University of Kentucky
UKnowledge

Theses and Dissertations--Pharmacy

College of Pharmacy

2014

Synthesis and Biological Evaluation of Novel Resveratrol and Combretastatin A4 Derivatives as Potent Anti-Cancer Agents

Nikhil Reddy Madadi
University of Kentucky, madadinikhilreddy@gmail.com

Click here to let us know how access to this document benefits you.

Recommended Citation

Madadi, Nikhil Reddy, "Synthesis and Biological Evaluation of Novel Resveratrol and Combretastatin A4 Derivatives as Potent Anti-Cancer Agents" (2014). *Theses and Dissertations--Pharmacy*. 42.
https://uknowledge.uky.edu/pharmacy_etds/42

This Doctoral Dissertation is brought to you for free and open access by the College of Pharmacy at UKnowledge. It has been accepted for inclusion in Theses and Dissertations--Pharmacy by an authorized administrator of UKnowledge. For more information, please contact UKnowledge@lsv.uky.edu.

STUDENT AGREEMENT:

I represent that my thesis or dissertation and abstract are my original work. Proper attribution has been given to all outside sources. I understand that I am solely responsible for obtaining any needed copyright permissions. I have obtained needed written permission statement(s) from the owner(s) of each third-party copyrighted matter to be included in my work, allowing electronic distribution (if such use is not permitted by the fair use doctrine) which will be submitted to UKnowledge as Additional File.

I hereby grant to The University of Kentucky and its agents the irrevocable, non-exclusive, and royalty-free license to archive and make accessible my work in whole or in part in all forms of media, now or hereafter known. I agree that the document mentioned above may be made available immediately for worldwide access unless an embargo applies.

I retain all other ownership rights to the copyright of my work. I also retain the right to use in future works (such as articles or books) all or part of my work. I understand that I am free to register the copyright to my work.

REVIEW, APPROVAL AND ACCEPTANCE

The document mentioned above has been reviewed and accepted by the student's advisor, on behalf of the advisory committee, and by the Director of Graduate Studies (DGS), on behalf of the program; we verify that this is the final, approved version of the student's thesis including all changes required by the advisory committee. The undersigned agree to abide by the statements above.

Nikhil Reddy Madadi, Student

Dr. Peter A. Crooks, Major Professor

Dr. Jim Pauly, Director of Graduate Studies

Synthesis and Biological Evaluation of Novel Resveratrol and Combretastatin A4 Derivatives as Potent Anti-Cancer Agents

DISSERTATION

A dissertation submitted in partial fulfillment of the
requirements for the degree of Doctor of Philosophy in the
College of Pharmacy
at the University of Kentucky

By

Nikhil Reddy Madadi

Lexington, KY

Director: Dr. Peter A. Crooks, Professor and Chairman of Pharmaceutical Sciences

University of Arkansas for Medical Sciences

Little Rock, Arkansas

2014

Copyright © Nikhil Reddy Madadi 2014

ABSTRACT OF DISSERTATION

SYNTHESIS AND BIOLOGICAL EVALUATION OF NOVEL RESVERATROL AND COMBRETASTATIN A4 DERIVATIVES AS POTENT ANTI-CANCER AGENTS

Resveratrol has been reported as a potential anticancer agent but cannot be used as an antitumor drug due to its chemical and metabolic instability. We have designed and synthesized 184 novel compounds related to resveratrol in an attempt to produce more potent and drug-like molecules. We have identified a tetrazole analog of resveratrol, ST-145(a) as a lead anticancer agent from the resveratrol analog series of compounds with a GI_{50} value of less than 10nM against almost all the human cancer cell lines in the National Cancer Institute's screening panel.

In a separate study, we tested the hypothesis that the limited bioavailability of resveratrol, can be improved by synthesizing analogs which would be glucuronidated at a lower rate than resveratrol itself. We demonstrated that ST-05 and ST-12(a) exhibit lower glucuronidation profiles when compared to resveratrol and that these synthesized stilbenoids likely represent useful scaffolds for the design of efficacious resveratrol analogs.

We have also initiated a new discovery program to identify selective CB1 and CB2 receptor ligands from a library of novel stilbene scaffolds structurally related to the resveratrol molecule. From the screened resveratrol analogs, two compounds were identified as selective CB2 and CB1 ligands. Compound ST-179 had 47-fold selectivity for CB2 (*Ki* = 284 nM) compared to CB1, while compound ST-160 was 2-fold selective for CB1 (*Ki* = 400 nM) compared to the CB2 receptor. These structural analogs have the potential for development as novel cannabinoid therapeutics for treatment of obesity and/or drug dependency.

Combretastatin A4 (CA-4) is one of the most potent antiangiogenic and antimitotic agents of natural origin. However, CA-4 suffers from chemical instability due to *cis-trans* isomerism in solution. To circumvent this problem, we have developed a facile procedure for the synthesis of novel 4,5-diaryl-2*H*-1,2,3-triazoles as CA-4 analogs to constrain the molecule to its *cis*-configuration. Twenty three triazoles were prepared as CA-4 analogs and submitted for anticancer screening. Among these CA-4 analogs, ST-467 and ST-145(b) can be considered as lead anticancer agents from this series, and further investigation against various cancer cell types in vivo with this class of compound may provide novel therapeutic avenues for treatment.

Keywords: combretastatin, resveratrol, triazole, tetrazole, cannabinoid

Nikhil Reddy Madadi
Signature of Student

9-8-2014
Date

SYNTHESIS AND BIOLOGICAL EVALUATION OF NOVEL RESVERATROL AND COMBRETASTATIN A4 DERIVATIVES AS POTENT ANTI-CANCER AGENTS

By

Nikhil Reddy Madadi

Dr. Peter A. Crooks

Director of dissertation

Dr. Jim Pauly

Director of graduate studies

09-29-2014

Date

DEDICATION

This work is dedicated to my parents (Madadi Venkat Reddy and Madadi Ratnamala), my wife (Madadi Prathibha) and my sister (Yerramreddy Nikitha) for their love, support and patience.

ACKNOWLEDGEMENTS

First of all, I would like to thank my supervisor Dr. Peter A. Crooks for his continuous encouragement and support throughout my graduate studies at the University of Kentucky and at the University of Arkansas for Medical Sciences. Without his guidance and motivational support, this dissertation would not have been possible. He gave me tremendous independence in my research, and expert advice whenever I needed help. I will always be grateful and proud to work under such a highly accomplished and remarkable researcher.

I am further thankful to Dr. Kyung-Bo Kim for agreeing to serve as the co-chair of my committee and providing insightful comments about my project. I would also like to thank Dr. Palli Subba Reddy and Dr. Val Adams for serving as my committee members and for being constructive and supportive during the course of doctoral studies. I am also very grateful to Dr. Isabel Mellon for readily agreeing to serve as my outside examiner. I am greatly privileged to have such a wonderful committee.

Special thanks are due to our collaborator Dr. Paul Prather at the UAMS for giving me the opportunity to work in his lab and for introducing me to cannabinoid receptor studies. I am also thankful to the graduate students Lirit and Max in Dr. Prather's lab for teaching me the lab techniques. I am also very grateful to our collaborator Dr. Radominska Pandya at the UAMS for all the support and encouragement with the resveratrol project discussed in Data Set 1. Her collaborative spirit and enthusiasm are incredible. Thanks are also due to our collaborator Dr. Robert Eoff at the UAMS for helping me with computational docking studies. Dr. Amit Ketkar from Eoff's lab was very helpful with the computational docking studies of CA-4 analogs. Thanks are also due to Dr. Howard Hendrickson and Dr. Lin Song for providing analytical support and for conducting analytical experiments for my projects.

Acknowledgements are also due to our collaborator Dr. Monica Guzman at the Cornell University for carrying out anticancer studies on my compounds. Likewise, gratitude is

also warranted to the National Cancer Institute (NCI) for screening my compounds for anticancer activity and providing such an enormous and useful data set. I would also like to thank Dr. Mark Leggas at the University of Kentucky for doing anticancer screening studies on some of my CA-4 analogs. I would also like to thank Dr. Sean Parkin at the UK for providing crystallographic data on a number of my compounds.

I would also like to thank all my present and past colleagues in Dr. Crooks' lab who turned out to be my friends both in the lab and outside the lab. Special thanks are due to Yerramreddy Thirupathi Reddy for introducing me to practical organic chemistry and for teaching me organic chemistry techniques during my initial days of my graduate studies. I would like to thank Dr. Penthala, Dr. Shoban, Dr. Venu, Dr. Shyam and Dr. Sateesh for being such wonderful friends and lab-mates all these years. Thanks are also due to Dr. Zheng and Dr. Zaineb for being critics of my work and for providing valuable suggestions during group meetings.

Special thanks are also due to my roommates and friends Dr. Satisha U.V. Praveen and Dr. Shyam for being very accommodating during my stay in Little Rock. Acknowledgements are also due to my friends Mahendra, Subramanyam and Ramesh for making my stay in Lexington memorable.

I want to thank my parents (Madadi Venkat Reddy and Madadi Ratnamala) and my sister (Yerramreddy Nikitha) for their love and affection. They have always been there to encourage and inspire me. Last but certainly not least, I wish to thank my wife, Prathiba for her love, encouragement and support.

TABLE OF CONTENTS

Acknowledgements v

List of Tables x

List of Schemes xiii

List of Figures xv

Chapter 1: Goals of the study and literature review 1

1.1 Hypothesis 1

1.2 Overall Aims 1

1.3 Introduction to cancer 3

1.4 Natural products as anti-cancer drugs 4

1.5 National Cancer institute (NCI) Anticancer screening program 11

1.6 Introduction to resveratrol 13

1.6.1 Molecular targets of resveratrol 16

1.6.2 Pharmacokinetics of resveratrol 19

1.7 Introduction to Combretastatin A4 20

Chapter 2: Synthesis of resveratrol analogues as anti-cancer agents 28

2.1 Previous SAR studies on resveratrol 28

2.2 Synthesis of *(E)*-stilbenes as resveratrol analogues 31

2.2.1 Analytical data of the synthesized *trans*-stilbene analogues 44

2.3 Synthesis of *(E)*-3,5,4'-trimethoxy resveratrol analogues with substitutions at the C2 position on the stilbene 55

2.3.1 Prior studies with this scaffold 55

2.3.2 Chemistry and analytical data 57

2.4 Synthesis of (*Z*)-2,3-diaryl substituted acrylonitriles as anticancer agents 71

2.4.1 Prior studies with this scaffold 71

2.4.2 Chemistry and analytical data 74

2.5 Synthesis of (*E*)-2,3-diaryl substituted acrylonitriles as anticancer agents 104

2.6 Synthesis of (*E*)-3-(3-hydroxy-4-methoxyphenyl)-2-(3,4,5-trimethoxyphenyl)

acrylic acid for anticancer activity and UDP-glucuronosyltransferases studies..... 105
2.7 Synthesis of (*Z*)-5-(2-(2H-tetrazol-5-yl)-2-(3,4,5-trimethoxyphenyl)vinyl) -2-methoxy- phenol (ST-145(a)) as second generation *trans* stilbenes..... 107
Chapter 3: Anticancer activities of synthesized resveratrol analogs..... 110
3.1 NCI-60 Human Tumor Cell Line Screen..... 110
3.2 Methodology used for the *in vitro* screen at the NCI..... 110
3.3 Anticancer activity at NCI of simple stilbenes as resveratrol analogues 112
3.4 Anticancer evaluation of *(E)*-3,5,4'-trimethoxy resveratrol analogues with substitutions at the C2 position on the stilbene..... 115
3.5 Anticancer activity of (*E/Z*)-2,3-diaryl substituted acrylonitriles as anticancer agents..... 120
3.6 *In vitro* toxicity and tubulin affinity study against Acute Myeloid Leukemia cell line MV-411 128
3.7Anticancer activity of (*Z*)-5-(2-(2H-tetrazol-5-yl)-2-(3,4,5-trimethoxyphenyl)vinyl)-2-methoxyphenol (ST-145(a)) as second generation *trans* stilbenes..... 132
3.8 *In vitro* toxicity study of ST-145(a) against Acute Myeloid Leukemia cell line MV-411 135
3.9 Conclusion..... 135
Chapter 4: Preparation of 4,5 disubstituted-2*H*-1,2,3-triazoles as potent and stable combretastatin A4 analogues 138
4.1 Introduction 138
4.2 Methodology Development and Design of 4,5 disubstitutes-2H-1,2,3-triazoles ... 141
4.3 Chemistry..... 145
4.4 Analytical data..... 151
4.5 Biological Evaluation..... 158
4.5.1 Anticancer activity against a panel of NCI 60 human cancer cells 158
4.5.2 Anticancer evaluation of ST-145(b) versus 9LSF rat gliosarcoma cells via colony formation assay 166
4.6 Conclusion..... 167
Chapter 5: Resveratrol derivatives as selective high affinity cannabinoid receptor ligands and correlation with their anti-cancer properties. 169
5.1 Introduction 169

5.2 Standard Operating Procedure for cannabinoid affinity screening 172
5.3 CB1 and CB2 receptor competitive binding data from screening assay with resveratrol analogs 173
5.4 Discussion and Conclusion 176
Chapter 6: Summary 177
Appendices 183
Data Set 1: Novel Resveratrol-Based Substrates for Human Hepatic, Renal, and Intestinal UDP-Glucuronosyltransferases 183
7.1 Introduction 176
7.2 Source of Human Microsomes and Recombinant UGTs. 185
7.3 Screening of Human Microsomes and Recombinant UGTs 185
7.4 Enzyme Kinetics Assays 186
7.5 Data Analysis 187
7.6 Glucuronide Product Analysis 188
7.7 Analysis of Glucuronide Product Structures by ESI-HPLC-MS 188
7.8 Glucuronide Metabolites Analysis by HPLC−UV−VIS and HPLC−MS/MS 189
7.9 Screening of Recombinant UGTs for glucuronidating ST-12a and ST-05 192
7.10 Glucuronidation of ST-12(a) and ST-05 by Human Hepatic and Intestinal Microsomes 193
7.11 Kinetic Analysis of NI-12a and NI-ST-05 with selected Recombinant UGTs 194
7.12 Conclusion 198
Data Set 2: NCI single dose percentage growth results for the simple stilbene analogues 200
Data Set 3: CB1 and CB2 competitive binding screening at 1µM concentration 224
Data Set 4: NMR spectral data of selected compounds 230
References 241
Vita 255

List of Tables

Table 1.1 Effects of resveratrol on various human cancer cell lines. Adapted from (Athar, Back et al. 2009) 17

Table 2.1 Structures of the synthesized *trans*-stilbenes and the starting materials (benzyl carbaldehyde and Wittig salt) used 33

Table 2.2 Structures of the synthesized diarylacrylonitrile products and the starting materials (aldehyde and phenylacetonitrile precursors) utilized in their preparation 75

Table 3.1 Growth inhibition (GI_{50}/µM) and Total Growth Inhibition (TGI/µM) data for compound ST-198 against human cancer cells 114

Table 3.2 Tryphan blue assay results; IC_{50} values (µM) for resveratrol analogs (RES-09, RES-10, RES-14, RES-27, RES-13, RES-16, RES-23 and RES-18**)** against lung and breast cancer 116

Table 3.3 Growth inhibition **(**GI_{50}/µM) and cytotoxicity (LC_{50}/µM) data for compounds RES-11, RES-17, RES-59, ST-100 and ST-127 against human cancer cells 119

Table 3.4 Growth inhibition **(**GI_{50}/µM) and Total Growth Inhibition (TGI/µM) data for compounds ST-198, ST-148, ST-147 and ST-124 against human cancer cells 121

Table 3.5 Growth inhibition **(**GI_{50}/µM) and Total Growth Inhibition (TGI/µM) data for compounds ST-507, ST-507(a), ST-145 and ST-510 against human cancer cells 122

Table 3.6 Growth inhibition **(**GI_{50}/µM) and Total Growth Inhibition (TGI/µM) data for compounds ST-179, ST-163, ST-178 and ST-180 against human cancer cells 123

Table 3.7 Growth inhibition **(**GI_{50}/µM) and Total Growth Inhibition (TGI/µM) data for compounds ST-257, ST-260, ST-261 and ST-253 against human cancer cells 125

Table 3.8 Growth inhibition **(**GI_{50}/µM) and Total Growth Inhibition (TGI/µM) data for compounds ST-252 and ST-173 against human cancer cells 126

Table 3.9 Growth inhibition **(**GI_{50}/µM), Total Growth Inhibition (TGI/µM) and cytotoxicity (LC_{50}/µM) data for compound ST-145(a) against human cancer

cells 132
Table 4.1 Optimization of the reaction conditions for the synthesis of 4-(3,4-dichloro)-5-(3,4-dimethoxyphenyl)-2*H*-1,2,3-triazole 144
Table 4.2 Synthesis of 4,5-disubstituted-2*H*-1,2,3-triazoles from their corresponding (*Z*)-2,3-diaryl substituted acrylonitriles 147
Table 4.3 Percentage growth inhibition of NCI 60 cancer cells by compounds (ST-124(a), ST-440, ST-442, ST-447, ST-452 and ST-467) with 10µM concentration.....159
Table 4.4 Percentage growth inhibition of NCI 60 cancer cells by compounds (ST-471, ST-475, ST-482, ST-492, ST-497 and ST-145(b)) with 10µM concentration 161
Table 4.5 Growth inhibition **(**GI_{50}/µM) and Total Growth Inhibition (TGI/µM) data for compounds ST-497, ST-124(a), ST-467 against NCI human cancer cells.....163
Table 4.6: Growth inhibition **(**GI_{50}/µM) and Total Growth Inhibition (TGI/µM) data for compounds ST-282, ST-482 and ST-452 against NCI human cancer cells ...165
Table 5.1 Ki values of ST-179, ST-165, and ST-160 for CB1 and CB2 receptors 175
Table 7.1 Glucuronidation Kinetics for NI-12(a) and NI-ST-05 Metabolites. Glucuronidation activities of selected recombinant UGTs were measured by incubating membrane fractions with increasing concentrations of substrate (see Figures 7.7 and 7.8) at a constant concentration of UDP-GlcUA (3 mM). Reactions were centrifuged, supernatants separated by HPLC, and curve fits and kinetic constants determined using GraphPad Prism 4 software. *Values estimated based on an incomplete data set. 196
Table 8.1 Percentage growth inhibition of NCI 60 human cancer cells by compounds (ST-191, ST-192, ST-193, ST-194, ST-197, ST-198 and ST-209) with 10µM conc.....200
Table 8.2 Percentage growth inhibition of NCI 60 human cancer cells by compounds (ST-212, ST-220, ST-226, ST-227, ST-233, ST-234 and ST-236 with 10µM conc.....201
Table 8.3 Percentage growth inhibition of NCI 60 human cancer cells by compounds (ST-239, ST-247, ST-294, ST-297, ST-309, ST-315 and ST-320) with 10µM conc.....203
Table 8.4 Percentage growth inhibition of NCI 60 human cancer cells by compound ST-321 with 10µM conc.....205

Table 8.5 Percentage growth inhibition of NCI 60 human cancer cells by compounds (RES-14, RES-17, RES-18, RES-27, RES-16 and RES-54) with 10µM conc206
Table 8.6 Percentage growth inhibition of NCI 60 human cancer cells by compounds (RES-57, RES-11, RES-75, RES-59, RES-80 and RES-62**)** with 10µM conc208
Table 8.7 Percentage growth inhibition of NCI 60 human cancer cells by compounds (ST-132(a), ST-127, ST-128 and ST-138 with 10µM conc 209
Table 8.8 Percentage growth inhibition of NCI 60 human cancer cells by compounds (ST-139, ST-98, ST-100 and ST-89**)** with 10µM conc.....211
Table 8.9 Percentage growth inhibition of NCI 60 human cancer cells by compounds (ST-101, ST-113, ST-148, ST-147, ST-145, ST-145(a), ST-161) with 10µM conc 213
Table 8.10 Percentage growth inhibition of NCI 60 human cancer cells by compounds (ST-162, ST-163, ST-164, ST-165, ST-168, ST-169 and ST-170) with 10µM conc 215
Table 8.11 Percentage growth inhibition of NCI 60 human cancer cells by compounds (ST-171, ST-173, ST-174, ST-175, ST-176, ST-177 and ST-178) with 10µM conc 216
Table 8.12 Percentage growth inhibition of NCI 60 human cancer cells by compounds (ST-179, ST-180, ST-181, ST-183, ST-152, ST-153 and ST-112) with 10µM conc 218
Table 8.13 Percentage growth inhibition of NCI 60 human cancer cells by compounds (TMR-03, TMR-01, ST-252, ST-253, ST-257, ST-260, ST-261) with 10µM conc 220
Table 8.14 Percentage growth inhibition of NCI 60 human cancer cells by compounds (ST-287, ST-288, ST-507, ST-507(A), ST-509, ST-510, ST-124**)** with 10µM conc 221

List of Schemes

Scheme 2.1 Synthesis of *(E)*-stilbenes as resveratrol analogues.Reagents and conditions: (a) 5% NaOMe, MeOH, reflux.. 32

Scheme 2.2 Synthesis of resveratrol analogs with heterocyclic ring substitutions at the C2 Position. (a) MeI, K_2CO_3, acetone; (a) $POCl_3$, DMF, 0 ^oC, 69% yield; (b) barbituric acid or thiobarbituric acid, methanol, RT, 6 hrs, 95-96% yield; (c) five membered active methylene compound, NH_4OAc, AcOH, MWI, 1-2 min, 94-97% yield; (d) isobarbituric acid, ethanol, reflux, 4 hrs, 60% yield**.**.....58

Scheme 2.3 Synthesis of resveratrol analogs with bicyclic and acrylonitrile substitutions at the C2 position. (a) Quinuclidinone, 20% NaOH, EtOH, reflux; (b) $NH_2OH.HCl$, AcONa, EtOH; (c) Phenylacetonitrile, NaOMe, EtOH, 6hrs reflux. 62

Scheme 2.4 Synthesis of resveratrol analogs with hydroxamine, benzylalcohol, bromo, cyano and imidazole substitutions at the C2 position. (a) NH_4OH, NaOAc, ethanol, reflux 4hrs; (b) $NaBH_4$, methanol; (c) imidazole, neat, MW 180 ^0C, 5min (f) N-bromosuccinamide, $CHCl_3$; (g) Aq.NH_3, I_2, THF. 66

Scheme 2.5 Synthesis of resveratrol analogs with methyl, benzylalcohol and bromo substitutions at the C2 position. (a) MeI, K_2CO_3, acetone, reflux 12hrs. (c) *N*-bromosuccinamide, $CHCl_3$; (e) $NaBH_4$, methanol.....67

Scheme 2.6 Synthesis of (*Z*)-2,3-diaryl substituted acrylonitriles; reagents and conditions: (a) 5% NaOMe, MeOH, reflux. 74

Scheme 2.7 Synthesis of (*E*)-substituted diarylacrylonitrile analogs 104

Scheme 2.8 Synthesis of (*E*)-3-(3-hydroxy-4-methoxyphenyl)-2-(3,4,5trimethoxyphenyl) acrylic acid (ST-12(a)) (a) TEA, Ac2O, 140 °C, 40% yield.....106

Scheme 2.9 Synthesis of ST-145(a).....108

Scheme 4.1 1,2,3 triazole synthesis by Huisgen Azide-alkyne 1,3 dipolar cyclization ..142

Scheme 4.2 Proposed mechanism and optimization of the reaction conditions for the synthesis of 4-(3,4-dichloro)-5-(3,4-dimethoxyphenyl)-2*H*-1,2,3-triazole and synthesis of its methylated product. 144

Scheme 4.3 Synthesis of 4,5-disubstituted 2*H*-1,2,3-triazoles from (*Z*)-2,3-diarylacrylonitriles 145
Scheme 4.4 Synthesis of 4,5-disubstituted 2*H*-1,2,3-triazoles; reagents and conditions: (a) 5% NaOMe, MeOH, reflux. (b) NaN_3, NH_4Cl, DMF/H_2O. 146

List of Figures

Figure 1.1 Structure of resveratrol and Combretastatin A4 3
Figure 1.2 Structures of Vinblastine and Vincristine 4
Figure 1.3 Structures of Podophyllotoxin, Etoposide and Teniposide 5
Figure 1.4 Structures of Camptothecin, Topotecan and Irinotecan 6
Figure 1.5 Structures of Actinomycin D and Mitomycin C 7
Figure 1.6 Structures of Daunorubin and Doxorubin 8
Figure 1.7 Structures of *p*-Propenyl phenol, Diethylstilbestrol, Tamoxifen and Gilvec 9
Figure 1.8 Structure of resveratrol 13
Figure 1.9 Sources of resveratrol from various plant species 14
Figure 1.10 Resveratrol citations appearing on pubmed from 1978 to 2013 16
Figure 1.11 Microtubule dynamic instability, where the coexistence of polymerization and depolymerizing microtubules are imperative for the dynamic stability 23
Figure 1.12 Structures of polymerizing and depolymerizing agents on tubulin assembly 24
Figure 1.13 Structures of Combretastatin A4 (CA4), CA4P and PMS 26
Figure 2.1 Structures of resveratrol and its O-methylated derivatives 29
Figure 2.2 Isomerization of *cis*-3,5,4'-trimethoxystilbene to *trans*-3,5,4' – trimethoxystilbene 30
Figure 2.3 Structures of *trans*-3,5,4'-trimethoxystilbene and its potent analogs 56
Figure 2.4 Crystal structures of compound RES-27, RES-17 and RES-54 66
Figure 2.5 Structures of literature reported potent anti-cancer agents in the phenylacrylonitrile series 70
Figure 2.6 Scaffolds of reported potent anticancer agents in the stilbene and phenylacrylonitrile series 71
Figure 2.7 Structures of potent aromatase inhibitory (XC), ST-145 and ST-145(a**)** 107
Figure 3.1 Structures of ST-198 and ST-148 113
Figure 3.2 Lead compounds ST-507, ST-507(a), ST-145 and ST-510 exhibit potent anti-leukemia activity. MV-411 cells were treated with the indicated compounds for 24 and 48 h. Cell viability was determined by Annexin V staining. Percent viability was calculated as the percent of annexin v-/7-AAD-cells relative to

control 129
Figure 3.3 Structures of the lead cyano stilbenes tested ST-507, ST-507(a), ST-145 and ST-510 against MV-411 cells (AML).....130
Figure 3.4 Microtubule depolymerization assay with the lead compounds ST-507, ST-507(a), ST-145 and ST-510 131
Figure 3.5 Lead compound ST-145(a) exhibited potent anti-leukemia activity against MV-411 cells. 135
Figure 3.6 Triage flow chart of resveratrol analogues that were submitted for anticancer screening in the NCI panel of 60 human cancer cell lines 136
Figure 3.7 Structures of the lead resveratrol analogs ST-145(a), ST-145 and ST-510 ...136
Figure 4.1 Structures of Combretastatin A4 (CA-4) (A), Colchicine (B), and reported anti-tubulin compounds (C-I) 140
Figure 4.2 Structures of CA4 and *cis* constraines heterocyclic CA4 analogs 141
Figure 4.3 X-ray Crystal structures of compounds ST-464 and ST-447(a).....158
Figure 4.4 Dose response curve of ST-145(b) versus 9LSF rat gliosarcoma cells.....167
Figure 4.5 Lead 4,5-diaryl-2*H*-1,2,3-triazoles as potent CA4 analogs.....168
Figure 5.1 Structures of Anandamide, Tetrahydrocannabinol, N-benzyl indole-quinuclidinones, Carboxamido-5-aryl-isoxazole.....170
Figure 5.2 Structures of synthetic cannabinoids JWH-133, WIN 55, SR 144528 and AM252 171
Figure 5.3 Structures of prenylated stilbenoids *trans*-arachidin-1 and *trans*-arachidin-3.....172
Figure 5.4 Structures of TMR, ST-124, ST-179, ST-165 and ST-160 173
Figure 5.5 CB1 and CB2 competitive binding screen at 1µM concentration with TMR, ST-124, ST-179, ST-165 and ST-160.....174
Figure 5.6 Affinity (*Ki*) of compounds ST-179(A), ST-165(B) and ST-160(C) for mouse brain CB1Rs (mCB1) and human CB2Rs (hCB2) 176
Figure 7.1 Structures of resveratrol analogs *trans*-arachidin-1, *trans*-arachidin-3, ST-05, DNR-1 and ST-12(a).....184
Figure 7.2 Metabolism of ST-12(a) and ST-05 with human liver microsomes.....189
Figure 7.3 Extracted ion chromatogram (m/z 361) and (+)-ESI mass spectra of ST-12(a) and its glucuronide conjugate NH4+ adducts. Spectra of ST-12(a)

glucuronides (two isomers of tR = 16.0 and 16.3 min) showed an [M + NH_4]
+
peak (m/z 554) plus a fragment ion resulting from neutral loss of the glucuronide moiety (m/z 361).....191
Figure 7.4 Structures and Mass spectra of ST-05 and its glucuronide conjugates. Spectrum of ST-05 glucuronide (tR = 21.4 min) showed an [M+ H]+ peak (m/z 490) plus a major peak corresponding to the ST-05 substrate (m/z 314).....191
Figure 7.5 Glucuronidation of NI-12a and ST-05 by human recombinant UGTs. UGT1A1,1A3, 1A4, 1A6, 1A7, 1A8, 1A9, 1A10, 2B4, 2B7, 2B15, 2B17 (5 µg of protein) were evaluated for their ability to glucuronidate DNR-1, ST-12(a), and ST-05. No activity was observed toward DNR-1, and UGT2B7, 2B4, 2B15, and 2B17 were not active toward any compound. Activities are expressed in nanomoles per milligram of protein per minute.....193
Figure 7.6 Glucuronidation activities of Human Liver Microsomes and Human Intestinal Microsomes toward NI-12a and NI-ST-05. Human liver microsomes from 10 different donors, a pooled liver sample, and hepatosomes and human intestine microsomes from 13 different donors were analyzed. Each substrate concentration was 0.25 mM for HIM, with a molar excess of UDP-GlcUA; the reactions were incubated for 60 minutes. Activities are expressed in nmol/mg protein/min.....194
Figure 7.7 Steady state kinetic curves for the glucuronidation of NI-12a by selected human recombinant UGTs. Glucuronidation activities for wildtype UGT1A7, 1A8, 1A9, and 1A10 were measured by incubating membrane fractions containing recombinant UGTs with increasing concentrations (shown in figure) of the substrates at a constant concentration of UDP-GlcUA (3 mM) for 60 min at 37 °C. Curve fits and kinetic constants were determined using GraphPad Prism 4 software. The graphical fits of the data (mean ± SD) are shown. 197
Figure 7.8 Steady state kinetic curves for the glucuronidation of ST-05 by selected human recombinant UGTs. Glucuronidation activities for wildtype UGT1A1, 1A9, and 1A10 were measured by incubating membrane fractions containing recombinant UGTs with increasing concentrations (shown in figure) of the

substrates at a constant concentration of UDP-GlcUA (3 mM) for 60 min at 37 °C. Curve fits and kinetic constants were determined using GraphPad Prism 4 software. The graphical fits of the data (mean ± SD) are shown. 198
Figure 7.9 Glucuronidation rates of Resveratrol, ST-05 and ST-12(a) 198
Figure 8.1 CB1 and CB2 competitive binding screen at 1µM concentration with ST-179, ST-173, ST-165, ST-172, ST-171 and ST-167.....224
Figure 8.2 CB1 and CB2 competitive binding screen at 1µM concentration with ST-177, ST-162, ST-164, ST-184, ST-178 and ST-161.....225
Figure 8.3 CB1 and CB2 competitive binding screen at 1µM concentration with ST-190, ST-175, ST-181, ST-185, ST-169 and ST-183.....226
Figure 8.4 CB1 and CB2 competitive binding screen at 1µM concentration with ST-192, ST-193, ST-194, ST-195, ST-196 and ST-197.....227
Figure 8.5 CB1 and CB2 competitive binding screen at 1µM concentration with ST-198, ST-179(repeat), ST-188, ST-166, ST-176 and ST-191 228
Figure 8.6 CB1 and CB2 competitive binding screen at 1µM concentration with ST-153, ST-155, ST-147(a) and ST-156 229
Figure 8.7 ^{1}H NMR spectral data of compound ST-145(a).....230
Figure 8.8 1D NOE of compound ST-145(a). Blue circled hydrogen is excited.....231
Figure 8.9 1D NOE of compound ST-145(a). Blue circled hydrogen is excited.....232
Figure 8.10 ^{1}H NMR spectral data of compound ST-145 233
Figure 8.11 ^{13}C NMR spectral data of compound ST-145 234
Figure 8.12 ^{1}H NMR spectral data of compound ST-510 235
Figure 8.13 ^{13}C NMR spectral data of compound ST-510 236
Figure 8.14 ^{1}H NMR spectral data of compound ST-467 237
Figure 8.15 ^{13}C NMR spectral data of compound ST-467 238
Figure 8.16 ^{1}H NMR spectral data of compound ST-145(b) 239
Figure 8.17 ^{13}C NMR spectral data of compound ST-145(b) 240

Chapter 1:

Goals of the study and literature review

1.1 Hypothesis:

The central hypothesis of this work is that the anti-cancer activity, metabolic stability and chemical stability of resveratrol can be improved by structural modification of the stilbene molecule. The second hypothesis of this work was that the anti-cancer activity and chemical stability (*cis-trans* isomerization) of the related compound, combretastatin A4, can be improved by replacing the ethylene bridge with a heterocyclic ring system, thereby constraining the molecule to the *cis* configuration.

1.2 Overall Aims:

Cancer is the second most life threatening disease after cardiovascular disease, affecting more than six million people per year worldwide. Drastic changes in lifestyle during the beginning of 20^{th} century have increased the risk of humans developing different types of cancers. Although to date, significant research has carried out to improve treatment of various forms of cancer, there is still a lack of effective chemotherapeutic treatment to cure most forms of cancer completely. In this respect, considerable effort has been focused on identifying molecules with anti-cancer properties from both natural and synthetic sources. Herein, two medicinal chemistry projects related to the natural product molecules resveratrol and combretastatin A4, both of which possess anticancer properties, are presented.

Resveratrol (3,5,4-trihydroxystilbene) is a well-known phytoalexin found in grapes, peanuts, red wine and other foods. It has been reported as a potential chemotherapeutic agent due to its striking inhibitory effects on cellular events associated with cancer initiation, promotion, and progression. In clinical studies, resveratrol has demonstrated the ability to reduce tumor cell proliferation in patients with colorectal cancer. However, resveratrol has some limitations which preclude its use in cancer treatment, since it cannot be used as a drug because of its chemical and metabolic instability. This project has been designed to improve the chemical and metabolic stability and the anti-cancer potency of the resveratrol molecule with structural modifications designed to make the molecule more drug like.

Combretastatin A4 (CA-4), a natural product structurally related the resveratrol molecule was first isolated from the South African willow tree, *combretum caffrum*, by Pettit and co-workers (Pettit, Singh et al. 1995). It is one of the most potent antiangiogenic and antimitotic agents of natural origin. Combretastatin A4 is structurally and functionally similar to a well-known microtubule-targeting agent, colchicine. Its phosphate prodrug (CA-4P) is currently in phase 3 clinical trial for the treatment of anaplastic thyroid cancer, and it has successfully retarded tumor growth in a wide spectrum of tumor models. However, recent studies have reported the chemical instability of CA-4 due to *cis*-*trans* isomerization to the more thermodynamically stable, but less potent *trans*-CA-4 isomer (Nathwani, Hughes et al. 2013). This project has been designed to improve the chemical stability and the anti-cancer potency of the resveratrol molecule with structural modifications designed to constrict the *cis* configuration of CA-4.

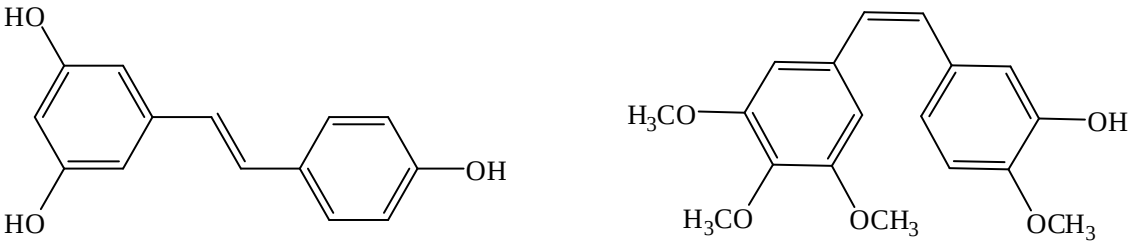

Resveratrol **Combretastatin A4**

Figure 1.1 Structure of resveratrol and Combretastatin A4

1.3 Introduction to cancer

Cancer is the second most common cause of death in America after cardiovascular disease. About 567,628 Americans died of cancer in 2009 alone, almost 11,000 per week. About 23 % of deaths in the United States during 2008-2009 were caused by cancer (Heron 2012). The cost for the treatment of cancer in the US in 2009 was estimated to be $216.6 billion and was expected to double over the next few years. Thus, curing cancer is one of the biggest challenges the scientific community is facing in the 21st century.

Cancer is a disease characterized by unrestrained growth and abnormal spread of cells. If the invasion of these abnormal cells to other tissues is not controlled, it may lead to death. This abnormality in the cells can be caused by both internal stimuli (hormones, immune system, inherited mutations and mutations from metabolism) and external stimuli (chemicals, radiation, infectious microorganisms). Both the internal and external factors may act together to initiate the development of cancer (Heron 2012).

1.4 Natural products as anti-cancer drugs

Since 1940, a systematic search for novel natural products with interesting biological properties has been initiated by pharmaceutical organizations and health institutes all around the world. By 1958 Charles Beer had isolated a pure compound from the leaves of the Madagascar periwinkle that depleted white cells and named the compound vinblastine (Noble, Beer et al. 1959). During the same period, the Eli Lilly Company discovered that vinblastine prolonged the life of mice carrying the leukemia cell line P1534. Vinblastine is currently being used in the treatment of testicular teratoma and Hodgkin's lymphoma (Gobbi, Broglia et al. 2003). Later, another *Vinca* alkaloid, vincristine was isolated which was used to treat a host of rare childhood cancers such as Wilms tumour, neuroblastoma, rhabdomyosarcoma and Ewing's sarcoma (Johnson, Armstrong et al. 1963).

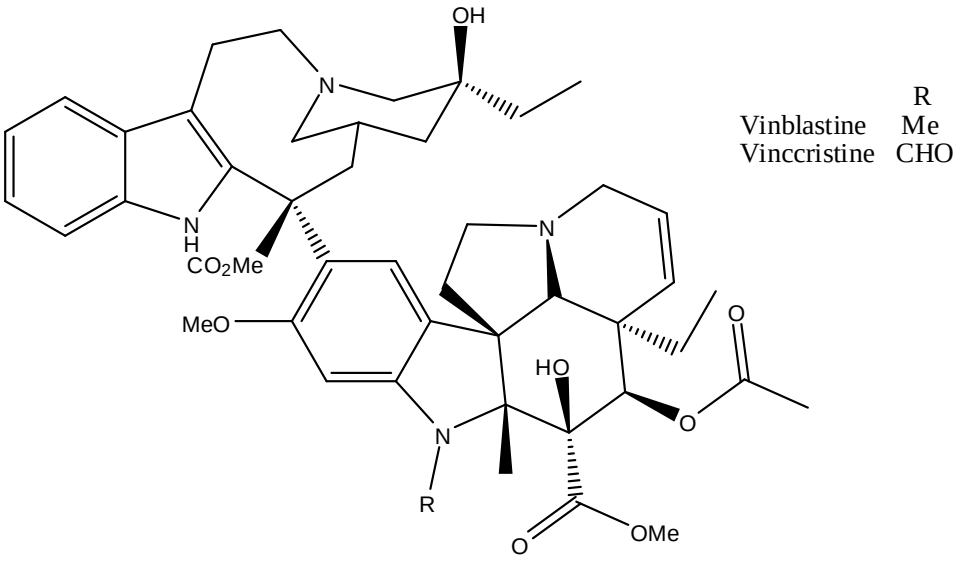

Figure 1.2 Structures of Vinblastine and Vincristine.

Reports of the use of *Podophyllum peltatum* (Mayapple) for the treatment of cancer around 950 AD from the "*Leech book of Bald"* intrigued the NCI to screen extracts from the plant, and thy discovered podophyllotoxin as a potent anticancer drug (Ma, Khan et al. 2005). However, due to high toxicity in clinical trials the drug was withdrawn. Further SAR studies focused on synthesizing glycoside analogues of podophyllotoxin; this approach yielded two successful drugs: Etoposide and Teniposide (**Figure 1.3**). Etoposide is currently being used to treat testicular and small cell lung cancers, Teniposide, on the other hand, is used to treat acute lymphoblastic leukemia and rare childhood cancers such as neuroblastoma (Ma, Khan et al. 2005).

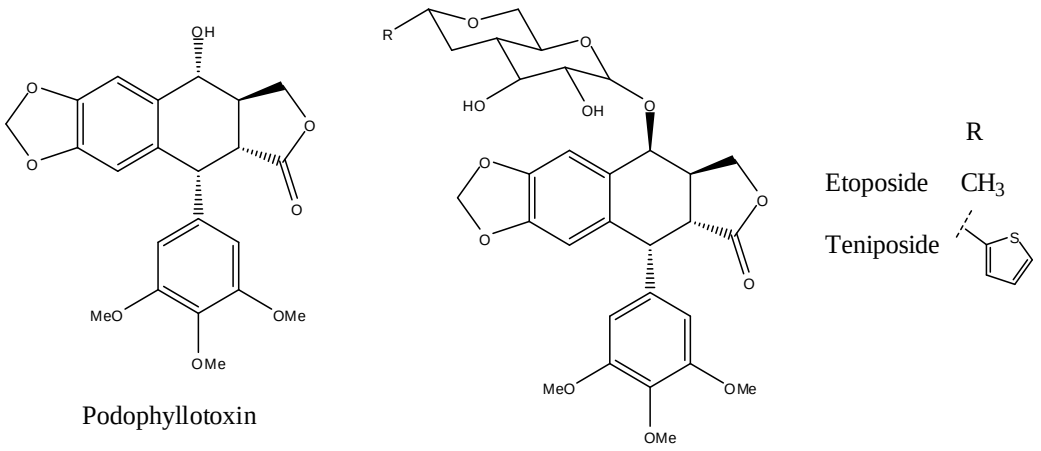

Figure 1.3 Structures of Podophyllotoxin, Etoposide and Teniposide.

In 1958, Monroe Wall discovered and isolated the natural product camptothecin from *Carmptotheca acuminata*, a tree native to China and Tibet. It was found to have potent antitumor activity against leukemia cell line L1210. The exact structure was elucidated in

1966, and its water soluble analogues, topotecan and irinotecan (**Figure 1.4**) are used in the treatment of colon and ovarian cancer, respectively (Thomas, Rahier et al. 2004).

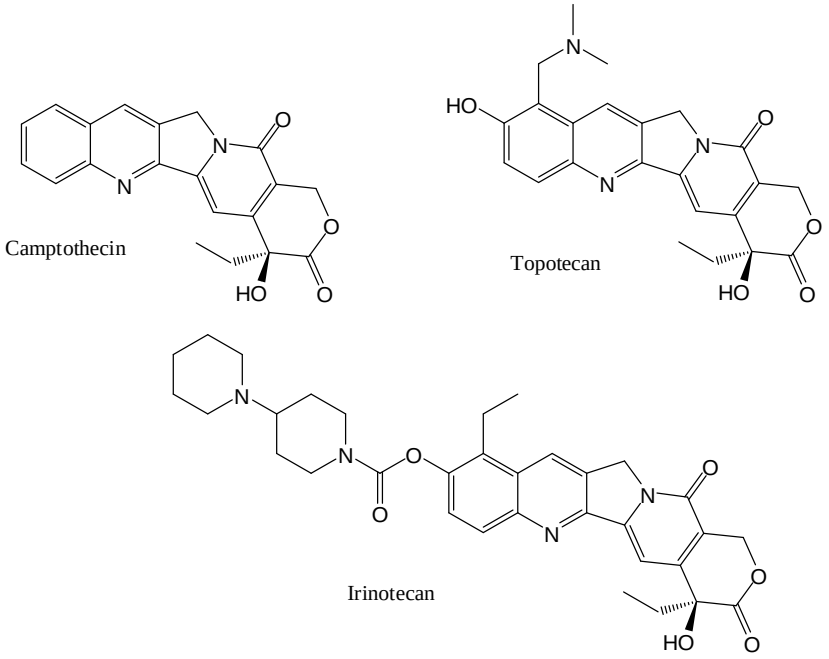

Figure 1.4 Structures of Camptothecin, Topotecan and Irinotecan.

The discovery of penicillium by Fleming in 1928 lead scientists to look into microorganisms as a source of useful natural products and this led to the discovery of several anticancer agents. In 1960, Dr. Faber discovered the anticancer properties of actinomycin D (**Figure 1.5**) and reported its potential for treating Wilms tumour in children (Farber, D'Angio et al. 1960). The discovery of actinomycin D introduced a new class of antitumor agents from microorganisms.

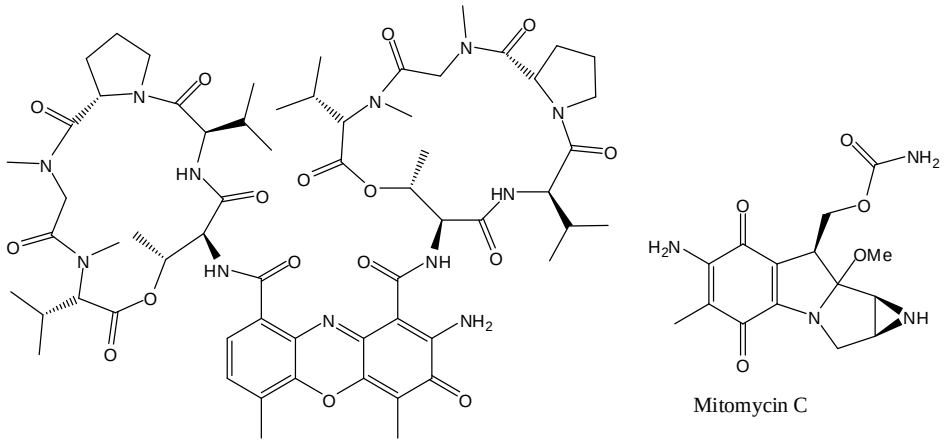

Figure 1.5: Structures of Actinomycin D and Mitomycin C.

Mitomycin C was first isolated by Wakaki from *Streptomyces caespitosus* in 1958. It was found to be highly toxic towards cancer cells but lacked selectivity, causing bone-marrow depression, vomiting, and kidney, liver and heart toxicity. The toxicity of mitomycin C was attributed to its bio-reduced product, which can form covalent bonds to DNA, similar to alkylating agents (Nguy, Chiu et al. 1987).

Anthracyclines are a more useful class of anticancer antibiotics. The Arcamone group first isolated them in the early 1960s, and they were found to possess potent antitumor properties. In the coming years, hundreds of analogues were synthesized and developed to yield drugs such as Doxorubicin and Daunorubicin, with a broad spectrum of anticancer activity (Arcamone, Franceschi et al. 1964).

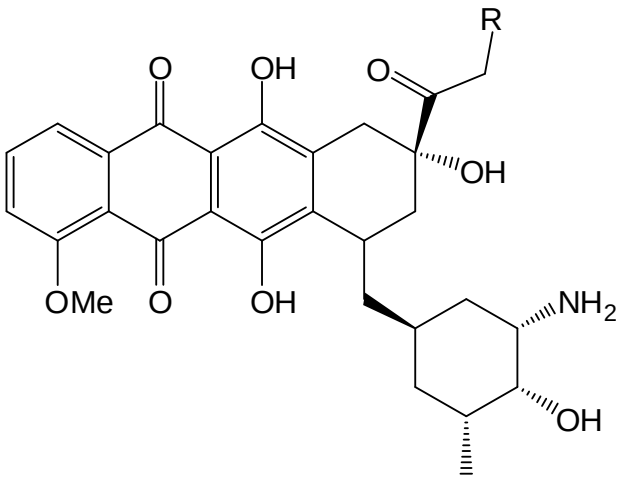

	R
Daunorubicin	H
Doxorubicin	OH

Figure 1.6 Structures of Daunorubicin and Doxorubicin.

Another area of developing anticancer agents is the use of hormone mimics. In the early 1930s Dodd and coworkers reported that a dimer of *p*-propenyl phenol had potent oestrogenic activity and mimicked the activity of estrogen (Hasenbrink, Sievernich et al. 2006). This lead to the synthesis of a series of dimeric structures, among which diethylstilbestrol was found to be a potent compound against breast cancer. Further modifications to the diethylstilbestrol structure led to the discovery of Tamoxifen (Early Breast Cancer Trialists' Collaborative 1992).

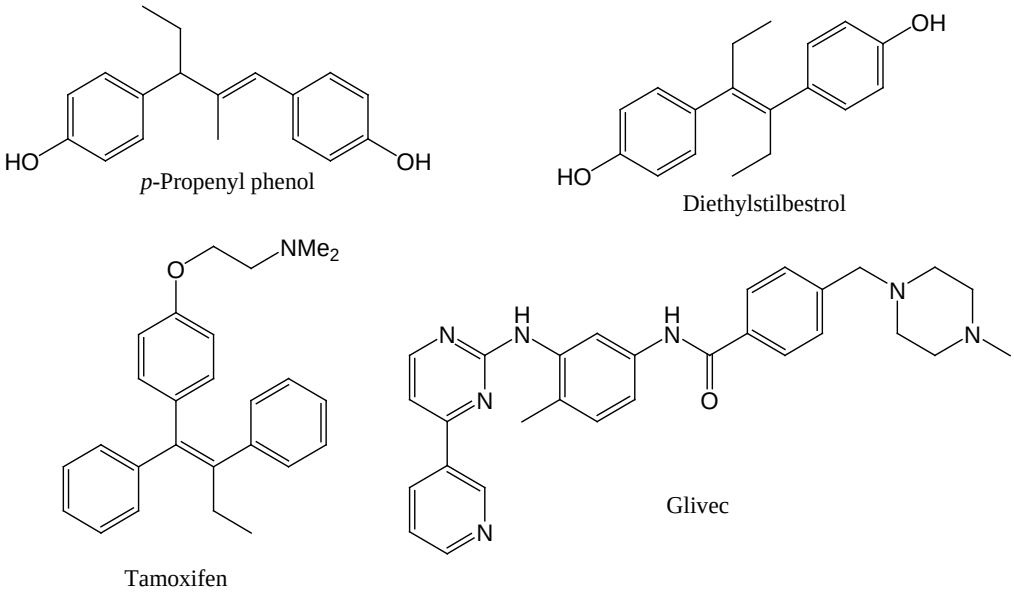

Figure 1.7 Structures of *p*-Propenyl phenol, Diethylstilbestrol, Tamoxifen and Glivec.

The initial discoveries in the field of chemotherapy were mostly cytotoxic agents with little selectivity for cancer cells. However, as our understanding of cancer improved, complimented with computational docking studies, high throughput screening protocols and bioinformatics, chemotherapy is now becoming more selective in targeting cancer cells.

By 2001, the first target-based cancer drug, Gleevec (**Figure 1.7**), was approved by the FDA for the treatment of chronic myelogenous leukemia (CML). If treated with Gleevec in the early stages of CML, nearly 100% of the diagnosed patients went into remission, and no major side effects were reported (Capdeville, Buchdunger et al. 2002).

Cancer chemotherapy is used as the primary mode of treatment for cancer and is also utilized as an adjuvant to other treatment options. However, it often is associated with

side effects and poor selectivity. Throughout history, natural products have been a rich source of compounds with excellent pharmacological activities and few side effects. The huge structural diversity of natural products isolated from natural sources can serve as lead compounds for the discovery of new anticancer agents, and their potencies and drug likeness properties can be further optimized by appropriate chemical modifications. Most of the anticancer drugs currently available on the market are from natural sources (Gordaliza 2007). The search for potent and selective semi-synthetically derived anticancer agents from parent natural products continues to be an important part of drug discovery process. Currently, close to 30 molecules of natural origin are in various stages of clinical trials for the treatment of cancer. Researchers and pharmaceutical companies devoted to the search for new cancer drugs are exploring new natural products emerging from variable sources, with the hope of finding potent, selective, drug-like and non-toxic molecules.

There are more than 100 types of malignancies that have been recognized to date. Almost any cell types can become cancerous (Heron 2012). In the last 50 years our understanding of cancer has improved greatly, but many forms of cancer still lack effective treatment options. In an effort to find anticancer drug leads, pharmaceutical companies often screen large chemical libraries which include natural products. Natural products are a rich source of complex molecules that are biologically relevant. The method used to develop new drugs from a prototype or a lead molecule of known biological activity is known as pharmacomodulation. The main aim of pharmacomodulation is to establish a correlation between the pharmacophore in the structure and its biological activity. By understanding the structure activity relationships (SAR) of the natural product and its analogs, by semi-

synthetically altering the functional groups in the molecule, additionally complimented with high throughput screening protocols, computational docking studies and bioinformatics, medicinal chemists can produce compounds that are far more effective as clinical agents in terms of potency and pharmacokinetic parameters.

1.5 National Cancer institute (NCI) Anticancer screening program

Screening natural products from different sources for activity against various human cancer cells gained momentum after the discovery of vinblastine in the 1950s. The National Cancer Institute (NCI) has been screening thousands of natural products and their derivatives and has been encouraging researchers to submit semi-synthetically produced derivatives for testing against its panel of 60 human tumor cell lines of nine different classifications (Rubinstein, Shoemaker et al. 1990). Numerous anticancer drugs have been discovered because of the NCI initiative, e.g. paclitaxel, docetaxel, irinotecan and topotecan (Shoemaker 2006). The successful discovery of these agents demonstrates the potential of natural products in the treatment of cancer.

Since 1955, the NCI has employed both *in vitro* and *in vivo* screens to evaluate the activity of natural products, their analogs, and novel synthetic compounds. Up until 1990, the NCI used the P388 mouse leukemia cell line to assess the activity of submitted compounds (Boyd and Paull 1995). From 1991 onwards the NCI introduced a panel of 60 human cancer cell lines of nine different classifications for its *in vitro* screens. The classifications represent human cancer lines from leukemia, non-small cell lung, colon, CNS, melanoma, ovarian, renal, prostate, and breast cancers. Five different

concentrations, viz. 10^{-4} M, 10^{-5} M, 10^{-6} M, 10^{-7} M and 10^{-8} M, of the compounds are used to evaluate their growth inhibition properties after 48 hours of exposure to cells in culture. The NCI employs an effective triage system for the submitted compounds based on duplicates already screened and single dose screening results, prior to selecting them for five dose testing. According to Rubinstein et al. anti-cancer activity screening studies involves a two stage process in which only the compounds showing more than 60% growth inhibition in at least eight of the 60 tumor cell line panel with a single dose of 10μM are selected for the second stage (five dose testing) (Rubinstein, Shoemaker et al. 1990). The Sulforhodamine B (SRB) assay is used to quantify the cell growth and viability effects of the test compounds. SRB is a chemical which stains basic amino acids to afford a pink colored product in mild acidic conditions allowing colorimetric quantitation, which is proportional to the total biomass. The collected data, when compared to control cells, allows the determination of GI_{50} values (i.e. 50% Growth Inhibition, concentration of drug resulting in a 50% reduction in net protein increase compared to control cells), TGI values (Total Growth Inhibition, concentration of drug resulting in a 100% reduction in net protein increase compared with control cells) and LC_{50} values (Lethal Concentration, concentration of drug lethal to 50% of cells). The screens have identified many potent anticancer drugs, and on average, every year NCI screens close to 10,000 novel compounds against its 60 human cancer cells. We have utilized the NCI 60-cell cancer screen to gather large quantities of useful biological data for the synthesized molecules in this dissertation project against various human tumor cell lines.

Herein, two medicinal chemistry projects related to the natural product molecules resveratrol and combretastatin, which possess anticancer properties, are presented. The projects were designed to improve the chemical/metabolic stability and pharmacokinetic properties of the above-mentioned drug molecules.

1.6 Introduction to resveratrol

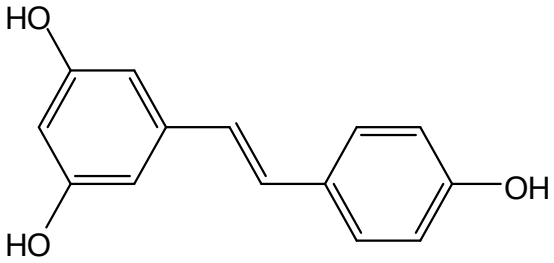

Resveratrol

Figure 1.8 Structure of resveratrol

The use of resveratrol in an ayurvedic herbal preparation can be dated back to thousands of years ago. Darakchasava is an ayurvedic herbal preparation of which the main ingredient is *Vitis vinifera L* (Baur, Pearson et al. 2006). This ayurvedic medicine was prescribed to patients with cardiovascular ailments. High performance liquid chromatography studies on darakchasava revealed the active ingredient to be resveratrol (Paul, Masih et al. 1999). Resveratrol (**Figure 1.8**) is a naturally occurring *E*-3,5,4'-trihydroxystilbene that was first isolated from the roots of white hellebore in 1940 (Baur and Sinclair 2006). The phytoalexin (resveratrol) is produced by a wide variety of plants in response to injury, stress, microbial infection and UV irradiation (Aggarwal, Takada et al. 2004). Although, red grapes have the highest concentration of resveratrol (50-100 mg

per gram) in the plant kingdom, Resveratrol was found in more than 80 plant species (**Figure 1.9**) (Baur and Sinclair 2006).

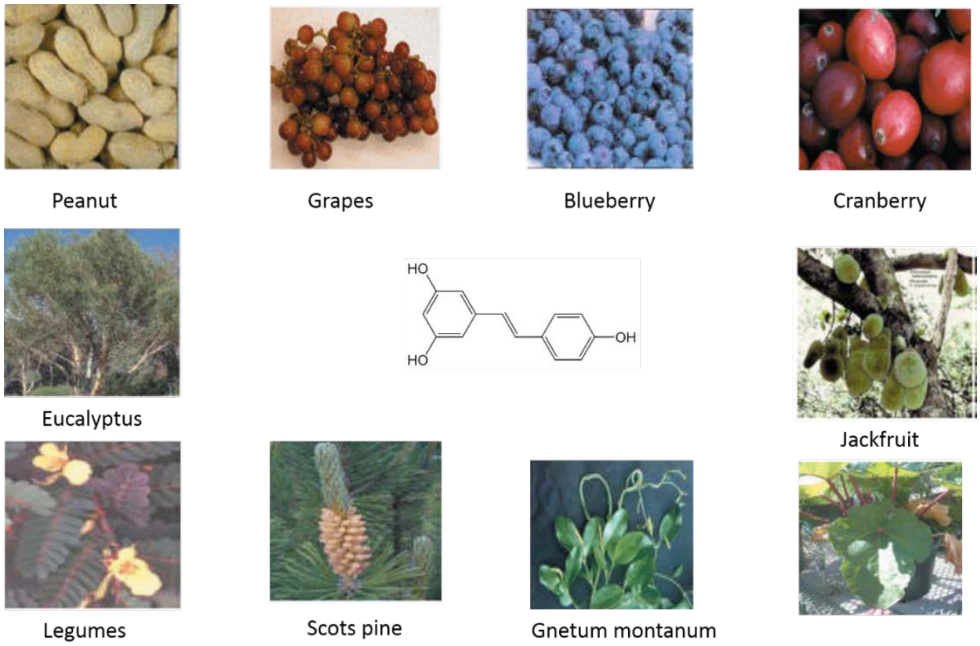

Figure 1.9 Sources of resveratrol from various plant species.

Resveratrol received tremendous attention after it was credited for the cardio-protective effects of red wine, famously known as the 'French paradox' (Kopp 1998). In 1997, Jang and coworkers reported that the topical application of resveratrol reduced mouse skin tumors to 2%, triggering extensive research on resveratrol (Jang, Cai et al. 1997). Since then, hundreds of reports (**Figure 1.10**) have shown that resveratrol can be used to treat a wide variety of diseases including cancer. Resveratrol has been reported as a potential chemotherapeutic agent due to its striking inhibitory effects on cellular events associated with cancer initiation, promotion, and progression *in vitro* (Aggarwal, Bhardwaj et al. 2004). In addition, there are several *in vitro* and *in vivo* reports on the biologically beneficial properties of resveratrol for coronary, hepatic, neurological, cardiovascular,

and inflammation conditions (Pace-Asciak, Rounova et al. 1996, Fauconneau, Waffo-Teguo et al. 1997, Jang, Kang et al. 1999, Aggarwal, Bhardwaj et al. 2004, Kim, Zhu et al. 2006). Also, resveratrol synergistically enhanced the anti-HIV activity of zidovudine, and has antiviral effects against the herpes simplex virus (Docherty, Fu et al. 1999, Heredia, Davis et al. 2000).

Below is a list of breakthrough findings on resveratrol's biological properties.

1) Resveratrol modulates low-density lipoprotein levels, reducing the risk for development of coronary heart disease (Frankel, Waterhouse et al. 1993).
2) Resveratrol reduced mouse skin tumors by 98%, indicating its chemo-preventive effects (Jang, Cai et al. 1997).
3) Resveratrol extends the life span of yeast, giving a boost to the sales of resveratrol supplements (Howitz, Bitterman et al. 2003).
4) Resveratrol has a positive effect on obesity and diabetes (Baur, Pearson et al. 2006) (Lagouge, Argmann et al. 2006).

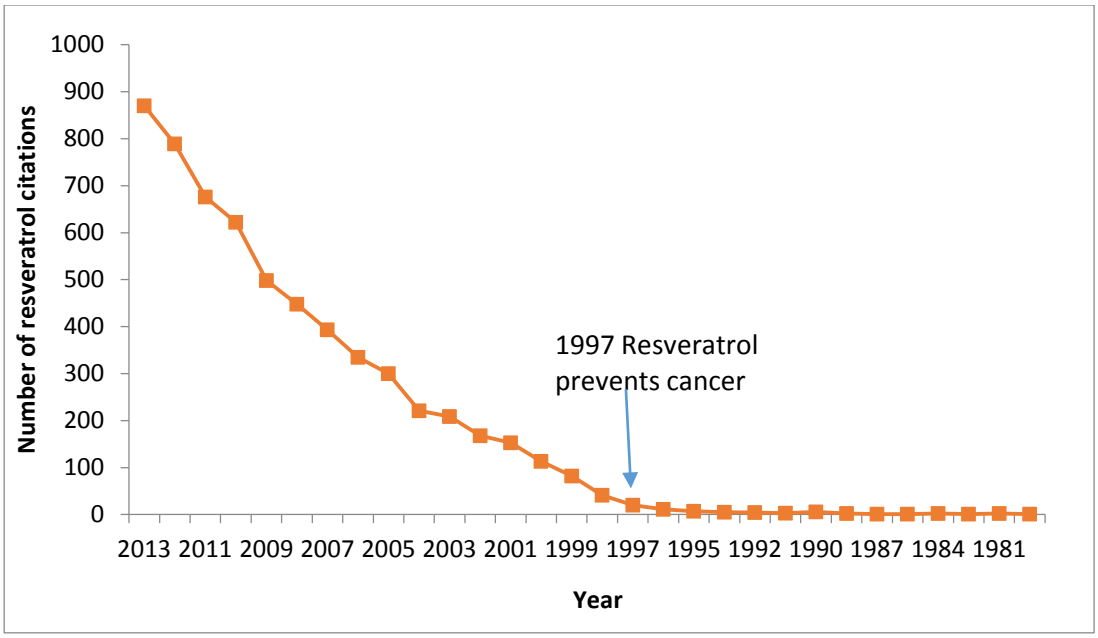

Figure 1.10 Resveratrol citations appearing on Pubmed from 1978 to 2013. The PubMed database was searched using the key word 'resveratrol'.

1.6.1 Molecular targets of resveratrol:

Extensive studies have been conducted to elucidate the mechanism of resveratrol as an anticancer agent. The studies revealed multiple molecular targets, which regulate cell growth, invasion, apoptosis, angiogenesis and metastasis. Resveratrol's direct and indirect targets include tumor suppressors p53 and Rb; cell cycle regulator cyclins, CDKs, p21WAF1, p27KIP and INK and the checkpoint kinases ATM/ATR; transcription factors NFκB, AP-1, c- Jun, and c-Fos; angiogenic and metastatic factors, VEGF and matrix metalloprotease 2/9; cyclooxygenases for inflammation; and apoptotic and survival regulators Bax, Bak, PUMA, Noxa, TRAIL, APAF, survivin, Akt, Bcl2 and Bcl-XL (Athar, Back et al. 2009). In addition to these targets, resveratrol is known to exhibit pro-oxidant activity in cancer cells causing apoptosis (Seve, Chimienti et al. 2005). Resveratrol is an ideal anticancer molecule due to its low toxicity and capacity to target

multiple molecular targets that may collectively promote cancerous cell growth and invasion. Since resveratrol is known to regulate multiple molecular targets and signaling pathways, it is important to elucidate the mechanism by which resveratrol influences these molecular targets. One assumption is that the resveratrol may act as an endogenous signaling molecule, or act through generation of mediators such as reactive oxygen species (ROS), or both (Athar, Back et al. 2009). The biological effects and molecular targets of resveratrol against various tumor cell lines are summarized in **Table 1.1**.

Table 1.1 Effects of resveratrol on various human cancer cell lines. Adapted from (Athar, Back et al. 2009)

Cell Type	Molecular target	Cellular effects	References
Breast cancer T47D MDA-MB-231 MDA-MB-468 MCF-7	p53, PTEN, p27, ROS, NO, QR, p21p70S6K, ppS6RP, Src-Stat3, pAkt, Bcl2, NF-jB, calpain, MMP-9, cyclin D, Cdk4, ribonucleotide reductase, CYP1A1, telomerase	Apoptosis Growth arrest Cell migration	(Lee and Safe 2001, Pozo-Guisado, Alvarez-Barrientos et al. 2002, Pozo-Guisado, Merino et al. 2005, Waite, Sinden et al. 2005, Lanzilli, Fuggetta et al. 2006, Alkhalaf 2007)
Prostate cancer LNCap PC-3 DU145 LAPC-4	Caspases 3/9, p53, p21, p27, Bax, Bak, Bid, Bad, MKP5PI3K, pAKT, cyclins B/D1/E, Cdk1/4, Bcl2, Src-Stat3, ROS	Apoptosis, G0/G1-arrest Proliferation rate, cell viability	(Awad, Burr et al. 2005, Aziz, Nihal et al. 2006, Benitez, Pozo-Guisado et al. 2007, Nonn, Duong et al. 2007)
Colon cancer HT-29 DLD1 HCT116	AMPK, ROS, cathepsin D, caspase-2, cytochrome c, ATF3 Cdk7, p34Cdc2	Apoptosis, lysosome leakage, G2-arrest, Cell growth	(Liang, Tsai et al. 2003, Hwang, Kwak et al. 2007, Trincheri, Nicotra et al. 2007)
Pancreatic cancer	MIC-1, cytochrome c,	Apoptosis	(Mouria, Gukovskaya et al. 2002, Golkar, Ding et al.

Table 1.1 (continued)

CD18 S2-013 panc-1	caspase-3 Src-Stat3, NF-jB	Cell growth	2007)
Leukemia HL-60	NO	Apoptosis, nuclear size, granularity Cell growth	(Quiney, Dauzonne et al. 2004, Stervbo, Vang et al. 2006)
Hepatoma HepG2	NO	Apoptosis, nuclear size, granularity Cell growth	(Stervbo, Vang et al. 2006)
B-cell Lymphoma LY1 LY8 LY18	p27, p53, CD69 BCL6, Myc, pAKT, pp70S6K	Apoptosis, G0/G1-arrest glycolysis	(Faber and Chiles 2006, Faber, Dufort et al. 2006)
Osteosarcoma SJSA1	pERK1/2, pp53(Ser15)	Apoptosis Cell growth	(Alkhalaf 2007)
Acute myeloid leukemia OCIM2 OCI/AML3	IL-1b, NF-jB	S-arrest, apoptosis	(Estrov, Shishodia et al. 2003)
Thyroid cancer PTC FTC	P53, p53(ser15), c-fos, c-jun, p21	Apoptosis	(Shih, Davis et al. 2002)
Gastric adenocarcinomas KATO-III RF-1	PKC, PKCa	G0/G1-arrest, apoptosis DNA synthesis	(Atten, Attar et al. 2001)

1.6.2 Pharmacokinetics of resveratrol:

Nearly all the reports claiming the biologically beneficial effects of resveratrol to date have been generated *in vitro* and in animal models. Thus, it is still unclear if these claims can be translated to humans. At higher doses, protective effects of resveratrol were observed. For example, a daily dose of 40 mg/kg increased the survival of mice with subcutaneous neuroblastomas from 0% to 70% (Chen, Tseng et al. 2004). However, in many *in vivo* studies, no notable chemopreventive effect of resveratrol was observed in animal models. For example, treatment with 1-5 mg/kg daily dose of resveratrol failed to affect the metastasis of breast cancer in mice, despite encouraging *in vitro* results. In one recent study, resveratrol acted as an ant-proliferative agent against ovarian cancer cells in vitro, but failed to exhibit this effect on the same cancerous cells *in vivo (Bove, Lincoln et al. 2002)*. Overall, numerous *in vitro* studies clearly showed promising results, but the drug did not yield consistent results *in vivo*.

The pharmacokinetic data of resveratrol reported in the literature is both confusing and contradicting. The high doses of resveratrol used in animal models (for example 100 ng - 1500 mg/Kg body weight) to achieve pharmacologically relevant concentration in plasma raises many questions about its translational effectiveness in humans. Resveratrol was found to have a short half-life of 8-10 min after oral administration, and was extensively metabolized to both sulfate and glucuronide phase 2 conjugates (Marier, Vachon et al. 2002). In the case of intravenous administration, resveratrol was completely converted to sulfate conjugates within 30 min in humans (Walle, Hsieh et al. 2004). The maximum tolerated dose of resveratrol has not been comprehensively determined; however,

300mg/Kg (body weight) showed no toxicity in rats, but toxic effects related to the kidney have been observed at 1 gram/Kg (body weight) (Crowell, Korytko et al. 2004).

Despite resveratrol's low bioavailability, it was speculated that the *in vivo* efficacy of resveratrol could be attributed to its metabolites. However, when resveratrol-3-sulfate was tested *in vitro* it failed to activate SIRT1 and inhibit cyclooxygenase (Yu, Shin et al. 2003). Another speculation is that the inactive metabolites of resveratrol could act as pool from which the resveratrol can be released into the tissues and stimulate the biological activity; however, no data on such findings have been reported.

Because of the extremely low bioavailability and rapid clearance from the circulation, resveratrol could not be used as a drug. One approach to addressing this problem is to modify resveratrol's structure to create analogs which would be metabolized at a slower rate than resveratrol itself (Greer, Madadi et al. 2014). Another approach is to synthesize potent resveratrol analogs that mimic its effect with improved bioavailability (Aggarwal, Takada et al. 2004). In the following chapters, both of these approaches have been tested.

1.7 Introduction to Combretastatin A4

Microtubules are believed to be one of the most promising targets for cancer chemotherapy since the tubulin interacting agent pacitaxel (**Figure 1.13**) was approved by the FDA for cancer treatment. Since then, the interest in tubulin targeting agents has significantly increased. Between 2007 and 2009, over 25% of the drug molecules that

entered clinical study were tubulin targeting agents (Butler 2008), and almost all of these drug molecules were natural products or analogs thereof.

It is important to evaluate the role of tubulin in the life cycle of the cell in order to understand the mechanism of action of tubulin targeting anti-cancer agents. The cytoskeleton present in the cytoplasm of eukaryotic cells is responsible for the organization of constituents of the cell, maintains cell shape and the movement of the various organelles within the cell. There are three types of filaments or fibers that makeup the cytoskeleton: they are the microfilaments, the intermediate filaments and the microtubules. Microtubules comprise of αβ-tubulin heterodimers and play an important role in cell division, cellular transport, and cell mortality, maintaining cell polarity and cell signaling (Jordan, Hadfield et al. 1998, Zhou and Giannakakou 2005). Microtubule polymerization involves coordinated assembly of αβ-tubulin dimers followed by GTP hydrolysis. Each α and β subunit of the heterodimer has one GTP molecule bound to it; the GTP attached to the α subunit is irreversible, whereas the GTP molecule attached to the β subunit is reversibly hydrolyzed during polymerization (Nogales, Wolf et al. 1998). Compromised or non-coordinated microtubule functioning may lead to apoptosis.

There are mainly three phases of microtubule polymerization

1. Nucleation (an oligomer consisting of 6-12 α-β-tubulin heterodimers is formed)
2. Polymer growth (a protofilament is formed where the GTP binds to αβ-tubulin dimers)

3. Steady-state equilibrium (addition and dissociation of tubulin subunits is balanced)

Treadmilling and dynamic instability are the two types of microtubule dynamics observed. In the treadmilling dynamics the subunits from the minus end of the microtubule flow to the plus end; this dynamics doesn't change the average length of the microtubules. On the other hand, dynamic instability is associated with alternative growth and shortening microtubule ends (Mitchison and Kirschner 1984). The transition from a growing phase to a shortening phase is termed as "catastrophe" and the transition from a shortening phase to a growing phase as "rescue", **Figure 1.13** illustrates the necessity for GTP hydrolysis for switching between catastrophe and rescue. Microtubules are stabilized and destabilized by microtubule-associated proteins (MAP). MAPs such as plus and tracking proteins (TIP) interact with the microtubule ends to regulate the microtubule dynamics (Akhmanova and Steinmetz 2008). Since the microtubule dynamics play an important role in mitosis and basic cellular functions, microtubule targeting drugs are used in the treatment of various forms of cancer (Jordan and Wilson 2004, Singh, Rathinasamy et al. 2008).

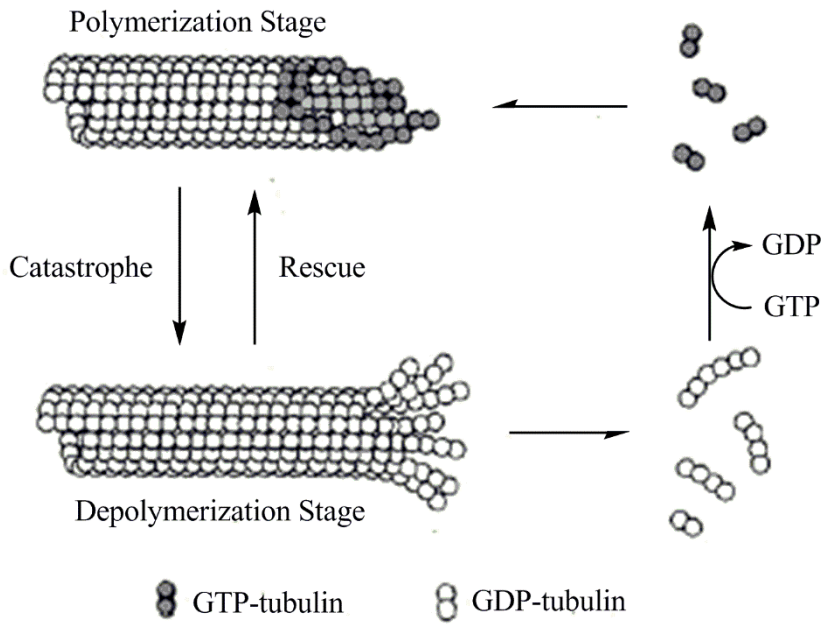

Figure 1.11 Microtubule dynamic instability, where the coexistence of polymerization and depolymerizing microtubules are imperative for dynamic stability.

Anticancer agents that have polymerizing and depolymerizing effects on tubulin assembly are known as Microtubule-interfering Agents (MIA). Both polymerization and depolymerization impairs the proper function of microtubules and stagnates the cell cycle at G2/M phase leading to apoptosis (Li, Wu et al. 2009). Anticancer drugs such as colchicine, vinblastine and vincristine act by depolymerizing mechanism, whereas drugs such as paclitaxel and docetaxel act through a polymerizing effect. There are many tubulin binding sites for the depolymerizing agents, such as the colchicine and the vinblastine binding sites (Ravelli, Gigant et al. 2004, Gigant, Wang et al. 2005). Additionally, when depolymerization agents such as estramustine and LY290181 (**Figure 1.12**) were treated with tubulin, they did not compete for the colchicine and vinblastine binding sites. Also, Chakraborti *et al.* using fluorescence spectroscopy, demonstrated that curcumin binds to tubulin at a site which is close to the vinblastine binding site

(Chakraborti, Das et al. 2011). This experiment suggests that each of these depolymerization agents have distinct binding site (Singh, Rathinasamy et al. 2008).

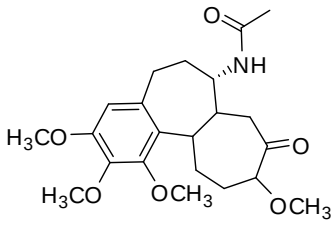

(A) Colchicine

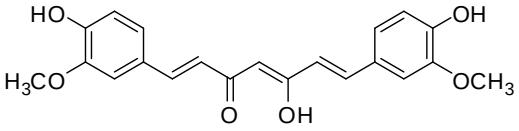

(B) Curcuminl

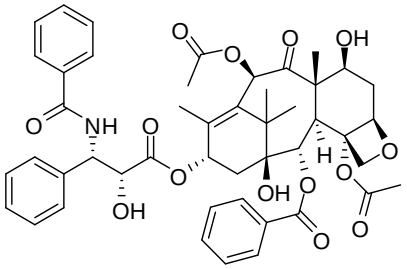

(C) Pacitaxel

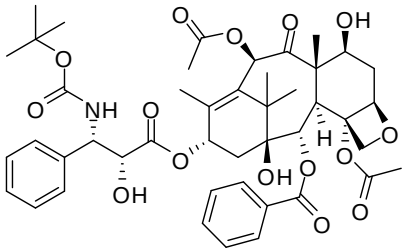

(D) Docetaxel

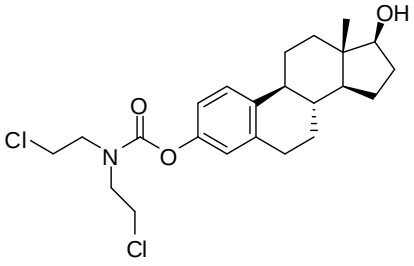

(E) Estramustine

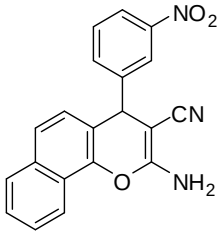

(F) LY290181

Figure 1.12 Structures of polymerizing and depolymerizing agents on tubulin assembly.

Microtubule targeting agents act as anticancer agents by causing the cells to arrest at the G2/M stage of the cell cycle promoting apoptosis, and/or by their vascular disrupting action. However, the mechanism by which they act is poorly understood. The relationship between mitotic block and apoptosis caused by 2',3,4,4',5-pentamethoxy-*trans*-stilbene (PMS) (**Figure 1.13**) was studied by Li and co-workers. The experiments suggested that

hyper phosphorylation of CDC2 or JNK by Bcl-2/Bcl-xL and activation of Bim by JNK could be a link between mitotic block and apoptosis (Li, Wu et al. 2009). Also, caspase-8 activation was observed during paclitaxel-induced apoptosis (Goncalves, Braguer et al. 2000).

Interestingly, there is also a strong correlation between microtubule targeting agents and their vascular disruption properties (Mason, Zhao et al. 2011). Anticancer agents that target the tumor vasculature are known as vascular-targeting agents (VTAs) and can be divided into two categories. They are

(a) Vascular disrupting agents (VDAs). Example: Combretastatin A4.

(b) Angiogenesis inhibiting agents (AIA). Example: Bevacizumab.

VDAs like combretastatin A4 influence tubulin polymerization by damaging the proliferating endothelial cells of the cancer vasculature, thereby decreasing blood flow to the tumor cells leading to cell death. VDAs like combretastatin A4 also have potential curative activities in retinal and choroidal neovascularization related diseases, since angiogenesis plays a key role in these disease conditions (Nambu, Nambu et al. 2003, Jockovich, Suarez et al. 2007).

A total of seventeen combretastatin compounds have been isolated from the South African bushwillow tree *Combretum caffrum* by Pettit and co-workers (Pettit, Singh et al. 1995). Among these compounds, a *cis*-stilbene: Combretastatin A4 (3'-hydroxy-3,4,4',5-tetramethoxy-cis-stilbene; CA-4; **Figure 1.13**), has emerged as a potent anti-cancer agent with promising anti-mitotic and anti-angiogenic activity (Tron, Pirali et al. 2006). CA4 functions as a microtubule targeting agent, interfering with microtubule dynamics and

perturbation of the mitotic cycle. Moreover, CA4 selectively inhibits the formation of new blood vessels in cancerous cells, sparing the normal cell population (Thorpe 2004).

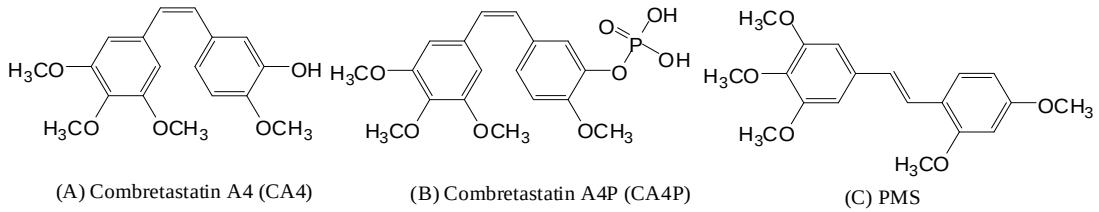

Figure 1.13 Structures of Combretastatin A4 (CA4), CA4P and PMS.

CA4 is well known anticancer agent for inhibition of tubulin polymerization *in vitro*. CA4 binds to the β-tubulin at the colchicine binding site, promoting the disturbance of the dynamic equilibrium of microtubule formation (Mikstacka, Stefanski et al. 2013). Also, CA4 exerts its antitumor affects against multi-drug resistant (MDR) cancer cells (Chaudhary, Pandeya et al. 2007). However, CA4 itself cannot be used as a drug because of its poor water solubility leading to low bioavailability, and due to its chemical instability, since it forms the thermodynamically more stable and less potent *trans* CA4 (Hsieh, Liou et al. 2005) isomer. The low bioavailability of CA4 was addressed by preparing the water soluble phosphate salt (disodium CA-4-3-O-phosphate) of CA4 (CA4P). Currently, CA4P (**Figure 1.13**) has been moved into phase III clinical trial by the pharmaceutical company OXiGENE for the treatment of anaplastic thyroid cancer (Siemann, Chaplin et al. 2009). Another approach utilized for improving the bioavailability of CA4 was to prepare nitrothiophene ether-linked conjugates of CA4, which could function as bioreductively activated prodrugs (Thomson, Naylor et al. 2006).

Also, formulations that employ nanoparticles to selectively deliver CA4 and improve its bioavailability have also been reported (Calligaris, Verdier-Pinard et al. 2010).

The chemical instability (isomerization) of CA4 has been addressed by designing and synthesizing a series of *cis*-constrained derivatives of CA4. Extensive studies have been conducted to stabilize CA4 by replacing the double bond bridge with heterocyclic ring systems such as β-lactam, azetidone, thiazoles, tetrazoles, imidazoles, pyrazoles, oxazolones, triazoles, and furanones (Shirai, Takayama et al. 1998, Tron, Pagliai et al. 2005, Carr, Greene et al. 2010, Beale, Bond et al. 2012, Banimustafa, Kheirollahi et al. 2013, Mikstacka, Stefanski et al. 2013, Demchuk, Samet et al. 2014).

Our approach is to design and synthesize triazole modified CA4 analogues that are more water soluble and also incapable of undergoing *cis-trans* isomerization of CA4.

Copyright © Nikhil Reddy Madadi 2014

Chapter 2

Synthesis of resveratrol analogues as anti-cancer agents

2.1 Previous SAR studies on resveratrol analogues

Resveratrol binds with multiple molecular targets *in vitro*, and exhibits cytotoxic effects against breast, skin, gastric, colon, esophageal, prostate, and pancreatic cancer cells, and leukemia cells (Jang, Cai et al. 1997, Aggarwal, Bhardwaj et al. 2004). However, resveratrol has some limitations which preclude its use in cancer treatment, and it cannot be used as an antitumor drug due to its photosensitivity and metabolic instability (Goldberg, Ng et al. 1995). Literature results indicate that the *in vivo* effectiveness of resveratrol in animal models is limited by its poor systemic bioavailability (Athar, Back et al. 2009). Thus, there is a need for the design and synthesis of novel resveratrol analogs that retain the potent anti-cancer agents of the parent compound, have good chemical and metabolic stability, and are devoid of photosensitivity problems.

Extensive structure activity relationship (SAR) studies on the resveratrol molecule for its anticancer activity and chemical/metabolic stability have been conducted on synthetically prepared derivatives and natural products which resemble resveratrol. The studies revealed that maintaining the stilbene skeleton is necessary for good metabolic stability and for retaining resveratrol's medicinal properties. Also, replacing the extensively metabolized hydroxyl groups with methoxyl groups improves resveratrol's bioavailability.

Wang and co-workers compared the anticancer effects of resveratrol and its natural derivatives pterostilbene, *trans*-3,5,4’ -trimethoxy-stilbene, pinostilbene and desoxyrhapontigenin against human prostate cancer cell line LNCaP (**Figure 2.1**). They reported that *trans*-3,5,4’ -trimethoxy-stilbene was the most effective compound among resveratrol and its natural derivatives, causing G2/M blockage in the cell cycle leading to apoptosis (Wang, Schoene et al. 2010).

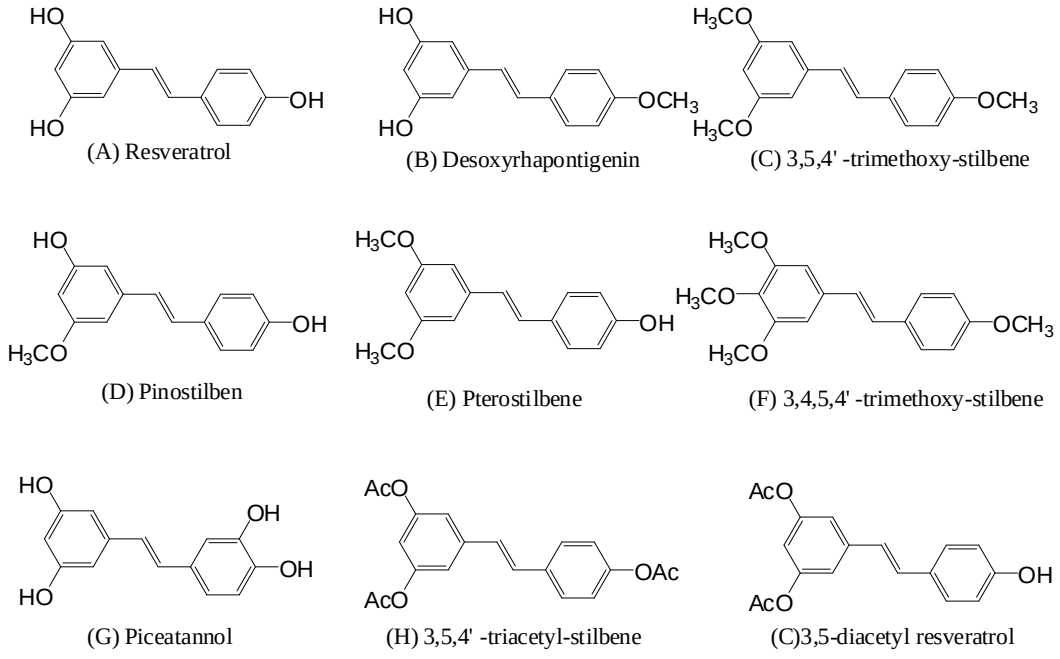

Figure 2.1 Structures of resveratrol and its O-methylated derivatives.

Chen and co-workers synthesized and evaluated a series of methoxylated resveratrol derivatives for their anti-cancer properties against three different human cancer cell lines, i.e. K562, HT29, and HePG2. They reported that *trans*-3,5,4’ -trimethoxy-stilbene

(TMR) and *trans*-3,4,5,4’ -trimethoxy-stilbene (**Figure 2.1**) were the most effective anti-cancer agents among the synthesized analogs and showed better cytotoxicity compared to resveratrol itself. SAR analysis revealed that methoxy substitutions at positions 3, 4, and 5 on the A ring and at position 4’ of the B ring promoted cytotoxicity, and that incorporation of halogeno substituents such as bromo, chloro and fluoro, or nitro groups into the B ring was detrimental to anticancer activity (Chen, Hu et al. 2013).

Dias et al. evaluated resveratrol, *trans*-3,5,4’ –trimethoxystilbene (TMR), piceatannol, pterostilbene, *trans*-3,5-diacetyl-4’ hydroxyl stilbene, and *trans*-3,5,4’-triacetylstilbene, and characterized their effects on PCa cells in vitro using a cell proliferation assay. Also, they compared the chemopreventative effects of oral resveratrol, *trans*-3,5,4’ –trimethoxystilbene, piceatannol in LNCaP-Luc xenografts. Among all these stilbenes examined, *trans*-3,5,4’ –trimethoxystilbene was the most potent in inhibiting cell proliferation, and its permeability into the tumor tissues was the highest (Dias, Li et al. 2013).

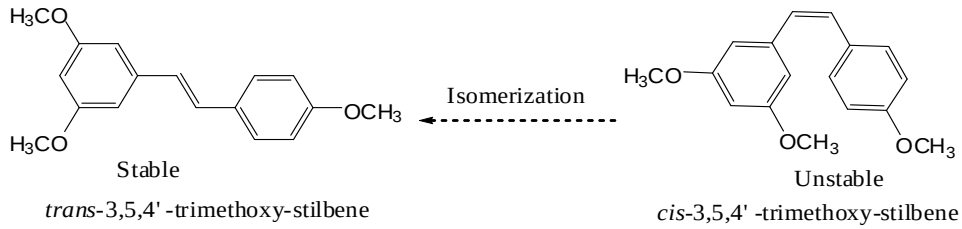

Figure 2.2 Isomerization of *cis*-3,5,4’-trimethoxystilbene to *trans*-3,5,4’-trimethoxystilbene.

Paul et al. compared the anticancer activity of *trans*-3,5,4'-trimethoxystilbene with *cis*-3,5,4'-trimethoxystilbene against the colon cancer cell lines HT-29 and Caco-2. Also, *in vivo* studies using HT-29 xenografts in immunodeficient mice were conducted with both these isomers. Tumor volume was significantly lowered in groups of mice when *trans*-3,5,4'-trimethoxystilbene was used compared to *cis*-3,5,4'-trimethoxystilbene, Also *cis*-3,5,4'-trimethoxystilbene was found to be chemically unstable and isomerized to *trans*-3,5,4'-trimethoxystilbene in solution (Paul, Mizuno et al. 2010).

From these studies, it is evident that *trans*-3,5,4'-trimethoxystilbene (TMR) is the most potent and stable analog of resveratrol, and has better bioavailability than resveratrol. *Trans*-3,5,4'-trimethoxy-stilbene is a natural resveratrol analogue extracted from the plant species *Pterobolium hexapetallum* (Aggarwal, Bhardwaj et al. 2004) and the molecule has been reported to have anticancer and antiangiogenic activities (Belleri, Ribatti et al. 2005). The trimethoxylated substitution pattern on *trans*-3,5,4'-trimethoxystilbene molecule might improve metabolic stability and intestinal absorption. Moreover, conversion of the phenolic substituents to methoxy substituents increases the lipophilicity and cell membrane permeability properties of the molecule and enhances bioavailability.

2.2 Synthesis of *(E)*-stilbenes as resveratrol analogues

Based on the structure-activity relationship analysis reported previously, it is evident that O-methylation of resveratrol leads to an enhanced cytotoxic activity. In our continuing

quest for improving the potencies of our newly identified lead anti-cancer agents, we have synthesized a wide range of such (*E)*-stilbene resveratrol analogs.

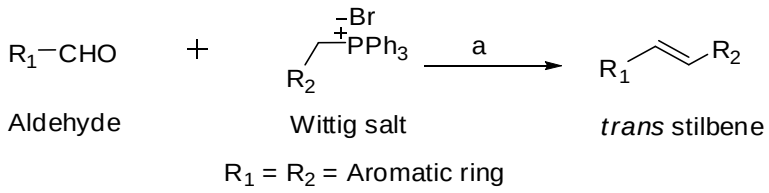

Scheme 2.1 Synthesis of *(E)*-stilbenes as resveratrol analogues. Reagents and conditions: (a) 5% NaOMe, MeOH, reflux.

The general procedure for the synthesis of *trans* 2,3-disubstituted stilbenes is illustrated in **Scheme 2.1**. *Trans* 2,3-disubstituted stilbenes were synthesized by reacting substituted benzyl carbaldehydes (1 mmol) with an appropriately substituted benzyl Wittig salt (1.2 mmol) in 5% NaOMe in methanol. The reaction mixture was stirred at room temperature for about 2-3 hours for the reaction to come to completion and the final product crashed out of the solution. The resulting precipitate was filtered, washed with methanol, then water and dried to yield the desired compound in yields ranging from 60-75% (Scheme **2.1**). If necessary, further purification can be carried out by flash column chromatography. The minor *cis*-stilbene product could be separated during the filtration and methanol wash. A total of seventy four *trans* stilbenes were synthesized via this general procedure and their structures are presented in **Table 2.1**.

Table 2.1: Structures of the synthesized *trans*-stilbenes and the starting materials (benzyl carbaldehyde and Wittig salt) used.

Table 2.1 (Continued)

	Aldehyde	Wittig salt	Stilbene
1.	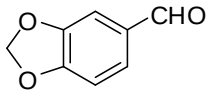	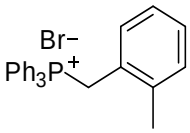	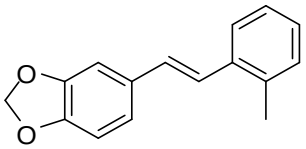 ST-188
2.	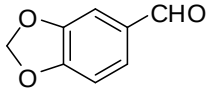	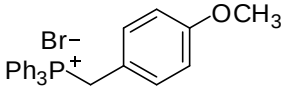	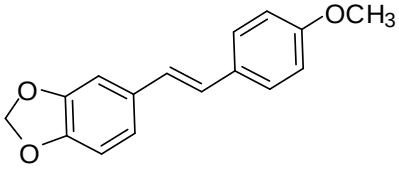 ST-186
3.	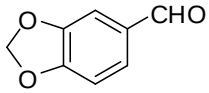	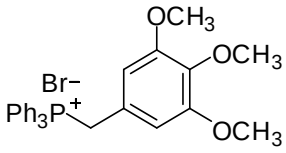	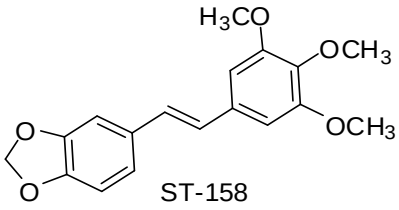 ST-158
4.	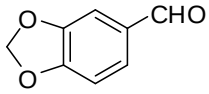	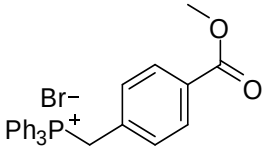	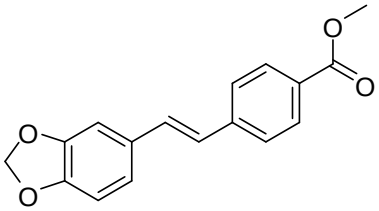 ST- 190
5.	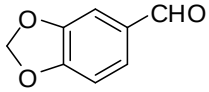	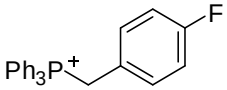	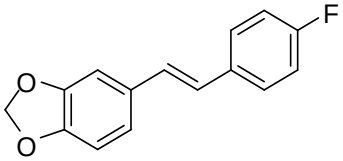 ST-191
6.	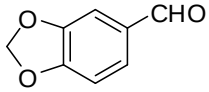	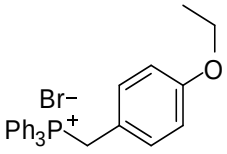	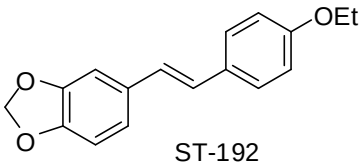 ST-192

Table 2.1 (Continued)

7.	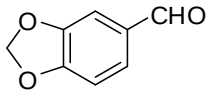	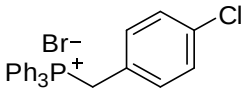	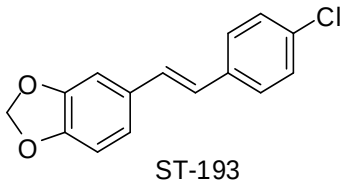 ST-193
8.	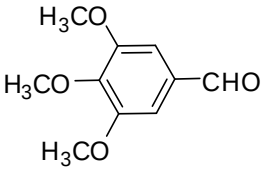	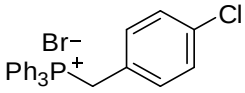	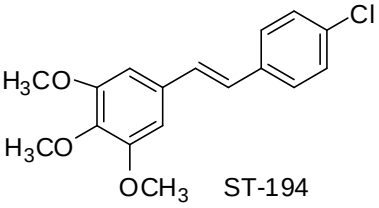 ST-194
9.	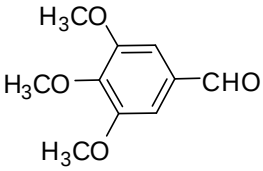	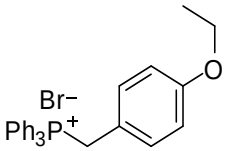	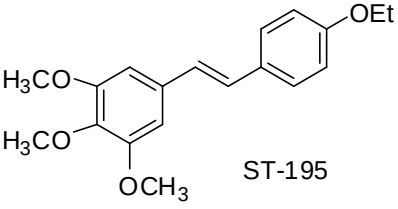 ST-195
10.	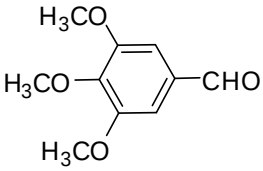	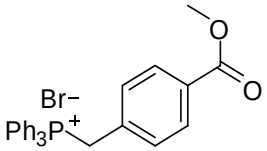	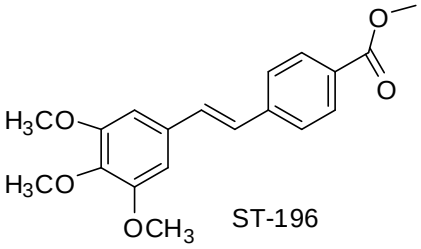 ST-196
11.	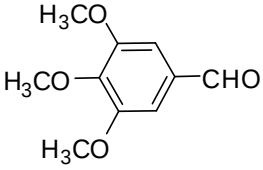	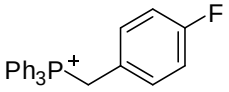	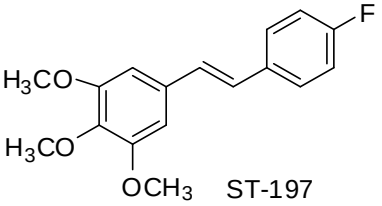 ST-197
12.	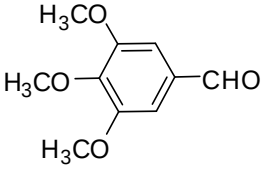	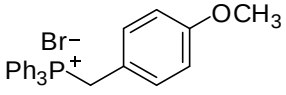	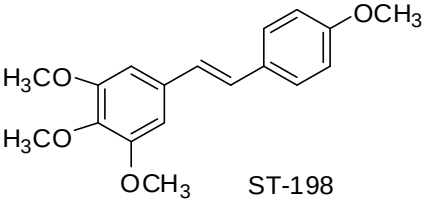 ST-198

Table 2.1 (Continued)

13.	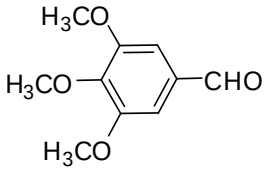	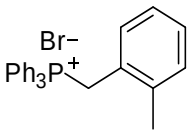	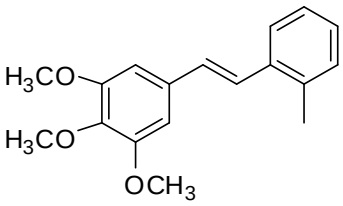 ST-200
14.	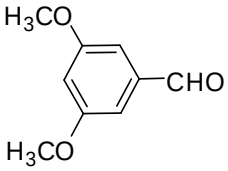	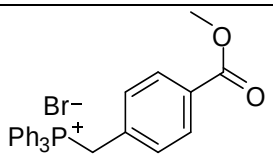	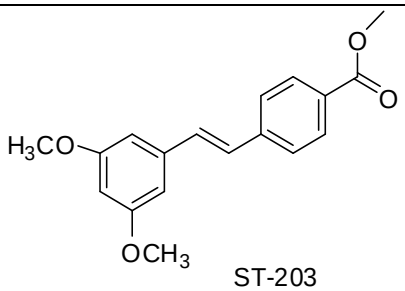 ST-203
15.	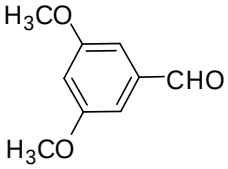	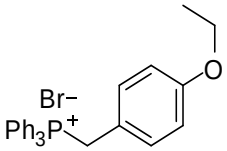	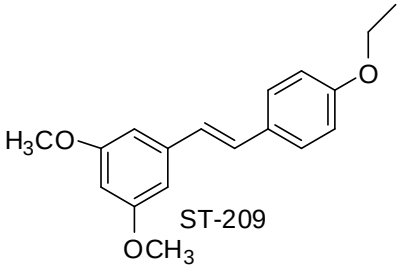 ST-209
16.	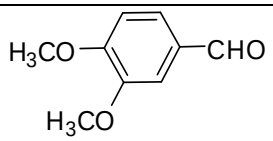	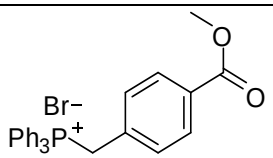	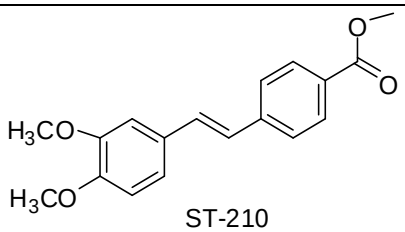 ST-210
17.	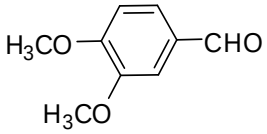	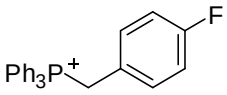	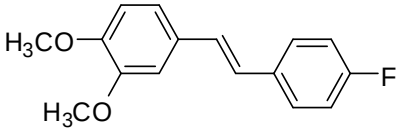 ST-211

Table 2.1 (Continued)

18.	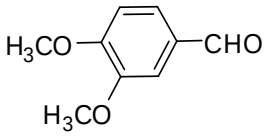	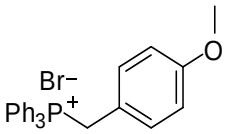	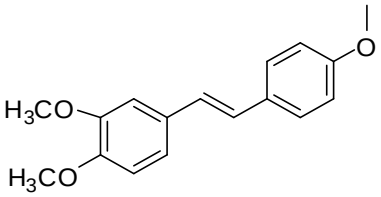 ST-212
19.	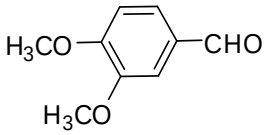	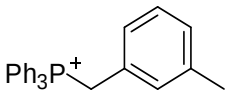	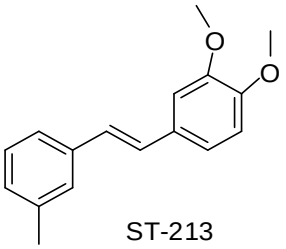 ST-213
20.	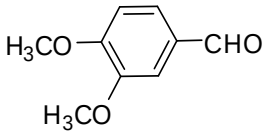	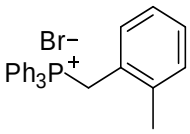	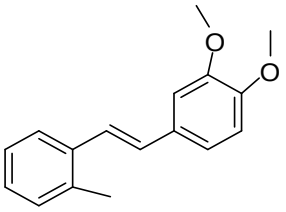 ST-214
21.	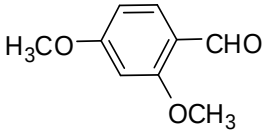	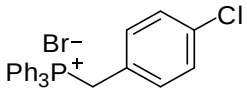	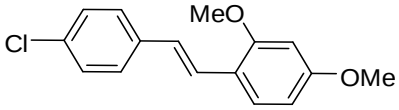 ST-219
22.	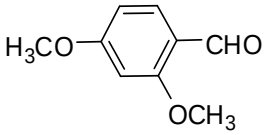	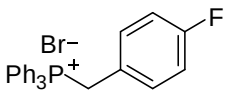	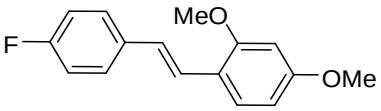 ST-222
23.	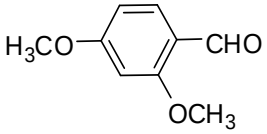	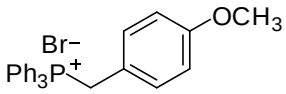	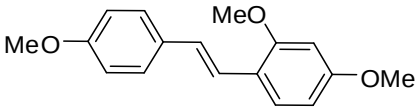 ST-223
24.	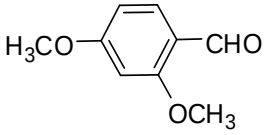	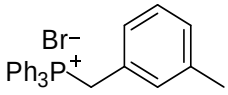	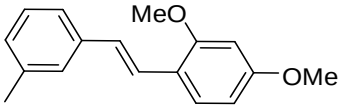 ST-224

Table 2.1 (Continued)

25.	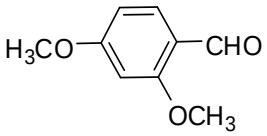	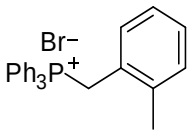	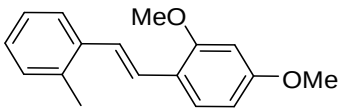 ST-225
26.	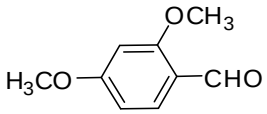	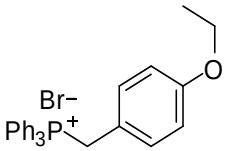	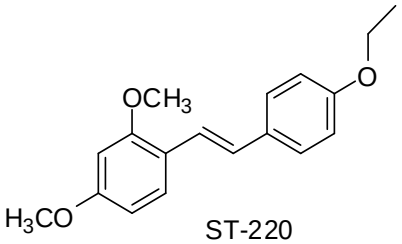 ST-220
27.	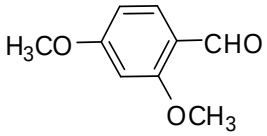	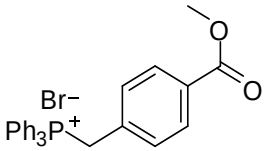	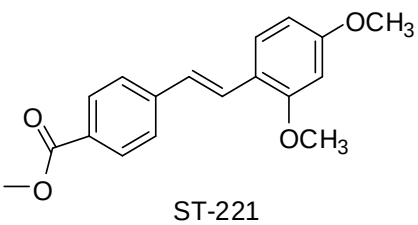 ST-221
28.	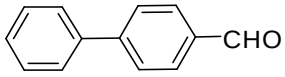	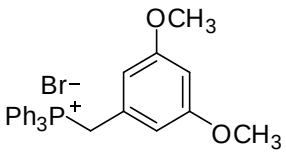	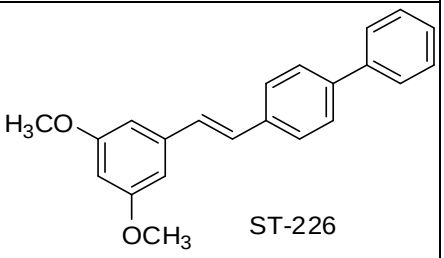 ST-226
29.	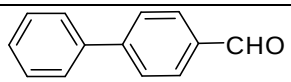	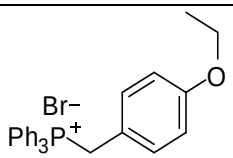	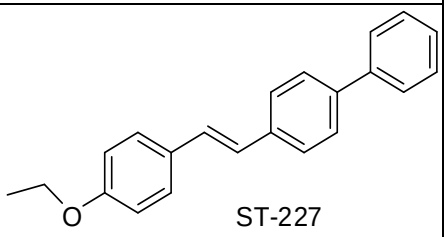 ST-227
30.	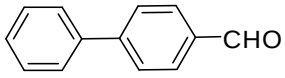	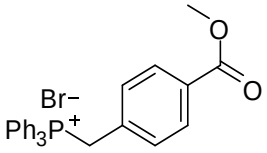	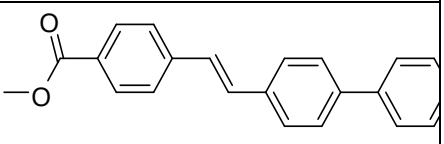 ST-228

Table 2.1 (Continued)

31.	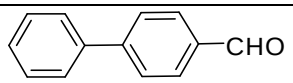	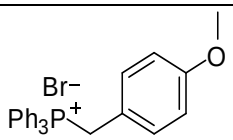	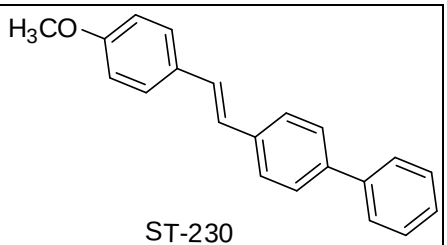 ST-230
32.	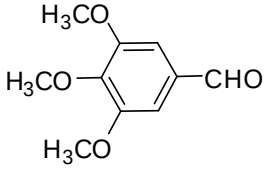	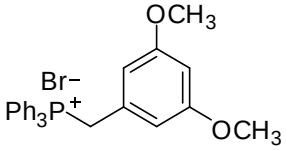	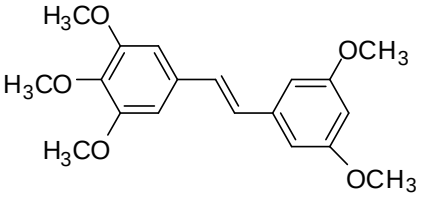 ST-233
33.	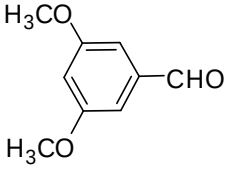	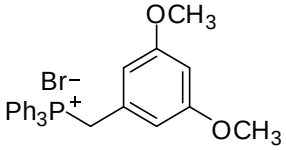	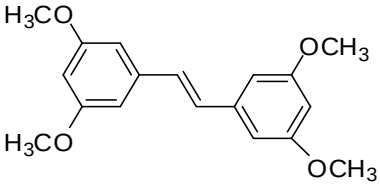 ST-234
34.	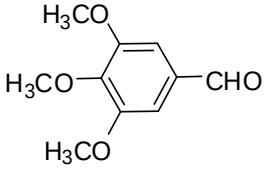	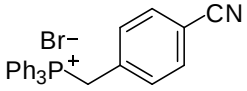	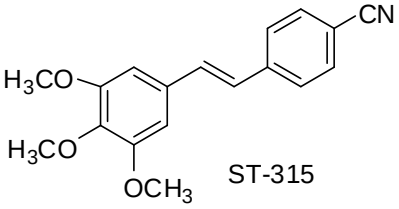 ST-315
35.	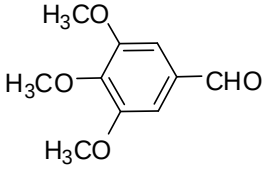	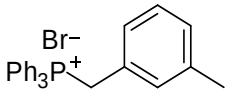	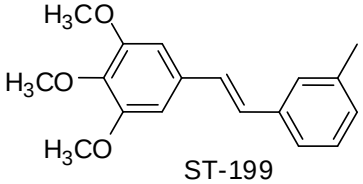 ST-199
36.	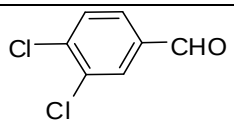	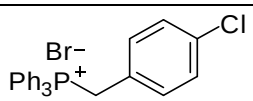	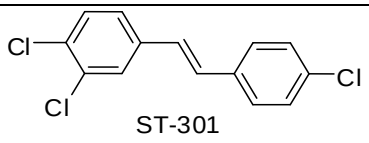 ST-301

Table 2.1 (Continued)

37.	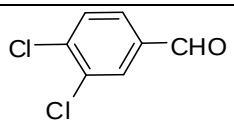	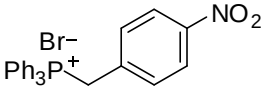	ST-302
38.	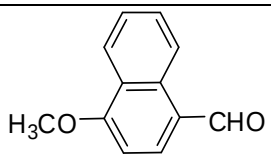	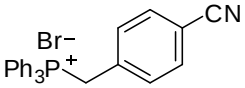	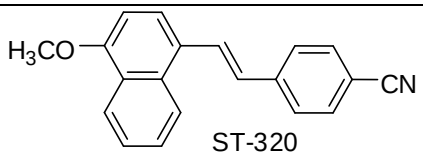 ST-320
39.	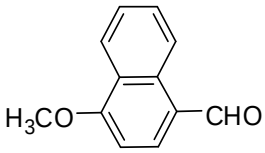	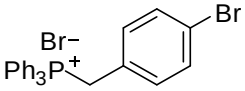	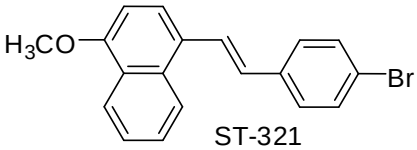 ST-321
40.	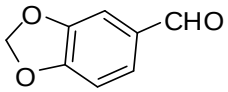	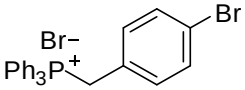	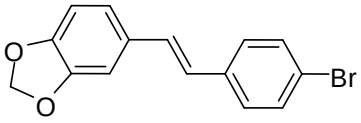 ST-312
41.	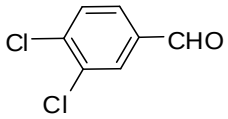	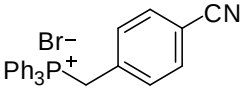	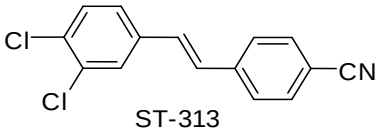 ST-313
42.	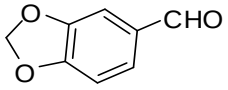	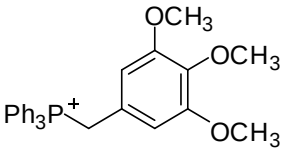	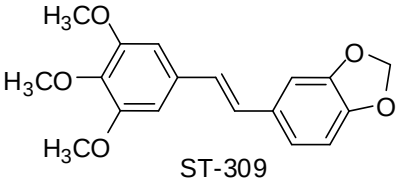 ST-309
43.	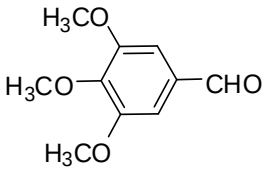	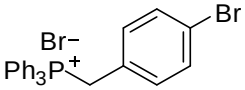	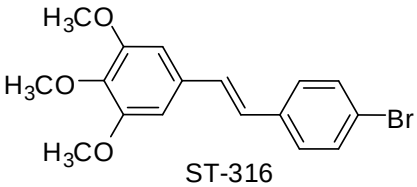 ST-316
44.	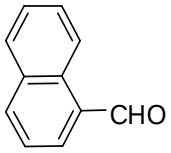	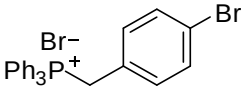	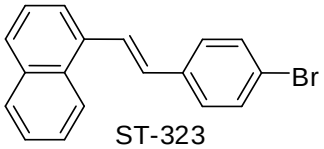 ST-323

Table 2.1 (Continued)

45.	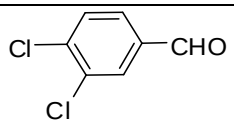	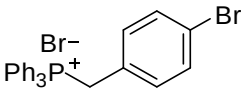	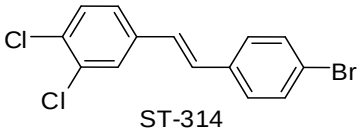 ST-314
46.	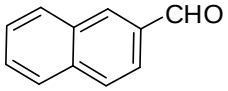	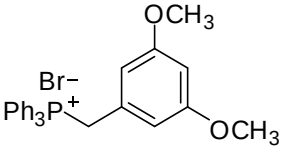	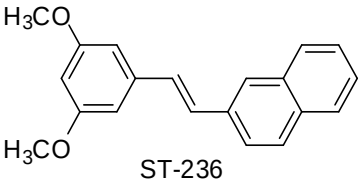 ST-236
47.	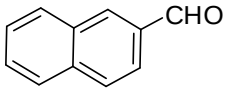	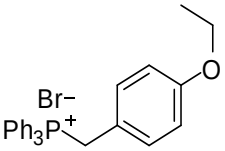	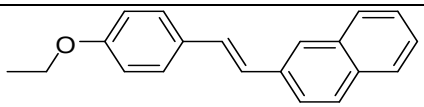 ST-237
48.	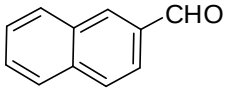	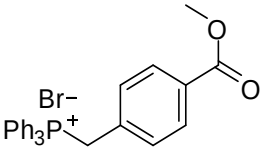	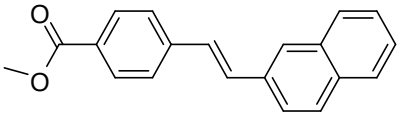 ST-238
49.	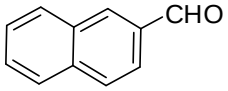	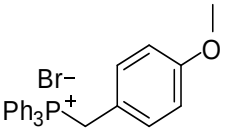	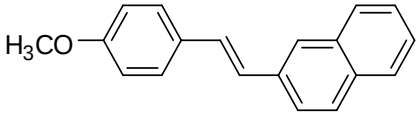 ST-239
50.	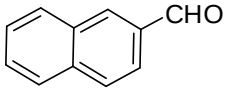	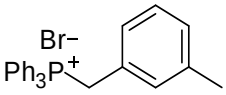	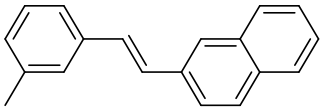 ST-240
51.	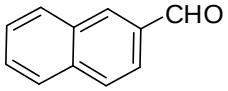	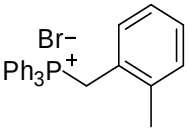	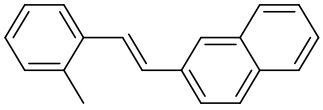 ST-241
52.	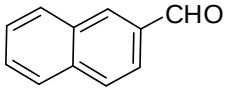	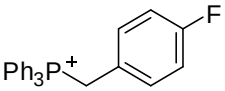	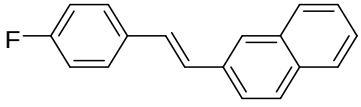 ST-242

Table 2.1 (Continued)

53.	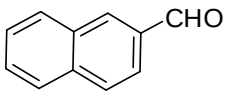	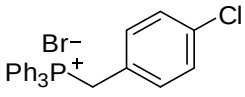	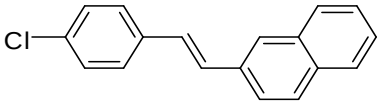 ST-243
54.	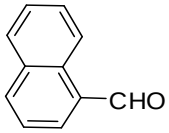	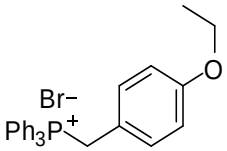	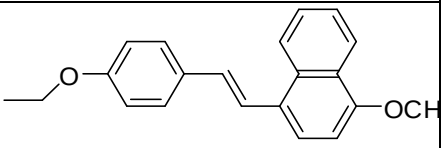 ST-245
55.	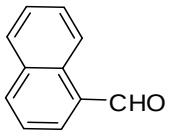	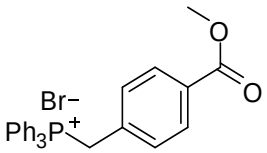	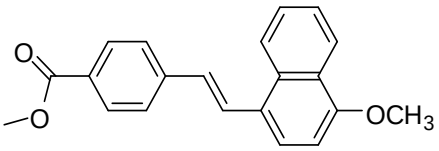 ST-246
56.	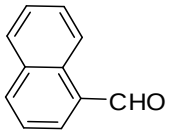	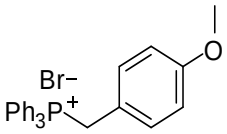	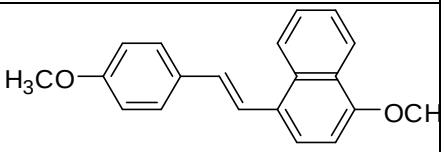 ST-247
57.	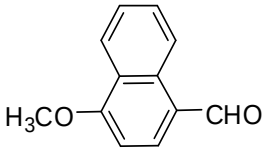	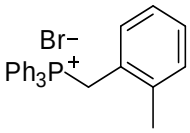	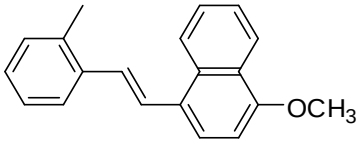 ST-249
58.	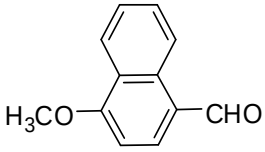	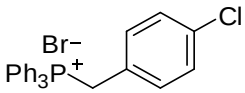	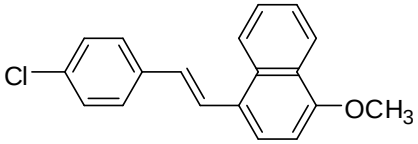 ST-251
59.	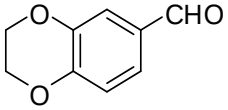	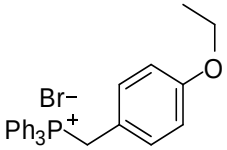	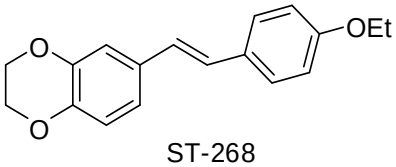 ST-268

Table 2.1 (Continued)

60.	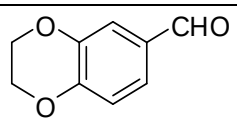	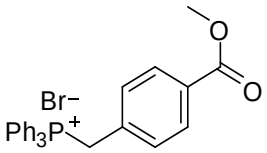	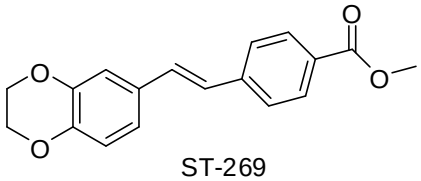 ST-269
61.	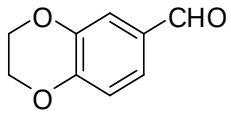	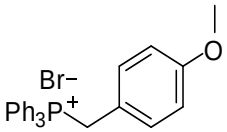	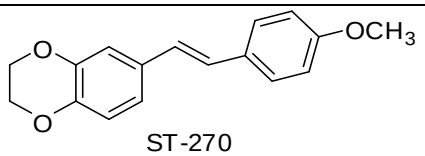 ST-270
62.	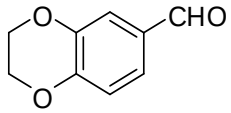	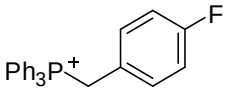	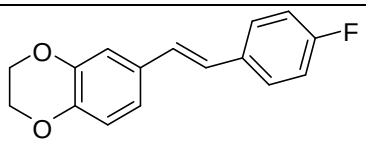 ST-273
63.	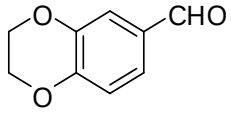	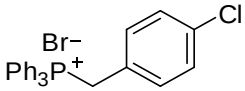	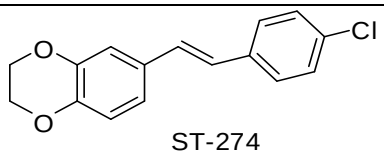 ST-274
64.	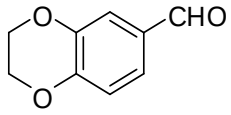	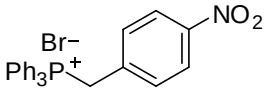	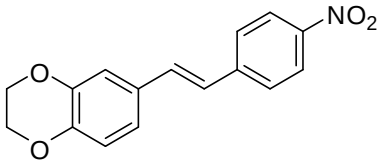 ST-275
65.	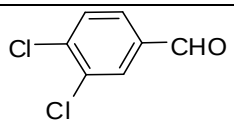	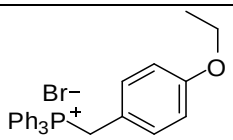	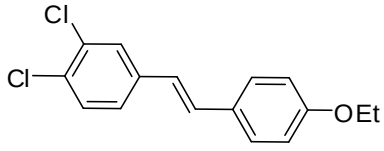 ST-295
66.	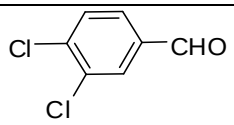	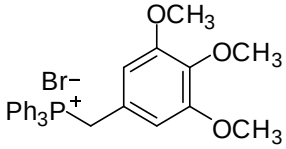	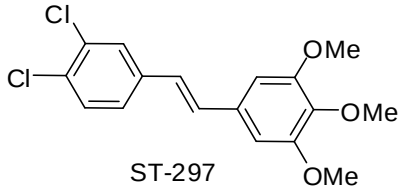 ST-297

Table 2.1 (Continued)

67.	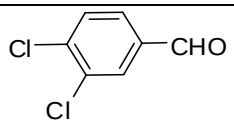	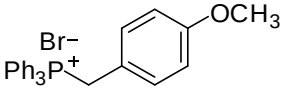	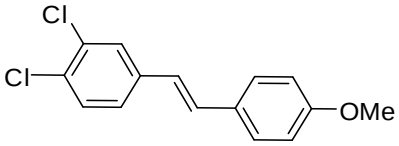 ST-294
68.	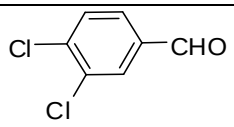	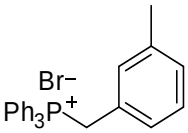	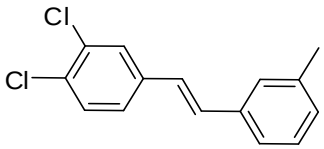 ST-298
69.	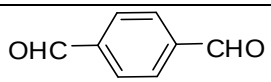	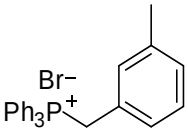	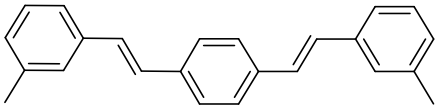 ST-283
70.	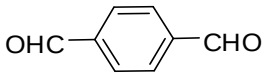	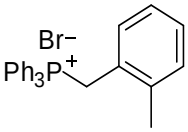	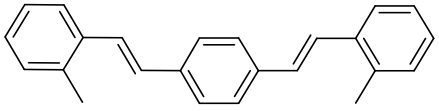 ST-284
71.	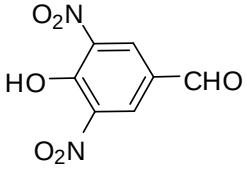	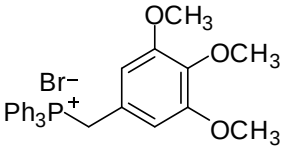	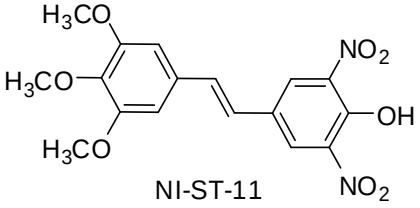 NI-ST-11
72.	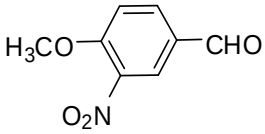	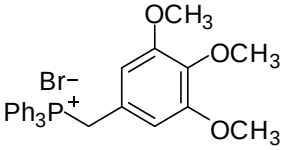	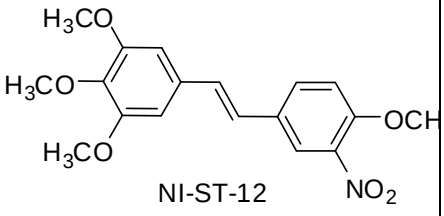 NI-ST-12

Table 2.1 (Continued)

73.	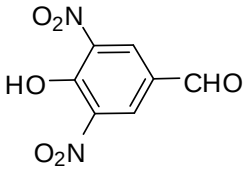	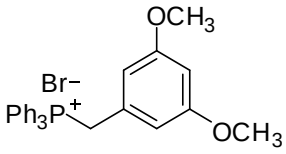	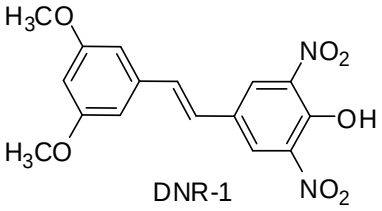 DNR-1
74.	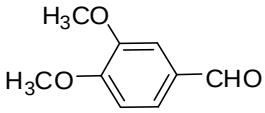	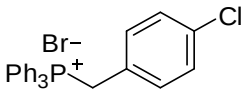	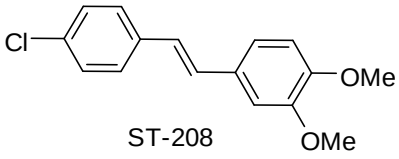 ST-208

2.2.1 Analytical data for the synthesized *trans*-stilbene analogues

ST-196 : ^{1}H NMR (400 MHz, DMSO-d_6): δ 3.68 (s, 3H, -OCH_3), 3.84 (s, 6H, -OCH_3), 3.85 (s, 3H, -OCH_3), 6.98 (s, 2H, -ArH), 7.34 (d, *J* =7.2 Hz, 2H, ArH), 7.72 (d, *J* =8.4 Hz, 2H, ArH), 7.968 (d, *J* =8 Hz, 2H, ArH) ppm. ^{13}C NMR (100 MHz, DMSO-d_6): 52.4, 56.3, 60.5, 60.5, 104.76, 126.8, 127.0, 128.4, 130.1, 131.9, 132.6, 142.4, 153.5, 166.4 ppm.

ST-192 : ^{1}H NMR (400 MHz, DMSO-d_6): δ1.32 (t, *J* =12.8 Hz, 3H, -CH_3), 4.03 (d, *J* =6.8 Hz, 2H, -CH_2), 6.02 (s, 2H, -CH_2), 6.91 (d, *J* =6.8 Hz, 3H, ArH), 6.96-7.02 (m, 3H, ArH), 7.22 (s,1H, ArH), 7.47 (d, *J* =7.6 Hz, 2H, ArH) ppm. ^{13}C NMR (100 MHz, DMSO-d_6): 15.0, 63.4, 101.4, 105.5, 108.7, 115.0, 121.5, 126.2, 126.7, 127.9, 130.1, 132.4, 147.0, 148.2, 158.4 ppm.

ST-191 : ^{1}H NMR (400 MHz, DMSO-d_6): δ6.04 (s, 2H, -CH_2), 6.92 (d, *J* =8 Hz, 1H, ArH),), 7.02 (d, *J* =9.2 Hz, 1H, ArH), 7.12 (s,2H, ArH), 7.18 (t, *J* =17.6 Hz, 2H, ArH), 7.26 (d, *J* =1.2 Hz, 1H, ArH), 7.06-7.57 (m, 2H, ArH) ppm. ^{13}C NMR (100 MHz,

DMSO-d_6): 101.5, 105.6, 108.8, 115.8, 116.0, 122.0, 125.9, 128.4, 128.5, 128.5, 131.9, 134.3, 147.3, 148.3 ppm.

ST-193 : ^{1}H NMR (400 MHz, DMSO-d_6): δ6.04 (s, 2H, -CH_2), 6.92 (d, *J* =7.6 Hz, 1H, ArH),), 7.04 (d, *J* =9.2 Hz, 1H, ArH), 7.12 (d, *J* =16.4 Hz, 1H, ArH), 7.21 (d, *J* =16.4 Hz, 1H, ArH), 7.27 (d, *J* =1.2 Hz, 1H, ArH), 7.41 (d, *J* =8.8 Hz, 2H, ArH), 7.57 (d, *J* =8.8 Hz, 2H, ArH) ppm. ^{13}C NMR (100 MHz, DMSO-d_6): 101.6, 105.8, 108.8, 122.3, 125.7, 128.2, 129.0, 129.5, 131.7, 131.9, 136.6, 147.5, 148.3 ppm.

ST-188 : ^{1}H NMR (400 MHz, DMSO-d_6): δ 2.38 (s,3H, CH_3), 6.04 (s, 2H, -CH_2), 6.92 (d, *J* =8 Hz, 1H, ArH),), 7.05-7.01 (m, 2H, ArH), 7.14-7.19 (m, 3H, ArH), 7.28 (d, *J* =16.0 Hz, 1H, ArH), 7.33 (d, *J* =1.6 Hz, 1H, ArH), 7.61 (d, *J* =6.8 Hz, 1H, ArH) ppm. ^{13}C NMR (100 MHz, DMSO-d_6): 19.9, 101.5, 106.0, 108.7, 122.1, 124.6, 125.2, 126.5, 127.6, 129.8, 130.7, 132.3, 135.7, 136.4, 147.3, 148.3 ppm.

ST-186: ^{1}H NMR (400 MHz, DMSO-d_6): δ 3.76 (s, 3H, -OCH_3), 6.02 (s, 2H, -ArH), 6.88-6.93 (m, 3H, ArH), 6.97-7.04 (m, 3H, ArH), 7.23 (s, 1H, -ArH), 7.49 (d, *J* =8.8 Hz, 2H, ArH) ppm. ^{13}C NMR (100 MHz, DMSO-d_6): 55.5, 55.6, 101.4, 105.5, 108.8, 114.5, 121.6, 126.3, 126.7, 127.9, 130.3, 132.3, 147.0, 148.2, 159.1 ppm.

ST-198 : ^{1}H NMR (400 MHz, DMSO-d_6): δ 3.64 (s, 3H, -OCH_3), 3.74 (s, 3H, -OCH_3), 3.79 (s, 6H, -OCH_3), 6.85 (s, 2H, -ArH), 6.91 (d, *J* =8.8 Hz, 2H, ArH), 6.97 (d, *J* =16.4 Hz, 1H, ArH), 7.11 (d, *J* =16.4 Hz, 1H, ArH), 7.11 (d, *J* =8.8 Hz, 1H, ArH) ppm. ^{13}C NMR (100 MHz, DMSO-d_6): 55.56, 56.29, 60.50, 103.99, 114.64, 126.73, 127.87, 128.03, 130.20, 133.56, 137.42, 153.48, 159.29 ppm.

ST-194 : ^{1}H NMR (400 MHz, DMSO-d_6): δ 3.67 (s, 3H, -OCH_3), 3.83 (s, 6H, -OCH_3), 6.93 (s, 2H, -ArH), 6.93 (s, 2H, -ArH), 7.21 (s, 2H, -ArH), 7.43 (d, *J* =8.4 Hz, 2H, ArH), 7.60 (d, *J* =8.4 Hz, 1H, ArH) ppm. ^{13}C NMR (100 MHz, DMSO-d_6): 56.3, 60.5, 104.4, 126.8, 128.3, 129.1, 129.9, 132.1, 132.9, 136.5, 137.9, 153.5 ppm.

ST-190 : ^{1}H NMR (400 MHz, DMSO-d_6): δ 3.84 (s, 3H, -OCH_3), 6.05 (s, 2H, -CH_2), 6.94 (d, *J* =8 Hz, 1H, ArH), 7.08 (d, *J* =16.4 Hz, 1H, ArH), 7.36 (d, *J* =16.8 Hz, 2H, ArH), 7.68 (d, *J* =8.8 Hz, 2H, ArH), 7.94 (d, *J* =8.4 Hz, 2H, ArH) ppm. ^{13}C NMR (100 MHz, DMSO-d_6): 52.4, 101.6, 105.9, 108.8, 122.8, 125.8, 126.7, 128.2, 130.0, 131.5, 142.5, 147.9, 148.3, 166.4 ppm.

ST-195 : ^{1}H NMR (400 MHz, DMSO-d_6): δ 1.33 (t, *J* =14.0 Hz, 3H, -CH_3), 3.66 (s, 3H, -OCH_3), 3.82 (s, 6H, -OCH_3), 4.04 (dd, *J* =20.8 Hz, *J* =6.8 Hz, 2H, -CH_2), 6.88 (s, 2H, -ArH), 6.93 (d, *J* =8.8 Hz, 2H, ArH), 7.03 (d, *J* =16.4 Hz, 1H, ArH), 7.17 (d, *J* =16.4 Hz, 1H, ArH), 7.51 (d, *J* =8.4 Hz, 1H, ArH) ppm. ^{13}C NMR (100 MHz, DMSO-d_6): 15.0, 56.2, 60.4, 63.4, 103.9, 115.0, 126.6, 127.8, 128.0, 130.0, 133.5, 137.3, 153.4, 158.5 ppm.

ST-200 : ^{1}H NMR (400 MHz, DMSO-d_6): δ 2.41 (s, 3H, -CH_3), 3.68 (s, 3H, -OCH_3), 3.84 (s, 6H, -OCH_3), 6.94 (s, 2H, -ArH), 7.05 (d, *J* =16 Hz, 1H, ArH), 7.19-7.16 (m, 3H, ArH), 7.37 (d, *J* =16.4 Hz, 1H, ArH), 7.63 (d, *J* =9.6 Hz, 1H, ArH) ppm. ^{13}C NMR (100 MHz, DMSO-d_6): 20.0, 56.3, 60.5, 104.5, 125.5, 125.9, 126.5, 127.7, 130.4, 130.7, 133.4, 135.8, 136.4, 137.8, 153.5 ppm.

ST-197: ^{1}H NMR (400 MHz, DMSO-d_6): δ 3.67 (s, 3H, -OCH_3), 3.83 (s, 6H, -OCH_3), 6.92 (s, 2H, -ArH), 7.11-7.25 (m, 4H, ArH), 7.19-7.16 (m, 3H, ArH), 7.62 (dd, *J* =14.8

Hz, *J* =6.0Hz, 2H, -CH_2) ppm. ^{13}C NMR (100 MHz, DMSO-d_6): 56.3, 60.5, 104.3, 115.9, 116.1, 127.0, 128.5, 128.6, 128.9, 128.9, 133.1, 134.2, 134.2, 137.7, 153.4, 160.7, 163.2 ppm.

ST-203 : ^{1}H NMR (400 MHz, DMSO-d_6): δ 3.78 (s, 6H, -OCH_3), 3.85 (s, 3H, -OCH_3), 6.46 (s, 1H, -ArH), 6.83 (s, 2H, ArH), 7.35 (s, 2H, ArH), 7.73 (d, *J* =8 Hz, 2H, ArH), 7.96 (d, *J* =8 Hz, 2H, ArH) ppm. ^{13}C NMR (100 MHz, DMSO-d_6): 52.4, 55.6, 100.9, 105.3, 127.1, 128.2, 128.7, 130.0, 131.7, 139.0, 142.2, 161.1, 166.4 ppm.

ST-209 : ^{1}H NMR (400 MHz, DMSO-d_6): δ 1.33 (t, *J* =11.2 Hz, 3H, -CH_3), 3.75 (s, 3H, -OCH_3), 3.81 (s, 3H, -OCH_3), 4.03 (d, *J* =6.4 Hz, 2H, -CH_2), 6.90-6.92 (m, 3H, -ArH), 7.02-7.05 (m, 3H, -ArH), 7.20 (s, 1H, -ArH), 7.49 (d, *J* =8.0 Hz, 2H, ArH) ppm. ^{13}C NMR (100 MHz, DMSO-d_6): 15.1, 55.9, 63.4, 109.4, 112.2, 115.0, 119.9, 126.4, 126.5, 127.8, 130.3, 130.8, 148.8, 149.3, 158.3 ppm.

ST-210: ^{1}H NMR (400 MHz, DMSO-d_6): δ 3.78 (s, 3H, -OCH_3), 3.83 (s, 3H, -OCH_3),), 3.85 (s, 3H, -OCH_3), 6.98 (d, *J* =8.4 Hz, 1H, ArH), 7.16 (d, *J* =9.6 Hz, 1H, ArH), 7.24 (d, *J* =16.4 Hz, 1H, ArH), 7.29 (d, *J* =1.6 Hz, 1H, ArH), 7.37 (d, *J* =16.4 Hz, 1H, ArH), 7.71 (d, *J* =8.4 Hz, 2H, ArH) ppm. ^{13}C NMR (100 MHz, DMSO-d_6): 52.4, 55.9, 109.8, 112.1, 1210.0, 125.4, 126.6, 128.1, 1293.9, 130.0, 131.8, 142.7, 149.4, 149.7, 166.4 ppm.

ST-212 : ^{1}H NMR (400 MHz, DMSO-d_6): δ 3.76 (s, 3H, -OCH_3), 3.76 (s, 3H, -OCH_3), 3.81 (s, 3H, -OCH_3), 6.94-6.91 (m, 3H, ArH), 7.10-6.98 (m, 3H, ArH), 7.20 (s, 1H, -ArH), 7.51 (d, *J* =8.4 Hz, 1H, ArH) ppm. ^{13}C NMR (100 MHz, DMSO-d_6): 55.5, 55.9, 55.9, 109.4, 112.2, 114.5, 119.9, 126.3, 126.5, 127.8, 130.4, 130.7, 148.8, 149.3, 159.0 ppm.

ST-211: ^{1}H NMR (400 MHz, DMSO-d_6): δ 3.76 (s, 3H, -OCH_3), 3.82 (s, 3H, -OCH_3), 6.95 (d, *J* =8.4 Hz, 1H, ArH), 7.07-7.23 (m, 6H, ArH), 7.59 (t, *J* =14 Hz, 2H, ArH) ppm. ^{13}C NMR (100 MHz, DMSO-d_6): 55.9, 55.9, 109.6, 112.1, 115.8, 116.0, 120.3, 125.5, 128.3, 128.3, 128.8, 130.3, 134.4, 149.1, 149.3 ppm.

ST-213 : ^{1}H NMR (400 MHz, DMSO-d_6): δ 2.32 (s, 3H, -CH_3), 3.76 (s, 3H, -OCH_3), 3.82 (s, 3H, -OCH_3), 6.95 (d, *J* =8.4 Hz, 1H, ArH), 7.04-7.26 (m, 6H, ArH), 7.35 (d, *J* =8 Hz, 1H, ArH), 7.39 (s, 1H, ArH) ppm. ^{13}C NMR (100 MHz, DMSO-d_6): 21.4, 55.9, 55.9, 109.6, 112.2, 120.2, 123.8, 126.7, 127.0, 128.3, 128.6, 128.9, 130.4, 137.7, 138.1, 149.1, 149.3 ppm.

ST-214 : ^{1}H NMR (400 MHz, DMSO-d_6): δ 2.33 (s, 3H, -CH_3), 3.77 (s, 3H, -OCH_3), 3.81 (s, 3H, -OCH_3), 6.94 (d, *J* =8 Hz, 1H, ArH), 7.02-7.25 (m, 6H, ArH), 7.34 (d, *J* =8 Hz, 1H, ArH), 7.41 (s, 1H, ArH) ppm. ^{13}C NMR (100 MHz, DMSO-d_6): 20.9, 55.7, 55.9, 101.3, 116.2, 124.2, 125.8, 126.5, 127.6, 128.5, 128.7, 129.9, 132.8, 134.3, 136.1, 149.7, 151.4 ppm.

ST-220: ^{1}H NMR (400 MHz, DMSO-d_6): δ 1.35 (t, *J* =11.2 Hz, 3H, -CH_3), 3.74 (s, 3H, -OCH_3), 3.80 (s, 3H, -OCH_3), 4.02 (d, *J* =6.4 Hz, 2H, -CH_2), 6.90-6.92 (m, 3H, -ArH), 7.02-7.04 (m, 3H, -ArH), 7.21 (s, 1H, -ArH), 7.48 (d, *J* =8.0 Hz, 2H, ArH) ppm. ^{13}C NMR (100 MHz, DMSO-d_6): 15.3, 55.8, 63.4, 109.4, 112.2, 115.0, 119.9, 126.4, 126.5, 127.8, 130.3, 130.8, 148.9, 149.1, 158.5 ppm.

ST-121 : ^{1}H NMR (400 MHz, DMSO-d_6): δ 3.67 (s, 3H, -OCH_3), 3.85 (s, 3H, -OCH_3), 3.87 (s, 3H, -OCH_3), 6.97 (s, 2H, -ArH), 7.36 (d, *J* =7.2 Hz, 2H, ArH), 7.71 (d, *J* =8.0 Hz, 2H, ArH), 7.98 (d, *J* =8.4 Hz, 2H, ArH) ppm. ^{13}C NMR (100 MHz, DMSO-d_6): 51.1,

54.3, 57.5, 60.1, 101.1, 123.8, 127.0, 128.4, 131.1, 131.8, 137.1, 142.8, 150.1, 161.6 ppm.

ST-226: ^{1}H NMR (400 MHz, DMSO-d_6): δ 3.77 (s, 6H, -OCH_3), 6.46 (d, J =6.4 Hz, 2H, -CH_2), 6.83 (s, 1H, ArH), 7.23-7.37 (m, 5H, -ArH), 7.73-7.86 (m, 6H, -ArH) ppm. ^{13}C NMR (100 MHz, DMSO-d_6): 55.6, 100.9, 105.3, 127.1, 128.2, 128.5, 128.7, 130.0, 131.7, 139.0, 142.2, 152.1 ppm.

ST-227 : ^{1}H NMR (400 MHz, DMSO-d_6): δ 1.33 (t, J =12.4 Hz, 3H, -CH_3), 4.04 (dd, J =20.8 Hz, J =6.8 Hz, 2H, -CH_2), 6.88 (d, J =6.8 Hz, 2H, -CH_2), 6.93 (d, J =8.8 Hz, 2H, ArH), 7.25-7.38 (m, 6H, -ArH), 7.71-7.77 (m, 4H, -ArH) ppm. ^{13}C NMR (100 MHz, DMSO-d_6): 15.3, 56.2, 103.9, 115.0, 126.6, 126.8, 127.8, 128.0, 130.0, 131.1, 132.5, 133.5, 137.3, 153.4, 154.5 ppm.

ST-228: ^{1}H NMR (400 MHz, DMSO-d_6): δ 3.67 (s, 3H, -OCH_3), 6.97 (s, 2H, -ArH), 7.36 (d, J =7.2 Hz, 2H, ArH), 7.71 (d, J =8.0 Hz, 2H, ArH), 7.98 (d, J =8.4 Hz, 2H, ArH) ppm. ^{13}C NMR (100 MHz, DMSO-d_6): 51.1, 101.1, 111.2, 115.4, 120.6, 123.8, 127.0, 127.4, 127.8, 128.4, 131.1, 137.1, 142.8, 150.1, 161.6 ppm.

ST-230: ^{1}H NMR (400 MHz, DMSO-d_6): δ 3.73 (s, 3H, -OCH_3), 6.97 (d, J =7.2 Hz, 2H, ArH), 7.36 (d, J =7.2 Hz, 2H, ArH), 7.46-7.53 (m, 11H, -ArH) ppm. ^{13}C NMR (100 MHz, DMSO-d_6): 55.8, 111.5, 125.3, 125.6, 126.7, 129.5, 130.2, 131.4, 140.5, 142.3, 158.3 ppm.

ST-237 : ^{1}H NMR (400 MHz, DMSO-d_6): δ 1.34 (t, J =13.6 Hz, 3H, -CH_3), 4.06 (dd, J =20.8 Hz, J =6.8 Hz, 2H, -CH_2), 6.96 (d, J =8.4 Hz, 2H, ArH), 7.23-7.37 (m, 2H, -ArH), 7.46-7.50 (m, 2H, -ArH), 7.58 (d, J =8.4 Hz, 2H, ArH), 7.82-7.90 (m, 3H, -ArH), 6.37 (s,

1H, -ArH) ppm. ^{13}C NMR (100 MHz, DMSO-d_6): 15.1, 63.5, 115.1, 123.9, 126.1, 126.4, 126.8, 128.0, 128.1, 128.3, 128.5, 129.1, 129.9, 132.7, 133.7, 135.4, 158.7 ppm.

ST-233 : ^{1}H NMR (400 MHz, DMSO-d_6): δ 3.67 (s, 3H, -OCH_3), 3.78 (s, 6H, -OCH_3), 3.83 (s, 6H, -OCH_3), 6.40 (s, 1H, -ArH), 6.77 (d, *J* =2 Hz, 2H, ArH), 6.92 (s, 2H, ArH), 7.13-7.24 (m, 2H, -ArH) ppm. ^{13}C NMR (100 MHz, DMSO-d_6): 55.6, 56.2, 60.5, 100.3, 104.3, 104.6, 128.2, 129.5, 133.0, 137.7, 139.6, 153.4, 161.0 ppm.

ST-234: ^{1}H NMR (400 MHz, DMSO-d_6): δ 3.73 (s, 12H, -OCH_3), 6.43 (s, 2H, -ArH), 6.77 (d, *J* =8 Hz, 2H, ArH), 6.92 (s, 4H, ArH) ppm. ^{13}C NMR (100 MHz, DMSO-d_6): 55.6, 99.6, 105.2, 127.4, 140.2, 158.4 ppm.

ST-238: ^{1}H NMR (400 MHz, DMSO-d_6): δ 3.73 (s, 3H, -OCH_3), 7.18-7.30 (m, 3H, ArH), 7.45-7.55 (m, 3H, ArH), 7.75 (d, *J* =7.6 Hz, 1H, ArH), 7.87-7.90 (m, 3H, ArH), 8.01 (s, 1H, ArH) ppm. ^{13}C NMR (100 MHz, DMSO-d_6): 55.6, 121.5, 124.7, 125.4, 126.7, 126.8, 127.4, 128.0, 128.3, 128.6, 130.2, 130.8, 132.1, 133.7, 135.3, 136.5, 140.1 ppm.

ST-239 : ^{1}H NMR (400 MHz, DMSO-d_6): δ 3.75 (s, 3H, -OCH_3), 6.81 (d, *J* =8.4 Hz, 2H, ArH), 7.25-7.36 (m, 2H, -ArH), 7.45-7.59 (m, 2H, -ArH), 7.61 (d, *J* =8.0 Hz, 2H, ArH), 7.80-7.97 (m, 4H, -ArH), 6.37 (s, 1H, -ArH) ppm. ^{13}C NMR (100 MHz, DMSO-d_6): 55.5, 110.4, 122.4, 125.2, 125.4, 126.1, 128.2, 128.3, 128.3, 128.8, 129.1, 129.5, 132.8, 132.9, 133.2, 152.3 ppm.

ST-240: ^{1}H NMR (400 MHz, DMSO-d_6): δ 2.43 (s, 3H, -CH_3), 7.08-7.26 (m, 3H, ArH), 7.45-7.52 (m, 3H, ArH), 7.71 (d, *J* =8 Hz, 1H, ArH), 7.84-7.99 (m, 4H, ArH) ppm. ^{13}C

NMR (100 MHz, DMSO-d_6): 19.7, 119.5, 121.5, 124.1, 125.7, 126.8, 126.9, 128.0, 128.3, 128.6, 131.1, 132.9, 133.4, 133.9, 134.3, 134.4, 135.3 ppm.

ST-241: ^{1}H NMR (400 MHz, DMSO-d_6): δ 2.45 (s, 3H, -CH_3), 7.19-7.31 (m, 3H, ArH), 7.48-7.59 (m, 3H, ArH), 7.73 (d, *J* =7.6 Hz, 1H, ArH), 7.89-7.92 (m, 3H, ArH), 8.03 (s, 1H, ArH) ppm. ^{13}C NMR (100 MHz, DMSO-d_6): 20.03, 124.25, 125.5, 126.4, 126.6, 126.8, 126.9, 128.0, 128.3, 128.6, 130.1, 130.8, 133.0, 133.7, 135.3, 136.0, 136.2 ppm.

ST-242: ^{1}H NMR (400 MHz, DMSO-d_6): δ 6.82 (d, *J* =8.0 Hz, 2H, ArH), 7.22-7.35 (m, 2H, -ArH), 7.46-7.61 (m, 2H, -ArH), 7.72 (d, *J* =8.4 Hz, 2H, ArH), 7.82-7.999 (m, 4H, -ArH), 6.65 (s, 1H, -ArH) ppm. ^{13}C NMR (100 MHz, DMSO-d_6): 113.5, 122.4, 125.2, 125.4, 125.5, 127.2, 128.2, 128.3, 128.8, 129.1, 129.5, 132.8, 133.7, 135.4, 159.5 ppm.

ST-243: ^{1}H NMR (400 MHz, DMSO-d_6): δ 7.19-7.31 (m, 3H, ArH), 7.48-7.59 (m, 3H, ArH), 7.73 (d, *J* =7.6 Hz, 1H, ArH), 7.89-7.92 (m, 3H, ArH), 8.03 (s, 1H, ArH) ppm. ^{13}C NMR (100 MHz, DMSO-d_6): 111.7, 125.5, 126.4, 126.6, 126.8, 126.9, 128.0, 128.3, 128.6, 130.1, 131.8, 133.1, 133.5, 134.3, 135.0, 154.2 ppm.

ST-245: ^{1}H NMR (400 MHz, DMSO-d_6): δ 1.34 (t, *J* =11.2 Hz, 3H, -CH_3), 3.99 (s, 3H, -OCH_3), 4.05 (dd, *J* =20.4 Hz, *J* =6.8 Hz, 2H, -CH_2), 6.95 (d, *J* =8.4 Hz, 2H, ArH), 7.02 (d, *J* =7.6 Hz, 1H, ArH), 7.11 (d, *J* =16 Hz, 1H, ArH), 7.51-7.65 (m, 4H, -ArH), 7.75-7.82 (m, 2H, -ArH), 8.21 (d, *J* =8.0 Hz, 1H, ArH), 8.35 (d, *J* =8.4 Hz, 1H, ArH) ppm. ^{13}C NMR (100 MHz, DMSO-d_6): 15.3, 55.8, 63.4, 109.4, 112.2, 115.0, 119.9, 126.4, 126.5, 127.8, 130.3, 130.8, 148.9, 149.1, 158.5 ppm.

ST-246: ^{1}H NMR (400 MHz, DMSO-d_6): δ 3.64 (s, 3H, -OCH_3), 3.75 (s, 3H, -OCH_3), 6.37 (s, 1H, -ArH), 6.74 (d, *J* =1.6 Hz, 2H, ArH), 6.89 (s, 1H, ArH), 7.16 (dd, *J* =42 Hz, *J*

=16.4 Hz, 2H, -CH_2) ppm. ^{13}C NMR (100 MHz, DMSO-d_6): 55.6, 56.2, 60.5, 100.3, 104.3, 104.6, 128.2, 129.5, 133.0, 137.7, 139.6, 153.4, 161.0 ppm.

ST-247: ^{1}H NMR (400 MHz, DMSO-d_6): δ 3.65 (s, 3H, -OCH_3), 3.67 (s, 3H, -OCH_3), 6.75 (d, *J* =8.0 Hz, 2H, ArH), 7.12 (d, *J* =8.4 Hz, 1H, ArH), 7.11 (d, *J* =8.4 Hz, 1H, ArH), 7.51-7.65 (m, 4H, -ArH), 7.75-7.82 (m, 2H, -ArH), 8.19 (d, *J* =8.4 Hz, 1H, ArH), 8.24 (d, *J* =8.0 Hz, 1H, ArH) ppm. ^{13}C NMR (100 MHz, DMSO-d_6): 55.8, 55.9, 104.6, 112.2, 116.1, 120.4, 126.4, 126.5, 127.8, 130.3, 131.4, 144.1, 145.5, 158.5 ppm.

ST-268: ^{1}H NMR (400 MHz, DMSO-d_6): δ 1.35 (t, *J* =12.4 Hz, 3H, -CH_3), 4.01 (dd, *J* =16.4 Hz, *J* =8.0 Hz, 2H, -CH_2), 4.15 (s, 4H, -CH_2), 6.85 (d, *J* =8.8 Hz, 1H, ArH), 7.06-7.13 (m, 4H, ArH), 7.15 (t, *J* =17.6 Hz, 2H, ArH), 7.56-7.60 (m, 2H, ArH) ppm. ^{13}C NMR (100 MHz, DMSO-d_6): 15.1, 59.1, 64.4, 64.6, 115.1, 115.8, 116.0, 117.6, 120.2, 125.9, 128.2, 128.3, 128.4, 128.5, 131.9, 134.3, 145.1, 149.1 ppm.

ST-269 : ^{1}H NMR (400 MHz, DMSO-d_6): δ 3.85 (s, 3H, -OCH_3), 4.26(s, 4H, -CH_2), 6.88 (d, *J* =8.4 Hz, 1H, ArH), 7.10-7.18 (m, 3H, ArH), 7.32 (d, *J* =16.4 Hz, 1H, ArH), 7.69 (d, *J* =8.4 Hz, 2H, ArH), 7.93 (d, *J* =8.4 Hz, 2H, ArH) ppm. ^{13}C NMR (100 MHz, DMSO-d_6): 52.4, 64.4, 64.6, 115.5, 117.7, 120.7, 125.8, 126.7, 128.2, 130.0, 130.5, 131.3, 142.5, 143.9, 144.2, 166.4 ppm.

ST-270: ^{1}H NMR (400 MHz, DMSO-d_6): δ 3.76 (s, 3H, -OCH_3), 4.24 (s, 4H, -CH_2), 6.83 (d, *J* =8 Hz, 1H, ArH), 6.93 (d, *J* =8.4 Hz, 2H, ArH), 6.97-7.07 (m, 4H, ArH), 7.49 (d, *J* =8.8 Hz, 2H, ArH) ppm. ^{13}C NMR (100 MHz, DMSO-d_6): 55.5, 64.4, 64.5, 114.5, 114.8, 117.6, 119.9, 126.0, 126.7, 127.9, 130.3, 131.4, 143.2, 143.9, 159.1 ppm.

ST-273: ^{1}H NMR (400 MHz, DMSO-d_6): δ 4.25 (s, 4H, -CH_2), 6.85 (d, *J* =8.8 Hz, 1H, ArH), 7.07-7.11 (m, 4H, ArH), 7.18 (t, *J* =17.6 Hz, 2H, ArH), 7.57-7.61 (m, 2H, ArH) ppm. ^{13}C NMR (100 MHz, DMSO-d_6): 64.4, 64.6, 115.1, 115.8, 116.0, 117.6, 120.2, 125.9, 128.2, 128.3, 128.4, 128.5, 130.9, 134.3, 143.6, 143.9 ppm.

ST-274: ^{1}H NMR (400 MHz, DMSO-d_6): δ 4.25 (s, 4H, -CH_2), 6.84 (d, *J* =8.4 Hz, 1H, ArH), 7.05-7.17 (m, 4H, ArH), 7.40 (d, *J* =8.4 Hz, 2H, ArH), 7.57 (d, *J* =8.8 Hz, 2H, ArH) ppm. ^{13}C NMR (100 MHz, DMSO-d_6): 64.4, 64.6, 115.2, 117.6120.4, 1255.7, 128.2, 129.0, 129.2, 130.8, 131.8, 136.9, 136.6, 143.8, 143.9 ppm.

ST-275: ^{1}H NMR (400 MHz, DMSO-d_6): δ 4.19 (s, 4H, -CH_2), 6.79 (d, *J* =8.8 Hz, 1H, ArH), 7.10-7.15 (m, 4H, ArH), 7.21 (t, *J* =17.6 Hz, 2H, ArH), 7.59-7.63 (m, 2H, ArH) ppm. ^{13}C NMR (100 MHz, DMSO-d_6): 64.7, 64.7, 113.2, 115.8, 116.1, 119.8, 123.7, 123.9, 128.5, 129.1, 129.4, 129.5, 131.5, 136.3, 144.4, 146.5 ppm.

ST-295: ^{1}H NMR (400 MHz, DMSO-d_6): δ 1.32 (t, *J* =12.8 Hz, 3H, -CH_3), 4.04 (d, *J* =6.4 Hz, 2H, -CH_2), 6.94 (d, *J* =8.4 Hz, 2H, ArH), 7.07 (d, *J* =16.4 Hz, 1H, ArH), 7.32 (d, *J* =16.4 Hz, 1H, ArH), 7.50-7.59 (m, 4H, ArH), 7.82 (s, 1H, ArH) ppm. ^{13}C NMR (100 MHz, DMSO-d_6): 15.1, 63.5, 115.0, 1238, 126.5, 128.0, 128.5, 129.4, 130.9, 131.1, 131.8, 138.9, 159.1 ppm.

ST-297: ^{1}H NMR (400 MHz, DMSO-d_6): δ 3.68 (s, 3H, -OCH_3), 3.82 (s, 6H, -OCH_3), 6.93 (s, 2H, ArH), 7.23 (d, *J* =16.4 Hz, 1H, ArH), 7.33 (d, *J* =16.4 Hz, 1H, ArH), 7.56 (d, *J* =8.4 Hz, 1H, ArH), 7.63 (d, *J* =8.4 Hz, 1H, ArH), 7.85 (s, 1H, ArH) ppm. ^{13}C NMR (100 MHz, DMSO-d_6): 56.3, 60.5, 104.6, 125.6, 126.7, 128.2, 129.7, 131.2, 131.4, 131.9, 132.6, 138.1, 138.6, 153.4 ppm.

ST-294: ^{1}H NMR (400 MHz, DMSO-d_6): δ 3.77 (s, 3H, -OCH_3), 6.96 (d, *J* =8.4 Hz, 2H, ArH), 7.08 (d, *J* =16.4 Hz, 1H, ArH), 7.32 (d, *J* =16.4 Hz, 1H, ArH), 7.52-7.58 (m, 4H, ArH), 7.81 (s, 1H, ArH) ppm. ^{13}C NMR (100 MHz, DMSO-d_6): 55.5, 114.6, 123.9, 126.5, 128.0, 128.5, 129.4, 129.5, 130.8, 131.1, 131.8, 138.8, 159.8 ppm.

ST-298: ^{1}H NMR (400 MHz, DMSO-d_6): δ 2.33 (s, 3H, -CH_3), 7.12 (d, *J* =7.2 Hz, 1H, ArH), 7.24-7.42 (m, 4H, ArH), 7.61 (dd, *J* =8.4 Hz, *J* =15.2 Hz, 2H, ArH), 7.88 (s, 1H, ArH) ppm. ^{13}C NMR (100 MHz, DMSO-d_6): 21.4, 124.5, 126.1, 126.9, 127.6, 128.4, 129.1, 129.3, 131.2, 131.3, 136.8, 138.2, 138.5 ppm.

ST-290: ^{1}H NMR (400 MHz, DMSO-d_6): δ 7.22 (s, 1H, ArH), 7.91-7.93 (m, 3H, ArH), 7.88 (s, 1H, ArH), 8.30-8.34 (m, 3H, ArH) ppm. ^{13}C NMR (100 MHz, DMSO-d_6): 106.7, 108.0, 117.9, 121.9, 124.8, 126.7, 137.5, 140.2, 146.1, 147.4, 149.6 ppm.

ST-283: ^{1}H NMR (400 MHz, DMSO-d_6): δ 2.33 (s, 6H, ArH), 7.46 (d, *J* =6.8 Hz, 2H, ArH), 7.24-7.28 (m, 6H, ArH), 7.38-7.44 (m, 4H, ArH), 7.60 (s, 4H, ArH) ppm. ^{13}C NMR (100 MHz, DMSO-d_6): 19.8, 121.5, 123.5, 124.1, 125.5, 126.4, 127.4, 127.6, 128.2, 128.8, 135.2 ppm.

ST-284: ^{1}H NMR (400 MHz, DMSO-d_6): δ 2.42 (s, 6H, ArH), 7.12-7.21 (m, 8H, ArH), 7.46 (d, *J* =16.4 Hz, 2H, ArH), 7.64-7.69 (m, 6H, ArH) ppm. ^{13}C NMR (100 MHz, DMSO-d_6): 19.2, 124.2, 124.8, 124.9, 125.5, 126.4, 127.4, 127.4, 128.6, 129.5, 136.7 ppm.

NI-ST-11: ^{1}H NMR (400 MHz, DMSO-d_6): δ 3.67 (s, 3H, -OCH_3), 3.82 (s, 6H, -OCH_3), 6.93 (s, 2H, -ArH), 7.32 (s, 2H, -ArH), 8.41 (s, 2H, -ArH) ppm. ^{13}C NMR (100 MHz,

DMSO-d_6): 56.7, 56.8, 61.0, 104.9, 124.8, 127.5, 129.1, 131.5, 133.2, 138.5, 141.4, 146.0, 154.0 ppm.

NI-ST-12: ^{1}H NMR (400 MHz, DMSO-d_6): δ 3.67 (s, 3H, -OCH_3), 3.82 (s, 6H, -OCH_3), 3.94 (s, 3H, -OCH_3), 6.92 (s, 2H, -ArH), 7.24 (s, 2H, -ArH), 7.34 (d, *J* =8.0 Hz, 1H, ArH), 7.85 (d, *J* =8.0 Hz, 1H, ArH), 8.09 (s, 1H, -ArH), 8.52 (s, 2H, -ArH) ppm. ^{13}C NMR (100 MHz, DMSO-d_6): 56.6, 60.2, 103.6, 112.4, 114.6, 124.6, 127.4, 127.5, 130.5, 131.2, 134.5, 140.4, 145.4, 149.5, 152.3 ppm.

DNR-1; ^{1}H NMR (400 MHz, DMSO-d_6): δ 3.76 (s, 6H, -OCH3), 6.33 (s, 1H, -ArH), 6.71 (s, 2H, -ArH), 6.83 (d, 1H, -ArH, J = 16.4 Hz), 7.12 (d, 1H, -ArH J = 16 Hz), 8.10 (s, 2H, -ArH) ppm. ^{13}C NMR (DMSO-d6, ppm): δ 55.5, 99.6, 104.2, 110.0, 113.5, 124.2, 128.1, 128.5, 140.7, 143.6, 159.7, 161.0 ppm.

ST-208 : ^{1}H NMR (400 MHz, DMSO-d_6): δ 3.77 (s, 3H, -OCH_3), 3.81 (s, 3H, -OCH_3), 6.94 (d, 1H, -ArH J = 8 Hz), 7.09 (d, 1H, -ArH J = 9.6 Hz), 7.15 (s, 1H, -ArH), 7.19 (s, 1H, -ArH), 7.24 (d, *J* =1.6 Hz, 1H, ArH), 7.41 (d, 2H, -ArH J = 8 Hz), 7.59 (d, 2H, -ArH J = 8.4Hz) ppm. ^{13}C NMR (100 MHz, DMSO-d_6): 55.9, 109.6, 112.1, 120.6, 125.3, 128.1, 129.1, 129.7, 130.1, 131.8, 136.8, 149.3 ppm.

2.3 Synthesis of *(E)*-3,5,4'-trimethoxy resveratrol analogues with substitutions at the C2 position on the stilbene.

2.3.1 Prior studies with this scaffold

Structure-activity relationship studies on the resveratrol molecule identified *trans*-3,5,4'-trimethoxy-resveratrol as a lead drug candidate and further SAR studies revealed that

various substitutions at the C2 position on *trans*-3,5,4' -trimethoxy-resveratrol led to enhanced cytotoxic activity against a variety of tumor cell lines (**Figure 2.3**).

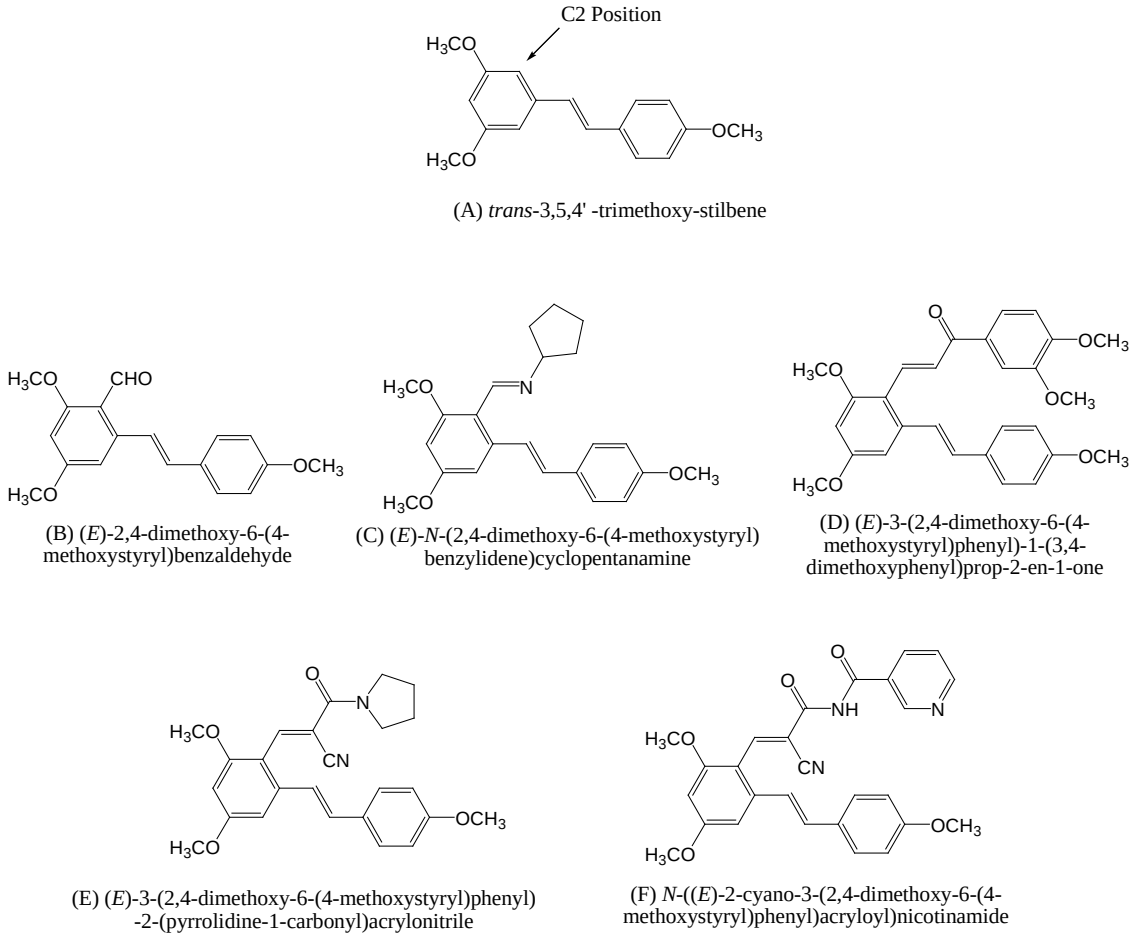

Figure 2.3 Structures of *trans*-3,5,4'-trimethoxystilbene and its potent analogs.

In 2006, Huang *et al*. reported that *O*-methylation of resveratrol caused an increase in cytotoxicity and that introduction of a formyl group (**B**) or an alkyl amine moiety (**C**) at the C2 position on the *trans*-3,5,4'-trimethoxystilbene scaffold (**A**) led to an enhanced cytotoxic activity (Huang, Ruan et al. 2007). In related studies, Ruan et al. have reported the antitumor activity of resveratrol derivatives possessing a chalcone moiety (**Figure 2.3**. Structure **D**); these analogues exhibited potent anti-proliferative and antitubulin

activities, and compound **D** inhibited the growth of cancer cell lines HepG2, B16-F10, and A549 with IC_{50} values of 0.2, 0.1, and 1.4 μg/mL, respectively.(Ruan, Lu et al. 2011). Recently, Raun and co-workers reported compounds **E** and **F** to be the most potent among the *trans*-3,5,4'-trimethoxystilbene acrylamides amine derivatives. Compounds **E** had the best cytotoxicity against the HuH-7 cell line and its IC_{50} was 4.5 μmol/L; and compound **F** had the best anti-tumor activity against the K562 cell line with an IC_{50} of 2.9 μmol/L.

2.3.2 Chemistry and analytical data

Based on the structure-activity relationship analysis of the above mentioned literature, it is evident that substitutions at the C2 position of the *trans*-3,5,4'-trimethoxystilbene scaffold (**Figure 2.3**, **A**) leads to enhanced cytotoxic activity along with increased tubulin binding capacity. In this respect, we have synthesized a range of *trans*-3,5,4'-trimethoxy resveratrol analogs with substitutions at the C2 position. We designed and synthesized a series of novel *trans*-3,5,4'-trimethoxy resveratrol analogs incorporating an α,β-unsaturated double bond conjugated to different five, and six membered heterocyclic and bicyclic quinuclidinone ring systems **Scheme 2.2** and **Scheme 2.3**. Also, we synthesized a series of 3,5,4'-trimethoxy resveratrol analogs with acrylonitrile substitutions at the C2 position **Scheme 2.3**.

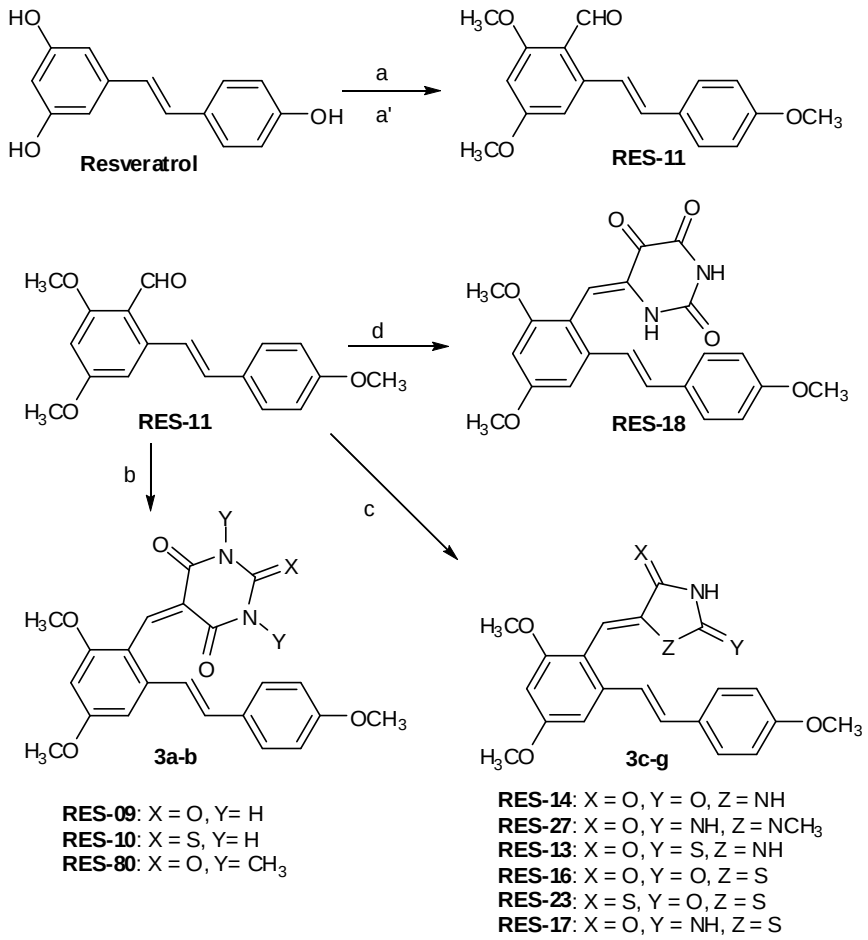

Scheme 2.2 Synthesis of resveratrol analogs with heterocyclic ring substitutions at the C2 position. (a) MeI, K_2CO_3, acetone; (a) $POCl_3$, DMF, 0 ^oC, 69% yield; (b) barbituric acid or thiobarbituric acid, methanol, RT, 6 hrs, 95-96% yield; (c) five membered active methylene compound, NH_4OAc, AcOH, MWI, 1-2 min, 94-97% yield; (d) isobarbituric acid, ethanol, reflux, 4 hrs, 60% yield**.**

The procedure for synthesizing compound **RES-11** involves *O*-methylating the hydroxyl groups on resveratrol with MeI/ K_2CO_3 in acetone followed by formylation of (*E*)-1,3-dimethoxy-5-(4-methoxystyryl) benzene in the presence of a slight excess of $POCl_3$ in DMF at 0 ^0C for 30 min yielding *trans*-2-formyl-3,4′,5-trimethoxy stilbene **(RES-11).**

(RES-11): ^1H NMR (DMSO-d_6):3.78 (s, 3H), 3.90 (s, 3H), 3.92 (s, 3H), 6.63 (s, 1H), 6.91 (s, 1H), 6.97 (d, 2H, *J* = 7.9 Hz), 7.21 (d, 1H, *J* = 16.2 Hz), 7.50 (d, 2H, *J* =7.9 Hz),

7.95 (d, 1H, *J* = 16.2 Hz), 10.41 (s, 1H) ppm. ^{13}C-NMR (DMSO-d_6): 55.8, 56.1, 101.2, 102.5, 109.8, 114.3, 129.4, 130.5, 131.4, 139.7, 162.5, 167.8, 193.5 ppm.

The novel resveratrol analogs (**RES-09** to **RES-27)** were then prepared by aldol condensation of **RES-11** with an appropriate active methylene compound, utilizing a variety of reaction conditions, i.e., ammonium acetate in acetic acid under microwave irradiation (MWI) conditions, by refluxing the reactants in ethanol, or by stirring the reaction at ambient temperature in methanol. The synthetic routes to the resveratrol analogs **RES-09** to **RES-27** are illustrated in **Scheme 2.2**.

RES-09: ^{1}HNMR (DMSO-d_6): δ 3.72-3.86 (m, 9H, 3 -OCH_3), 6.38 (d, 1H, *J*=24 Hz, C6H), 6.79 (d, 1H, C4H), 6.81-6.96 (m, 3H, C8H, C11H, C13H), 7.11 (s, 1H, C7H, C15H), 7.43-7.48 (m, 3H) ppm.^{13}C-NMR (DMSO-*d6*): δ 55.3, 55.5, 55.8, 55.8, 56.1, 97.3, 97.7, 102.2, 111.4, 113.8, 124.6, 127.6, 127.5, 129.1, 129.7, 129.9, 131.8, 132.4, 139.5, 159.0, 159.8, 162.6, 167.3, 169.8 ppm; mp: 146-148 ^{o}C.

RES-10: ^{1}H NMR (DMSO-d_6): δ 3.78 (d, 6H, -OCH_3), 3.84 (s, 3H, -OCH_3), 6.25(s, 1H, C6H), 6.73 (s, 1H,- Ar), 6.78 (d, 1H, *J*=1.8Hz, C4H), 6.89 (d, 2H, C7H ,C8H, *J*=8.7 Hz), 6.95 (d, 2H, C11H,C13H, *J*=4.5 Hz), 7.35 (d, 2H, *J*=8.7) ppm. ^{13}C-NMR (DMSO-d_6): δ 56.4, 55.7, 55.9,100.6, 101.7, 109.4, 114.5, 123.4, 129.7, 130.2, 131.4, 136.7, 148.4, 158.7, 158.9,160.4, 166.5, 166.9, 175.4 ppm; mp: 187-189^{o}C.

RES-80: ^{1}H NMR (DMSO-d_6): δ 2.74 (s, 3H, -CH_3), 3.20 (s, 3H, -CH_3), 3.64 (s, 3H, -OCH_3), 3.76 (s, 3H, -OCH_3), 3.78 (s, 3H, -OCH_3), 4.00 (s, 1H, ArH), 4.59 (s, 1H,-ArH), 6.32 (s, 1H, -ArH), 6.58 (s, 1H, ArH), 6.98 (s, 1H, ArH), 7.04 (d, 2H, *J*=8.4, ArH), 7.50 (d, 2H, *J*=8.4, ArH) ppm. ^{13}C-NMR (DMSO-d_6): δ 27.91, 28.5, 48.5, 55.7, 55.7,

55.8, 95.5, 99.4, 114.9, 127.0, 128.4, 147.1, 149.9, 151.9, 155.3, 159.5, 161.4. ppm; mp: 156-158^{o}C.

RES-14: ^{1}HNMR (DMSO-d_6): δ 3.57 (d, 6H, -OCH_3), 3.61 (s, 3H, -OCH_3), 6.35 (d, 1H, *J*=24 Hz, C6H), 6.75 (d, 1H, C4H), 6.82-6.94 (m, 3H, C8H, C11H, C13H), 7.17 (s, 2H, C7H, C15H), 7.39-7.48 (m, 2H) ppm.^{13}C-NMR (DMSO-*d6*): δ 55.6, 55.8, 56.2, 100.5, 102.3, 109.4, 114.3, 122.4, 124.5, 127.5, 130.4, 136.7, 154.3, 158.6, 159.1, 161.3, 163.6.ppm; mp: 123-125 ^{o}C.

RES-27: molecular formula: $C_{22}H_{23}N_{ST-624}$; ^{1}H NMR (DMSO-d_6): δ 2.84 (s, 3H, -NCH_3), 3.81 (d, 6H, -OCH_3), 3.89 (s, 3H, -OCH_3), 6.39(s, 1H, C6H), 6.75 (s, 1H, =CH), 6.79 (d, 1H, *J*=1.8Hz, C4H), 6.85 (d, 2H, C7H ,C8H, *J*=8.7 Hz), 6.99 (d, 2H, C11H,C13H, *J*=4.5 Hz), 7.38 (d, 2H, C10H,C14H, *J*=8.7) ppm. ^{13}C-NMR (DMSO-d_6): δ 29.9, 55.6, 55.7, 55.8, 97.5, 100.9, 106.3, 113.7,114.3, 114.4, 124.2, 128.1, 128.5, 129.8, 130.7, 135.3, 138.9, 158.8, 159.7, 160.8, 167.9, 176.2 ppm; mp: 162-165^{o}C.

RES-13: ^{1}HNMR (DMSO-d_6): δ 3.81-3.93 (m, 9H, 3 x -OCH_3),6.51 (s, 1H, C6H), 6.93-6.98 (m, 4H, C4H, C8H, C11H, C13H), 6.27 (d, 1H, C7H),7.45 (d, 2H, *J*=12.0 Hz, C10H, C14H), 8.34 (d, 1H, *J*=2 Hz, C15H), 11.21 (s, 1H, NH) ppm. ^{13}CNMR (DMSO-d_6): δ 55.6, 55.9, 56.1, 101.4, 114.3, 120.4, 126.4, 129.8, 131.4, 131.6, 137.5, 139.6, 157.5, 159.4, 161.3, 165.6, 175.9. ppm; mp: 112-114 ^{o}C.

RES-16: ^{1}HNMR (DMSO-d_6): δ 3.77 (s, 3H, -OCH_3), 3.91 (s, 3H, -OCH_3), 3.93 (s, 3H, -OCH_3),6.54 (s, 1H, C6H), 6.61 (d, 1H, C7H), 6.81-6.87 (m, 4H, C4H, C8H, C11H, C13H), 7.24 (d, 2H, *J*=12.0 Hz, C10H, C14H), 8.22 (d, 1H, *J*=2 Hz, C15H)

ppm. ^{13}CNMR (DMSO-d_6): δ 54.6, 55.1, 100.4, 102.4, 112.4, 116.0, 127.9, 130.4, 131.3, 136.7, 154.3, 160.7, 161.3, 167.6. ppm; mp: 143-144 ºC.

RES-23: Molecular formula: $C_{21}H_{19}NO_4S_2$; ^{1}HNMR (DMSO-d_6): δ 3.70-3.83 (m, 9H, 3 -OCH_3), 6.31 (d, 1H, *J*=20.1 Hz, C6H), 6.78 (d, 1H, C4H), 6.86-6.98 (m, 3H, C8H, C11H, C13H), 7.11 (s, 2H, C7H, C15H), 7.41-7.48 (m, 2H) ppm.^{13}C-NMR (DMSO-*d6*): δ 55.4, 55.5, 55.6, 55.9, 56.0, 97.8, 97.9, 103.2, 113.7, 114.6, 123.7, 126.9, 128.6, 128.7, 129.1, 129.8, 132.6, 139.5, 159.0, 159.8, 162.3, 167.6, 169.0 ppm; mp: 130-135 ºC.

RES-18: Molecular formula: $C_{22}H_{20}N_2O_6$; ^{1}HNMR (DMSO-d_6): δ 3.81-3.93 (m, 9H, 3 x -OCH_3),6.57 (s, 1H, C6H), 6.96-6.99 (m, 4H, C4H, C8H, C11H, C13H), 6.15 (d, 1H, C7H),7.54 (d, 2H, *J*=8.5 Hz, C10H, C14H), 8.32 (d, 1H, *J*=2 Hz, C15H), 11.0 (s, 1H, NH), 11.36 (s, 1H, NH) ppm. ^{13}CNMR (DMSO-d_6): δ 53.3, 55.5, 55.6, 55.9, 55.9, 56.2, 56.3, 97.55, 97.6, 102.1, 102.4, 114.5, 115.6, 121.3, 124.2, 128.6, 129.9, 131.9, 139.7, 149.7, 150.7 159.4, 159.7, 161.3, 162.4, 163.4 ppm; mp: 141-146 ºC.

RES-17: ^{1}HNMR (DMSO-d_6): δ 3.63 (s, 3H, -OCH_3), 3.82 (s, 3H, -OCH_3), 3.85 (s, 3H, -OCH_3),6.55 (s, 1H, C6H), 6.64 (d, 1H, C4H), 6.87-6.96 (m, 3H, C8H, C11H, C13H), 7.12 (d, 1H, C7H),7.35 (d, 2H, *J*=12.0 Hz, C10H, C14H), 8.34 (d, 1H, *J*=2 Hz, C15H) ppm. ^{13}CNMR (DMSO-d_6): δ 54.6, 54.7, 55.2, 110.4, 115.8, 121.3, 127.7, 128.6, 131.4, 131.8, 138.3, 139.9, 147.5, 156.8, 162.3, 165.6, 169.5 ppm; mp: 157-159 ºC.

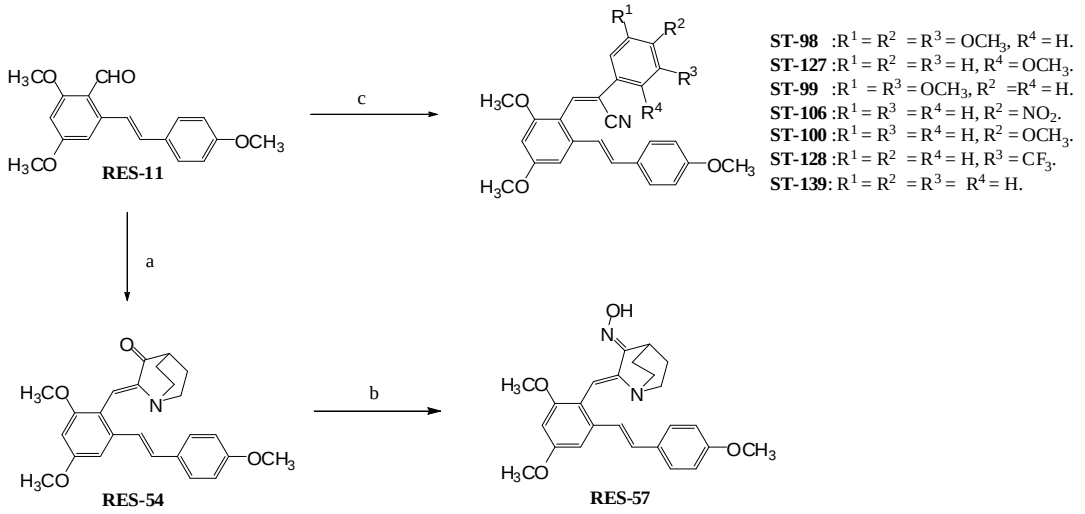

Scheme 2.3 Synthesis of resveratrol analogs with bicyclic and acrylonitrile substitutions at the C2 position (a) Quinuclidinone, 20% NaOH, EtOH, reflux; (b) $NH_2OH.HCl$, AcONa, EtOH; (c) Phenylacetonitrile, NaOMe, EtOH, 6hrs reflux.

The synthetic procedure for synthesizing compounds **ST-98-ST-139** is shown in **Scheme 2.3**. *Trans*-2-formyl-3,4′,5-trimethoxystilbene (**RES-11**) (1 mmol) and an appropriate phenylacetonitrile (1.1 mmol) were dissolved in 10 volumes of EtOH. 50% w/v aq. NaOMe was then added and mixture was refluxed for 6 hrs. The reaction was monitored by TLC (Thin Layer Chromatography). Once the reaction was completed the organic solvent was rota evaporated and purified by flash column chromatography with an EA/hexane solvent system, to afford analogs **(ST-98)-(ST-139)** in yields ranging from 60-90%.

ST-98: ^{1}H NMR (DMSO-d_6): δ 3.71 (s, 3H, -OCH_3), 3.75 (s, 3H, -OCH_3), 3.82 (s, 3H, -OCH_3), 3.85 (s, 6H, -OCH_3), 3.89 (s, 3H, -OCH_3), 6.61 (s, 1H, ArH), 6.94 (d, J=8.4 Hz, 2H), 7.00 (S, 3H, ArH), 7.08 (d, J=16 Hz, 2H), 7.28 (d, J=16 Hz, 2H), 7.49 (d, J=8.4 Hz, 1H), 7.98 (s, 1H, ArH) ppm. ^{13}C-NMR (DMSO-d_6): δ 55.1, 55.3, 55.8, 56.1, 56.4, 98.2,

101.5, 104.7, 108.1, 110.5, 115.4, 117.6, 114.2, 121.4, 127.6, 131.7, 134.2, 159.7, 160.7, 162.8 166.7 ppm.

ST-127: ^{1}H NMR (DMSO-d_6): δ 3.74 (s, 3H, -OCH_3), 3.81 (s, 6H, -OCH_3), 3.84 (s, 3H, -OCH_3), 3.89 (s, 3H, -OCH_3), 6.60 (s, 1H, ArH), 6.93 (d, J=8.4 Hz, 2H), 6.97 (s, 1H, ArH), 7.03-7.07 (m, 2H), 7.28 (m, 2H), 7.33 (s, 1H, ArH), 7.47 (d, J=8.4 Hz, 2H), 7.89 (s, 1H, ArH) ppm. ^{13}C-NMR (DMSO-d_6): δ 55.3, 55.4, 56.2, 56.4, 56.8, 56.9, 97.5, 100.8, 104.7, 108.4, 111.5, 111.8, 114.5, 124.7, 129.5, 131.4, 134.8, 138.4, 147.5, 149.6, 158.7, 163.8, 164.5 ppm.

ST-99: ^{1}H NMR (DMSO-d_6): δ 3.75 (s, 3H, -OCH_3), 3.81 (s, 9H, -OCH_3), 3.89 (s, 3H, -OCH_3), 6.61 (d, J=7.2 Hz, 2H), 6.87 (d, J=1.6 Hz, 2H), 6.94 (d, J=8.8 Hz, 2H), 6.98 (d, J=1.2 Hz, 1H), 7.07 (d, 1H, J=16.0 Hz, ArH), 7.27 (d, 1H, J=16.0 Hz, ArH),7.49 (d, 1H, J=8.4 Hz, ArH), 8.03 (s, 1H, ArH) ppm. ^{13}C-NMR (DMSO-d_6): δ 55.2, 55.8, 55.9, 99.5, 100.5, 101.7, 109.5, 118.6, 120.5, 114.2, 127.4, 131.4, 136.3, 158.5, 160.7, 161.5. ppm.

ST-100: ^{1}H NMR (DMSO-d_6): δ 3.75 (s, 3H, -OCH_3), 3.81 (s, 6H, -OCH_3), 3.89 (s, 3H, -OCH_3), 6.60 (S, 1H, ArH), 6.91-7.07 (m, 6H, *J*= 64.8 Hz ArH), 7.22 (d, 1H, *J*= 16.4 Hz, ArH), 7.45 (d, 2H, ArH ,*J*= 8.4 Hz), 7.68 (d, 2H, ArH and *J*= 8 Hz), 7.83 (s, 1H, ArH). ^{13}C-NMR (DMSO-d_6): δ 55.6, 55.9, 55.9, 56.1, 98.2, 102.2, 114.7, 115.5, 117.2, 117.6, 123.7, 126.1, 128.5, 129.6, 129.7, 129.9, 131.6, 133.8, 138.9, 139.4, 158.9, 159.7, 161.6 ppm.

ST-128: ^{1}H NMR (DMSO-d_6): δ 3.78 (s, 3H, -OCH_3), 3.86 (s, 3H, -OCH_3), 3.88 (s, 3H, -OCH_3), 6.18 (s, 1H, ArH), 6.75 (d, J=8.6 Hz, 2H), 6.83 (s, 2H, ArH), 7.12 (d, 1H, J=16.0 Hz, ArH), 7.28 (d, 1H, J=16.0 Hz, ArH), 7.43-7.50 (m, 6H, ArH), 7.77 (d, 2H, *J*= 8.4 Hz, ArH), 8.01 (s, 1H, ArH). ^{13}C-NMR (DMSO-d_6): δ 55.7, 55.2, 56.4, 99.1, 101.2, 114.7, 117.3, 117.9, 118.9, 124.8, 126.6, 127.6, 128.2, 129.5, 129.8, 131.9, 135.4, 138.5, 140.2, 158.6, 158.8, 162.4 ppm.

ST-139: ^{1}H NMR (DMSO-d_6): δ 3.74 (s, 3H, -OCH_3), 3.82 (s, 3H, -OCH_3), 3.89 (s, 3H, -OCH_3), 6.13 (s, 1H, ArH), 6.93 (d, J=8.8 Hz, 2H), 6.98 (s, 2H, ArH), 7.08 (d, 1H, J=16.4 Hz, ArH), 7.22 (d, 1H, J=16.4 Hz, ArH), 7.45-7.51 (m, 6H, ArH), 7.76 (d, 2H, *J*= 7.2 Hz, ArH), 7.98 (s, 1H, ArH). ^{13}C-NMR (DMSO-d_6): δ 55.5, 55.9, 56.1, 98.2, 102.2, 114.7, 115.5, 117.1, 117.59, 123.6, 126.0, 128.4, 129.5, 129.6, 129.9, 131.9, 133.8, 138.9, 139.4, 158.8, 159.6, 161.6 ppm.

For preparing compound **ST-54**, *E*-2,4-dimethoxy-6-(4-methoxystyryl)benzaldehyde (**RES-11**) and quinuclidinone (1.2 mmol) were added to 10 volumes of methanol and the resulting mixture stirred at room temperature. The final product **ST-54**, crashed out of the solution once the reaction was complete in 1-2 hrs. The final product was filtered and recrystallized from methanol to afford **ST-54** in 80% yield. In the next step, compound **ST-54** (1mmol), hydroxylamine HCl (1.1 mmol) and sodium acetate (1.5 mmol) were dissolved in 10 volumes of ethanol and the mixture was heated under reflux for 6 hrs. A white precipitate was formed, which was later filtered off to afford **ST-57** in 65% yield **(Scheme 2.3)**.**ST-54**: ^{1}H NMR (DMSO-d_6): δ 1.96 (d, J=3 Hz, 4H), 2.63 (s, 1H), 2.90–2.92 (m, 4H), 3.72–3.82 (m, 6H), 3.86 (s, 3H), 6.39 (d, J=3 Hz, 1H), 6.78 (d, J=3 Hz,

1H), 6.86 (d, J=9 Hz, 2H), 6.95 (d, J=6 Hz, 2H), 7.26 (s, 1H), 7.38 (d, J=6 Hz, 2H) ppm .^{13}C NMR (DMSO-d6): δ 26.1, 41.0, 48.2, 49.7, 55.6, 55.7, 55.9, 97.9, 101.6, 114.3, 123.9, 125.4, 127.9, 128.0, 129.8, 130.2, 138.4, 158.8, 159.5, 160.9 ppm. mp: 178–180 °C.

ST-57: ^{1}H NMR (DMSO-d_6): δ 1.98 (d, J=3 Hz, 4H), 2.43 (s, 1H), 2.73–2.76 (m, 4H), 3.79–3.84 (m, 6H), 4.13 (s, 3H), 6.46 (d, J=4 Hz, 1H), 6.84 (d, J=4.4 Hz, 1H), 6.89 (d, J=9 Hz, 2H), 6.93 (d, J=6 Hz, 2H), 7.28 (s, 1H), 7.41 (d, J=8.4 Hz, 2H) ppm.^{13}C NMR (DMSO-d6): δ 26.1, 41.0, 48.2, 49.7, 55.6, 55.7, 55.9, 97.9, 101.6, 114.3, 123.9, 125.4, 127.9, 128.0, 129.8, 130.2, 138.4, 158.8, 159.5, 160.9 ppm. mp: 142–145 °C.

X-ray crystallographic data for the representative compounds **RES-27, RES-17** and **RES-54** were obtained which confirmed the *Z*-geometry (**Figure 2.4**) in these analogs (Madadi, Reddy et al. 2010, Madadi, Parkin et al. 2012).

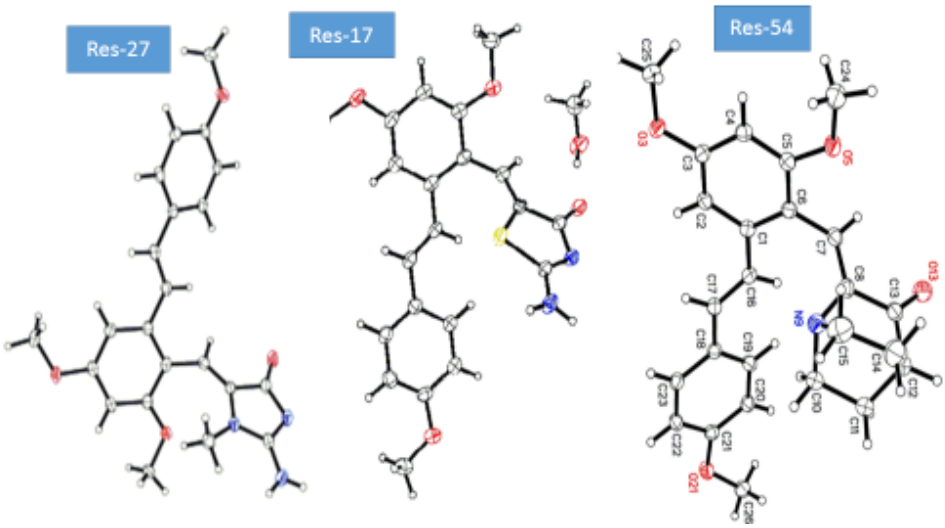

Figure. 2.4 Crystal structures of compounds **RES-27**, **RES-17** and **RES-54**.

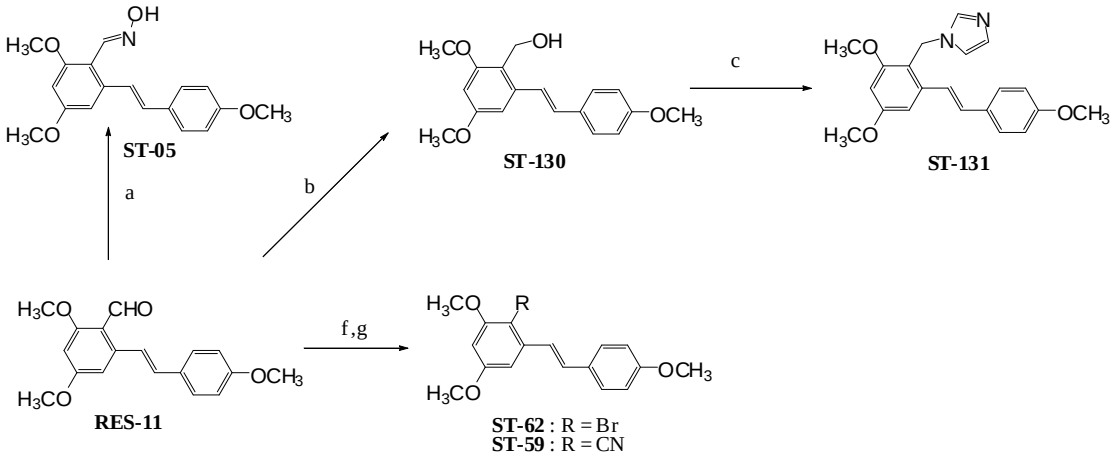

Scheme 2.4 Synthesis of resveratrol analogs with hydroxamine, benzylalcohol, bromo, cyano and imidazole substitutions at the C2 position (a) NH_4OH, NaOAc, ethanol, reflux 4hrs; (b) $NaBH_4$, methanol; (c) imidazole, neat, MW 180 ^{0}C, 5min (f) N-bromosuccinamide, $CHCl_3$; (g) Aq.NH_3, I_2, THF.

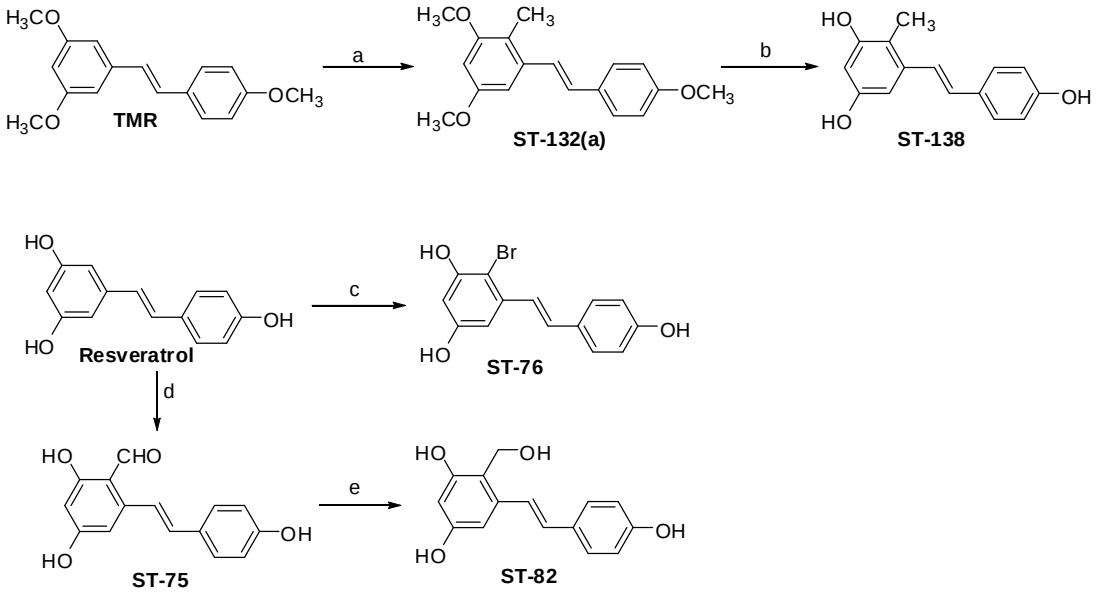

Scheme 2.5: Synthesis of resveratrol analogs with methyl, benzylalcohol and bromo substitutions at the C2 position (a) MeI, K_2CO_3, acetone, reflux 12hrs. (c) *N*-bromosuccinamide, $CHCl_3$; (e) $NaBH_4$, methanol.

We wanted to compare the anti-cancer activity of C2 conjugated five and six-membered heterocyclic and bicyclic quinuclidinone ring systems with simpler and smaller functionalities. Below are the analytical data and reaction conditions for the synthesized compounds:

ST-138: ^{1}H NMR (400 MHz, DMSO-d_6): δ 3.32 (s, 3H, -CH_3), 6.22 (d, *J* =2 Hz, 1H, ArH), 6.45 (d, *J* =2 Hz, 1H, ArH), 6.74 (d, *J* =8.4 Hz, 2H, ArH), 6.82 (d, *J* =16 Hz, 2H, ArH), 7.12 (d, *J* =16 Hz, 2H, ArH), 7.41 (d, *J* =7.2 Hz, 8.8H, ArH), 8.91 (s, 1H, -OH), 9.09 (s, 1H, -OH), 9.53 (s, 1H, -OH) ppm. ^{13}C NMR (100 MHz, DMSO-d_6): 11.2, 103.0, 112.8, 115.9, 123.9, 128.2, 128.8, 129.4, 138.1, 155.8, 156.4, 157.5 ppm.

ST-76: δ 6.38 (s, 1H, ArH), 6.63 (s, 1H, ArH), 6.79 (d, *J* =5.6 Hz, 2H, ArH), 6.96 (d, *J* =16.4 Hz, 1H, ArH), 7.18 (d, *J* =16 Hz, 1H, ArH), 7.41 (d, *J* =6 Hz, 2H, ArH), 9.44 (s,

1H, -OH), 9.62 (s, 1H, -OH), 9.99 (s, 1H, -OH) ppm. ^{13}C NMR (100 MHz, DMSO-d_6): 101.2, 102.8, 104.4, 110.0, 116.0, 124.5, 128.1, 128.5, 131.2, 138.5, 155.3, 157.5, 158.0 ppm.

ST-75: δ 6.58 (s, 1H, ArH), 6.72 (s, 1H, ArH), 6.80 (d, *J* =5.6 Hz, 2H, ArH), 6.92 (d, *J* =16.4 Hz, 1H, ArH), 7.06 (d, *J* =16 Hz, 1H, ArH), 7.52 (d, *J* =6 Hz, 2H, ArH), 9.19 (s, 1H, -CHO), 9.95 (s, 1H, -OH), 10.45 (s, 1H, -OH), 10.66 (s, 1H, -OH) ppm. ^{13}C NMR (100 MHz, DMSO-d_6): 98.7, 101.8, 103.3, 116.7, 116.0, 124.5, 128.1, 128.5, 134.4, 138.5, 157.5, 157.9, 193.1 ppm.

ST-82: δ 3.59 (s, 2H, -CH_2), 6.10 (s, 1H, ArH), 6.46 (s, 1H, ArH), 6.77 (d, *J* =9.2 Hz, 2H, ArH), 6.81 (s, 1H, ArH), 7.19 (d, *J* =16.0 Hz, 1H, ArH), 7.40 (d, *J* =8.4 Hz, 1H, ArH) ppm. ^{13}C NMR (100 MHz, DMSO-d_6): 43.9, 101.9, 103.0, 109.5, 111.5, 115.5, 123.1, 127.9, 128.3, 129.6, 138.2, 157.0, 157.2, 158.8 ppm.

ST-05: *E*-2,4-Dimethoxy-6-(4-methoxystyryl)benzaldehyde (**RES-11**) (1mmol), hydroxylamine HCl (1.1 mmol) and sodium acetate (1.5 mmol) were dissolved in 10ml of ethanol and the resulting mixture was heated under reflux for 4 hrs. A white precipitate was formed, which was later filtered off to afford **ST-05** in 80% yield. ^{1}H NMR (DMSO-d_6): δ 3.77 (s, 3H, -OCH_3), 3.81 (s, 3H, -OCH_3), 3.85 (s, 3H, -OCH_3), 6.54 (s, 1H, -ArH), 6.89 (s, 1H, -ArH), 6.93-6.96 (d, 2H, -ArH; *J* = 8.4 Hz), 7.11-7.15 (d, 1H, -ArH; *J* = 16.4 Hz), 7.45-7.47 (d, 2H, -ArH; *J* = 8 Hz), 7.59-7.63 (d, 1H, -ArH; *J* = 16.4Hz), 8.30 (s, 1H, -ArH), 11.15 (s, 1H, -OH) ppm. ^{13}C-NMR (DMSO-d_6): δ 55.6, 55.8, 55.3, 98.0, 102.7, 110.0, 112.6, 114.6, 126.4, 128.3, 130.1, 130.5, 138.7, 145.2, 159.4, 159.7, 161.0 ppm.

ST-130: *E*-2,4-Dimethoxy-6-(4-methoxystyryl)benzaldehyde (**RES-11**) (1mmol) was dissolved in methanol and cooled to 0 ^{0}C and $LiBH_4$(1.0 mmol) was added. The reaction mixture was allowed to stir for 1 hr at ambient temperature. The reaction was monitored by TLC, and after consumption of the starting materials, the reaction mixture was concentrated and extracted into ethyl acetate followed by concentration on a rotary evaporator. Flash column chromatography was carried out using an EA/hexane solvent system to afford **ST-130** in 85% yield. **(ST-130**): ^{1}H NMR ($CDCl_3$): δ 3.83 (s, 3H, -OCH_3), 3.85 (s, 3H, -OCH_3), 3.86 (s, 3H, -OCH_3), 4.79 (s, 2H, CH2), 6.41 (s, 2H, CH2), 6.72 (d, J=2.0 Hz, 1H), 6.91 (d, 2H, J=8.8 Hz, ArH), 6.98 (d, 1H, J=16.0 Hz, ArH), 7.36 (d, 1H, J=16.0 Hz, ArH), 7.47 (d, 2H, *J*= 8.4 Hz, ArH) ppm. ^{13}C-NMR (DMSO-d_6): δ 56.1, 56.7, 56.8, 58.6, 99.4, 99.8, 101.2, 114.5, 121.3, 124.5, 125.4, 129.7, 131.2, 136.4, 153.4, 156.7, 159.6 ppm.

ST-131: Compound **ST-130** (1mmol) and imidazole (5mmol) were added to a synthetic microwave vial and irradiated for 2 min at 80 ^{0}C using a Biotage Initiator synthetic microwave. The reaction was monitored by TLC. After the starting material had completely disappeared, ethyl acetate was added and the excess imidazole was washed out with water. The ethyl acetate solvent was removed on a rotavaporator to yield **ST-131** in 95 % yield. ^{1}H NMR (DMSO-d_6): δ 3.78 (s, 3H, -OCH_3), 3.83 (s, 3H, -OCH_3),3.85 (s, 3H, -OCH_3), 5.29 (s, 2H, -CH_2), 6.55-6.56(d, *J*=2 Hz, 1H, ArH), 6.79 (S, 1H, ArH), 6.86-6.87(d, *J*=2Hz, 1H, ArH), 6.94-6.97(d, J=8.4 Hz, 2H, ArH), 7.12-7.16 (d, *J*=16 Hz, 1H, ArH), 7.41-7.46 (d, *J*=16.4 Hz, 1H, ArH), 7.57 (s, 1H, ArH), 7.61-7.63 (d, *J*= 8.8 Hz, 2H, ArH) ppm. ^{13}C-NMR (DMSO-d_6): δ 55.6, 55.7, 56.3, 98.2, 102.1, 110.0, 114.6, 115.3, 119.3, 122.6, 128.5, 128.7, 129.9, 131.9, 137.3, 139.3, 159.3, 159.7, 160.7 ppm.

ST-62: To a solution of *trans*-2-formyl-3,4′,5-trimethoxystilbene (**RES-11**) (1.4 mmol) in $CHCl_3$ (need volume), was added drop-wise at 0-5 ^{0}C *N*-bromosuccinimide (1.7 mmol). The reaction mixture was stirred for 2 hrs and was monitored by TLC. After compound **RES-11** was consumed the mixture was added to 10 volumes of water and then extracted with 4 volumes of CH_2Cl_2. Removal of impurities from the product was achieved by column chromatography using a silica gel column and an ethyl acetate/hexane solvent system to afford **ST-62** in 65% yield. ^{1}H NMR ($CDCl_3$): δ 3.83 (s, 3H), δ 3.86 (s, 3H), δ 3.88 (s, 3H), 6.41 (s, 1H), 6.79 (s, 1H), 6.89 (d, 2H, J=8.8 Hz, ArH), 6.94 (d, 1H, J=16.0 Hz, ArH), 7.37 (d, 1H, J=16.0 Hz, ArH), 7.50 (d, 2H, J=8.8 Hz, ArH) ppm; ^{13}C-NMR ($CDCl_3$): δ 55.1, 55.8, 100.3, 104.6, 105.1, 114.2, 127.4, 137.8, 157.9, 160.2 ppm.

ST-59: *Trans*-2-formyl-3,4′,5-trimethoxystilbene (**RES-11**)(1 mmol) was dissolved in 1ml of THF and 10 ml of 28% aqueous NH_3 solution. Iodine (1.1 mmol) was added and the mixture stirred at room temperature for 1hr. The reaction mixture was quenched with $Na_2S_2O_3$ followed by extraction with diethyl ether to afford the nitrile product **ST-59** in 55% yield. ^{1}H NMR ($CDCl_3$): δ 3.79 (s, 3H), δ 3.82 (s, 3H, -OCH_3), δ 3.83 (s, 3H, -OCH_3), 6.46 (s, 3H, -OCH_3), 6.82 (s, 1H), 6.87 (d, 2H, J=8.8 Hz, ArH), 6.97 (d, 1H, J=16.0 Hz, ArH), 7.39 (d, 1H, J=16.0 Hz, ArH), 7.52 (d, 2H, J=8.8 Hz, ArH) ppm; ^{13}C-NMR ($CDCl_3$): δ 56.4, 56.7, 56.9, 98.6, 99.8, 103.2, 114.5, 121.3, 124.5, 125.4, 128.7, 131.2, 136.4, 154.4, 156.7, 160.6 ppm.

ST-132(a): (*E*)-1,3-Dimethoxy-5-(4-methoxystyryl)benzene (1 mmol) was dissolved in 10 volumes of anhydrous acetone. MeI (2 eq) and K_2CO_3 (5 eq) were added to the solution and the mixture refluxed overnight to afford (*E*)-1,5-dimethoxy-3-(4-methoxystyryl)-2-methylbenzene (**ST-132(a)**) along with a mixture of unidentified

methylated products. The resveratrol analog (**ST-132(a)**) was isolated by silica gel chromatography utilizing ethyl acetate/hexane as eluting solvent in 40 % yield. (**ST-132(a)**): molecular formula: $C_{18}H_{20}O_3$; ^{1}H NMR (DMSO-d_6): δ 3.82-3.85 (t, *J*= 13.6 Hz, 9H, -OCH_3), 6.40-6.41(d, *J*= 2.4 Hz, 1H, ArH), 6.72-6.73(d, *J*= 2.4 Hz, 1H, ArH), 6.90-6.94 (m, *J*=18 Hz, 3H, ArH), 7.21-7.25 (d, *J*=16 Hz, 1H, ArH), 7.45-7.48 (d, *J*= 8.8 Hz, 1H, ArH) ppm. ^{13}C-NMR (DMSO-d_6): δ 10.9, 55.3, 55.4, 55.6, 97.7, 101.2, 114.1, 117.1, 124.9, 127.8, 129.9, 130.4, 138.1, 158.3, 158.6, 159.3. ppm. mp: 55-57 ^{o}C.

2.4 Synthesis of (*Z*)-2,3-diaryl substituted acrylonitriles as anticancer agents.

2.4.1 Prior studies with this scaffold

In 2011, Tarleton and coworkers serendipitously discovered a family of 2-phenylacrylonitriles (**Figure 2.5**, **A**) with potent growth inhibition properties against a panel of ten human cancer cell lines: HT29 and SW480 (colon cancer), MCF-7 (breast cancer), A2780 (ovarian cancer), H460 (lung cancer), A431 (skin cancer), DU145 (prostate cancer), BEC-2 (neuroblastoma), SJ-G2 (glioblastoma), and MIA (pancreatic cancer) (Tarleton, Gilbert et al. 2011). They reported (*Z*)-2-(3,4-dichlorophenyl)-3-(4-nitrophenyl)acrylonitrile (**Figure 2.5**, **A**) as the lead compound from their studies with a GI_{50} value of 0.127 μM against the (ER+ve) human breast cancer cell line, MCF-7 with a 543-fold selectivity towards MCF-7 cells compared with nine other non-breast derived cancer cell lines.

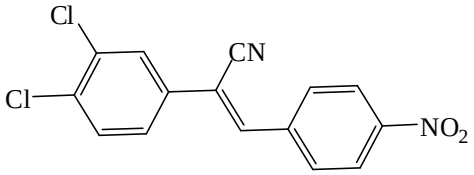

(A) 2-phenylacrylonitriles

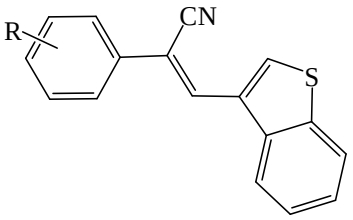

(B) (Z)-benzothiophene acrylonitriles

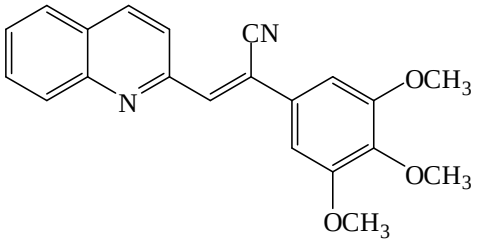

(C) (Z)-3-(quinolin-2-yl)-2-(3,4,5-trimethoxyphenyl)acrylonitrile

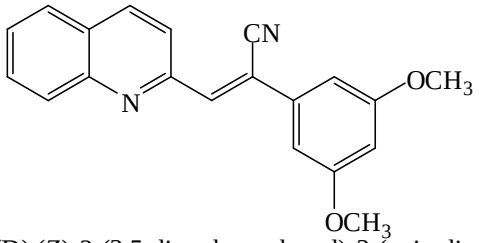

(D) (Z)-2-(3,5-dimethoxyphenyl)-3-(quinolin-2-yl)acrylonitrile

Figure 2.5 Structures of literature reported potent anti-cancer agents in the phenylacrylonitrile series.

Recently, our laboratory has reported on a series of (*Z*)-benzothiophene acrylonitrile analogues (**Figure 2.5**, **B**) as potent anti-cancer agents with GI_{50} values generally in the range 10–100 nM against a panel of 60 human cancer cell lines. Of interest, these compounds are also able to overcome cell-associated P-glycoprotein mediated resistance, since they were equipotent in inhibiting OVCAR8 and NCI/ADR-RES cell growth (Penthala, Sonar et al. 2013).

Also, our laboratory has synthesized and evaluated a series of (*Z*)-quinolinyl acrylonitrile derivatives **(Figure 2.5, C, D)** as anticancer agents against a panel of 60 human cancer cell lines**.** Of these compounds, (Z)-3-(quinolin-2-yl)-2-(3,4,5-trimethoxyphenyl)acrylonitrile (**Figure 2.5, C**) showed potent cytotoxicity against MDA-

MB-435 melanoma and NCI-H522 non-small cell lung cancer line with GI_{50} values of 33 nM and 37 nM, respectively. (Z)-2-(3,5-Dimethoxyphenyl)-3-(quinolin-2-yl)acrylonitrile (**Figure 2.5, D**) also displayed potent growth inhibitory activity against NCI-H522 non-small cell lung cancer lines with a GI_{50} value of 94 nM (Penthala, Janganati et al. 2014).

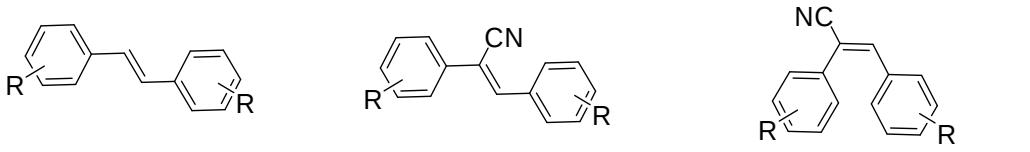

(**E**) (*E*)-diaryl stilbenes (**F**) (*Z*)-diarylacrylonitriles (**G**) (*E*)-diarylacrylonitriles

Figure 2.6 Scaffolds of reported potent anticancer agents in the stilbene and phenylacrylonitrile series.

Of interest, Ohsumi *et al.* had reported (*E*)-substituted diarylacrylonitrile analogs (**Figure 2.6, G**) as effective anti-cancer agents against murine solid tumors, but failed to mention or compare the activity of their *Z*-isomers (Ohsumi, Nakagawa et al. 1998). In the current work the stilbene structural fragments present in resveratrol are modified by introducing a cyano group on the double bond bridge and incorporating methoxy substituents into the phenyl rings to improve the compound's potency. Also, a small structure-anticancer activity relationship (SAR) study was performed by comparing the GI_{50} and TGI values from the cytotoxic assay of the synthesized substituted stilbenes (**Figure 2.6, E**) and (*E/Z*)-substituted diarylacrylonitriles analogs (**Table 2.2**).

2.4.2 Chemistry and analytical data

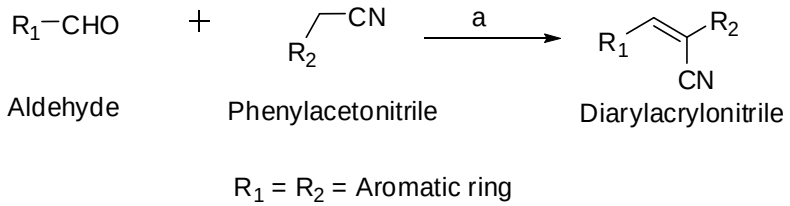

Scheme 2.6 Synthesis of (*Z*)-2,3-diaryl substituted acrylonitriles; reagents and conditions: (a) 5% NaOMe, MeOH, reflux.

A series of (*Z*)-substituted diarylacrylonitrile analogs (**Table 2.2**) were synthesized by reacting substituted benzyl carbaldehydes with their corresponding substituted phenylacetonitriles in 5% sodium methoxide/methanol. The reaction mixture was stirred at room temperature for 2-3 hours. On completion of the reaction, the desired product crashed out of the solution. The precipitate was filtered off, washed with water and dried to yield the final compound in yields ranging from 70-95 % (**Scheme 2.6**). Compounds with (*Z*)-geometry can convert to their corresponding (*E*)-isomer under certain reaction conditions. This conversion is also dependent on the nature of substituents and functionalities (electron donating or accepting) on the aryl rings. However, base-catalyzed condensation reactions have been reported to form exclusively *Z*-isomer products (Penthala, Sonar et al. 2013).

Table 2.2 Structures of the synthesized diarylacrylonitrile products and the starting materials (aldehyde and phenylacetonitrile precursors) utilized in their preparation

	Aldehyde precursor	Phenylacetonitrile precursor	Diarylacrylonitrile product
1.	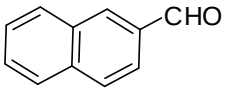	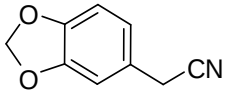	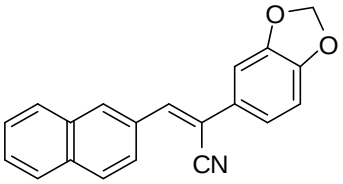 ST-215
2.	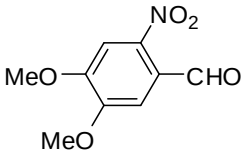	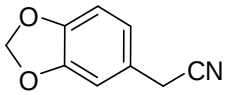	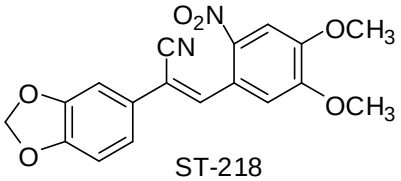 ST-218
3.	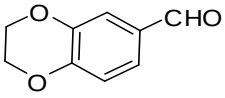	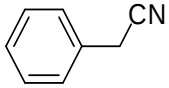	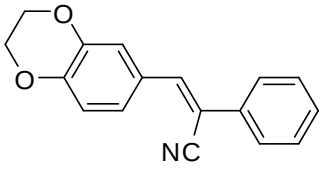 ST-254
4.	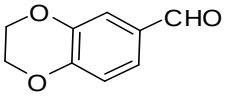	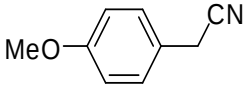	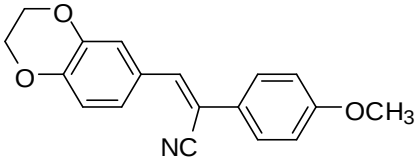 ST-252

Table 2.2 (continued)

5.	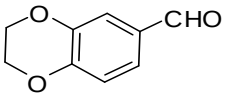	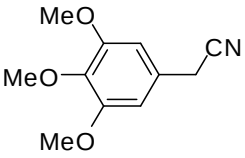	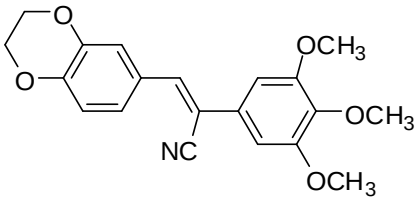 ST-253
6.	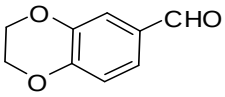	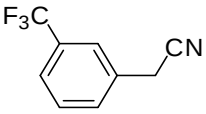	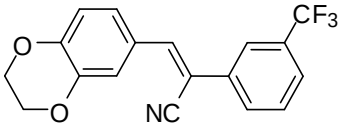 ST-255
7.	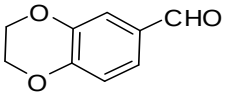	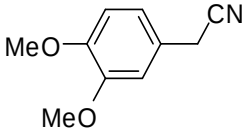	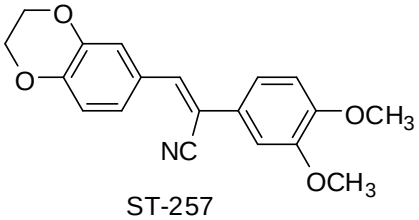 ST-257
8.	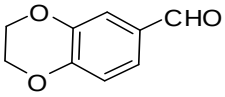	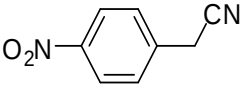	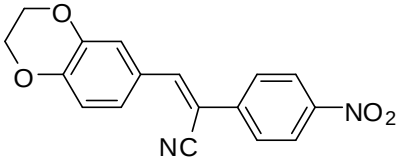 ST-258
9.	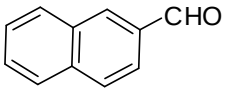	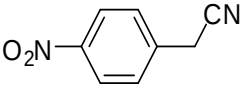	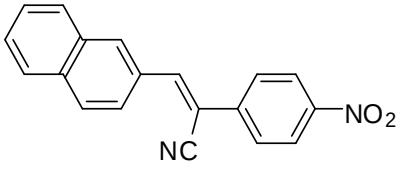 ST-259
10	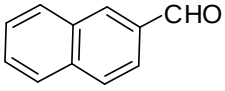	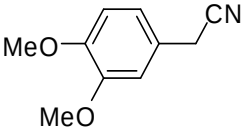	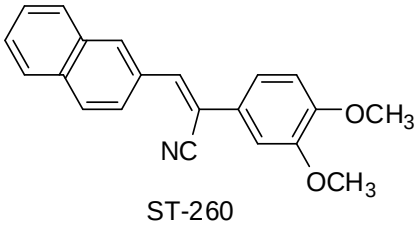 ST-260

Table 2.2 (continued)

11	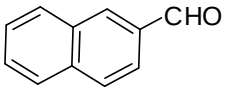	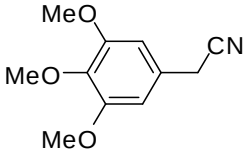	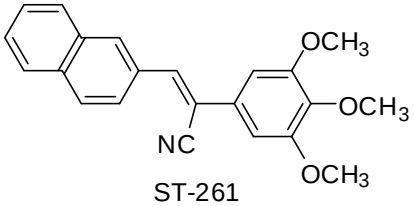 ST-261
12	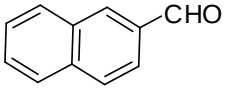	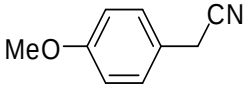	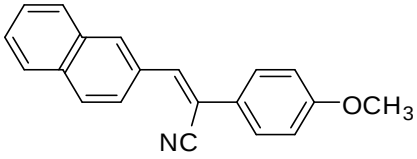 ST-262
13	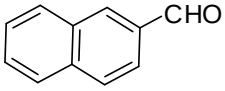	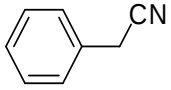	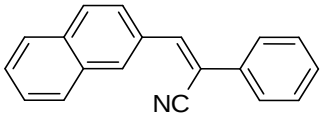 ST-263
14	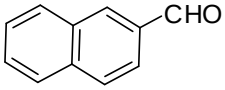	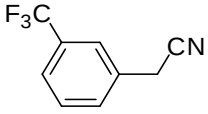	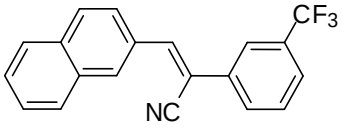 ST-264
15	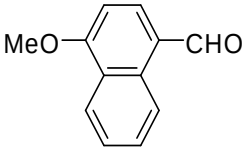	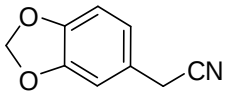	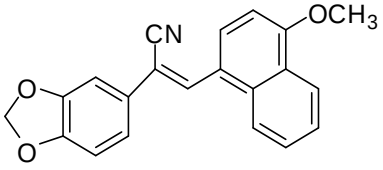 ST-179

Table 2.2 (continued)

16	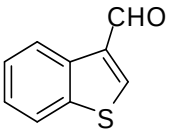	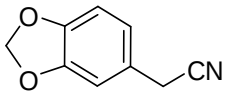	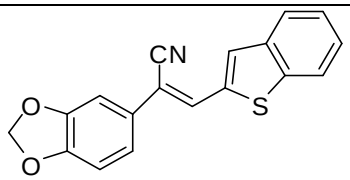 ST-180
17	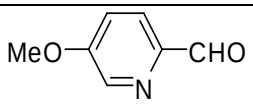	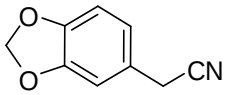	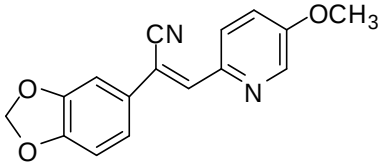 ST-181
18	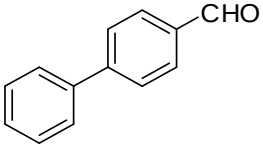	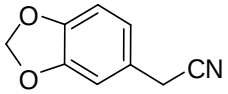	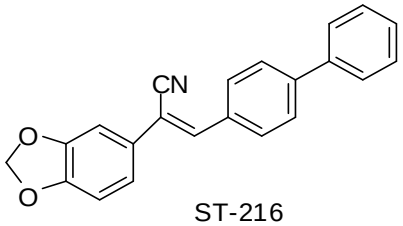 ST-216
19	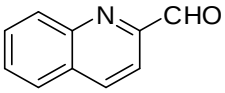	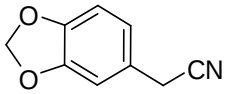	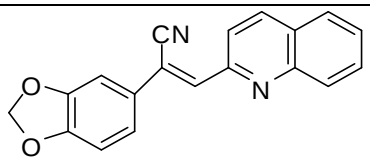 ST-183
20	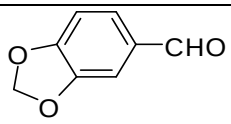	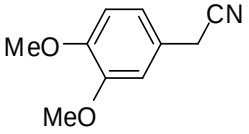	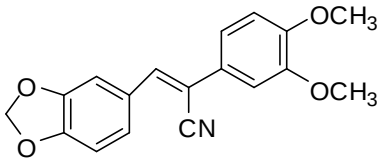 ST-185
21	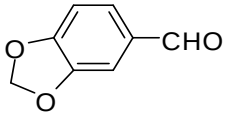	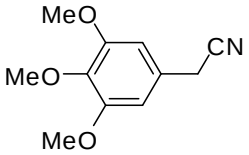	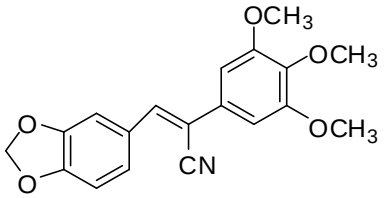 ST-160

Table 2.2 (continued)

22	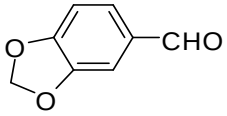	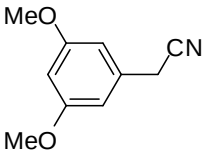	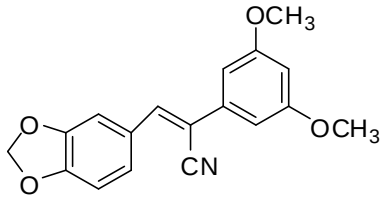 ST-155
23	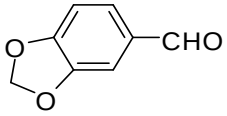	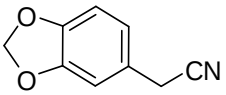	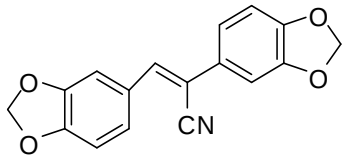 ST-161
24	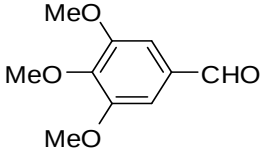	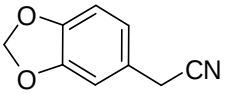	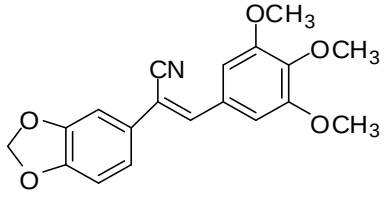 ST-162
25	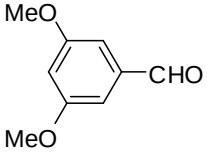	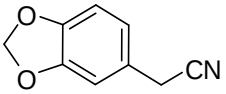	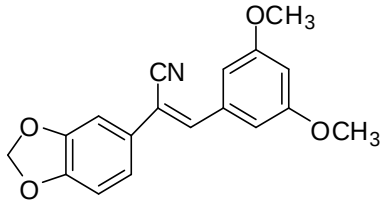 ST-164
26	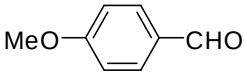	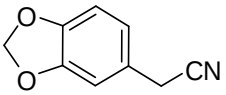	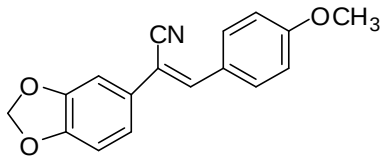 ST-163
27	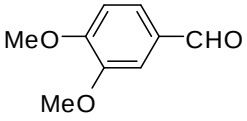	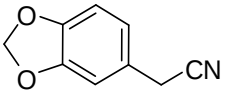	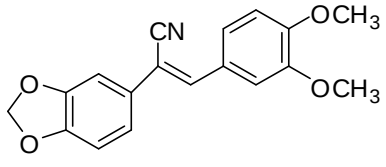 ST-165

Table 2.2 (continued)

28	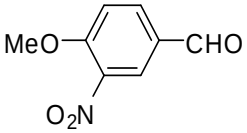	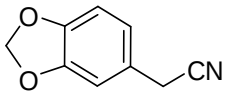	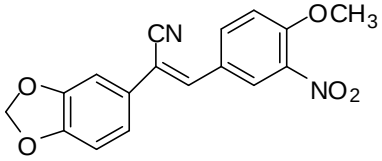 ST-166
29	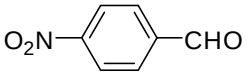	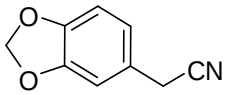	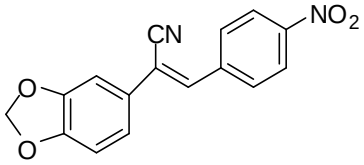 ST-167
30	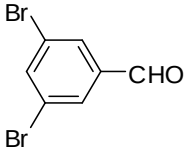	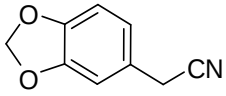	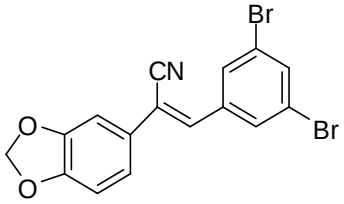 ST-168
31	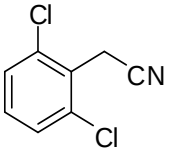	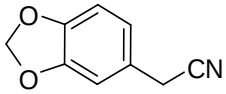	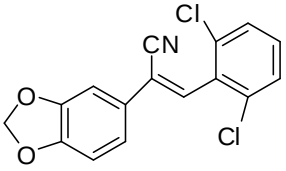 ST-169
32	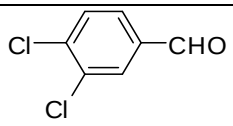	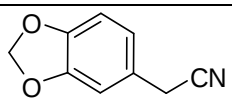	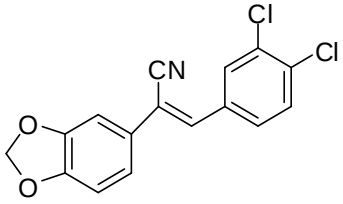 ST-170

Table 2.2 (continued)

33	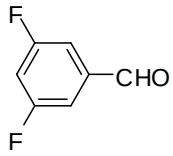	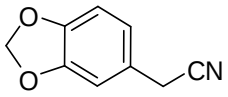	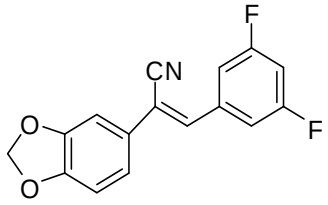 ST-171
34	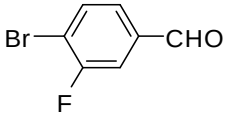	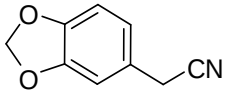	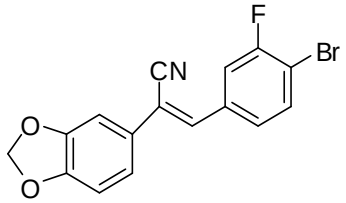 ST-172
35	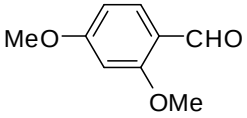	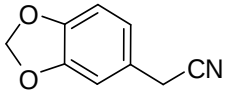	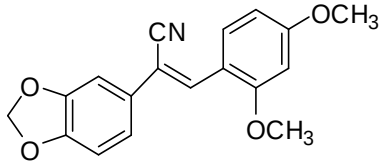 ST-173
36	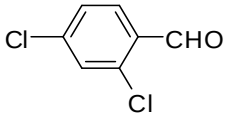	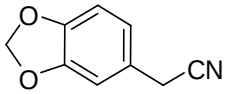	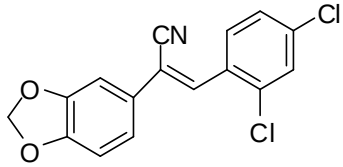 ST-174
37	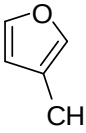	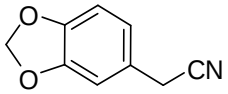	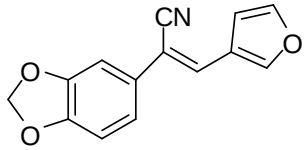 ST-175
38	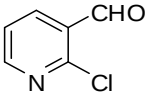	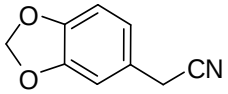	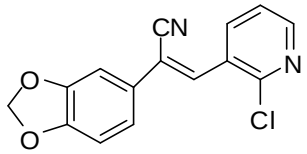 ST-176

Table 2.2 (continued)

39	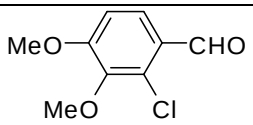	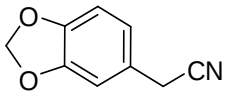	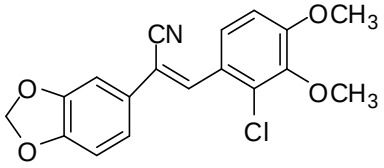 ST-177
40	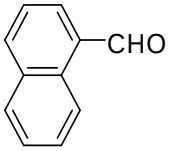	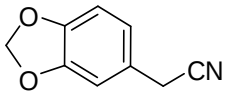	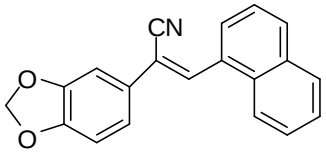 ST-178
41	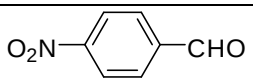	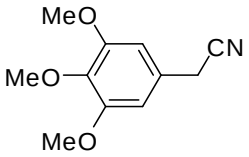	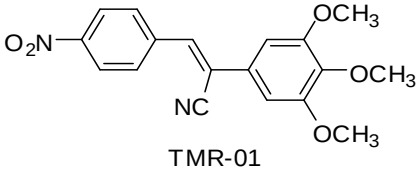 TMR-01
42	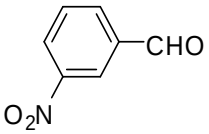	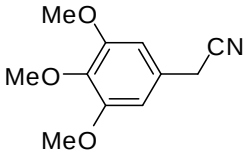	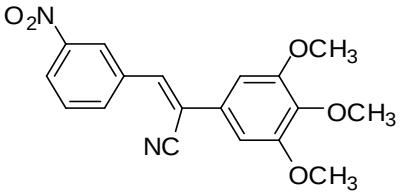 TMR-03
43	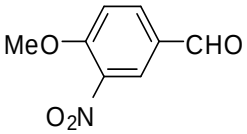	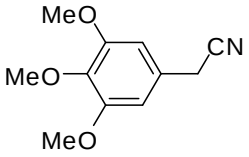	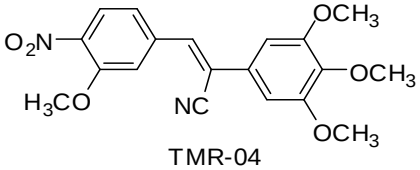 TMR-04
44	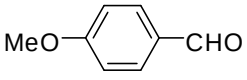	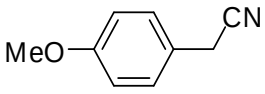	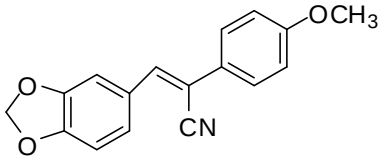 ST-153

Table 2.2 (continued)

45	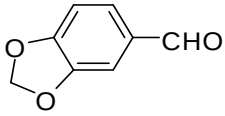	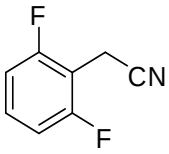	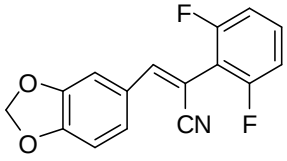 ST-184
46	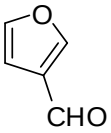	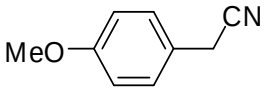	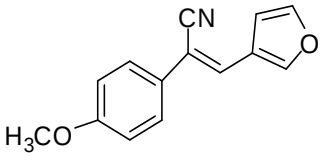 ST-288
47	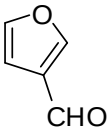	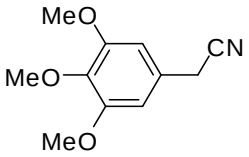	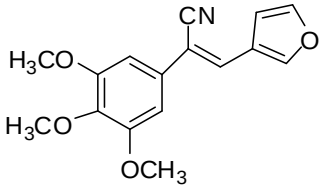 ST-287
48	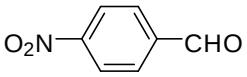	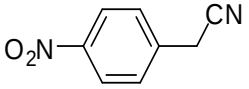	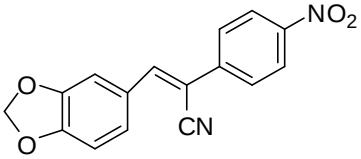 ST-156
49	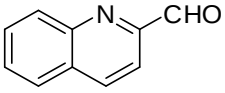	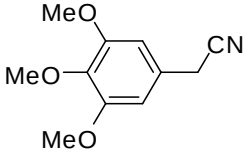	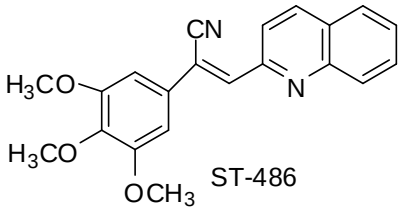 ST-486
50	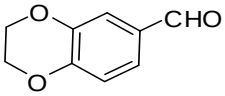	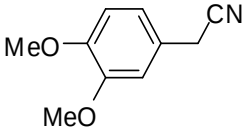	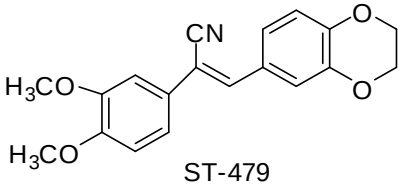 ST-479

Table 2.2 (continued)

51	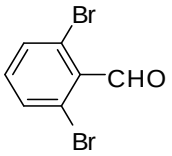	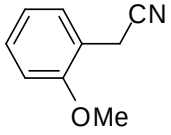	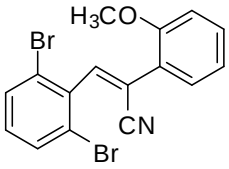 ST-152
52	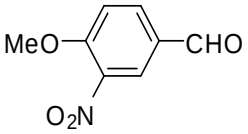	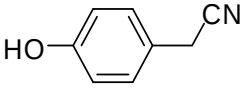	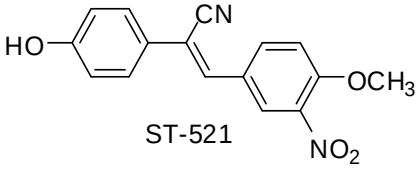 ST-521
53	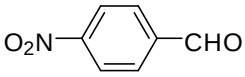	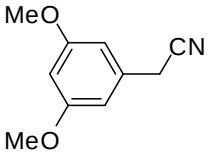	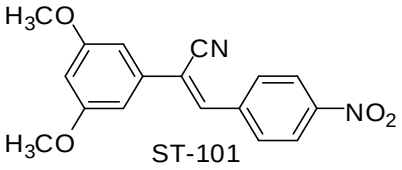 ST-101
54	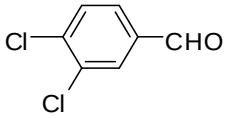	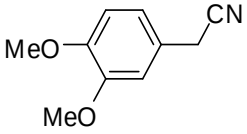	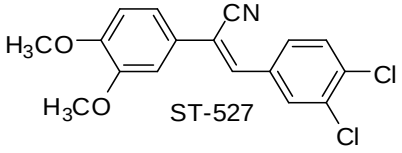 ST-527
55	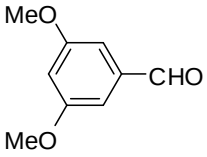	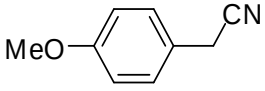	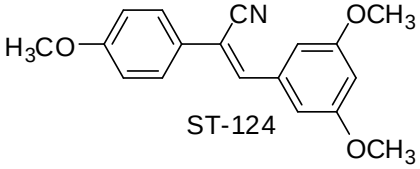 ST-124
56	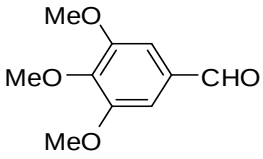	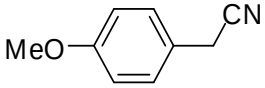	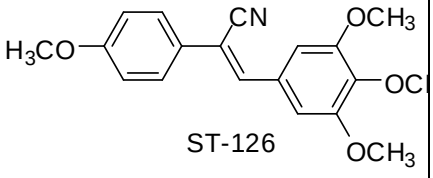 ST-126
57	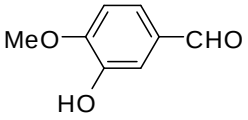	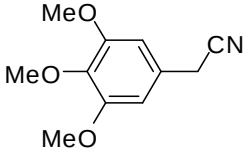	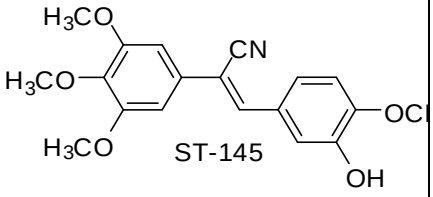 ST-145

Table 2.2 (continued)

58	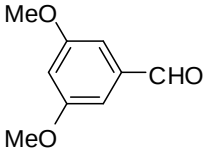	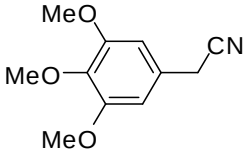	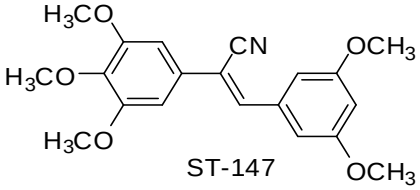 ST-147
59	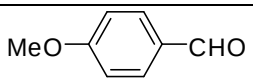	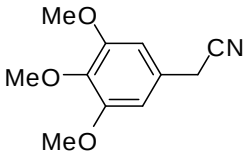	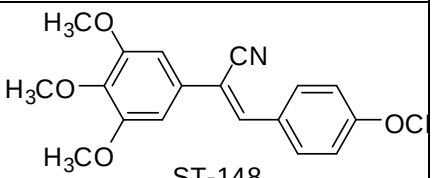 ST-148
60	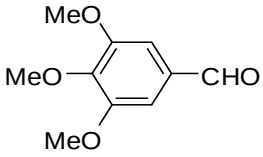	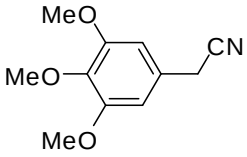	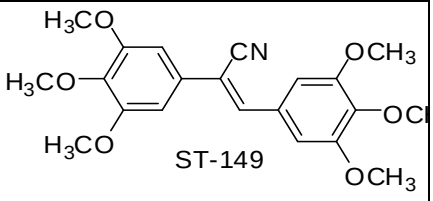 ST-149
61	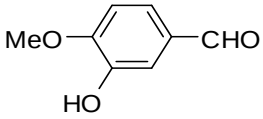	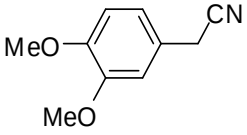	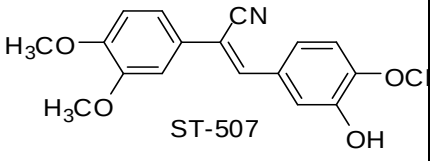 ST-507
62	-	-	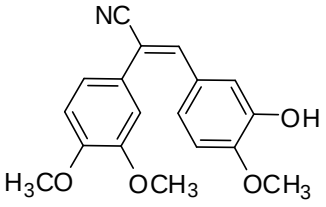 ST-507(A) *
63	-	-	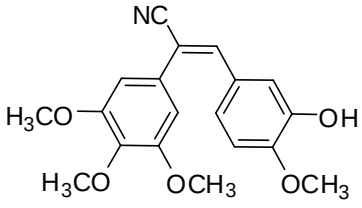 ST-510 *

Table 2.2 (continued)

64	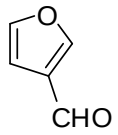	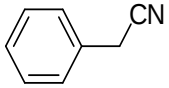	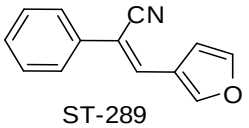 ST-289
65	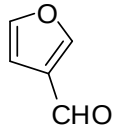	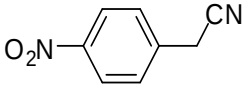	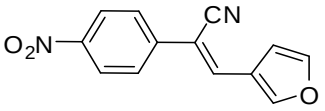 ST-290
66	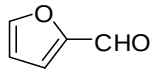	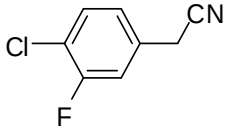	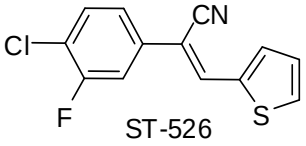 ST-526
67	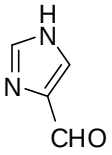	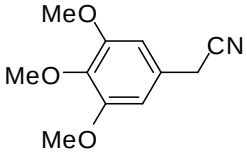	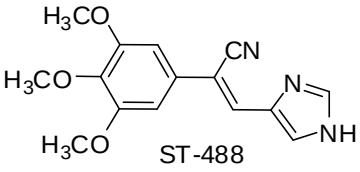 ST-488
68	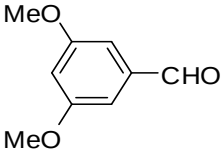	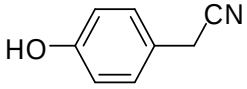	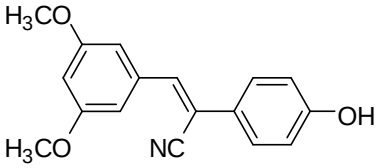 ST-512
69	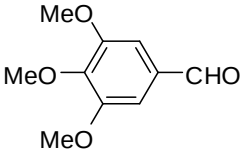	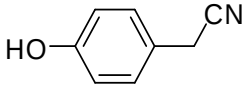	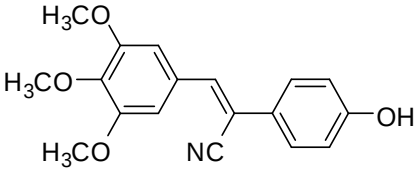 ST-514
70	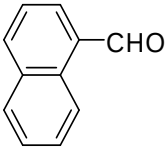	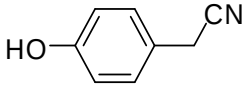	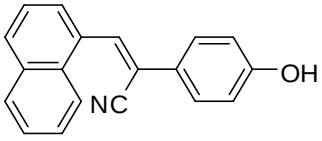 ST-516

Table 2.2 (continued)

71	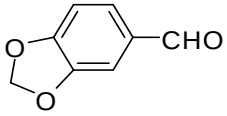	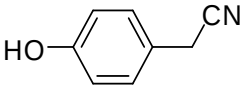	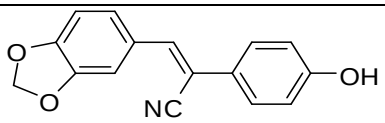 ST-517
72	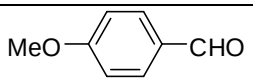	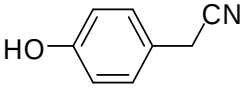	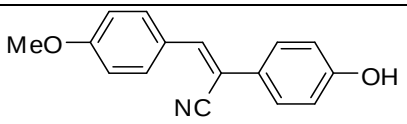 ST-520
73	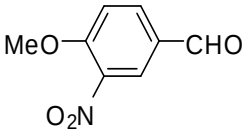	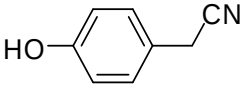	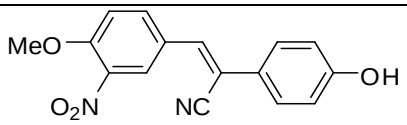 ST-521
74	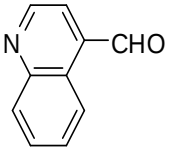	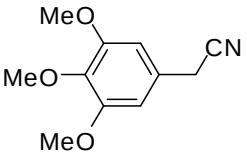	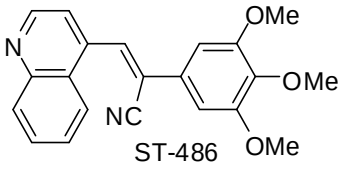 ST-486

* Synthetic route presented in **Scheme 2.7**.

ST-215: ^{1}H NMR (400 MHz, DMSO-d_6): δ 6.13 (s, 2H, -ArH), 7.55 (t, J =14.8 Hz, 2H, ArH), 7.61-7.65 (m, 2H, ArH), 7.85 (d, J =7.2 Hz, 2H, ArH), 7.91 (t, J =13.6 Hz, 2H, ArH), 8.07 (d, J =8.4 Hz, 2H, ArH), 8.11 (d, J =8.4 Hz, 2H, ArH), 8.21 (s, 1H, -ArH), 8.47 (s, 1H, -ArH) ppm. ^{13}C NMR (100 MHz, DMSO-d_6): 111.3, 115.5, 121.4, 126.2, 126.3, 127.4, 128.1, 128.2, 128.9, 129.6, 129.7, 130.8, 131.8, 133.1, 134.4, 134.3, 141.5, 145.8 ppm.

ST-218: ^{1}H NMR (400 MHz, DMSO-d_6): δ 3.86 (s, 3H, -OCH_3), 4.06 (s, 3H, -OCH_3), 6.12 (s, 2H, -ArH), 7.05 (d, J =8.0 Hz, 1H, ArH), 7.20 (d, J =7.6 Hz, 1H, ArH), 7.39 (s, 1H, -ArH), 7.56 (d, J =8.4 Hz, 1H, ArH), 7.95 (s, 1H, -ArH), 8.23 (d, J =10.8 Hz, 1H,

ArH), 8.42 (d, *J* =1.2 Hz, 1H, ArH) ppm. ^{13}C NMR (100 MHz, DMSO-d_6): 57.5, 57.6, 102.2, 105.5, 105.6, 109.0, 110.2, 115.4, 115.5, 118.1, 121.1, 126.3, 126.6, 128.0, 134.9, 135.0, 138.7, 138.8, 139.3, 148.7, 148.8, 153.6 ppm.

ST-252: ^{1}H NMR (400 MHz, DMSO-d_6): δ 3.71 (s, 3H, -OCH_3), 4.31 (d, *J* =5.6 Hz, 4H, -CH_2), 7.12 (d, *J* =8.8 Hz, 1H, ArH), 7.54 (d, *J* =8 Hz, 1H, ArH), 7.58 (s, 1H, ArH), 7.70-7.79 (m, 2H, ArH), 7.98 (d, *J* =12.8 Hz, 2H, ArH), 8.06 (s, 1H, -ArH) ppm. ^{13}C NMR (100 MHz, DMSO-d_6): 64.4, 64.9, 107.9, 117.9, 118.0, 118.1, 118.7, 123.8, 123.8, 123.9, 125.9, 126.0, 127.3, 128.4, 129.5, 134.4, 142.6, 144.4, 149.8, 151.3 ppm.

ST-253: ^{1}H NMR (400 MHz, DMSO-d_6): δ 3.32 (s, 3H, -OCH_3), 3.70 (s, 3H, -OCH_3), 3.86 (s, 6H, -OCH_3), 4.25 (s, 4H, -ArH), 6.97 (s, 2H, -ArH), 7.09 (d, *J* =7.6 Hz, 1H, ArH), 7.44 (d, *J* =8.4 Hz, 1H, ArH), 7.58 (s, 1H, -ArH), 7.91 (s, 1H, -ArH) ppm. ^{13}C NMR (100 MHz, DMSO-d_6): 56.54, 60.60, 102.36, 103.64, 107.95, 108.03, 109.24, 118.74, 126.18, 128.29, 130.05, 138.67, 142.56, 148.24, 149.74, 153.67 ppm.

ST-254: ^{1}H NMR (400 MHz, DMSO-d_6): δ 4.31 (d, *J* =5.6 Hz, 4H, -CH_2), 7.03 (d, *J* =7.6 Hz, 1H, ArH), 7.34-7.51 (m, 4H, ArH), 7.56 (s, 1H, ArH), 7.72 (d, *J* =7.6 Hz, 2H, ArH), 7.90 (s, 1H, -ArH) ppm. ^{13}C NMR (100 MHz, DMSO-d_6): 64.4, 64.9, 107.9, 117.9, 118.0, 118.1, 118.7, 123.8, 123.8, 123.9, 125.9, 126.0, 127.3, 129.3, 129.5, 134.4, 142.6, 142.7, 143.8, 146.2 ppm.

ST-255: ^{1}H NMR (400 MHz, DMSO-d_6): δ 4.30 (d, *J* =5.6 Hz, 4H, -CH_2), 7.03 (d, *J* =8.8 Hz, 1H, ArH), 7.51 (d, *J* =8 Hz, 1H, ArH), 7.58 (s, 1H, ArH), 7.69-7.767 (m, 2H, ArH), 7.98 (d, *J* =12.8 Hz, 2H, ArH), 8.06 (s, 1H, -ArH) ppm. ^{13}C NMR (100 MHz,

DMSO-d_6): 64.4, 64.9, 107.9, 117.9, 118.0, 118.1, 118.7, 123.8, 123.8, 123.9, 125.9, 126.0, 127.3, 129.3, 129.5, 134.4, 142.6, 142.7, 143.8, 146.2 ppm.

ST-258: ^{1}H NMR (400 MHz, DMSO-d_6): δ 4.11 (s, 4H, -ArH), 7.12 (d, *J* =8.4 Hz, 1H, ArH), 7.19 (d, *J* =9.2 Hz, 1H, ArH), 7.41 (d, *J* =1.2 Hz, 1H, ArH), 8.01-8.07 (m, 4H, ArH), 8.31 (d, *J* =9.2 Hz, 2H, ArH) ppm. ^{13}C NMR (100 MHz, DMSO-d_6): 102.4, 105.9, 109.1, 114.0, 1177.6, 121.9, 124.4, 127.7, 130.4, 138.8, 138.9, 140.6, 148.0, 149.1, 151.1 ppm.

ST-259: ^{1}H NMR (400 MHz, DMSO-d_6): δ 7.49 (d, *J* =8.8 Hz, 2H, ArH), 7.69-7.75 (m, 2H, ArH), 7.82 (t, *J* =14.0 Hz, 2H, ArH), 8.01 (t, *J* =14.0 Hz, 2H, ArH), 8.13 (d, *J* =8.8 Hz, 2H, ArH), 8.34 (s, 1H, -ArH), 8.35 (s, 1H, -ArH) ppm. ^{13}C NMR (100 MHz, DMSO-d_6): 109.2, 118.1, 122.5, 123.0, 125.2, 125.3, 125.7, 126.1, 127.5, 127.6, 128.1, 128.2, 128.4, 129.0, 129.1, 129.2, 130.1, 130.3, 130.6, 130.8, 131.2, 131.4, 131.4, 132.6, 133.5, 138.4, 144.2, 149.9 ppm.

ST-260: ^{1}H NMR (400 MHz, DMSO-d_6): δ 3.71 (s, 3H, -OCH_3), 3.75 (s, 3H, -OCH_3), 7.07 (d, *J* =8.4 Hz, 1H, ArH), 7.31 (d, *J* =8.0 Hz, 1H, ArH), 7.62-7.66 (m, 4H, ArH), 7.95 (d, *J* =7.2 Hz, 1H, ArH), 7.95-8.01 (m, 2H, ArH), 8.15 (m, 1H, ArH), 8.21 (s, 1H, ArH) ppm. ^{13}C NMR (100 MHz, DMSO-d_6): 56.07, 56.35, 102.26, 106.24, 109.02, 114.71, 118.10, 121.53, 124.76, 125.91, 127.06, 127.13, 127.41, 128.05, 129.01, 130.66, 131.47, 132.08, 133.48, 141.05, 148.81, 148.86 ppm.

ST-261: ^{1}H NMR (400 MHz, DMSO-d_6): δ 3.74 (s, 3H, -OCH_3), 3.90 (s, 6H, -OCH_3), 7.16 (s, 2H, -ArH), 7.84 (t, *J* =14 Hz, 1H, ArH), 7.91 (d, *J* =8.4 Hz, 1H, ArH), 8.04 (t, *J* =19.6 Hz, 2H, ArH), 8.22 (s, 1H, -ArH), 8.53 (d, *J* =8.4 Hz, 1H, ArH) ppm. ^{13}C NMR

(100 MHz, DMSO-d_6): 56.6, 60.6, 104.4, 114.9, 117.8, 123.0, 128.0, 128.1, 128.3, 129.3, 129.7, 130.8, 137.5, 139.5, 140.7, 147.6, 152.3, 153.6 ppm.

ST-262: ^{1}H NMR (400 MHz, DMSO-d_6): δ 3.79 (s, 3H, -OCH_3), 7.49 (t, *J* =14.8 Hz, 2H, ArH), 7.54-7.58 (m, 2H, ArH), 7.79 (d, *J* =8.0 Hz, 2H, ArH), 7.91 (t, *J* =8.4 Hz, 2H, ArH), 8.02 (d, *J* =8.0 Hz, 2H, ArH), 8.19 (d, *J* =8.0 Hz, 2H, ArH), 8.27 (s, 1H, -ArH), 8.31 (s, 1H, -ArH) ppm. ^{13}C NMR (100 MHz, DMSO-d_6): 55.3, 112.4, 114.5, 121.4, 122.2, 126.8, 127.4, 128.1, 128.2, 128.9, 129.6, 129.7, 130.8, 132.3, 133.0, 135.1, 135.4, 143.3, 147.3 ppm.

ST-263: ^{1}H NMR (400 MHz, DMSO-d_6): δ 7.47 (t, *J* =14.4 Hz, 1H, ArH), 7.54 (t, *J* =14.8 Hz, 2H, ArH), 7.60-7.63 (m, 2H, ArH), 7.83 (d, *J* =7.2 Hz, 2H, ArH), 7.99 (t, *J* =13.6 Hz, 2H, ArH), 8.07 (d, *J* =8.4 Hz, 2H, ArH), 8.13 (d, *J* =8.4 Hz, 2H, ArH), 8.21 (s, 1H, -ArH), 8.43 (s, 1H, -ArH) ppm. ^{13}C NMR (100 MHz, DMSO-d_6): 110.9, 118.5, 125.4, 126.2, 126.3, 127.4, 128.1, 128.2, 128.9, 129.6, 129.7, 130.8, 131.8, 133.0, 134.0, 134.3, 143.3, 143.4 ppm.

ST-264: ^{1}H NMR (400 MHz, DMSO-d_6): δ 7.61 (t, *J* =13.6 Hz, 2H, ArH), 7.74-7.82 (m, 2H, ArH), 7.98 (t, *J* =14.4 Hz, 2H, ArH), 8.07 (t, *J* =16.8 Hz, 2H, ArH), 8.13 (d, *J* =8.8 Hz, 2H, ArH), 8.38 (s, 1H, -ArH), 8.45 (s, 1H, -ArH) ppm. ^{13}C NMR (100 MHz, DMSO-d_6): 109.2, 118.1, 122.5, 123.0, 125.2, 125.3, 125.7, 126.1, 127.5, 127.6, 128.1, 128.2, 128.4, 129.0, 129.1, 129.2, 130.2, 130.3, 130.6, 130.8, 130.9, 131.4, 131.4, 132.9, 134.2, 135.4, 145.1, 145.2 ppm.

ST-179: ^{1}H NMR (400 MHz, DMSO-d_6): δ 3.85(s, 3H, -OCH_3), 6.09 (s, 2H, -ArH), 7.59 (d, *J* =14.2 Hz, 2H, ArH), 7.59-7.63 (m, 2H, ArH), 7.81 (d, *J* =8.0 Hz, 2H, ArH),

7.91 (t, *J* =14.8 Hz, 2H, ArH), 7.98 (d, *J* =8.0 Hz, 2H, ArH), 8.02 (d, *J* =8.0 Hz, 2H, ArH), 8.12 (s, 1H, -ArH), 8.24 (s, 1H, -ArH) ppm. ^{13}C NMR (100 MHz, DMSO-d_6): 56.52, 109.2, 112.1, 118.4, 121.2, 123.3, 125.4, 126.1, 128.2, 128.9, 129.6, 129.7, 130.8, 131.8, 133.1, 134.4, 141.5, 142.4 ppm.

ST-181: ^{1}H NMR (400 MHz, DMSO-d_6): δ 3.81 (s, 3H, -OCH_3), 6.11 (s, 2H, -CH2), 6.56 (t, *J* =4 Hz, 1H, ArH), 6.82 (s, 1H, ArH), 7.11 (d, *J* =7.6 Hz, 1H, ArH), 7.46 (d, *J* =7.6 Hz, 1H, ArH), 7.59 (d, *J* =8 Hz, 1H, ArH), 7.96 (s, 1H, -ArH) ppm. ^{13}C NMR (100 MHz, DMSO-d_6): 55.0, 101.0, 102.3, 104.2, 107.7, 108.8, 118.6, 126.4, 128.1, 136.3, 142.3, 148.2, 148.9, 155.1 ppm.

ST-216: ^{1}H NMR (400 MHz, DMSO-d_6): δ 6.08 (s, 2H, -CH2), 7.47-7.52 (m, 4H, ArH), 7.60-7.71 (m, 5H, ArH), 8.07 (d, *J* =8.4 Hz, 2H, ArH), 8.13 (d, *J* =8.4 Hz, 2H, ArH ppm. ^{13}C NMR (100 MHz, DMSO-d_6): 108.1, 112.3, 114.3, 114.6, 116.7, 125.4, 126.2, 126.3, 127.4, 127.8, 128.1, 128.5, 129.6, 129.7, 130.8, 131.8, 133.1, 133.2, 134.3, 141.0, 142.8 ppm.

ST-185: ^{1}H NMR (400 MHz, DMSO-d_6): δ 3.76 (s, 3H, -OCH_3), 3.81 (s, 3H, -OCH_3), 6.19 (s, 2H, -ArH), 7.12 (d, *J* =8.0 Hz, 1H, ArH), 7.16 (d, *J* =8.4 Hz, 1H, ArH), 7.30 (s, 1H, -ArH), 7.39 (s, 1H, -ArH), 7.79 (s, 1H, -ArH) ppm. ^{13}C NMR (100 MHz, DMSO-d_6): 55.6, 56.1, 102.2, 105.5, 106.0, 109.0, 109.8, 118.71, 120.7, 128.5, 129.7, 132. 4, 141.1, 148.6, 153.4 ppm.

ST-156: ^{1}H NMR (400 MHz, DMSO-d_6): δ 6.11 (s, 2H, -ArH), 7.10 (d, *J* =8.4 Hz, 1H, ArH), 7.15 (d, *J* =8.8 Hz, 1H, ArH), 7.41 (d, *J* =4.0 Hz, 1H, ArH), 8.11-8.15 (m, 4H, ArH), 8.31 (d, *J* =8.0 Hz, 2H, ArH) ppm. ^{13}C NMR (100 MHz, DMSO-d_6): 101.4, 102.1,

105.9, 109.1, 114.0, 1177.6, 121.9, 124.4, 127.7, 130.4, 138.8, 138.9, 140.6, 148.0, 149.1, 151.1 ppm.

ST-145: ^{1}H NMR (400 MHz, DMSO-d_6): δ 3.69 (s, 3H, -OCH_3), 3.86 (s, 9H, -OCH_3), 6.97 (s, 2H, -ArH), 7.07-7.09 (d, *J* =8.4 Hz, 1H, ArH), 7.38 (d, *J* =8.4 Hz, 1H, ArH), 7.51 (S, 1H, ArH), 7.84 (S, 1H, ArH), 9.42 (S, 1H, -OH) ppm. ^{13}C NMR (100 MHz, DMSO-d_6): 56.08, 56.52, 60.58, 103.52, 107.09, 112.39, 115.61, 118.88, 122.96, 130.37, 138.45, 143.00, 146.93, 150.50, 153.63 ppm. HRMS (ESI): *m/z* calcd for C19H19NO5 [M-H] 342.1341; found 342.1331.

ST-507: yellow solid; ^{1}H NMR (400 MHz, DMSO-d_6): δ 3.79 (s, 3H, -OCH_3), 3.84(s, 3H, -OCH_3), 3.85(s, 3H, -OCH_3), 7.04-7.07 (t, *J* =15.2 Hz, 2H, ArH), 7.20 (dd, *J* =2, 8.8 Hz, 1H, ArH), 7.29 (S, 1H, ArH), 7.35 (dd, *J* =1.6, 8.4 Hz, 1H, ArH), 7.49 (S, 1H, ArH), 7.77(S, 1H, ArH), 9.38 (S, 1H, -OH) ppm. ^{13}C NMR (100 MHz, DMSO-d_6): 55.93, 55.96, 56.02, 56.13, 56.16, 56.23, 107.16, 108.79, 112.23, 112.34, 112.39, 115.41, 115.65, 118.94, 118.97, 119.08, 122.75, 127.20, 127.29, 141.15, 141.37, 146.90, 149.53, 149.91, 150.22 ppm.

ST-198: ^{1}H NMR (400 MHz, DMSO-d_6): δ 3.64 (s, 3H, -OCH_3), 3.74 (s, 3H, -OCH_3), 3.79 (s, 6H, -OCH_3), 6.85 (s, 2H, -ArH), 6.91 (d, *J* =8.8 Hz, 2H, ArH), 6.97 (d, *J* =16.4 Hz, 1H, ArH), 7.11 (d, *J* =16.4 Hz, 1H, ArH), 7.11 (d, *J* =8.8 Hz, 1H, ArH) ppm. ^{13}C NMR (100 MHz, DMSO-d_6): 55.56, 56.29, 60.50, 103.99, 114.64, 126.73, 127.87, 128.03, 130.20, 133.56, 137.42, 153.48, 159.29 ppm.

ST-148: ^{1}H NMR (400 MHz, DMSO-d_6): δ 3.67 (s, 3H, -OCH_3), 3.81 (s, 3H, -OCH_3), 3.83 (s, 6H, -OCH_3), 6.96 (s, 2H, -ArH), 7.07 (d, *J* =8.4 Hz, 1H, ArH), 7.89-7.91(m, 3H,

ArH) ppm. ^{13}C NMR (100 MHz, DMSO-d_6): 55.88, 56.2, 60.59, 103.58, 107.54, 114.92, 118.89, 126.72, 130.22, 131.47, 138.56, 142.59, 153.65, 161.48 ppm.

ST-147: ^{1}H NMR (400 MHz, DMSO-d_6): δ 3.71 (s, 3H, -OCH_3), 3.80 (s, 6H, -OCH_3), 3.87 (s, 6H, -OCH_3), 6.65 (s, 1H, -ArH), 7.01 (s, 2H, -ArH), 7.12 (d, *J* =2 Hz, 2H, ArH), 7.96 (s, 1H, -ArH) ppm. ^{13}C NMR (100 MHz, DMSO-d_6): 56.32, 57.05, 61.10, 103.39, 104.39, 107.97, 111.57, 118.82, 130.18, 136.34, 139.49, 143.28, 154.16, 161.49 ppm.

ST-124: ^{1}H NMR (400 MHz, DMSO-d_6): δ 3.79 (s, 6H, -OCH_3), 3.81 (s, 3H, -OCH_3), 3.71 (s, 6H, -OCH_3), 6.62 (s, 1H, -ArH), 7.05-7.10 (m, 4H, ArH), 7.69 (d, *J* =8.8 Hz, 2H, ArH), 7.84 (s, 1H, -ArH) ppm. ^{13}C NMR (100 MHz, DMSO-d_6): 55.1, 55.4, 55.6, 111.4, 114.5, 115.9, 118.8, 126.7, 134.2, 135.1, 138.6, 142.9, 147.1, 149.1 ppm.

ST-126: ^{1}H NMR (400 MHz, DMSO-d_6): δ 3.58 (s, 3H, -OCH_3), 3.63 (s, 3H, -OCH_3), 3.71 (s, 6H, -OCH_3), 7.12 (s, 2H, -ArH), 7.15 (d, *J* =8.0 Hz, 2H, ArH), 7.21 (d, *J* =8.8 Hz, 2H, ArH), 7.36 (s, 1H, -ArH) ppm. ^{13}C NMR (100 MHz, DMSO-d_6): 55.88, 55.2, 56.9, 101.5, 104.5, 114.9, 118.8, 126.7, 134.2, 135.1, 138.6, 142.9, 154.5, 155.8 ppm.

ST-177: ^{1}H NMR (400 MHz, DMSO-d_6): δ 3.84 (s, 3H, -OCH_3), 3.86 (s, 3H, -OCH_3), 6.13 (s, 2H, -ArH), 6.67 (d, *J* =8.4 Hz, 2H, ArH), 7.00 (d, *J* =8.0 Hz, 1H, ArH), 7.12- (d, *J* =8.4 Hz, 1H, ArH), 7.25 (s, 1H, -ArH), 7.78 (s, 1H, -ArH), 7.92 (d, *J* =8.8 Hz, 1H, ArH) ppm. ^{13}C NMR (100 MHz, DMSO-d_6): 55.99, 56.31, 98.79, 120.11, 105.75, 106.09, 108.38, 109.08, 115.85, 118.84, 120.48, 129.02, 129.40, 136.61, 148.34, 148.68, 159.61, 163.15 ppm.

ST-178: ^{1}H NMR (400 MHz, DMSO-d_6): δ 6.14 (s, 2H, -CH_2), 7.07 (d, *J* =8.4 Hz, 1H, ArH), 7.31 (d, *J* =8.0 Hz, 1H, ArH), 7.62-7.66 (m, 4H, ArH), 7.95 (d, *J* =7.2 Hz, 1H,

ArH), 8.01 (m, 2H, ArH), 8.16 (m, 1H, ArH), 8.61 (s, 1H, ArH) ppm. ^{13}C NMR (100 MHz, DMSO-d_6): 102.26, 106.24, 109.02, 114.71, 118.10, 121.53, 124.76, 125.91, 127.06, 127.13, 127.41, 128.05, 129.01, 130.66, 131.47, 132.08, 133.48, 140.07, 148.80, 148.95 ppm.

ST-180: ^{1}H NMR (400 MHz, DMSO-d_6): δ 6.12 (s, 2H, -CH_2), 7.03 (d, *J* =8.0 Hz, 1H, ArH), 7.21 (d, *J* =8.4 Hz, 1H, ArH), 7.43-7.46 (m, 4H, ArH), 7.95 (s, 2H, ArH), 8.05 (d, *J* =7.6 Hz, 1H, ArH), 8.28 (s, 1H, ArH) ppm. ^{13}C NMR (100 MHz, DMSO-d_6): 102.30, 105.61, 109.02, 109.14, 118.16, 121.23, 123.15, 125.12, 125.66 127.08, 127.89, 131.72, 1234.80, 137.98, 138.59, 140.67, 148.84, 148.89 ppm.

ST-160: ^{1}H NMR (400 MHz, DMSO-d_6): δ 3.32 (s, 3H, -OCH_3), 3.70 (s, 3H, -OCH_3), 3.86 (s, 6H, -OCH_3), 6.14 (s, 2H, -ArH), 6.97 (s, 2H, -ArH), 7.09 (d, *J* =7.6 Hz, 1H, ArH), 7.44 (d, *J* =8.4 Hz, 1H, ArH), 7.58 (s, 1H, -ArH), 7.91 (s, 1H, -ArH) ppm. ^{13}C NMR (100 MHz, DMSO-d_6): 56.54, 60.60, 102.36, 103.64, 107.95, 108.03, 109.24, 118.74, 126.18, 128.29, 130.05, 138.67, 142.56, 148.24, 149.74, 153.67 ppm.

ST-163: ^{1}H NMR (400 MHz, DMSO-d_6): δ 3.83 (s, 3H, -OCH_3), 6.09 (s, 2H, -ArH), 7.01 (d, *J* =8.4 Hz, 1H, ArH), 7.07 (d, *J* =8.8 Hz, 2H, ArH), 7.15 (d, *J* =10.4 Hz, 1H, ArH), 7.36 (d, *J* =1.6 Hz, 1H, ArH),7.83 (s, 1H, -ArH), 7.88 (d, *J* =8.8 Hz, 1H, ArH) ppm. ^{13}C NMR (100 MHz, DMSO-d_6): 56.54, 60.60, 102.36, 103.64, 107.95, 108.03, 109.24, 118.74, 126.18, 128.29, 130.05, 138.67, 142.56, 148.24, 149.74, 153.67 ppm.

ST-173: ^{1}H NMR (400 MHz, DMSO-d_6): δ 3.84 (s, 3H, -OCH_3), 3.86 (s, 3H, -OCH_3), 6.09 (s, 2H, -ArH), 6.67 (d, *J* =8.4 Hz, 2H, ArH), 7.00 (d, *J* =8.0 Hz, 2H, ArH), 7.12- (d, *J* =8.4 Hz, 1H, ArH), 7.25 (s, 1H, -ArH), 7.78 (s, 1H, -ArH), 7.92 (d, *J* =8.8 Hz, 1H,

ArH) ppm. ^{13}C NMR (100 MHz, DMSO-d_6): 55.99, 56.31, 98.79, 120.11, 105.75, 106.09, 108.38, 109.08, 115.85, 118.84, 120.48, 129.02, 129.40, 136.61, 148.34, 148.68, 159.61, 163.15 ppm.

ST-162: ^{1}H NMR (400 MHz, DMSO-d_6): δ 3.74 (s, 3H, -OCH_3), 3.82 (s, 6H, -OCH_3), 6.11 (s, 2H, -ArH), 7.03 (d, *J* =7.6 Hz, 1H, ArH), 7.18 (d, *J* =8.0 Hz, 1H, ArH), 7.31 (s, 2H, -ArH), 7.39 (s, 1H, -ArH), 7.87 (s, 1H, -ArH) ppm. ^{13}C NMR (100 MHz, DMSO-d_6): 56.26, 56.37, 60.60, 102.22, 105.56, 107.08, 109.00, 109.08, 118.71, 120.87, 128.50, 129.57, 139.74, 141.61, 148.62, 148.78, 153.24 ppm.

ST-521: ^{1}H NMR (400 MHz, DMSO-d_6): δ 3.95 (s, 3H, -OCH_3), 6.13 (d, *J* =8.4 Hz, 2H, ArH), 7.21 (d, *J* =8.4 Hz, 2H, ArH), 7.27 (S, 1H, ArH), 7.44 (d, *J* =9.2 Hz, 1H, ArH), 8.06 (d, *J* =8.4 Hz, 1H, ArH), 8.26 (S, 1H, ArH) ppm. ^{13}C NMR (100 MHz, DMSO-d_6): 57.3, 112.3, 112.7, 115.1, 119.2, 119.9, 124.3, 126.3, 127.5, 128.8, 133.8, 139.5, 151.7, 174.8 ppm.

ST-149: ^{1}H NMR (400 MHz, DMSO-d_6): δ 3.71-3.75 (m, 6H, -OCH_3), 3.84 (s, 6H, -OCH_3), 3.87 (s, 6H, -OCH_3), 7.00 (s, 2H, -ArH), 7.32 (s, 2H, ArH), 7.94 (s, 1H, ArH) ppm. ^{13}C NMR (100 MHz, DMSO-d_6): 60.5, 60.6, 103.6, 107.2, 109.4, 118.7, 129.4, 129.8, 138.8, 139.9, 142.8, 153.2, 153.6 ppm.

ST-152: ^{1}H NMR (400 MHz, DMSO-d_6): δ 3.88 (s, 3H, -OCH_3), 7.07 (t, *J* =15.2 Hz, 1H, ArH), 7.17 (d, *J* =8.4 Hz, 1H, ArH), 7.49 (d, *J* =7.2 Hz, 2H, ArH), 7.65 (s, 1H, ArH), 7.97 (s, 1H, ArH), 8.08 (s, 2H, ArH) ppm. ^{13}C NMR (100 MHz, DMSO-d_6): 56.3, 111.4, 112.5, 117.5, 121.4, 123.2, 123.8, 130.3, 130.8, 131.8, 135.1, 138.0, 143.2, 157.0 ppm.

ST-153: ^{1}H NMR (400 MHz, DMSO-d_6): δ 3.80 (s, 3H, -OCH_3), 6.13 (s, 2H, -ArH), 7.06 (t, *J* =18 Hz, 3H, ArH), 7.41 (d, *J* =9.6 Hz, 1H, ArH), 7.55 (s, 1H, -ArH), 7.65 (d, *J* =8.4 Hz, 2H, ArH), 7.79 (s, 1H, -ArH) ppm. ^{13}C NMR (100 MHz, DMSO-d_6): 55.7, 55.85, 102.2, 107.7, 107.8, 107.9, 109.2, 115.0, 115.2, 118.8, 125.8, 126.7, 127.4, 128.5, 140.7, 140.8, 148.1, 149.4, 160.2 ppm.

ST-164: ^{1}H NMR (400 MHz, DMSO-d_6): δ 3.79 (s, 6H, -OCH_3), 6.11 (s, 2H, -ArH), 6.62 (s, 1H, -ArH), 7.05 (d, *J* =7.6 Hz, 1H, ArH), 7.10 (s, 2H, -ArH), 7.21 (d, *J* =7.6 Hz, 1H, ArH), 7.39 (s, 1H, -ArH), 7.85 (s, 1H, -ArH) ppm. ^{13}C NMR (100 MHz, DMSO-d_6): 55.7, 102.2, 102.7, 105.7, 107.3, 109.0, 110.6, 118.3, 121.1, 128.3, 135.9, 141.4, 148.7, 148.8, 160.9 ppm.

ST-165: ^{1}H NMR (400 MHz, DMSO-d_6): δ 3.80 (s, 3H, -OCH_3), 3.83 (s, 3H, -OCH_3), 6.10 (s, 2H, -ArH), 7.03 (d, *J* =8 Hz, 1H, ArH), 7.11 (d, *J* =8.4 Hz, 1H, ArH), 7.18 (d, *J* =10.4 Hz, 1H, ArH), 7.37 (d, *J* =2 Hz, 1H, ArH), 7.52 (d, *J* =10 Hz, 1H, ArH), 7.62 (d, *J* =1.6 Hz, 1H, ArH), 7.83 (s, 1H, -ArH) ppm. ^{13}C NMR (100 MHz, DMSO-d_6): 55.7, 55.8, 56.0, 56.1, 102.1, 105.5, 105.5, 107.1, 109.0, 112.1, 119.0, 120.5, 123.7, 126.8, 128.8, 141.6, 141.7, 148.3, 148.3, 148.9, 151.1 ppm.

ST-168: ^{1}H NMR (400 MHz, DMSO-d_6): δ 6.14 (s, 2H, -ArH), 7.17 (d, *J* =8.4 Hz, 1H, ArH), 7.28 (t, *J* =16.0 Hz, 2H, ArH), 7.41 (d, *J* =8.4 Hz, 1H, ArH), 7.51-7.56 (m, 3H, ArH) ppm. ^{13}C NMR (100 MHz, DMSO-d_6): 101.3, 106.2, 107.8, 107.9, 109.4, 112.7, 112.9, 117.6, 124.6, 124.8, 126.3, 126.9, 127.3, 130.5, 148.4, 150.6, 151.0, 158.5, 158.6 ppm.

ST-486: ^{1}H NMR (400 MHz, DMSO-d_6): δ 3.74 (s, 3H, -OCH_3), 3.90 (s, 6H, -OCH_3), 7.16 (s, 2H, -ArH), 7.84 (t, *J* =14 Hz, 1H, ArH), 7.91 (d, *J* =8.4 Hz, 2H, ArH), 8.04 (t, *J* =19.6 Hz, 2H, ArH), 8.22 (s, 1H, -ArH), 8.53 (d, *J* =8.4 Hz, 1H, ArH) ppm. ^{13}C NMR (100 MHz, DMSO-d_6): 56.6, 60.6, 104.4, 114.9, 117.8, 123.0, 128.0, 128.1, 128.3, 129.3, 129.7, 130.8, 137.5, 139.5, 140.7, 147.6, 152.3, 153.6 ppm.

ST-479: ^{1}H NMR (400 MHz, DMSO-d_6): δ 3.79 (s, 3H, -OCH_3), 3.84 (s, 3H, -OCH_3), 4.31 (d, *J* =4 Hz, 4H, ArH), 7.01 (d, *J* =8.0 Hz, 1H, ArH), 7.05 (d, *J* =8.4 Hz, 1H, ArH), 7.22 (d, *J* =8.4 Hz, 1H, ArH), 7.28 (s, 1H, -ArH), 7.44 (d, *J* =8.4 Hz, 1H, ArH), 7.52 (s, 1H, -ArH), 7.80 (s, 1H, -ArH) ppm. ^{13}C NMR (100 MHz, DMSO-d_6): 56.0, 56.1, 64.4, 64.8, 107.9, 108.9, 112.2, 117.7, 117.9, 118.8, 119.1, 123.5, 127.0, 127.6, 140.5, 143.7, 145.8, 149.5, 150.0 ppm. HRMS (ESI): *m/z* calcd for C19H18NO4 [M-H] 324.1236; found 324.1224.

ST-161: ^{1}H NMR (400 MHz, DMSO-d_6): δ 6.10 (s, 2H, -ArH), 6.13 (s, 2H, -ArH), 7.04 (d, *J* =8.4 Hz, 1H, ArH), 7.09 (d, *J* =8.4 Hz, 1H, ArH), 7.17 (d, *J* =8.4 Hz, 1H, ArH), 7.37 (d, *J* =1.6 Hz, 1H, ArH), 7.42 (d, *J* =8.0 Hz, 1H, ArH), 7.54 (s, 2H, -ArH), 7.82 (s, 1H, -ArH) ppm. ^{13}C NMR (100 MHz, DMSO-d_6): 102.1, 12.3, 105.5, 105.6, 107.6, 107.8, 107.9, 109.0, 109.2, 118.7, 120.7, 125.9, 128.3, 128.6, 141.2, 141.3, 148.1, 148.4, 148.7, 149.5 ppm.

ST-156: ^{1}H NMR (400 MHz, DMSO-d_6): δ 6.17 (s, 2H, -ArH), 7.15 (d, *J* =8.0 Hz, 1H, ArH), 7.55 (d, *J* =8.4 Hz, 1H, ArH), 7.65 (d, *J* =1.6 Hz, 1H, ArH), 7.99 (d, *J* =9.2 Hz, 1H, ArH), 8.19 (s, 1H, -ArH), 8.34 (d, *J* =8.8 Hz, 1H, ArH) ppm. ^{13}C NMR (100 MHz,

DMSO-d_6): 102.6, 105.8, 108.1, 108.2, 109.4, 118.1, 124.7, 127.0, 127.5, 127.7, 140.8, 146.3, 146.4, 147.4, 148.3, 150.7 ppm.

ST-175: ^{1}H NMR (400 MHz, DMSO-d_6): δ 6.19 (s, 2H, -ArH), 7.23 (s, 1H, -ArH), 7.26 (s, 1H, -ArH), 7.29 (d, *J* =7.6 Hz, 1H, ArH), 7.32 (s, 1H, -ArH), 7.51 (d, *J* =7.6 Hz, 2H, ArH), 7.56 (d, *J* =8.0 Hz, 1H, ArH) ppm. ^{13}C NMR (100 MHz, DMSO-d_6): 102.9, 108.7, 118.2, 121.7, 129.6, 131.5, 138.8, 144.3, 145.9, 153.6 ppm.

ST-287: ^{1}H NMR (400 MHz, DMSO-d_6): δ 3.88 (s, 3H, -OCH_3), 3.93 (s, 6H, -OCH_3), 6.81 (s, 2H, -ArH), 7.23 (s, 1H, -ArH), 7.26 (s, 2H, -ArH), 7.32 (s, 1H, -ArH), 7.52 (s, 1H, -ArH), 7.95 (s, 1H, -ArH) ppm. ^{13}C NMR (100 MHz, DMSO-d_6): 56.2, 56.3, 60.9, 102.9, 108.7, 110.1, 118.2, 121.7, 129.6, 131.5, 138.8, 144.3, 145.8, 145.9, 153.6 ppm.

ST-288: ^{1}H NMR (400 MHz, DMSO-d_6): δ 3.84 (s, 3H, -OCH_3), 6.95 (d, *J* =8.0 Hz, 2H, ArH), 7.21 (s, 1H, -ArH), 7.28 (s, 1H, ArH), 7.50 (s, 1H, -ArH), 7.56 (d, *J* =9.2 Hz, 2H, ArH), 7.91 (s, 1H, -ArH) ppm. ^{13}C NMR (100 MHz, DMSO-d_6): 55.3, 55.4, 108.7, 109.8, 114.4, 118.3, 121.9, 126.4, 126.8, 129.9, 144.2, 145.3, 145.4, 160.1 ppm.

ST-166: ^{1}H NMR (400 MHz, DMSO-d_6): δ 4.00 (s, 3H, -OCH_3), 6.12 (s, 2H, -ArH), 7.05 (d, *J* =8.0 Hz, 1H, ArH), 7.20 (d, *J* =7.6 Hz, 1H, ArH), 7.39 (s, 1H, -ArH), 7.56 (d, *J* =8.4 Hz, 1H, ArH), 7.95 (s, 1H, -ArH), 8.23 (d, *J* =10.8 Hz, 1H, ArH), 8.42 (d, *J* =1.2 Hz, 1H, ArH) ppm. ^{13}C NMR (100 MHz, DMSO-d_6): 57.6, 102.2, 105.5, 105.6, 109.0, 110.2, 115.4, 115.5, 118.1, 121.1, 126.3, 126.6, 128.0, 134.9, 135.0, 138.7, 138.8, 139.3, 148.7, 148.8, 153.6 ppm.

ST-172: ^{1}H NMR (400 MHz, DMSO-d_6): δ 6.12 (s, 2H, -ArH), 7.06 (d, *J* =8.0 Hz, 1H, ArH), 7.20 (d, *J* =10.4 Hz, 1H, ArH), 7.39 (d, *J* =2 Hz, 1H, ArH), 7.56 (t, *J* =17.2 Hz,

1H, ArH), 7.91-7.97 (m, 2H, -ArH), 8.23 (dd, *J* =8.8 Hz, *J* =2.4 Hz, 1H, ArH) ppm. ^{13}C NMR (100 MHz, DMSO-d_6): 102.3, 105.7, 105.8, 108.9, 109.0, 109.1, 111.4, 117.6, 117.9, 117.9, 121.9, 127.9, 130.5, 130.6, 130.7, 132.6, 134.5, 134.6, 138.7, 148.7, 149.0, 158.0, 160.5 ppm.

ST-167: ^{1}H NMR (400 MHz, DMSO-d_6): δ 6.13 (s, 2H, -ArH), 7.08 (d, *J* =8.4 Hz, 1H, ArH), 7.28 (d, *J* =9.2 Hz, 1H, ArH), 7.47 (d, *J* =1.2 Hz, 1H, ArH), 8.08-8.10 (m, 4H, ArH), 8.36 (d, *J* =9.2 Hz, 2H, ArH) ppm. ^{13}C NMR (100 MHz, DMSO-d_6): 102.4, 105.9, 109.1, 114.0, 1177.6, 121.9, 124.4, 127.7, 130.4, 138.8, 138.9, 140.6, 148.0, 148.8, 149.4 ppm.

ST-184: ^{1}H NMR (400 MHz, DMSO-d_6): δ 6.17 (s, 2H, -ArH), 7.13 (d, *J* =8.0 Hz, 1H, ArH), 7.29 (t, *J* =16.4 Hz, 2H, ArH), 7.46 (d, *J* =6.8 Hz, 1H, ArH), 7.55-7.63 (m, 3H, ArH) ppm. ^{13}C NMR (100 MHz, DMSO-d_6): 94.0, 102.6, 107.8, 107.9, 109.4, 112.7, 112.9, 117.6, 126.9, 127.3, 130.5, 148.4, 150.6, 151.0, 158.5, 158.6, 160.9, 161.0 ppm.

ST-101: ^{1}H NMR (400 MHz, DMSO-d_6): δ 3.81 (s, 6H, -OCH_3), 6.71 (s, 1H, -ArH), 7.21 (s, 2H, -ArH), 8.04 (d, *J* =9.2 Hz, 2H, ArH), 8.25 (s, 1H, -ArH), 8.37 (d, *J* =8.8 Hz, 2H, ArH) ppm. ^{13}C NMR (100 MHz, DMSO-d_6): 55.8, 99.5, 99.6, 105.4, 118.5, 124.5, 125.6, 125.8, 132.4, 136.5, 140.8, 147.1 ppm.

TMR-01: ^{1}H NMR (400 MHz, DMSO-d_6): δ 3.72 (s, 3H, -OCH_3), 3.87 (s, 6H, -OCH_3), 7.06 (s, 2H, -ArH), 8.12 (d, *J* =8.8 Hz, 2H, ArH), 8.17 (s, 1H, -ArH), 8.38 (d, *J* =8.4 Hz, 2H, ArH) ppm. ^{13}C NMR (100 MHz, DMSO-d_6): 56.5, 60.6, 104.2, 114.3, 117.6, 124.5, 130.5, 139.5, 140.25, 140.4, 148.1, 153.7 ppm.

TMR-03: ^{1}H NMR (400 MHz, DMSO-d_6): δ 3.72 (s, 3H, -OCH_3), 3.87 (s, 6H, -OCH_3), 7.05 (s, 2H, -ArH), 7.83 (t, *J* =16 Hz, 1H, ArH), 8.19 (s, 1H, -ArH), 8.29 (d, *J* =8.4 Hz, 1H, ArH), 8.36 (d, *J* =8.0 Hz, 1H, ArH), 8.73 (s, 1H, -ArH) ppm. ^{13}C NMR (100 MHz, DMSO-d_6): 56.5, 60.6, 104.0, 113.1, 117.7, 124.3, 125.0, 129.0, 131.0, 134.9, 135.7, 139.3, 140.1, 148.4, 153.7 ppm.

TMR-04: ^{1}H NMR (400 MHz, DMSO-d_6): δ 3.71 (s, 3H, -OCH_3), 3.86 (s, 6H, -OCH_3), 4.01 (s, 3H, -OCH_3), 7.01 (s, 2H, -ArH), 7.60 (d, *J* =9.2 Hz, 1H, ArH), 8.07 (s, 1H, -ArH), 8.29 (d, *J* =8.8 Hz, 1H, ArH), 8.44 (s, 1H, -ArH) ppm. ^{13}C NMR (100 MHz, DMSO-d_6): 55.4, 56.2, 56.3, 60.9, 102.9, 108.7, 110.1, 118.2, 121.7, 124.2, 124.5, 124.8, 129.6, 131.5, 138.8, 144.3, 145.8, 145.9, 153.6 ppm.

ST-155: ^{1}H NMR (400 MHz, DMSO-d_6): δ 3.86 (s, 6H, -OCH_3), 6.14 (s, 2H, -CH2), 6.56 (t, *J* =4 Hz, 1H, ArH), 6.85 (d, *J* =2 Hz, 1H, ArH), 7.11 (d, *J* =7.6 Hz, 1H, ArH), 7.46 (d, *J* =7.6 Hz, 1H, ArH), 7.59 (d, *J* =8 Hz, 1H, ArH), 7.96 (s, 1H, -ArH) ppm. ^{13}C NMR (100 MHz, DMSO-d_6): 55.9, 101.0, 102.3, 104.2, 107.7, 108.1, 109.2, 118.6, 126.4, 128.1, 136.3, 143.3, 148.2, 149.9, 161.3 ppm.

ST-512: ^{1}H NMR (400 MHz, DMSO-d_6): δ 3.58 (s, 3H, -OCH_3), 3.61 (s, 3H, -OCH_3), 6.52 (d, *J* =8.0 Hz, 2H, ArH), 6.87 (d, *J* =8.4 Hz, 2H, ArH), 6.95 (s, 2H, -ArH), 7.12 (s, 1H, -ArH), 7.36(s, 1H, -ArH), 9.15 (s, 1H, -OH) ppm. ^{13}C NMR (100 MHz, DMSO-d_6): 57.9, 58.2, 101.5, 104.8, 115.4, 118.8, 125.0, 127.5, 129.8, 139.5, 145.2, 151.1, 151.5 ppm.

ST-514: ^{1}H NMR (400 MHz, DMSO-d_6): δ 3.73 (s, 3H, -OCH_3), 3.82 (s, 6H, -OCH_3), 6.89 (d, *J* =8.8 Hz, 2H, ArH), 7.29 (s, 2H, -ArH), 7.57 (d, *J* =8.4 Hz, 2H, ArH), 7.75(s,

1H, -ArH), 9.94 (s, 1H, -OH) ppm. ^{13}C NMR (100 MHz, DMSO-d_6): 56.3, 60.6, 106.9, 109.4, 116.3, 118.8, 125.0, 127.5, 129.8, 139.5, 140.1, 153.2, 158.9 ppm.

ST-516: ^{1}H NMR (400 MHz, DMSO-d_6): δ 7.55 (d, *J* =14.8 Hz, 2H, ArH), 7.61-7.65 (m, 2H, ArH), 7.85 (d, *J* =7.2 Hz, 2H, ArH), 7.91 (t, *J* =8.6 Hz, 1H, ArH), 8.07 (d, *J* =8.4 Hz, 2H, ArH), 8.11 (d, *J* =8.4 Hz, 2H, ArH), 8.21 (s, 1H, -ArH), 9.94 (s, 1H, -OH) ppm. ^{13}C NMR (100 MHz, DMSO-d_6): 111.3, 115.5, 121.4, 126.2, 126.3, 127.4, 128.1, 128.2, 128.9, 129.6, 129.7, 130.8, 131.8, 133.1, 134.4, 134.3, 141.5, 145.8 ppm.

ST-520: ^{1}H NMR (400 MHz, DMSO-d_6): δ 3.79 (s, 3H, -OCH_3), 6.89 (d, *J* =8.4 Hz, 2H, ArH), 6.89 (d, *J* =8.4 Hz, 2H, ArH), 6.89 (d, *J* =8.0 Hz, 2H, ArH), 7.29 (s, 2H, -ArH), 7.57 (d, *J* =8.0 Hz, 2H, ArH), 9.94 (s, 1H, -OH) ppm. ^{13}C NMR (100 MHz, DMSO-d_6): 55.8, 107.7, 114.8, 116.3, 119.0, 125.3, 127.0, 127.3, 131.1, 139.8, 158.6, 161.0 ppm.

ST-517: ^{1}H NMR (400 MHz, DMSO-d_6): δ 6.12 (s, 2H, -ArH), 6.87 (d, *J* =8.4 Hz, 2H, ArH), 7.07 (d, *J* =8.4 Hz, 1H, ArH), 7.38 (d, *J* =10 Hz, 1H, ArH), 7.52-7.54 (m, 3H, ArH), 7.71 (s, 1H, -ArH), 9.88 (s, 1H, -OH) ppm. ^{13}C NMR (100 MHz, DMSO-d_6): 56.3, 60.6, 106.9, 109.4, 116.3, 118.8, 125.0, 127.5, 129.8, 139.5, 140.1, 153.2, 158.9 ppm.

ST-315: ^{1}H NMR (400 MHz, DMSO-d_6): δ 3.68 (s, 3H, -OCH_3), 3.83 (s, 6H, -OCH_3), 6.97 (s, 2H, -ArH), 7.28-7.43 (m, 3H, ArH), 7.76 (d, *J* =8 Hz, 2H, ArH), 7.83 (d, *J* =7.2 Hz, 2H, ArH) ppm. ^{13}C NMR (100 MHz, DMSO-d_6): 56.3, 60.5, 104.9, 110.4, 114.5, 119.5, 124.8, 125.1, 126.5, 127.3, 133.0, 153.5 ppm.

ST-301: ^{1}H NMR (400 MHz, DMSO-d_6): δ 7.28 (d, *J* =16.4 Hz, 1H, ArH), 7.41 (d, *J* =16.4 Hz, 1H, ArH), 7.46 (d, *J* =8.4 Hz, 2H, ArH), 7.57-7.64 (m, 4H, ArH), 7.89 (d, *J* =2

Hz, 1H, ArH) ppm. ^{13}C NMR (100 MHz, DMSO-d_6): 127.1, 127.2, 128.5, 128.8, 129.2, 129.9, 130.2, 131.2, 131.9, 132.9, 135.9, 138.2 ppm.

ST-321: ^{1}H NMR (400 MHz, DMSO-d_6): δ 4.00 (s, 3H, -OCH$_3$), 7.04 (d, *J* =8.4 Hz, 1H, ArH), 7.17 (d, *J* =16.0 Hz, 1H, ArH), 7.54-7.61 (m, 4H, ArH), 7.71 (d, *J* =8.4 Hz, 2H, ArH), 7.84 (d, *J* =8.0 Hz, 1H, ArH), 8.04 (d, *J* =16 Hz, 1H, ArH), 8.22 (d, *J* =8.4 Hz, 1H, ArH), 8.38 (d, *J* =8.0 Hz, 1H, ArH) ppm. ^{13}C NMR (100 MHz, DMSO-d_6): 56.1, 105.0, 120.6, 122.3, 124.2, 124.3, 125.2, 125.8, 126.2, 126.7, 127.2, 128.3, 129.0, 131.9, 132.0, 137.3, 155.3 ppm.

ST-302: ^{1}H NMR (400 MHz, DMSO-d_6): δ 7.52 (d, *J* =8.4 Hz, 2H, ArH), 7.65 (d, *J* =8.8 Hz, 2H, ArH), 7.85 (d, *J* =2.8 Hz, 2H, ArH), 7.95 (s, 1H, ArH), 8.25 (d, *J* =5.6 Hz, 1H, ArH) ppm. ^{13}C NMR (100 MHz, DMSO-d_6): 124.5, 127.6, 128.0, 128.9, 129.0, 130.9, 131.1, 131.3, 132.0, 137.6, 143.8, 146.9 ppm.

ST-312: ^{1}H NMR (400 MHz, DMSO-d_6): δ 6.03 (s, 2H, -ArH), 6.91 (s, 1H, -ArH), 7.01-7.10 (m, 2H, ArH), 7.22 (d, *J* =8 Hz, 1H, ArH), 7.27 (s, 1H, -ArH), 7.47-7.54 (m, 4H, ArH) ppm. ^{13}C NMR (100 MHz, DMSO-d_6): 101.5, 105.7, 108.8, 120.5, 122.3, 125.7, 128.5, 129.5, 131.7, 131.9, 137.0, 147.6, 148.3 ppm.

ST-313: ^{1}H NMR (400 MHz, DMSO-d_6): δ 7.44 (d, *J* =1.6 Hz, 2H, ArH), 7.59-7.65 (m, 2H, ArH), 7.77 (d, *J* =8.4 Hz, 2H, ArH), 7.84 (d, *J* =8.4 Hz, 2H, ArH), 7.91 (d, *J* =1.6 Hz, 2H, ArH) ppm. ^{13}C NMR (100 MHz, DMSO-d_6): 110.4, 119.3, 127.4, 127.7, 128.8, 129.5, 129.9, 130.8, 131.3, 132.0, 133.0, 137.7, 141.6 ppm.

ST-309: ^{1}H NMR (400 MHz, DMSO-d_6): δ 3.66 (s, 3H, -OCH$_3$), 3.83 (s, 6H, -OCH$_3$), 6.11 (s, 2H, -ArH), 6.83-6.88 (m, 4H, ArH), 7.04 (dd, *J* =1.2 Hz, *J* =1.8 Hz, 1H, ArH),

7.14 (d, *J* =16.4 Hz, 1H, ArH), 7.28 (d, *J* =16.4 Hz, 1H, ArH) ppm. ^{13}C NMR (100 MHz, DMSO-d_6): 51.6, 56.3, 60.5, 101.3, 130.2, 107.7, 120.1, 122.2, 122.8, 131.7, 153.5 ppm.

ST-316: ^{1}H NMR (400 MHz, DMSO-d_6): δ 3.67 (s, 3H, -OCH_3), 3.83 (s, 6H, -OCH_3), 6.93 (s, 2H, -ArH), 7.21 (s, 2H, -ArH), 7.55 (dd, *J* =8.8 Hz, *J* =13.6 Hz, 4H, ArH) ppm. ^{13}C NMR (100 MHz, DMSO-d_6): 56.3, 60.5, 104.4, 120.7, 126.9, 128.6, 129.7, 132.0, 132.9, 136.9, 137.9, 153.5 ppm.

ST-323: ^{1}H NMR (400 MHz, DMSO-d_6): δ 7.30 (d, *J* =16.4 Hz, 1H, ArH), 7.52-7.60 (m, 4H, ArH), 7.75 (d, *J* =8.4 Hz, 2H, ArH), 7.89 (dd, *J* =3.6 Hz, *J* =8.4 Hz, 2H, ArH), 8.96 (d, *J* =9.2 Hz, 1H, ArH), 8.14 (d, *J* =16 Hz, 1H, ArH), 8.43 (d, *J* =8.0 Hz, 1H, ArH) ppm. ^{13}C NMR (100 MHz, DMSO-d_6): 121.1, 123.6, 124.2, 126.2, 1263, 126.4, 126.7, 128.5, 128.9, 129.3, 130.5, 131.2, 132.0, 133.8, 134.4, 137.0 ppm.

ST-314: ^{1}H NMR (400 MHz, DMSO-d_6): δ 7.25-7.38 (m, 2H, ArH), 7.53-7.63 (m, 6H, ArH), 7.88 (s, 1H, -ArH) ppm. ^{13}C NMR (100 MHz, DMSO-d_6): 121.5, 127.1, 127.2, 128.5, 129.0, 129.9, 130.2, 131.2, 131.9, 132.1, 136.2, 138.2 ppm.

ST-199: ^{1}H NMR (400 MHz, DMSO-d_6): δ 2.32 (s, 3H, -CH_3), 3.67 (s, 3H, -OCH_3), 3.83 (s, 6H, -OCH_3), 6.93 (s, 2H, -ArH), 7.08 (d, *J* =7.6 Hz, 1H, ArH), 7.17 (s, 2H, -ArH), 7.25 (t, *J* =15.2 Hz, 1H, ArH), 7.37 (d, *J* =7.6 Hz, 1H, ArH), 7.41 (s, 1H, -ArH) ppm. ^{13}C NMR (100 MHz, DMSO-d_6): 21.4, 56.2, 60.5, 104.2, 124.0, 127.2, 128.2, 128.6, 128.8, 129.0, 133.2, 137.4, 138.1, 153.4 ppm.

ST-160: ^{1}H NMR (400 MHz, DMSO-d_6): δ 3.70 (s, 3H, -OCH_3), 3.86 (s, 6H, -OCH_3), 6.14 (s, 2H, -CH2), 6.97 (s, 2H, -ArH), 7.11 (d, *J* =8 Hz, 1H, ArH), 7.46 (d, *J* =8 Hz, 1H,

ArH), 7.57 (s, 1H, -ArH), 7.91 (s, 1H, -ArH) ppm. ^{13}C NMR (100 MHz, DMSO-d_6): 56.5, 60.6, 102.3, 103.6, 107.9, 109.2, 126.1, 142.5, 148.2, 149.7, 153.6 ppm.

ST-488: ^{1}H NMR (400 MHz, DMSO-d_6): δ 3.68 (s, 3H, -OCH_3), 3.84 (s, 6H, -OCH_3), 6.93 (s, 2H, -CH2), 7.78 (s, 1H, -ArH), 7.85 (d, *J* =4 Hz, 2H, ArH) ppm. ^{13}C NMR (100 MHz, DMSO-d_6): 56.3, 56.5, 60.4, 60.6, 102.9, 104.6, 119.0, 122.7, 122.9, 130.3, 135.4, 135.6, 138.0, 138.2, 153.6 ppm.

ST-527: ^{1}H NMR (400 MHz, DMSO-d_6): δ 3.81 (s, 3H, -OCH_3), 3.85 (s, 3H, -OCH_3), 7.07 (d, *J* =4 Hz, 1H, ArH), 7.25 (d, *J* =8.8 Hz, 1H, ArH), 7.34 (d, *J* =16.2 Hz, 1H, ArH), 7.82 (d, *J* =8.0 Hz, 1H, ArH), 7.92 (d, *J* =4.0 Hz, 1H, ArH), 7.96 (s, 1H, -CH2), 8.11 (d, *J* =4 Hz, 1H, ArH) ppm. ^{13}C NMR (100 MHz, DMSO-d_6): 56.0, 56.1, 108.9, 112.2, 112.5, 117.9, 119.8, 126.1, 128.8, 131.2, 131.5, 132.0, 132.7, 135.0, 137.9, 149.6, 150.7 ppm.

ST-526: ^{1}H NMR (400 MHz, DMSO-d_6): δ 7.59 (d, *J* = 8.8 Hz, 1H, ArH), 7.74-7.79 (m, 3H, ArH), 7.87 (d, *J* =16.2 Hz, 2H, ArH), 7.97 (s, 1H, -CH2) ppm. ^{13}C NMR (100 MHz, DMSO-d_6): 108.0, 1169, 117.1, 117.7, 121.5, 125.0, 125.6, 126.4, 126.5, 129.2, 131.7, 135.1, 135.2, 136.0, 138.7, 156.3 ppm.

2.5 Synthesis of (*E*)-2,3-diaryl substituted acrylonitriles as anticancer agents.

Two (*E*)-2,3-diaryl substituted acrylonitriles (**Scheme 2.7**) were synthesized to compare their anti-cancer activities to the isomeric (*Z*)-2,3-diaryl substituted acrylonitriles.

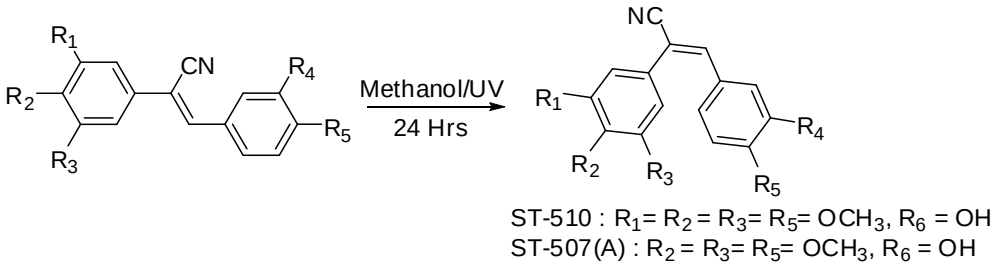

Scheme 2.7 Synthesis of (*E*)-substituted diarylacrylonitrile analogs**.**

The (*E)*-substituted diarylacrylonitrile analogs **ST-510,** and **ST-507(A)** were obtained by refluxing their *Z*-isomer counterparts **ST-145,** and **ST-507** in methanol under ultraviolet light for 24 hrs. The reaction was monitored by GC-MS. Once the reaction was complete, it was cooled to room temperature and the precipitate that formed was filtered off to yield the desired (*E)*-substituted diarylacrylonitrile analogs **ST-510,** and **ST-507(A)** (Scheme **2.7**).

ST-510: yellow solid; ^{1}H NMR (400 MHz, DMSO-d_6): δ 3.71 (s, 9H, -OCH_3), 3.75 (s, 3H, -OCH_3), 6.67 (s, 2H, -ArH), 6.72 (s, 1H, -ArH), 6.76 (d, *J* =8.4 Hz, 1H, ArH), 6.86 (d, *J* =8.4 Hz, 1H, ArH), 7.42 (S, 1H, ArH), 9.15 (S, 1H, -OH) ppm. ^{13}C NMR (100 MHz, DMSO-d_6): 55.86, 56.07, 56.35, 56.57, 60.53, 60.75, 106.20, 106.38, 110.00, 112.06, 116.65, 121.06, 123.51, 126.45, 128.59, 138.55, 144.67, 144.94, 146.46, 150.16, 153.92 ppm.

ST-507(A): brown solid; ^{1}H NMR (400 MHz, DMSO-d_6): δ 3.92 (s, 3H, -OCH_3), 3.96(s, 6H, -OCH_3), 7.04 (T, *J* =13.2 Hz, 2H, ArH), 7.12 (s, 1H, ArH), 7.22 (d, *J* =2, 8.4Hz, 1H, ArH), 7.31 (S, 1H, ArH), 7.35 (d, *J* =10.4 Hz, 1H, ArH) ppm. ^{13}C NMR (100 MHz, DMSO-d_6): 55.95, 56.07, 108.69, 108.74, 109.18, 110.59, 110.61, 111.26, 115.06,

115.19, 118.44, 118.75, 122.02, 122.12, 127.47, 127.66, 140.15, 140.24, 145.66, 148.25, 149.23, 149.76 ppm.

2.6 Synthesis of (E)-3-(3-hydroxy-4-methoxyphenyl)-2-(3,4,5-trimethoxyphenyl)acrylic acid for evaluation of anticancer activity and for UDP-glucuronosyltransferase studies.

(*E*)-3-(3-hydroxy-4-methoxyphenyl)-2-(3,4,5-trimethoxyphenyl)acrylic acid was designed to investigate its ability to act as a substrate for UDP-glucuronosyltransferases and to evaluate the anticancer activity of the compound.

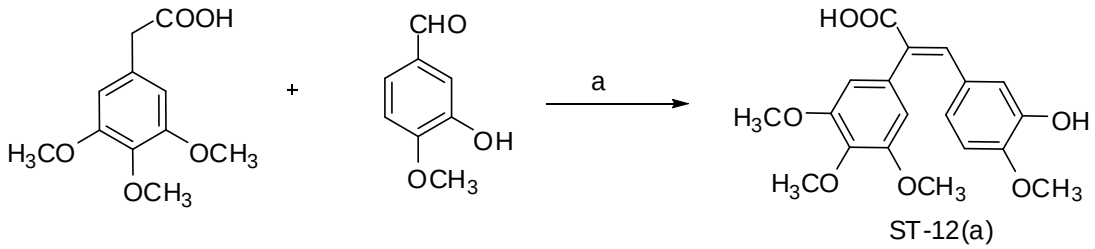

Scheme 2.8 Synthesis of (*E*)-3-(3-hydroxy-4-methoxyphenyl)-2-(3,4,5-trimethoxyphenyl)acrylic acid (**ST-12(a)**). (a) TEA, Ac2O, 140 °C, 40% yield.

3-Hydroxy-4- methoxybenzaldehyde (9) (1.0 mmol), 2-(3,4,5-trimethoxyphenyl)-acetic acid (10) (2.0 mmol) and triethylamine (3.2 mmol) were added to 5 mL of acetic anhydride. The resulting reaction mixture was refluxed at 140 °C for 4 h, with periodic monitoring by TLC. When the reaction was complete, 10 mL of ice-water was added and the mixture extracted with 10 ml of ethyl acetate. The organic phase was concentrated on a rotary evaporator and the desired product purified by silica gel flash column

chromatography using methanol/DCM as mobile phase to afford **ST-12(a)** in 35% yield (**Scheme 2.8**).

ST-12(a): ^{1}H NMR (CDCl3-d6, ppm): δ 3.43 (d, 12H,−OCH3, J = 15.2 Hz), 6.69 (d, 2H, −ArH, *J* = 2.8 Hz), 6.54 (s, 1H, −ArH), 6.61 (s, 1H, −ArH), 6.80 (s, 1H, −ArH), 8.93 (s, 1H, −ArH), 12.41 (s, 1H, −COOH) ppm. ^{13}C NMR ($CDCl_3$,): δ 55.9, 56.4, 60.6, 107.2, 110.0, 112.0, 118.0, 123.3, 127.4, 131.0, 132.5, 137.4, 139.5, 146.2, 149.3, 153.5, 169.0 ppm.

2.7 Synthesis of (*Z*)-5-(2-(2*H*-tetrazol-5-yl)-2-(3,4,5-trimethoxyphenyl)vinyl)-2-methoxyphenol (ST-145(a)) as second generation *trans*-stilbenes

Cushman and co-workers designed and synthesized a series of novel imidazole-containing resveratrol analogues and evaluated their inhibitory activities as aromatase and quinone reductase inhibitors. Among the synthesized compound **XC (Figure 2.7)** displayed potent aromatase inhibitory activity (IC_{50} = 36 nM) and showed promising anticancer activity against various human tumor cell lines (Sun, Hoshino et al. 2010). We planned to introduce a tetrazole ring resembling the imidazole pharmacophore present on **XC** as a structural modification of our lead compound (**ST-145**) to improve the compounds water solubility and anti-cancer activity. The pharmacological assay data for **ST-145(a)** is discussed in Chapter 3.

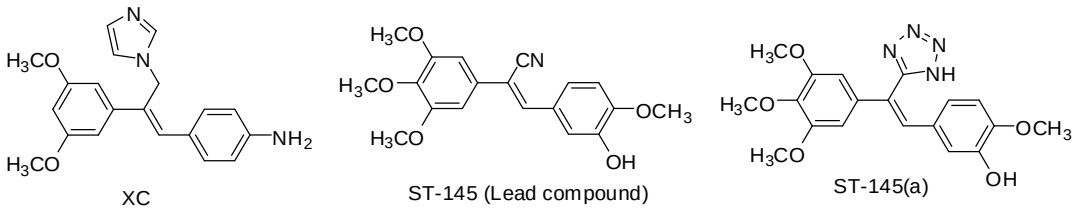

Figure 2.7 Structures of the potent aromatase inhibitor **XC**, **ST-145** and **ST-145(a)**.

(*Z*)-5-(2-(2*H*-tetrazol-5-yl)-2-(3,4,5-trimethoxyphenyl)vinyl)-2-methoxyphenol (**ST-145(a))** was synthesized as a second generation analogue and a structural analogue of the lead molecule (*Z*)-3-(3-hydroxy-4-methoxyphenyl)-2-(3,4,5-trimethoxyphenyl)acrylonitrile (**ST-145**). Initially we tried to synthesize **ST-145(a)** by reacting (*Z*)-3-(3-hydroxy-4-methoxyphenyl)-2-(3,4,5-trimethoxyphenyl)acrylonitrile with NH_4Cl/NaN_3 in anhydrous DMF condition, but only traces of the final tetrazole product were formed. Subsequently, we used tributyltin chloride/NaN_3 in DMF to afford (*Z*)-5-(2-(2*H*-tetrazol-5-yl)-2-(3,4,5-trimethoxyphenyl)vinyl)-2-methoxyphenol (**ST-145(a)**) in 58 % yield.

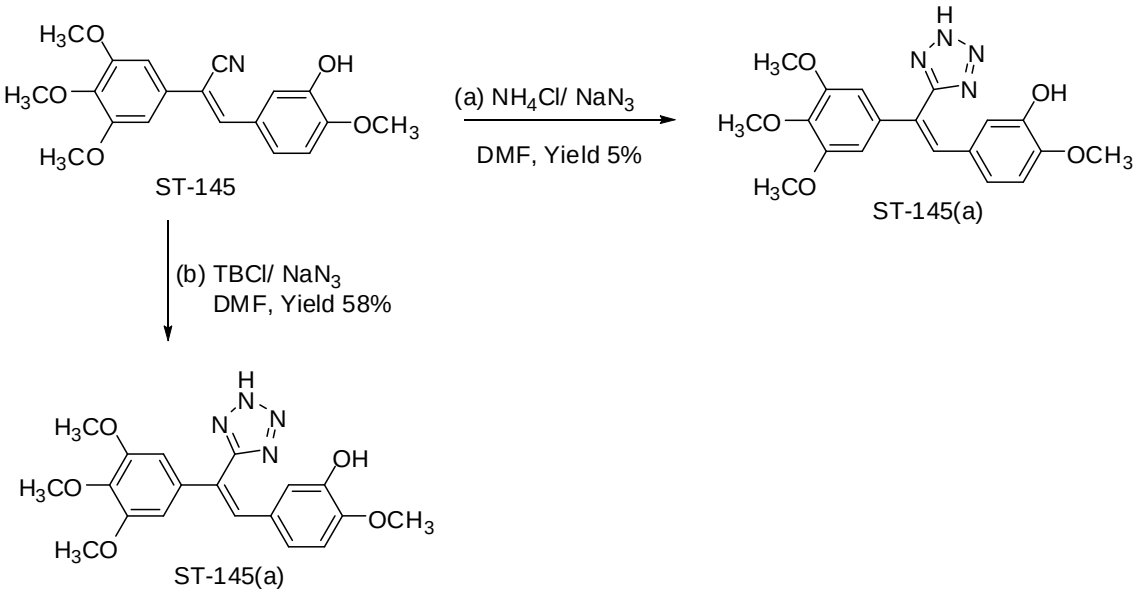

Scheme 2.9 Synthesis of **ST-145(a)**.

(**a**) A mixture of (*Z*)-3-(3-hydroxy-4-methoxyphenyl)-2-(3,4,5-trimethoxyphenyl)acrylonitrile (100mg; 1mmol), sodium azide (50mg; 5mmol) and ammonium chloride (42mg; 5mmol) was refluxed in 4ml of anhydrous DMF for 11 hrs. After the reaction was complete, 12ml of water was added and the resulting mixture was stirred for 10 min. The resulting aqueous solution was washed with five volumes of ethyl acetate three times, and the organic layers were combined and concentrated on a rotary evaporator. The residue was purified by DCM/methanol flash chromatography to yield (*Z*)-5-(2-(2*H*-tetrazol-5-yl)-2-(3,4,5-trimethoxyphenyl)vinyl)-2-methoxyphenol as a pale yellow solid in 5% yield. NOE experiments were carried out to confirm the structure of the *Z*-isomer product (**Figures 8.7, 8.8 and 8.9**).

(**b**) Tributyltin chloride (9.76 g, 0.03 mole) and sodium azide (1.95 g, 0.03) were stirred for 30 min at 15-30° C. *N*,*N*-dimethylformamide (1.46 g, 0.02 mole) was added and the

mixture stirred for 30 min. Thereafter, (*Z*)-3-(3-hydroxy-4-methoxyphenyl)-2-(3,4,5-trimethoxyphenyl)acrylo nitrile (3.21 g; 0.01 mol) was added followed by o-xylene (5 ml). The reaction mass was heated to 130-135° C and stirred for until completion of the reaction (TLC monitoring). The reaction mixture was then cooled to 20° C, and o-xylene (10 ml) and methylene chloride (10 ml) were added followed by water (10 ml). Hydrochloric acid (2.0 g, 35% w/w) was then slowly added at 20-25° C over 30 min and the slurry obtained was stirred for 60 min. The resulting solid was filtered off, washed with methylene chloride (5 ml) and dried to afford the desired tetrazole product as a pale yellow powder (58% yield).

ST-145 (a): ^{1}H NMR (400 MHz, DMSO-d_6): δ 3.89 (s, 3H, -OCH_3), 3.93 (s, 6H, -OCH_3), 3.97 (s, 3H, -OCH_3), 6.85 (s, 2H, ArH), 6.92-6.94 (d, *J* =8.4 Hz, 1H, ArH), 7.34 (s, 1H, ArH), 7.48-7.50(d, *J* =10.8 Hz, 2H, ArH) ppm. ^{13}C NMR (100 MHz, DMSO-d_6): 56.01, 56.28, 60.99, 103.10, 103.18, 109.26, 110.62, 115.08, 118.36, 122.34, 127.20, 130.49, 138.76, 141.48, 145.61, 148.44, 153.52 ppm.

Copyright © Nikhil Reddy Madadi 2014

Chapter 3

Anticancer activities of synthesized resveratrol analogs

3.1 NCI-60 Human Tumor Cell Line Screen

The biological evaluation of potential anticancer agents at the NCI is a two-stage process, starting with the screening of the submitted compounds against a panel of 60 human tumor cell lines at a single dose of 10 µM. The results from the single dose is reported as a mean graph and is analyzed by the algorithm software, COMPARE. The software is used for comparing the anticancer activity of various molecules at a same time. Using this software, compounds which showed promising growth inhibitory activity at 10 µM are then evaluated against the 60 cell panel at five concentration levels, viz. 10^{-4} M, 10-^{5} M, 10^{-6} M, 10^{-7} M and 10^{-8} M.

3.2 Methodology used for the *in vitro* anticancer screen at the NCI

RPMI 1640 medium with 5% fetal bovine serum and 2 mM L-glutamine is used for growing the NCI-60 human tumor cells. Initially the tumor cells are inoculated into 96-well microtiter plates in 100 microliters at plating densities starting from 5,000 to 40,000 cells/well. The range is dependent on the doubling time of individual tumor cell lines. The plates are then incubated at 37° C for 24 hours prior to addition of the submitted compounds (Shoemaker 2006).

After 24 hrs, two microtiter plates of each tumor cell line are fixed *in situ* with TCA. The optical density reading at this point represent the cell population for each tumor cell line at the time of compound addition (ODtzero). The experimental compounds are dissolved in DMSO at 400-fold concentration to the desired final maximum test concentration, and frozen. Then, an aliquot part of the frozen concentrate is thawed and diluted to twice the chosen maximum test concentration with medium containing 50 µg/ml gentamicin. Four more 10-fold serial dilutions are prepared to afford a total of five drug concentrations. A control sample with just DMSO is also prepared. Aliquots of 100 microliters of these different experimental drug dilutions controls are added to the appropriate microtiter wells containing 100 µl of medium, resulting in the required final drug concentrations, viz. 10^{-4} M, 10-^{5} M, 10^{-6} M, 10^{-7} M and 10^{-8} M and 0 M (control).

Once the compounds are added, the microtiter plates are incubated for 48 hrs at 37°C and 100 % relative humidity. Cold TCA is used to terminate the assay for adherent cells. Cells are fixed by the addition of 50 µl of cold 50 % (w/v) TCA and further incubated for 1 hr at 4°C. The supernatant is thrown away, and the microtiter plates are splashed five times with water and air dried. Sulforhodamine B (SRB) solution (100 microliters) at 0.4 % (w/v) in 1 % CH_3COOH is added to each well, and plates are incubated for another 10 minutes at room temperature. After SRB staining, free SRB is removed by washing five times with 1 % acetic acid. Bound SRB stain is successively dissolved with 10 mM trizma base, and the optical density is measured at a wavelength of 515 nm. The growth inhibitory or cytotoxicity effect of the test compounds in the above cellular assay is measured by determining percentage cell growth (PG) inhibition. Optical density (OD) measurements of SRB-derived color just before exposing the cells to the test compound

(ODtzero) and after 48hrs exposure to the test compound (ODtest) or the control vehicle (ODctrl) are recorded.

Growth percentage is calculated utilizing one of the two formulas below (Madadi, Penthala et al. 2014).

A negative growth percentage implies cytotoxicity.

If (OD test - ODtzero)≥0, then

PG = 100-(ODtest -ODtzero)/ (ODctrl- ODtzero)

and percentage growth is shown as positive.

If (ODtest - ODtzero) < 0, then

PG = 100 - (ODtest -ODtzero)/ODtzero and

percentage growth is shown as negative, which implies cell death.

Growth inhibitory or cytotoxicity effects of the test compounds are represented with three dose response parameters. They are:

1. GI_{50}: 50% growth inhibition, indicating concentration of drug resulting in a 50% reduction in net protein increase compared with control cells.
2. TGI: 100% growth inhibition, indicating concentration of drug resulting in a 100% reduction in net protein increase compared with control cells.
3. LC_{50}: lethal concentration, indicating concentration of drug lethal to 50% of cells.

3.3 Anticancer activity of simple stilbenes as resveratrol analogues

A total of 74 stilbenes analogues were synthesized (**Table 2.1**) and submitted to the NCI for screening against the panel of 60 human tumor cell lines, 22 analogs were selected for single dose screening at 10μM concentration. The single dose results with 10μM concentration are presented in the appendix section (**Table 8.1**- **Table 8.8**). From the 22 compounds selected for single dose screening, one compound (**ST-198**) showed promising anticancer activity and was selected for full five dose study. Of interest, Gosslau *et al*. also reported that **ST-198** potently inhibits the proliferation of cancer cells, with no inhibitory effect on normal cells (Gosslau, Pabbaraja et al. 2008). These results imply that for the stilbene to be active in the anticancer screens the trimethoxy substitution pattern on ring A and the *p*-methoxy group on ring B are essential structural elements. The GI_{50} and TGI values of compound **ST-198** against the panel of 60 human cancer cell lines are presented in **Table 3.1**. Interestingly, the introduction a cyano group on the stilbene double bond next to ring A (**ST-148**) dramatically improved the mean GI_{50} value against the panel of NCI 60 tumor cells from μM range to nM range and the data is presented in **Table 3.4**.

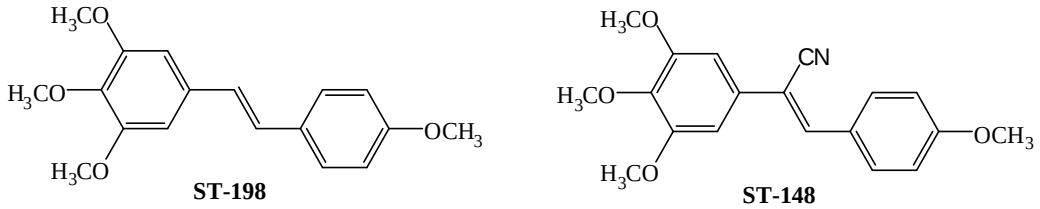

Figure 3.1 Structures of **ST-198** and **ST-148**.

Table 3.1 Growth inhibition (GI_{50}/μM) and Total Growth Inhibition (TGI/μM) data for compound **ST-198** against human cancer cells.

Table 3.1 (continued)

Panel/cell line	**ST-198**	
	GI_{50} (μM)	TGI (μM)
Leukemia CCRF-CEM	2.89	>100
HL-60(TB)	3.14	39.1
K-562	3.22	>100
MOLT-4	6.42	>100
RPMI-8226	3.93	>100
SR	3.04	>100
Non-Small Cell Lung Cancer A549/ATCC	3.70	>100
HOP-62	3.14	25.3
HOP-92	7.23	>100
NCI-H23	4.44	>100
NCI-H522	3.37	>100
Colon Cancer COLO 205	2.07	5.01
HCC-2998	3.59	>100
HCT-116	3.23	>100
HCT-15	2.82	>100
HT29	2.32	6.79
KM12	3.63	>100
SW-620	3.42	>100
CNS Cancer SF-268	7.59	>100
SNB-75	1.88	5.98
U251	3.07	16.8
Melanoma LOX IMVI	4.89	>100
M14	2.81	>100
MDA-MB-435	1.04	4.49
SK-MEL-2	3.95	22.7
SK-MEL-28	3.86	>100
SK-MEL-5	2.50	12.3
UACC-62	2.37	>100
Ovarian Cancer IGROV1	5.29	>100
OVCAR-3	3.45	14.4
OVCAR-4	4.00	>100
NCI/ADR-RES	3.01	31.9
SK-OV-3	3.34	59.7
Renal Cancer	5.42	64.8

Table 3.1 (continued)

786-0		
A498	0.74	4.56
ACHN	4.51	>100
CAKI-1	3.00	>100
UO-31	3.69	>100
Prostate Cancer PC-3	3.22	>100
DU-145	4.23	>100
Breast Cancer MCF7	1.66	>100
MDA-MB-231/ATCC	3.74	35.6
HS 578T	3.09	>100

3.4 Anticancer evaluation of *(E)*-3,5,4'-trimethoxy resveratrol analogues with substitutions at the C2 position on the stilbene.

Initially, analogs **RES-09, RES-10, RES-14, RES-27, RES-13, RES-16, RES-23** and **RES-18** were evaluated for their anti-proliferative activity against MCF-7 and MDA-231 breast cancer cell lines, and A549 and H460 lung cancer cell lines in the laboratory of Dr. Chendil Damadaran at the University of Kentucky, College of Medicine.

MCF-7, MDA-231, A-549 and H-460 cancer cells lines were purchased from the American Type Culture Collection (ATCC) (Manassas, VA) and were utilized to test the antitumor activity of the above C2-substituted resveratrol analogs. Breast cancer cell lines, MCF-7 and MDA-231 were grown in DMEM medium supplemented with 10% fetal bovine serum (FBS) and 1% L-glutamine, whereas lung cancer cell lines A549 and H460 were maintained and propagated in RPMI 1640 medium containing 2 µM L-glutamine, 4.5 g/L glucose, 10 µM HEPES, 1.0 µM sodium pyruvate and 10% FBS. All cell cultures were maintained at 37^{o}C in a 5% CO_2/95% air-humidified atmosphere. Anti-cancer activity of the resveratrol derived analogs **RES-09, RES-10, RES-14, RES-27,**

RES-13, RES-16, RES-23 and **RES-18** were assessed in cell viability assays (trypan blue dye exclusion) on both breast (MCF-7 and MDA-231) and lung (A-549 and H-460) cancer cells at 24 hours post-treatment at 5 concentrations of drug (1, 5, 10, 20 and 40 μM) and with vehicle (DMSO) alone. All assays were performed in triplicate. Results were expressed as percentage growth inhibition compared to control values. IC_{50} values for growth inhibition were derived from a nonlinear regression model based on sigmoidal dose-response curves and computed using GraphPad Prism 5 (Graphpad) (Koduru, Sowmyalakshmi et al. 2009).

Table 3.2. Tryphan blue assay results; IC_{50} values (μM) for resveratrol analogs (**RES-09, RES-10, RES-14, RES-27, RES-13, RES-16, RES-23** and **RES-18)** against lung and breast cancer cell lines

Entry	Lung cancer cell lines		Breast cancer cell lines	
	A-549	H-460	MCF-7	MDA-231
RES-09	10.6	13.3	11.8	5.57
RES-10	29.2	25.2	>40	7.59
RES-14	33.4	37.0	7.93	4.24
RES-27	6.19	1.20	14.8	0.99
RES-13	3.05	7.40	2.40	10.3
RES-16	7.52	19.3	3.96	10.1
RES-23	9.20	28.0	1.99	4.09
RES-18	7.34	24.0	1.28	12.3

We initially evaluated the abilities of the resveratrol analogues to inhibit the growth of the two human lung cancer cell lines A-549 and H-460 (**Table 3.2**). All eight compounds exhibited IC_{50} values < 37 μM in both cancer cell lines, and generally showed less growth inhibition against A549 lung cancer cells than H460 lung cancer cells. The

analogs were also tested for their anti-proliferative activity against estrogen positive MCF-7 and estrogen negative MDA-231 breast cancer cell lines. All the compounds showed growth inhibition against MCF-7 cell lines with IC_{50} values ranging from 0.99 µM to >40 µM. The pseudothiohydantoin analog (**RES-16,** IC_{50} = 2.61 µM) and the thiohydantoin analog (**RES-13,** IC_{50} = 3.05 µM) were identified as the most potent cytotoxic agents against A-549 lung cancer cells, whereas the creatinine analog (**RES-27**, IC_{50} = 1.2 µM) and thiohydantoin analog (**RES-13,** IC_{50} = 7.4 µM) were identified as the most potent cytotoxic agents against H460 lung cancer cells. The isobarbiturate analog (**RES-17**, IC_{50} = 1.28 µM) and the isorhodanine analog (**RES-18**, IC_{50} = 1.99 µM) were identified as potent cytotoxic agents against MCF-7 cells. The thiohydantoin analog (**RES-13,** IC_{50} = 2.4 µM) and the pseudothiohydantoin analog (**RES-16,** IC_{50} = 3.86 µM) also exhibited promising cytotoxicity against MCF-7 cells. The creatinine analog (**RES-27**, IC_{50} = 0.99 µM) and the isorhodanine analog (**RES-18**, IC_{50} = 4.09 µM) were identified as the most potent cytotoxic agents against MDA-231 cells.

From the library of resveratrol analogs synthesized, the following compounds: (*Z*)-2-amino-5-(2, 4-dimethoxy-6-(4-methoxystyryl)benzylidene) 1-methyl-1*H*-imidazol-4(5*H*)-one (**RES-27**), (*Z*)-2-amino-5-(2,4-dimethoxy-6-(4-methoxystyryl) benzylidene)thiazol-4(5H)-one (**RES-16**), (*Z*)-6-(2,4-dimethoxy-6-(4-methoxystyryl)benzylidene) dihydropyrimidine-2,4,5(3*H*)-trione (**RES-17**) and (*Z*)-5-(2,4-dimethoxy-6-(4-methoxystyryl) benzylidene)-4-thioxothiazolidin-2-one (**RES-18**) were identified as potent anti-proliferative agents against both lung and breast cancer cell lines.

Encouraged by the above results, a total of 31 resveratrol analogues with substitutions at the C2 position of the stilbene skeleton were submitted to NCI for evaluation in their cytotoxicity screening assays against 60 human tumor cell lines. The analogues **RES-11, RES-17, RES-59, ST-100 and ST-127**showed good activity in the 10 μM single dose screen, and were selected for five dose response studies for their *in vitro* cytotoxic effects on growth parameters against the 60 tumor cell line panel. Dose response curves were created by plotting cytotoxic effect against the log10 of the concentration for each cell line. The compound's cytotoxic effects were determined as their GI_{50}, TGI and LC_{50} values, which are presented in **Table 3.3**.

Among the compounds selected for five dose testing, acrylonitrile analogs **ST-100** and **ST-127** were found to be very effective against five particular human cancer cell lines; i.e. SR, NCI-H522, SF-539, MDA-MB-435 and RXF 393, with GI_{50} values that were less than 300 nM. Lung cancer cell line NCI-H522 appeared to be the most sensitive to the growth inhibition effects of **ST-100** and **ST-127**, exhibiting GI_{50} values of 240 nM and 250 nM, respectively. Compounds **ST-100** and **ST-127** also exhibited impressive growth inhibition against melanoma cancer cell line MDA-MB-435 with GI_{50} values of 240 nM and 280 nM, respectively. Importantly, compound **ST-100** showed promising growth inhibitory activity affording GI_{50} values < 1 μM for more than 50% of the human tumor cell lines in the panel. Compound **ST-127** was also effective against CNS cancer cell lines SF-295 (GI_{50} = 360 nM) and SF-539 (GI_{50} = 270 nM), renal cancer cell lines 786-0 (GI_{50} = 380 nM), CAKI-1 (GI_{50} = 500 nM), RXF 393 (GI_{50} = 310 nM), and breast cancer cell line MCF-7 (GI_{50} = 390 nM). Compound **ST-127** was also found to have an effective GI_{50} value of 280 nM against leukemia cancer cell line SR.

Table 3.3: Growth inhibition **(**GI_{50}/µM) and cytotoxicity (LC_{50}/µM) data for compounds **RES-11, RES-17, RES-59, ST-100 and ST-127** against human cancer cells.

Panel/cell line	RES-11		RES-17		RES-59		ST-100		ST-127	
	GI_{50} (µM)	LC_{50} (µM)	GI_{50} (µM)	LC_{50} (µM)	GI_{50} (µM)	LC_{50} (µM)	GI_{50} (µM)	LC_{50} (µM)	GI_{50} (µM)	LC_{50} (µM)
Leukemia CCRF-CEM	3.76	>100	2.86	>100	3.75	>100	0.75	>100	2.24	>100
HL-60(TB)	334	>100	2.13	>100	3.41	>100	1.66	>100	0.58	>100
K-562	0.58	>100	2.58	NA	NA	NA	**0.43**	>100	**0.43**	>100
MOLT-4	5.71	>100	2.06	>100	5.52	>100	4.38	>100	3.30	>100
RPMI-8226	5.47	>100	2.77	>100	3.88	>100	1.16	>100	2.85	>100
SR	0.52	>100	3.95	>100	1.51	>100	0.91	>100	**0.28**	>100
Lung Cancer A549/ATCC	5.06	>100	1.92	8.11	7.25	>100	0.91	>100	3.56	>100
HOP-62	4.35	>100	1.99	8.96	5.63	>100	0.97	>100	2.79	>100
NCI-H226	3.67	>100	5.37	52.3	8.54	>100	7.58	>100	17.3	>100
NCI-H322M	73.8	>100	1.97	>100	27.2	>100	4.66	>100	7.12	>100
NCI-H460	3.62	>100	2.23	32.6	3.85	>100	1.84	>100	3.47	>100
NCI-H522	4.40	>100	2.14	31.1	2.29	>100	**0.24**	>100	**0.25**	55.3
Colon Cancer COLO 205	5.49	>100	1.93	6.17	6.70	>100	1.24	>100	2.28	>100
HCC-2998	4.76	>100	1.53	6.05	8.65	>100	2.49	>100	5.47	>100
HCT-116	3.80	>100	1.75	7.25	3.94	>100	**0.49**	>100	1.29	>100
HCT-15	3.93	>100	2.14	>100	3.71	>100	0.65	>100	0.76	>100
HT29	2.89	>100	2.05	8.41	3.59	>100	0.69	>100	**0.48**	>100
KM12	2.13	>100	1.68	5.91	3.87	>100	0.78	>100	0.64	>100
SW-620	3.00	>100	1.59	5.78	4.61	>100	**0.50**	>100	0.71	>100
CNS Cancer SF-268	6.71	>100	1.67	6.06	7.20	>100	4.71	>100	4.18	>100
SF-295	3.79	>100	1.95	>100	2.37	87.6	**0.36**	>100	2.51	>100
SF-539	3.73	>100	2.06	11.2	3.21	90.0	**0.27**	>100	1.55	>100
SNB-19	6.63	>100	12.4	69.3	6.13	>100	>100	>100	8.77	>100
SNB-75	2.05	72.7	10.7	51.8	3.47	>100	**0.47**	>100	2.28	>100
U251	3.26	>100	2.18	44.9	5.22	>100	0.64	>100	2.77	>100
Melanoma M14	2.31	>100	2.16	>100	4.21	>100	1.38	>100	1.14	>100
MDA-MB-435	**0.36**	>100	3.61	>100	1.33	66.5	**0.24**	>100	**0.28**	>100
SK-MEL-28	3.06	>100	5.38	63.9	8.67	>100	0.75	>100	4.22	>100
SK-MEL-5	2.56	>100	5.97	43.2	3.28	>100	2.28	>100	2.44	>100
UACC-62	4.02	>100	2.89	35.6	2.80	>100	0.70	>100	NA	>100
Ovarian Cancer IGROV1	11.8	>100	2.77	61.3	13.8	>100	2.35	>100	5.28	>100
OVCAR-3	2.79	>100	1.93	9.87	3.73	79.0	0.63	>100	1.38	>100
OVCAR-4	10.7	>100	10.2	77.5	20.7	>100	**0.50**	>100	3.59	>100
OVCAR-5	9.15	>100	2.10	22.2	8.64	>100	6.71	>100	8.37	>100
OVCAR-8	4.58	>100	3.16	>100	17.2	>100	3.75	>100	3.37	>100
NCI/ADR-RES	1.02	>100	2.40	>100	3.30	>100	0.65	>100	0.71	>100

Table 3.3 (continued)

Renal Cancer 786-0	3.53	>100	12.7	57.8	4.06	>100	1.72	>100	3.25	>100
A498	2.44	>100	5.08	56.0	1.66	>100	**0.38**	>100	1.37	>100
ACHN	6.79	>100	2.21	18.6	6.96	>100	0.83	>100	4.25	>100
CAKI-1	3.12	>100	4.76	94.6	3.72	>100	**0.50**	>100	2.20	>100
RXF 393	2.16	>100	3.41	38.5	3.04	>100	**0.31**	>100	2.00	>100
SN12C	6.33	>100	2.55	38.9	4.72	>100	3.95	>100	4.68	>100
TK-10	13.6	>100	10.2	52.7	7.03	>100	>100	>100	1.95	>100
Breast Cancer MCF7	1.96	>100	1.44	7.89	3.30	>100	**0.39**	>100	0.72	>100
MDA-MB-231/ATCC	10.3	>100	2.76	65.7	2.19	>100	2.78	>100	2.83	>100
HS 578T	3.64	>100	2.55	>100	4.95	>100	0.68	>100	1.34	>100
BT-549	2.09	>100	3.91	49.8	6.36	>100	4.58	>100	1.31	>100
T-47D	7.28	>100	1.66	7.26	5.23	>100	0.80	>100	3.03	>100
MDA-MB-468	2.68	>100	1.66	7.10	1.93	>100	1.72	>100	1.70	>100

In conclusion, a library of novel resveratrol analogs with different substitutions on the C2 position of the stilbene skeleton was synthesized and evaluated for their growth inhibition properties against a panel of 60 human cancer cell lines. The acrylonitrile analog **ST-100** was found to be the lead compound with GI_{50} values < 1 μM for more than 50% of the cells in the panel. The novel acrylonitrile resveratrol analog **ST-100** represents a promising lead compound that may have clinical potential in treating a variety of solid and hematological cancers.

3.5 Anticancer activity of (*E/Z*)-2,3-diaryl substituted acrylonitriles as anticancer agents.

A total of 74 (*E/Z*)-2,3-diaryl substituted acrylonitriles were synthesized (Table DD) and submitted to the NCI for screening against the 60 human tumor cell panel, and 41 analogs were selected for single dose screening at 10μM. The single dose results are presented in the appendix (**Table 8.9- Table 8.14**). From the 41 compounds selected for single dose screening 18 compounds showed promising anticancer activity and were selected for full

five dose studies. The GI_{50} and TGI values of these 18 compounds against the panel of 60 human cancer cell lines are presented in **Tables 3.4** to **3.8**

Table 3.4: Growth Inhibition **(**GI_{50}/µM) and Total Growth Inhibition (TGI/µM) data for compounds **ST-198, ST-148, ST-147 and ST-124** against human cancer cells.

Panel/cell line	**ST-198**		**ST-148**		**ST-147**		**ST-124**	
	GI_{50} (µM)	TGI (µM)	GI_{50} (nM)	TGI (µM)	GI_{50} (µM)	TGI (µM)	GI_{50} (nM)	TGI (µM)
Leukemia CCRF-CEM	2.89	>100	36.7	58.7	51.2	>100	324	11.1
HL-60(TB)	3.14	39.1	22.0	6.32	68.6	>100	289	0.89
K-562	3.22	>100	<10	>100	3.14	>100	317	>100
MOLT-4	6.42	>100	36.2	33.5	28.2	>100	438	>100
RPMI-8226	3.93	>100	3.00	17.4	6.64	>100	339	10.5
SR	3.04	>100	<10	>100	4.14	>100	294	18.5
Non-Small Cell Lung Cancer A549/ATCC	3.70	>100	15.1	>100	6.35	>100	388	>100
HOP-62	3.14	25.3	30.1	>100	7.63	>100	516	>100
HOP-92	7.23	>100	23.9	15.7	3.57	69.5	NA	NA
NCI-H23	4.44	>100	57.8	>100	43.0	>100	537	>100
NCI-H522	3.37	>100	<10	0.02	20.5	>100	94.3	0.61
Colon Cancer COLO 205	2.07	5.01	13.1	0.03	5.16	42.7	270	0.63
HCC-2998	3.59	>100	43.5	>100	97.0	>100	349	16.7
HCT-116	3.23	>100	<10	>100	6.05	>100	333	>100
HCT-15	2.82	>100	<10	>100	4.47	>100	336	>100
HT29	2.32	6.79	<10	16.2	4.24	>100	289	1.03
KM12	3.63	>100	<10	13.6	4.97	>100	388	12.8
SW-620	3.42	>100	10.6	>100	5.17	>100	424	>100
CNS Cancer SF-268	7.59	>100	40.7	>100	25.3	>100	848	>100
SF-295	2.18	8.20	<10	30.3	5.33	>100	222	0.95
SF-539	2.18	5.70	<10	0.03	6.60	57.4	223	0.51
SNB-19	4.85	>100	59.7	>100	5.46	>100	988	>100
SNB-75	1.88	5.98	<10	>100	2.67	>100	295	59.2
U251	3.07	16.8	29.3	60.2	7.82	>100	343	30.6
Melanoma LOX IMVI	4.89	>100	14.1	>100	5.31	>100	580	>100
M14	2.81	>100	19.3	>100	4.45	94.1	288	>100
MDA-MB-435	1.04	4.49	<10	NA	1.63	7.58	173	0.48
SK-MEL-2	3.95	22.7	85.1	>100	5.44	79.7	887	>100
SK-MEL-28	3.86	>100	NA	>100	14.0	>100	498	>100
SK-MEL-5	2.50	12.3	12.7	0.06	4.70	68.1	278	1.36
UACC-62	2.37	>100	<10	>100	2.42	61.7	404	>100
Ovarian Cancer IGROV1	5.29	>100	26.3	>100	14.6	>100	532	>100

Table 3.4 (continued)

OVCAR-3	3.45	14.4	<10	NA	6.69	>100	300	0.73
OVCAR-4	4.00	>100	14.6	>100	7.48	>100	734	>100
NCI/ADR-RES	3.01	31.9	<10	86.8	3.25	38.3	274	>100
SK-OV-3	3.34	59.7	<10	58.3	14.4	>100	370	NA
Renal Cancer 786-0	5.42	64.8	21.6	>100	13.0	>100	425	13.8
A498	0.74	4.56	<10	0.02	1.29	43.3	252	2.08
ACHN	4.51	>100	10.6	>100	9.78	>100	532	>100
CAKI-1	3.00	>100	NA	NA	6.19	>100	544	20.9
UO-31	3.69	>100	<10	28.3	1.92	17.9	490	>100
Prostate Cancer PC-3	3.22	>100	10.1	>100	4.71	>100	363	>100
DU-145	4.23	>100	23.7	>100	71.2	>100	501	16.5
Breast Cancer MCF7	1.66	>100	<10	>100	4.35	>100	310	>100
MDA-MB-231/ATCC	3.74	35.6	28.3	>100	4.83	64.3	434	6.95
HS 578T	3.09	>100	<10	>100	16.7	>100	317	>100
MDA-MB-468	2.22	>100	21.1	20.5	3.44	57.0	294	2.45

Table 3.5: Growth Inhibition **(**GI_{50}/μM) and Total Growth Inhibition (TGI/μM) data for compounds **ST-507, ST-507(a), ST-145** and **ST-510** against human cancer cells.

Panel/cell line	**ST-507**		**ST-507(a)**		**ST-145**		**ST-510**	
	GI_{50} (nM)	TGI (μM)	GI_{50} (nM)	TGI (μM)	GI_{50} (nM)	TGI (μM)	GI_{50} (nM)	TGI (μM)
Leukemia CCRF-CEM	34.3	>100	38.9	46.5	<10	23.8	<10	>100
HL-60(TB)	29.9	NA	30.4	NA	<10	<0.01	<10	>100
K-562	22.6	>100	31.5	>100	<10	>100	<10	>100
MOLT-4	51.1	>100	73.8	22.7	<10	14.0	<10	>100
RPMI-8226	42.0	54.5	44.6	25.6	<10	2.21	<10	>100
SR	21.9	>100	26.6	49.6	<10	45.9	<10	>100
Non-Small Cell Lung Cancer A549/ATCC	218	>100	259	>100	<10	29.0	<10	>100
HOP-62	34.6	>100	33.3	93.1	<10	29.1	NA	NA
HOP-92	16900	>100	8650	85.1	<10	1.37	<10	NA
NCI-H23	76.3	>100	79.7	36.6	<10	17.9	<10	>100
NCI-H522	<10	0.05	12.9	0.07	<10	<0.01	<10	<0.01
Colon Cancer COLO 205	12400	47.1	12600	44.7	2990	24.9	301	11.1
HCC-2998	181	>100	172	34.5	26.1	12.1	<10	>100
HCT-116	36.4	>100	33.7	40.0	<10	10.3	<10	0.01
HCT-15	36.6	>100	32.9	12.5	<10	16.6	<10	>100
HT29	5780	>100	6230	>100	3180	46.9	320	4.61
KM12	22.9	>100	38.2	16.3	<10	19.5	<10	>100
SW-620	35.2	>100	38.6	78.7	<10	>100	<10	>100
CNS Cancer	66.3	>100	77.0	65.0	<10	60.4	<10	>100

SF-268								
SF-295	966	>100	5870	22.8	49.6	13.7	13.1	>100
SF-539	21.7	NA	23.1	NA	<10	<0.01	<10	<0.01
SNB-19	50.5	>100	43.7	>100	<10	>100	<10	>100
SNB-75	21.6	NA	16.8	NA	<10	41.1	<10	>100
U251	43.9	>100	47.3	>100	11.2	25.8	<10	>100
Melanoma LOX IMVI	58.2	>100	69.5	22.6	<10	19.5	<10	>100
M14	27.5	>100	22.8	NA	<10	14.8	<10	NA
MDA-MB-435	<10	<0.01	<10	0.02	<10	<0.01	<10	<0.01
SK-MEL-2	NA	>100	NA	49.8	<10	39.8	<10	>100
SK-MEL-28	11100	>100	12700	68.6	1010	24.5	<10	>100
SK-MEL-5	43.5	2.1	45.4	1.76	<10	0.02	<10	<0.01
UACC-62	20.9	>100	NA	35.8	<10	21.4	<10	>100
Ovarian Cancer IGROV1	61.3	>100	71.0	>100	<10	>100	<10	<0.01
OVCAR-3	17.3	NA	20.8	NA	<10	43.7	<10	>100
OVCAR-4	15600	>100	10700	56.5	<10	22.6	<10	>100
NCI/ADR-RES	16.2	>100	22.3	0.12	<10	NA	<10	>100
SK-OV-3	48.7	>100	53.7	54.6	16.9	43.5	<10	>100
Renal Cancer 786-0	3660	>100	2430	>100	<10	34.3	14.8	0.85
A498	20.0	NA	25.0	NA	<10	<0.01	<10	>100
ACHN	84.4	>100	85.6	48.8	<10	43.3	<10	>100
CAKI-1	>100	>100	423	>100	34.2	33.9	<10	>100
UO-31	57.2	>100	88.9	26.9	<10	19.3	<10	>100
Prostate Cancer PC-3	41.2	>100	39.3	50.1	<10	17.0	<10	>100
DU-145	36.5	>100	37.4	58.7	<10	39.6	<10	>100
Breast Cancer MCF7	35.3	>100	35.4	24.0	<10	12.1	<10	>100
MDA-MB-231/ATCC	44.9	>100	45.6	>100	<10	90.8	<10	>100
HS 578T	25.7	>100	27.7	NA	<10	92.2	<10	>100
MDA-MB-468	43.4	>100	44.6	30.2	<10	<0.01	<10	>100

Table 3.6: Growth Inhibition **(**GI_{50}/µM) and Total Growth Inhibition (TGI/µM) data for compounds **ST-179, ST-163, ST-178 and ST-180** against human cancer cells.

Panel/cell line	**ST-179**		**ST-163**		**ST-178**		**ST-180**	
	GI_{50} (µM)	TGI (µM)	GI_{50} (nM)	TGI (µM)	GI_{50} (µM)	TGI (µM)	GI_{50} (nM)	TGI (µM)
Leukemia CCRF-CEM	1.91	25.9	250	>100	3.65	>100	46.9	>100
HL-60(TB)	1.57	17.7	247	>100	3.50	55.2	25.7	>100
K-562	0.53	30.9	41.3	>100	0.79	70.7	36.4	>100
MOLT-4	3.71	>100	450	>100	4.99	>100	67.4	>100
RPMI-8226	3.85	>100	494	>100	4.49	>100	192	>100
SR	5.44	12.6	54.7	>100	1.60	21.2	35.5	>100
Non-Small Cell	2.65	>100	277	>100	500	>100	99.6	>100

Table 3.6 (continued)

Lung Cancer A549/ATCC								
HOP-62	2.14	14.5	308	62.8	3.77	>100	76.9	>100
HOP-92	12.0	63.2	>1000	>100	4.55	53.0	>1000	>100
NCI-H23	5.09	91.8	NA	>100	6.45	>100	325	>100
NCI-H522	2.37	7.78	43.0	0.51	2.89	9.73	15.6	0.057
Colon Cancer COLO 205	1.61	4.81	140	1.06	2.58	7.45	36.1	0.200
HCC-2998	5.42	>100	>1000	>100	11.0	>100	275	>100
HCT-116	2.41	>100	229	>100	3.72	>100	45.2	>100
HCT-15	0.75	>100	74.4	>100	1.77	>100	47.3	>100
HT29	1.60	>100	61.3	>100	3.02	22.6	33.0	13.1
KM12	2.39	>100	73.8	>100	3.77	>100	51.6	>100
SW-620	0.72	>100	122	>100	3.72	>100	50.1	>100
CNS Cancer SF-268	9.34	>100	730	>100	8.99	>100	>1000	>100
SF-295	1.91	10.5	202	13.1	2.96	>100	38.1	20.0
SF-539	1.58	6.97	249	1.42	2.71	11.0	45.1	>100
SNB-19	4.24	95.0	751	>100	6.29	>100	237	>100
SNB-75	1.14	4.88	NA	>100	2.45	9.44	27.5	18.2
U251	2.71	16.4	438	>100	3.85	>100	67.0	38.6
Melanoma LOX IMVI	3.96	>100	571	>100	4.22	>100	56.7	40.2
M14	1.68	>100	123	>100	3.13	>100	49.5	>100
MDA-MB-435	0.31	>100	27.5	0.095	0.43	6.20	25.4	0.104
SK-MEL-2	2.90	17.8	209	50.8	3.18	>100	43.5	>100
SK-MEL-28	4.52	>100	457	>100	5.84	>100	247	>100
SK-MEL-5	1.52	18.9	212	>100	3.20	2.04	57.3	2.67
UACC-62	1.51	41.1	594	>100	2.63	>100	56.3	>100
Ovarian Cancer IGROV1	4.07	>100	>1000	>100	5.95	>100	90.3	>100
OVCAR-3	3.04	NA	271	>100	4.18	28.4	37.9	>100
OVCAR-4	3.79	>100	NA	>100	8.25	>100	>1000	>100
NCI/ADR-RES	1.65	>100	79.2	>100	2.52	>100	42.4	>100
SK-OV-3	2.35	>100	404	>100	3.58	>100	56.2	>100
Renal Cancer 786-0	4.38	29.1	>1000	>100	5.62	50.6	887	>100
A498	0.41	5.38	201	6.17	1.17	7.08	31.6	2.50
ACHN	4.24	>100	525	>100	4.52	>100	63.2	>100
CAKI-1	2.06	>100	NA	>100	4.18	>100	48.9	>100
UO-31	6.24	>100	579	>100	6.48	>100	83.2	>100
Prostate Cancer PC-3	3.04	>100	321	>100	5.52	>100	55.6	>100
DU-145	3.49	>100	587	>100	6.94	>100	216	>100
Breast Cancer MCF7	0.61	>100	81.0	>100	1.99	>100	87.9	>100
MDA-MB-231/ATCC	2.43	>100	>1000	>100	5.11	>100	180	>100
HS 578T	2.63	80.5	466	>100	3.54	81.6	82.8	>100
MDA-MB-468	0.51	11.9	281	>100	2.11	62.6	383	45.7

Table 3.7: Growth Inhibition **(**GI_{50}/µM) and Total Growth Inhibition (TGI/µM) data for compounds **ST-257, ST-260, ST-261** and **ST-253** against human cancer cells.

Panel/cell line	ST-257		ST-260		ST-261		ST-253	
	GI_{50} (µM)	TGI (µM)	GI_{50} (nM)	TGI (µM)	GI_{50} (nM)	TGI (µM)	GI_{50} (nM)	TGI (µM)
Leukemia CCRF-CEM	3.76	>100	297	>100	52.2	>100	209	>100
HL-60(TB)	2.07	17.9	60.3	NA	30.9	NA	40.4	25.4
K-562	NA	>100	NA	NA	NA	NA	NA	NA
MOLT-4	8.85	>100	1010	>100	60.5	>100	622	>100
RPMI-8226	4.81	>100	34.2	76.2	53.4	>100	57.0	20.8
SR	0.93	31.5	67.9	21.1	31.7	>100	64.1	>100
Non-Small Cell Lung Cancer A549/ATCC	4.12	>100	146	>100	35.8	27.6	60.2	>100
HOP-62	2.98	>100	94.9	>100	44.2	17.4	51.5	>100
HOP-92	9.64	>100	1410	72.0	37.9	23.9	119	42.1
NCI-H23	6.61	>100	598	>100	48.1	16.5	158	>100
NCI-H522	2.80	>100	67.6	>100	2.73	87.9	51.1	>100
Colon Cancer COLO 205	2.77	12.3	131	0.42	22.2	0.04/0.08	121	0.38
HCC-2998	8.85	>100	331	>100	38.9	53.5	140	>100
HCT-116	2.71	>100	45.2	13.0	30.1	1.13	34.3	13.5
HCT-15	0.73	>100	57.4	>100	30.6	>100	39.2	>100
HT29	NA	>100	NA	NA	NA	NA	NA	>100
KM12	1.59	>100	80.3	>100	39.7	>100	54.4	>100
SW-620	1.04	>100	54.3	>100	37.8	>100	44.2	>100
CNS Cancer SF-268	5.38	>100	651	>100	51.4	43.2	113	>100
SF-295	2.49	21.8	41.1	13.1	28.4	13.1	28.6	33.5
SF-539	2.56	>100	48.8	0.47	25.0	0.09/2.47	25.2	0.07
SNB-19	4.08	>100	414	>100	60.6	62.0	199	>100
SNB-75	2.16	>100	91.3	>100	44.4	16.3	34.2	>100
U251	3.97	44.3	218	>100	36.4	10.3	49.8	60.7
Melanoma LOX IMVI	4.92	>100	145	>100	31.1	>100	64.4	>100
M14	1.63	>100	48.1	NA	25.6	NA	34.7	NA
MDA-MB-435	0.26	1.21	25.9	0.092	20.9	0.06	21.4	NA
SK-MEL-2	1.84	>100	558	>100	NA	NA	NA	>100
SK-MEL-28	4.59	>100	155	>100	49.1	>100	62.5	>100
SK-MEL-5	0.84	33.9	66.4	11.9	23.2	0.06	33.1	0.18
UACC-62	1.04	>100	35.1	>100	38.7	>100	35.3	>100
Ovarian Cancer IGROV1	9.40	>100	660	>100	76.2	>100	633	>100
OVCAR-3	2.16	10.1	51.8	29.4	36.4	4.55	36.2	>100
OVCAR-4	11.2	>100	927	>100	77.8	>100	266	>100
NCI/ADR-RES	1.52	>100	56.2	>100	31.0	>100	32.7	>100
SK-OV-3	3.24	58.1	113	15.5	30.9	0.09	43.1	>100
Renal Cancer	3.88	>100	62.4	>100	34.6	>100	38.4	16.8

Table 3.7 (continued)

786-0								
A498	1.35	9.26	49.8	90.0	32.8	2.50	26.3	13.8
ACHN	7.61	>100	306	>100	46.2	>100	79.8	>100
CAKI-1	2.92	>100	91.1	>100	50.9	>100	50.1	>100
UO-31	501	>100	761	>100	2040	>100	NA	>100
Prostate Cancer PC-3	4.57	>100	160	>100	41.0	>100	56.3	>100
DU-145	4.69	>100	381	>100	38.8	21.2	135	>100
Breast Cancer MCF7	0.86	>100	157	>100	32.0	>100	40.2	56.5
MDA-MB-231/ATCC	4.69	>100	376	52.7	26.8	0.07	170	>100
HS 578T	5.56	>100	154	>100	38.6	>100	71.2	>100
MDA-MB-468	1.11	>100	94.0	5.64	27.4	0.28	34.0	0.77

Table 3.8: Growth Inhibition **(**GI_{50}/µM) and Total Growth Inhibition (TGI/µM) data for compounds **ST-252** and **ST-173** against human cancer cells.

Table 3.8 (continued)

Panel/cell line	**ST-252**		**ST-173**	
	GI_{50} (µM)	TGI (µM)	GI_{50} (µM)	TGI (µM)
Leukemia CCRF-CEM	>100	>100	1.56	24.8
HL-60(TB)	>100	>100	1.49	>100
K-562	NA	>100	0.39	>100
MOLT-4	>100	>100	2.81	>100
RPMI-8226	>100	>100	3.23	>100
SR	2.76	>100	0.53	47.0
Non-Small Cell Lung Cancer A549/ATCC	21.7	>100	2.65	>100
HOP-62	>100	>100	3.30	>100
HOP-92	>100	>100	7.42	>100
NCI-H23	>100	>100	6.33	>100
NCI-H522	>100	>100	2.58	8.98
Colon Cancer COLO 205	>100	>100	1.59	3.77
HCC-2998	7.78	>100	11.9	>100
HCT-116	6.33	>100	2.68	>100
HCT-15	2.10	>100	0.87	>100
HT29	NA	>100	0.71	>100

Table 3.8 (continued)

KM12	4.26	>100	2.25	>100
SW-620	3.93	>100	1.23	>100
CNS Cancer SF-268	>100	>100	9.36	>100
SF-295	10.6	>100	1.75	>100
SF-539	73.1	>100	1.61	4.31
SNB-19	>100	>100	6.95	>100
SNB-75	21.9	>100	NA	>100
U251	>100	>100	3.59	>100
Melanoma LOX IMVI	NA	>100	5.33	>100
M14	3.87	>100	1.32	>100
MDA-MB-435	0.51	4.50	0.30	>100
SK-MEL-2	36.8	>100	0.72	>100
SK-MEL-28	>100	>100	4.47	>100
SK-MEL-5	3.54	>100	2.58	>100
UACC-62	8.68	>100	2.32	>100
Ovarian Cancer IGROV1	>100	>100	8.80	>100
OVCAR-3	37.1	>100	3.10	>100
OVCAR-4	24.9	>100	1.65	5.73
NCI/ADR-RES	4.45	>100	2.41	>100
SK-OV-3	>100	>100	2.75	>100
Renal Cancer 786-0	35.8	>100	4.93	>100
A498	>100	>100	1.33	8.62
ACHN	>100	>100	4.92	>100
CAKI-1	>100	>100	NA	>100
UO-31	>100	>100	6.66	>100
Prostate Cancer PC-3	>100	>100	3.03	>100
DU-145	>100	>100	3.62	>100
Breast Cancer MCF7	3.01	>100	0.85	>100
MDA-MB-231/ATCC	69.3	>100	3.36	>100
HS 578T	>100	>100	3.62	>100
MDA-MB-468	4.29	>100	0.69	>100

From the 74 (*E/Z*)-2,3-diaryl substituted acrylonitriles that were synthesized, analogues **ST-145** and **ST-510** were found to be the lead compounds from the five-dose studies against the panel of 60 human cancer cell lines. These compounds were remarkable in that they afforded GI_{50} values that were less than 10 nM against almost all human cancer cells in the NCI panel. Although, the GI_{50} values of the two isomers **ST-145** and **ST-510** are comparable, the *Z* isomer, **ST-145**, had the best TGI (Total Growth Inhibition) profile against HL-60(TB), NCI-H522, SF-539, MDA-MB-435, A-498, MDA-MB-468 tumor cell lines with values less than 10 nM.

3.6 *In vitro* toxicity and tubulin affinity study of ST-145, ST-510, ST-507 and ST-507(a) against acute myeloid leukemia (AML) cell line MV-411

Compounds **ST-507**, **ST-507(a)**, **ST-145** and **ST-510** were found to be very effective against the human leukemia sub-panel of cells, and especially the two analogs **ST-145** and **ST-510**, which had GI_{50} values of less than 10 nM across all the leukemic cells in the subpanel. At this point, we decided to test the lead compounds **ST-507**, **ST-507(a)**, **ST-145** and **ST-510** against acute myeloid leukemia MV-411 cells. The biological assays related to MV-411 cell lines were conducted by Dr. Monica Guzman's research group.

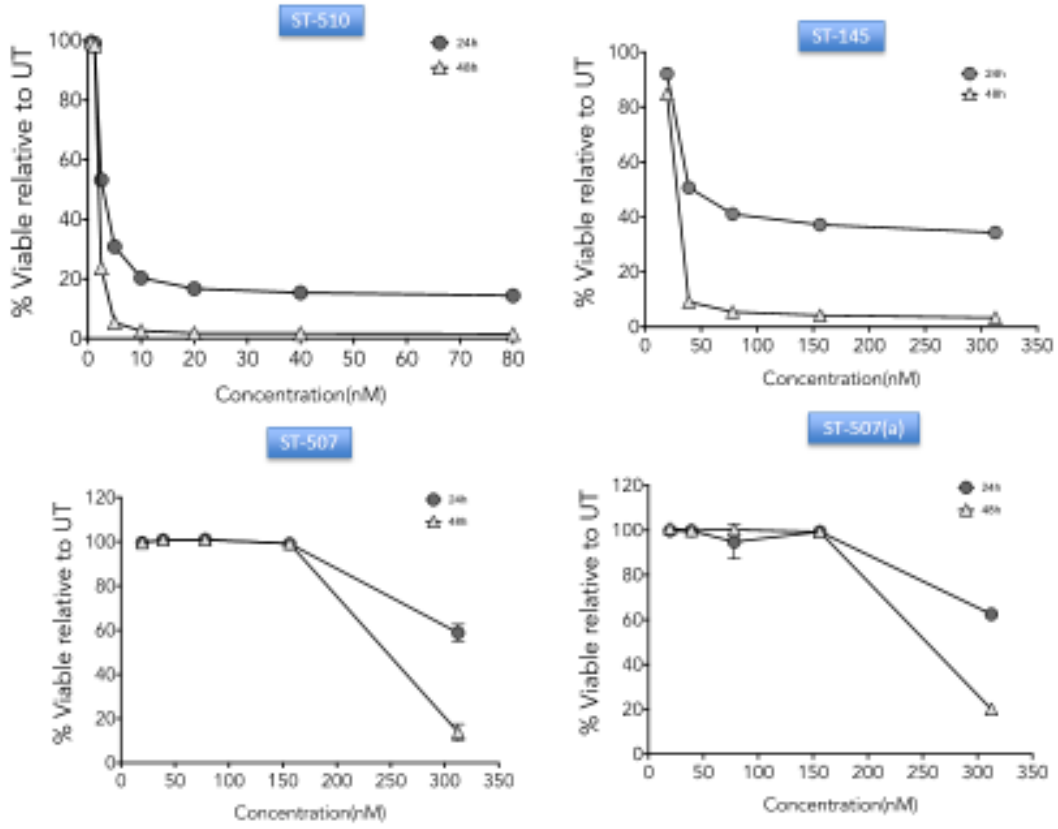

Figure 3.2. Lead compounds **ST-507**, **ST-507(a)**, **ST-145** and **ST-510** exhibit potent anti-leukemia activity. MV-411 cells were treated with the indicated compounds for 24 and 48 h. Cell viability was determined by Annexin V staining. Percent viability was calculated as the percent of annexin v-/7-AAD-cells relative to control.

MV-411 cells (AML cell line) were treated with increasing concentrations of the lead compounds **ST-507**, **ST-507(a)**, **ST-145** and **ST-510** for 24 and 48 hours. **Figure 3.2** shows the dose-response curves for each of the compounds at both time courses. We found that **ST-510** was the most potent anti-leukemia compound in the series, causing more than 80 percent cell death over both 24h and 48h drug treatments at concentrations below 5 nM (Figure **3.2** top left panel). Compound **ST-145** afforded an LD_{50} of ~30nM over 48 hours of drug treatment (Figure **3.2**). Compounds **ST-507** and **ST-507(a)**

presented LD_{50} values of ~238nM and ~280nM, respectively, at 48h (**Figure 3.2**). These data suggest that further investigation into the value of the above analogues as possible treatment for AML and associated leukemias is warranted, and may provide novel therapeutic avenues for treating this hematological malignancy.

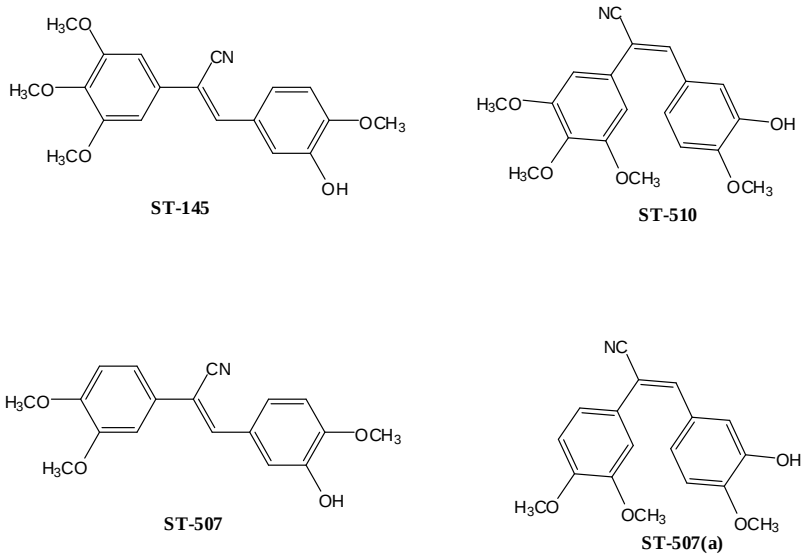

Figure 3.3: Structures of the lead cyano stilbenes **ST-507**, **ST-507(a)**, **ST-145** and **ST-510** tested against MV-411 (AML) cells.

We wanted to test our hypothesis that the mode of action of the cyano stilbene analogues as anticancer agents was through disruption of microtubule dynamics, resulting in the inhibition of mitosis. We investigated whether our lead compounds **ST-507**, **ST-507(a)**, **ST-145** and **ST-510** could interfere with microtubule polymerization by immunofluorescence using antibody against tyrosinated tubulin (a marker for dynamic microtubules) (Gundersen, Kalnoski et al. 1984, Baas and Black 1990). Through this study we also wanted to compare depolymerization activity in the presence of the *E/Z* cyano stilbenes.

MV4-11 cells were treated with the indicated doses (25, 50 and 100 nM) of **ST-507**, **ST-507(a)**, **ST-145** and **ST-510** for 2 hrs. Intracellular staining was performed using antibody against tyrosinated α-tubulin. Cells were stained with DAPI before mounting to the slides to show the cell nucleus. Cells were lysed in microtubule stabilizing buffer. The polymerized α-tubulin in the pellets (P) and unpolymerized α-tubulin in the supernatants (S) were detected by Western blotting using antibody against tyrosinated α-tubulin.

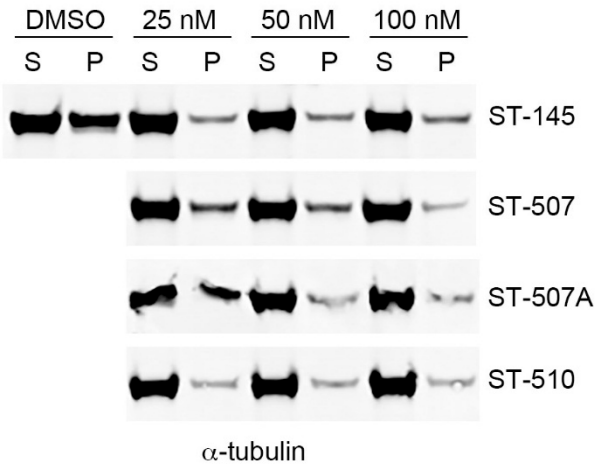

Figure 3.4: Microtubule depolymerization assay with the lead compounds **ST-507**, **ST-507(a)**, **ST-145** and **ST-510.**

Consistent with the superior anti-leukemia activity observed for **ST-510** over **ST-145** in MV4-11 cells, **ST-510** demonstrated a more potent inhibition of MT polymerization when compared to **ST-145** (Figure 3.5). Thus, our data strongly demonstrates that all four *E/Z* diarylacrylonitriles bind to tubulin directly to inhibit its polymerization.

In conclusion a library of *E/Z* diarylacrylonitriles analogs resembling resveratrol were synthesized and evaluated for their anticancer activity in an NCI panel of 60 human tumor cell lines and the lead compounds from the study (i.e. **ST-507**, **ST-507(a)**, **ST-145** and **ST-510)** were tested against MV-411 (Acute Myeloid Leukemia) cells. Analogs **ST-**

145 and **ST-510** were found to have potent anticancer properties that are likely mediated through interference with tubulin polymerization. This data suggests that further investigation into the clinical potential of these analogues for treatment of AML could provide novel therapeutics for treatment of this hematological malignancy.

3.7 Anticancer activity of (*Z*)-5-(2-(2*H*-tetrazol-5-yl)-2-(3,4,5-trimethoxyphenyl)vinyl)-2-methoxyphenol (ST-145(a)) as a second generation *trans* stilbene analogue

From the library of synthesized resveratrol analogs, **ST-145** was found to a lead anticancer agent. However, we wanted to synthesize second generation drug-like molecule with improved water solubility while preserving the potency of **ST-145**. **ST-145(a)** is a tetrazole substituted stilbene and was prepared as a second generation anticancer molecule in the resveratrol series. The GI_{50} TGI and LD_{50} values of the **ST-145(a)** against the panel of NCI 60 human cancer cell line panel are presented in **Table 3.9**.

Table 3.9: Growth Inhibition **(**GI_{50}/µM), Total Growth Inhibition (TGI/µM) and Cytotoxicity (LC_{50}/µM) data for compound **ST-145(a)** against human cancer cells.

Panel/cell line	**ST-145(a)**		
	GI_{50} (nM)	TGI (µM)	LC_{50} (µM)
Leukemia CCRF-CEM	<10	20.10	>100
HL-60(TB)	<10	NA	>100
K-562	<10	>100	>100
MOLT-4	<10	19.80	>100
RPMI-8226	<10	8.06	>100
SR	<10	25.50	>100
Non-Small Cell Lung Cancer A549/ATCC	<10	21.7	>100

Table 3.9 (continued)

HOP-62	<10	28.1	>100
HOP-92	<10	6.66	>100
NCI-H23	<10	48.5	>100
NCI-H522	<10	<0.01	>100
Colon Cancer COLO 205	970	11.1	44.0
HCC-2998	<10	32.1	>100
HCT-116	<10	20.1	>100
HCT-15	<10	27.0	>100
HT29	2200	59.8	>100
KM12	<10	11.9	54.4
SW-620	<10	57.7	>100
CNS Cancer SF-268	<10	40.3	>100
SF-295	528	18.6	61.9
SF-539	<10	<0.01	>100
SNB-19	<10	>100	>100
SNB-75	<10	23.7	96.3
U251	<10	NA	>100
Melanoma LOX IMVI	<10	25.4	>100
M14	<10	16.3	44.6
MDA-MB-435	<10	<0.01	95.4
SK-MEL-2	<10	23.3	63.9
SK-MEL-28	<10	28.5	78.7
SK-MEL-5	<10	<0.01	5.69
UACC-62	<10	18.4	47.0
Ovarian Cancer IGROV1	<10	25.7	>100
OVCAR-3	<10	NA	>100
OVCAR-4	<10	76.7	>100
NCI/ADR-RES	<10	>100	>100
SK-OV-3	<10	19.7	>100
Renal Cancer 786-0	<10	51.4	>100
A498	<10	<0.01	97.5
ACHN	<10	42.3	>100
RXF 393	<10	25.8	>100

Table 3.9 (continued)

UO-31	<10	16.4	>100
Prostate Cancer PC-3	<10	16.0	>100
DU-145	<10	15.3	74.1
Breast Cancer MCF7	<10	14.2	80.4
MDA-MB-231/ATCC	<10	59.6	>100
HS 578T	<10	47.7	>100
MDA-MB-468	<10	12.7	>100

ST-145(a) was selected for full dose response studies had very effective GI_{50} and TGI (Total Growth Inhibition) values against various human tumor cell lines. The majority of the LD_{50} values were >100μM against most of the human cancer cell lines, implying the compound is a potent anti-proliferative agent. **ST-145(a)** had impressive GI_{50} values of <10nM against almost all the cell lines in the panel except for colon cancer cell lines HT29 and COLO 205. The compound also showed potent TGI values of <10nM against non-small cell lung cancer cell line NCI-H522, CNS cancer cell line SF-539, Melanoma cell line MDA-MB-435 and renal cancer cell line A498.

3.8 *In vitro* toxicity study of ST-145(a) against Acute Myeloid Leukemia cell line MV-411

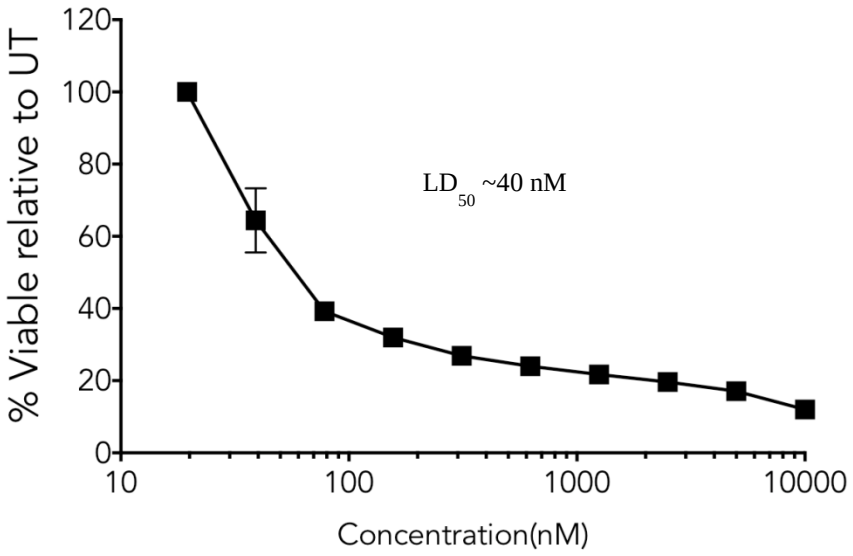

Figure 3.5. Lead compound ST-145(a) exhibited potent anti-leukemia activity against MV-411 cells.

MV-411 cells (AML cell line) were treated with increasing concentrations of the lead compound **ST-145(a)** for 48 hours. Cell viability was determined by Annexin V staining. Percent viability was calculated as the percent of annexin v-/7-AAD- cells relative to control. Compound **ST-145(a)** exhibited an LD_{50} <40nM after 48 hours of drug treatment (Figure **3.5**), and is worthy of further preclinical investigation as a possible treatment for AML. **ST-145(a)** may also have clinical potential in treating a variety of human cancers.

3.9 Conclusion

In conclusion, a large library of resveratrol analogs have been synthesized and evaluated for anticancer activity in the NCI panel of 60 human tumor cell lines. **Figure 3.6** illustrates the triage flow chart with the number of compounds submitted to the NCI (**180**) versus the number of compounds selected for 10μM single dose screening (**85**).

Out of **85** compounds screened, **25** showed promising growth inhibitory activity against human tumor cell lines and were selected for full dose-response study. The lead compounds emerging from these five-dose study were also tested for their tubulin binding activity and their cytotoxicity against MV-411 (Acute Myeloid Leukemia) cells was determined.

Figure 3.6: Triage flow chart of resveratrol analogues that were submitted for anticancer screening in the NCI panel of 60 human cancer cell lines.

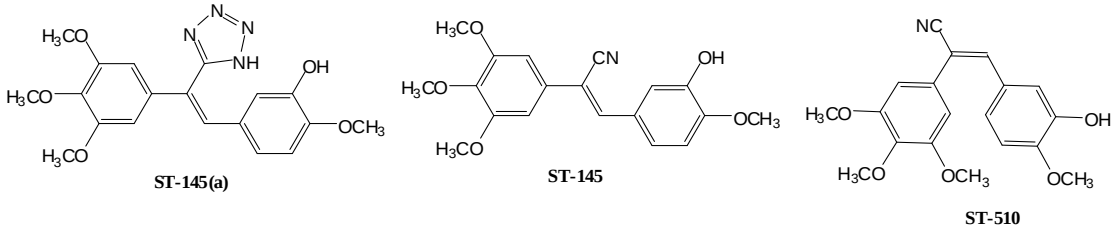

Figure 3.7: Structures of the lead resveratrol analogs **ST-145(a)**, **ST-145** and **ST-510**.

Three lead compounds, **ST-145(a), ST-145** and **ST-510 (Figure 3.7)** that may have clinical potential in treating a variety of human cancers have been discovered that have potent anticancer properties. The mechanism of action of these compounds are likely mediated through their interference with tubulin polymerization. Further investigation of this important class of compounds may provide novel therapeutic agents with clinical potential.

Copyright © Nikhil Reddy Madadi 2014

Chapter 4

Preparation of novel 4,5 disubstituted-2*H*-1,2,3-triazoles as combretastatin A4 analogues

4.1 Introduction

Although, significant research has been carried out to date to treat cancer, there is still a lack of effective chemotherapeutic treatment to cure it completely with minimal side effects. Also, considerable effort has been put into identifying molecules with anti-cancer properties from both natural and synthetic sources. More than 60% of the anticancer drugs currently available are from natural sources (Gordaliza 2007). The search for potent semi-synthetically derived anticancer agents from parent natural products continues to be an important part of the drug discovery process.

Antimitotic agents are a major class of cytotoxic drugs for the treatment of cancer, and drugs that target microtubule/tubulin dynamics are widely used in cancer chemotherapy (Jordan 2002). There are three major binding sites for tubulin. They are the vinca, taxane and colchicine domains. The vinca alkaloids such as vincristine and vinblastine, bind to the vinca domain and inhibit the assembly of microtubule structures and arrest mitosis (Hadfield, Ducki et al. 2003). Paclitaxel acts at the taxane domain and stabilizes microtubules interfering with the normal breakdown of microtubules during mitosis (Jordan and Wilson 2004). Our area of interest was the colchicine binding site. Colchicine binds to tubulin and inhibits microtubule polymerization. Anti-mitotic agents

such as combretastatin A-4 (CA-4) and related compounds have the capability of binding at the colchicine domain of tubulin. These natural products are structurally related to resveratrol and have received much attention lately, since the water-soluble phosphate salt of CA-4 is currently in phase III clinical trials for treatment of anaplastic thyroid cancer. The phosphate salt of of CA-4 is also in phase II clinical trials as a treatment for polypoidal choroidal vasculopathy and neovascular age-related macular degeneration (Young and Chaplin 2004, Cooney, Ortiz et al. 2005).

Combretastatin A4 (CA-4) is a *cis*-stilbene compound originating from the South African willow tree, *combretum caffrum.* CA-4 functions as a microtubule targeting agent, interfering with microtubule dynamics and perturbing the mitotic cycle (Tron, Pirali et al. 2006). When compared to colchicine, the vascular disrupting effects of CA-4 are well below the maximum tolerable dose with fewer side effects *in vivo* (Tozer, Kanthou et al. 2002). However, CA-4 suffers from chemical stability issues because of facile *cis*-*trans* isomerism in solution. CA-4 is a *cis*-configured stilbene which is readily converted to the thermodynamically more stable, but less potent *trans*-isomer (Hsieh, Liou et al. 2005). Extensive studies have been conducted in attempts to stabilize the *cis*-configuration of CA-4 by replacing the ethylene bridge in the molecule with heterocyclic ring systems such as β-lactam, azetidone, thiazole, tetrazole, imidazole, pyrazole, oxazolone, triazole, furanone moieties (Shirai, Takayama et al. 1998, Tron, Pagliai et al. 2005, Carr, Greene et al. 2010, Beale, Bond et al. 2012, Banimustafa, Kheirollahi et al. 2013, Demchuk, Samet et al. 2014).

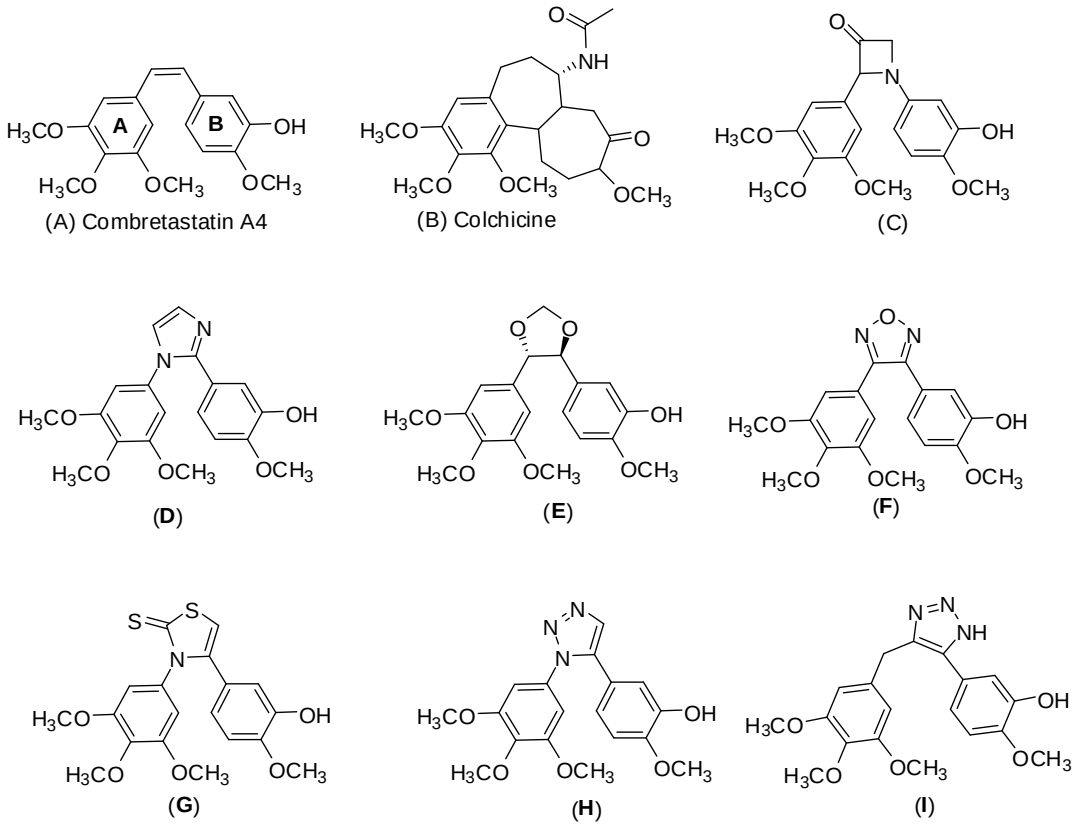

Figure 4.1: Structures of Combretastatin A4 (CA-4) (A), Colchicine (B), and heterocyclic anti-tubulin compounds (C-I).

In the work described herein, we report on the synthesis of novel and potent *cis*-constrained 4,5-disubstituted 2*H*-1,2,3-triazole combretastatin A-4 analogs which incorporates a unique heterocyclic moiety between the two aromatic rings to afford a chemically stable, *cis*-configured CA-4 scaffold. Evaluation of the anti-cancer properties of a sub-lbrary of these novel CA-4 analogues against the NCI panel of 60 human tumor cell lines has been performed, as well as with the determination of activity of these compounds in the tubulin polymerization assay.

4.2 Methodology, Development, and Design of 4,5 disubstitutes-2H-1,2,3-triazoles

1,2,3-Triazoles are an important class of heterocycles which have a wide range of applications in agricultural, industrial and pharmaceutical arenas . This ring system is present in a number of drugs with various biological properties, such as anti-cancer, anti-fungal, anti-viral, anti-consulvant (Pålhagen, Canger et al. 2001), and anti-HIV agents (Alvarez, Velazquez et al. 1994), Industrial applications include dyes, photostabilizers, photographic materials and anti-corrosives. Our laboratory is currently focusing on the development of anticancer agents structurally related to resveratrol and combretastatin A4 (CA-4) (Figure 4.1, A) (Pettit, Singh et al. 1995, Penthala, Janganati et al. 2014). CA-4 suffers from chemical instability in solution, due to *cis-trans* isomerism (Nathwani, Hughes et al. 2013). We are currently involved in identifying chemically stable analogues of *cis*-cyano-CA4 and related compounds that retain their potent anticancer properties One approach we are exploring is the replacement of the acrylonitrile moiety in these active anticancer agents with a heterocyclic ring system such as the triazole moiety, to afford geometrically stable triazole analogs of cyano-CA4 (Figure 4.2, C) that do not undergo *cis-trans* isomerism in solution.

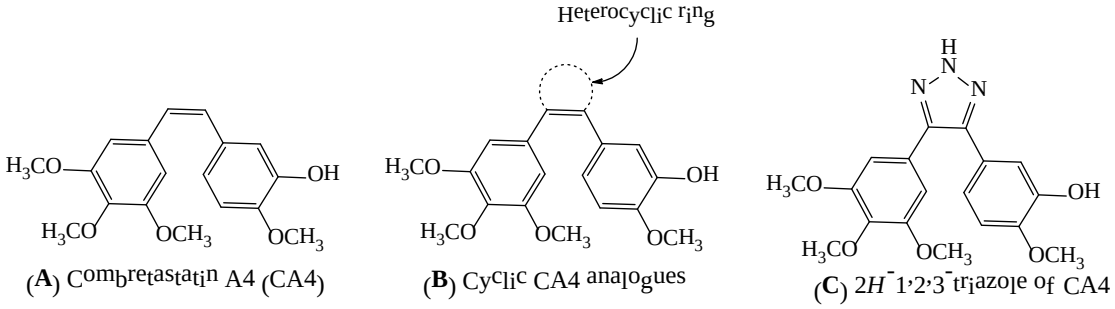

(**A**) Combretastatin A4 (CA4) (**B**) Cyclic CA4 analogues (**C**) 2*H*-1,2,3-triazole of CA4

Figure 4.2: Structures of CA4 and *cis* constraines heterocyclic CA4 analogs.

The conventional route for preparing 1,2,3-triazoles is via the Huisgen 1,3-dipolar cycloaddition of azides with alkynes (**Scheme 4.1**). However, the disadvantages of this synthetic approach are poor regioselectivity and long reaction times. A variety of triazoles can also be synthesized by the click chemistry methodologies developed by Sharpless et al. between azides and alkynes, to yield 1,5-disubstituted 1,2,3-triazoles (Krasiński, Fokin et al. 2004). However, inorganic azides (e.g. NaN_3) are not good substrates for this reaction, and these methods cannot be applied to the synthesis of internal alkynes. Recently, Majireck et al. and Tsai et al. have reported the synthesis of 4,5-disubstituted 2*H*-1,2,3-triazoles by cycloaddition of internal alkynes with alkyl azides or metal azides, but the disadvantage of this approach is the low yielding synthesis of the alkyne reactant, especially when an electron donating group is attached to the alkyne terminus (Majireck and Weinreb 2006, Tsai, Yang et al. 2009).

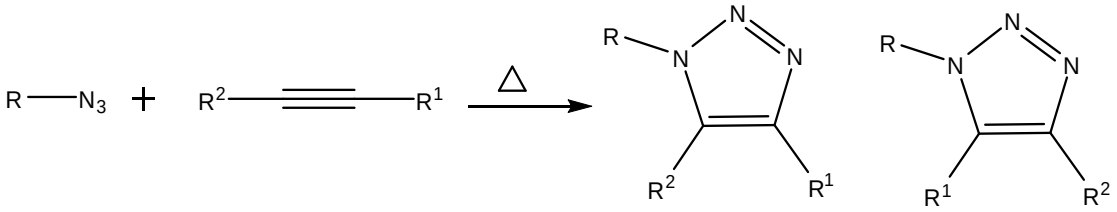

Scheme 4.1: 1,2,3 triazole synthesis by the Huisgen azide-alkyne 1,3 dipolar cyclization.

A less explored route for the synthesis of 2*H*-1,2,3-triazoles is the cycloaddition of azides with alkenes bearing a good leaving group. Zard et al. reported the synthesis of 4,5-disubstituted-1*H*-1,2,3-triazoles from nitroalkenes, but did not report any formation of 4,5-disubstituted 2*H*-1,2,3-triazoles via this approach (Quiclet-Sire and Zard 2005). Sengupta et al. have reported the synthesis of 4,5-disubstituted 2*H*-1,2,3-triazoles from

nitroalkenes, however, the presence of a vinyl group was necessary for the reaction to proceed (Sengupta, Duan et al. 2008).

Herein, we report a novel synthetic procedure for the synthesis of 4,5-disubstituted 2*H*-1,2,3-triazoles from (*Z*)-2,3-diaryl-substituted acrylonitriles by treatment with NaN_3/NH_4Cl in aqueous DMF (**Scheme 4.3**). The advantage of this methodological approach is that cyano-CA4 analogs bearing a broad range of aromatic functionalities can be easily converted to their corresponding 2*H*-1,2,3-triazole derivatives in one step.

Utilizing (*Z*)-3-(3,4-dichlorophenyl)-2-(3,4-dimethoxyphenyl) acrylonitrile as a model reactant, it was observed that using a combination of 10:1 volumes of DMF/H_2O as solvent significantly improved the yield of 4-(3,4-dichlorophenyl)-5-(3,4-dimethoxyphenyl)-2*H*-1,2,3-triazole compared to using DMF alone (**Scheme 4.3**). The reaction did not proceed in anhydrous THF. The rate of the reaction was found to be dependent on the molar amount of NaN_3/NH_4Cl used (**Table 4.1**). The optimum conditions for this reaction are: heating the reactant under reflux with 3 molar equivalents of NH_4Cl and 3 molar equivalents of NaN_3 in 10:1 volumes of DMF/H_2O. X-ray crystallographic studies on compounds **ST-464** and **ST-447(a)** confirmed the presence of a 2*H*-1,2,3-triazole ring system and the position of *N*-methylation (**Figure 4.3**).

Scheme 4.2: Proposed mechanism and optimization of the reaction conditions for the synthesis of 4-(3,4-dichloro)-5-(3,4-dimethoxyphenyl)-2*H*-1,2,3-triazole and synthesis of its methylated product.

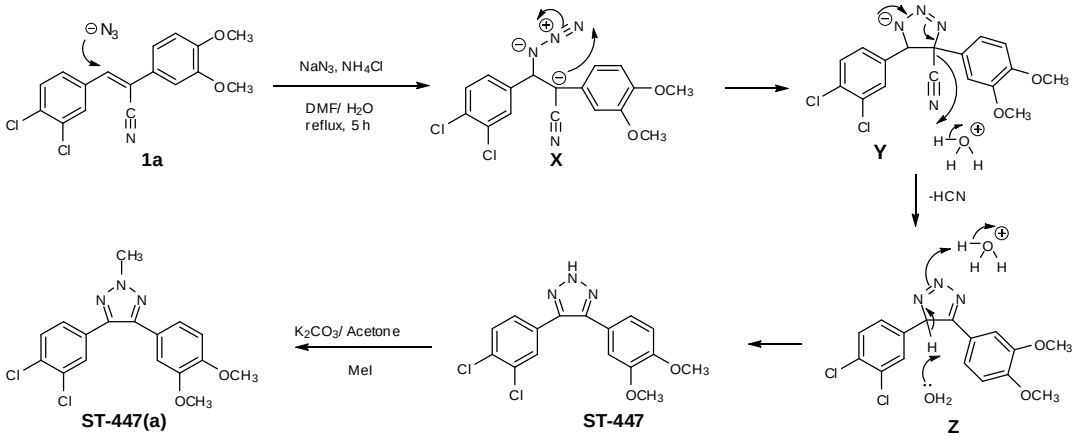

Table 4.1: Optimization of the reaction conditions for the synthesis of 4-(3,4-dichloro)-5-(3,4-dimethoxyphenyl)-2*H*-1,2,3-triazole .

Entry	Solvent	Reaction Conditions	Yield[a] (%)
1	DMF[c]	Reflux, 5 hrs, 3 eq NH_4Cl/ 3eq NaN_3	24
2	DMF/H_2O[b]	Reflux, 5 hrs, 3 eq NH_4Cl/ 3eq NaN_3	81
3	DMF/H_2O[b]	Reflux, 5 hrs, 1 eq NH_4Cl/ 1eq NaN_3	45
4	DMF/H_2O[b]	Reflux, 5 hrs, 3eq NaN_3	32
5	THF[c]	Reflux, 5 hrs, 3 eq NH_4Cl/ 3eq NaN_3	0

Previous reports have not elaborated on the mechanism of formation of the 2*H*-1,2,3-triazole ring in stilbenes of structure **1a (Scheme 4.3)** (Majireck and Weinreb 2006, Tsai, Yang et al. 2009). The proposed mechanism of triazole ring formation likely involves

initial Michael addition of azide ion at the unsubstituted sp2 olefinic carbon to afford compound **X** followed by cyclization to **Y (Scheme 4.2)**. Acid-catalyzed elimination of the cyano moiety then affords **ST-447**. It is evident from the optimization studies that NH_4Cl and water are essential components in the reaction **(Table 4.1**). All the reactions were conducted with (*Z*)-2,3-diarylacrylonitriles. However, we did examine the relative usefulness of utilizing (*E*)-2,3-diarylacrylonitriles in these reactions. Thus, (*E*)-3-(3-hydroxy-4-methoxyphenyl)-2-(3,4,5-trimethoxyphenyl)-acrylonitrile, the corresponding (*E*)-isomer of **1e (Table 4.2)**, was used as a starting material for the synthesis of compound **ST-145(b)**. The yield of the resulting 2*H*-1,2,3-triazole **ST-145(b)** was 21% compared to 59% when the (*Z*)-isomer was utilized under similar reaction conditions (**Table 4.2**; Entry 5), indicating that (*E*)-2,3-diarylacrylonitriles are less useful than their (*Z*)-counterparts in the synthesis of 2*H*-1,2,3-triazoles of structure **2 (Scheme 4.3)**. Also when (*E*)-1,3-dimethoxy-5-(4-methoxystyryl)benzene (**TMR)** was used as a starting material the reaction did not proceed (**Table 4.2)**.

4.3 Chemistry

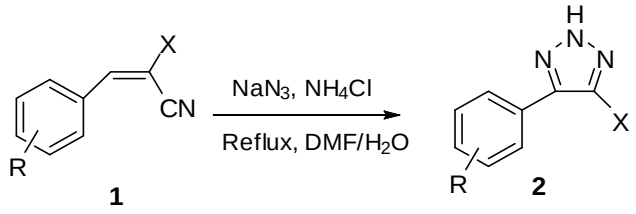

Scheme 4.3: Synthesis of 4,5-disubstituted 2*H*-1,2,3-triazoles from (*Z*)-2,3-diarylacrylonitriles.

General experimental procedure: A typical experimental procedure entailed refluxing a mixture of the (Z)-2,3-diarylacrylonitrile (**1, Scheme 4.3**), NaN_3 and NH_4Cl in a mole ratio of 1: 3: 3 in 10: 1 volumes of DMF/ H_2O for 5-12 hrs. The reaction was monitored by TLC and GC-MS. When the starting material had completely disappeared, cold water was added and the mixture was stirred over 10-15 min, during which time the final product precipitated out and could be filtered off. In the absence of a precipitate, the product was extracted into ethyl acetate, the organic extract washed with copious amounts of water, and the resulting organic liquor evaporated to dryness on a rotovaporator. The residue obtained was purified by flash column chromatography [need eluting solvent details] to afford the corresponding triazole (**2, Scheme 4.3**). Yields of the synthesized triazoles are presented in **Table 4.2**, and ranged from 59% to 87%.

A variety of cyano-CA4 analogs were subjected to treatment with NaN_3/DMF/H_2O under the above optimized reaction conditions, and their corresponding 4,5-disubstituted 2*H*-1,2,3-triazoles were obtained in modest to good yields (Table **2**). No significant side products were formed in the reactions shown in **Scheme 4.4**.

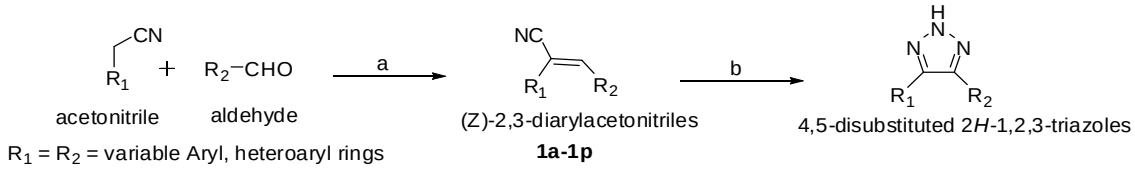

Scheme 4.4: Synthesis of 4,5-disubstituted 2*H*-1,2,3-triazoles; reagents and conditions: (a) 5% NaOMe, MeOH, reflux. (b) NaN_3, NH_4Cl, DMF/H_2O.

Table 4.2: Synthesis of 4,5-disubstituted-2*H*-1,2,3-triazoles from their corresponding (*Z*)-2,3-diaryl substituted acrylonitriles.

Entr-y	acetonitrile	aldehyde	(*Z*)-2,3-diarylacetonitriles (**1a-1w**)	4,5-disubstituted 2*H*-1,2,3-triazoles
1.	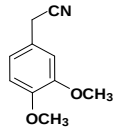	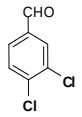	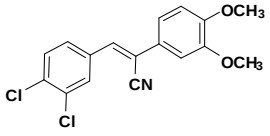 **1a**	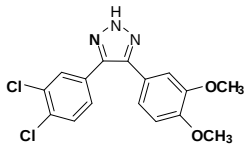 **ST-447**
2.	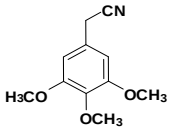	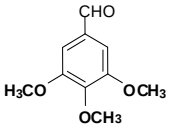	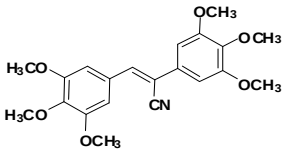 **1b**	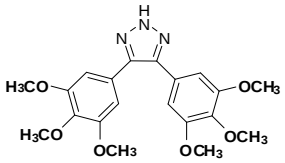 **ST-464**
3.	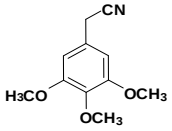	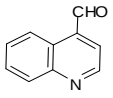	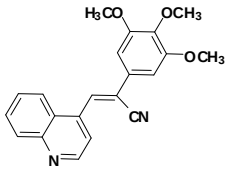 **1c**	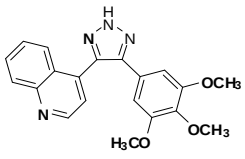 **ST-492**
4.	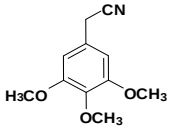	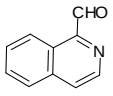	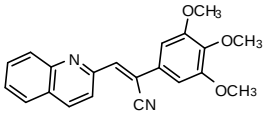 **1d**	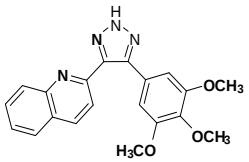 **ST-497**
5.	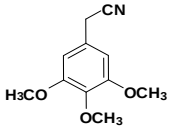	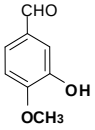	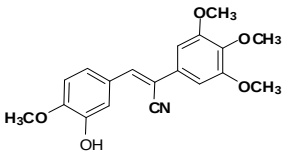 **1e**	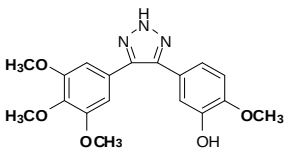 **ST-145(b)**

Table 4.2 (continued)

6.		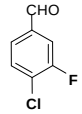	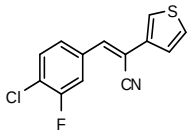 **1f**	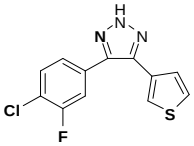 **ST-445**
7.	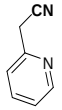	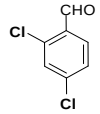	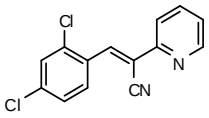 **1g**	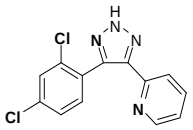 **ST-452**
8.	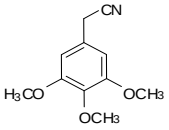	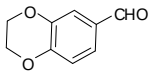	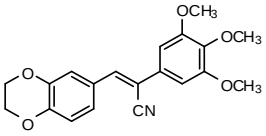 **1h**	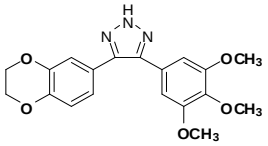 **ST-282**
9.	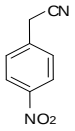	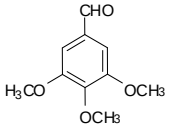	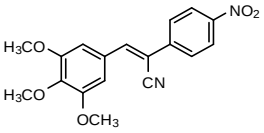 **1i**	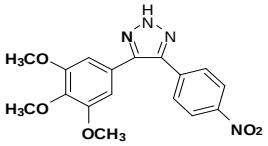 **ST-466**
10		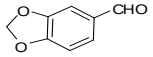	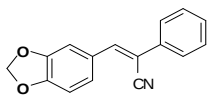 **1j**	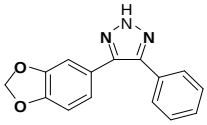 **ST-471**
11	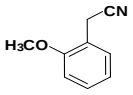	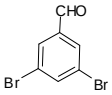	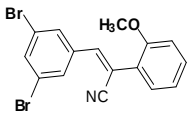 **1k**	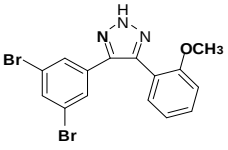 **ST-478**

Table 4.2 (continued)

12	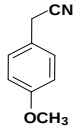	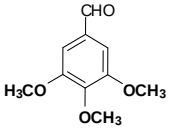	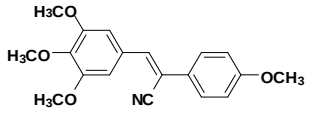 **1l**	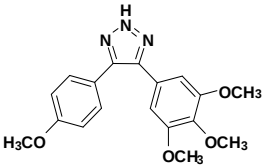 **ST-467**
13	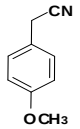	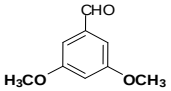	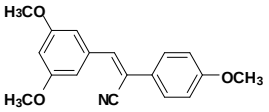 **1m**	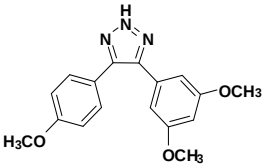 **ST-124(a)**
14		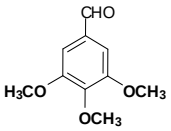	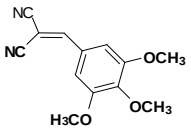 **1n**	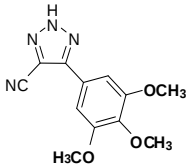 **ST-487**
15	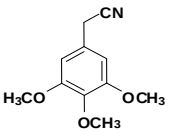	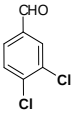	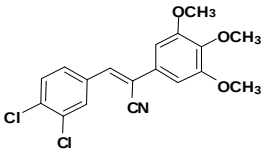 **1o**	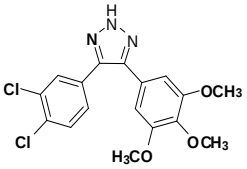 **ST-489**
16	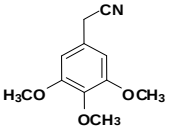		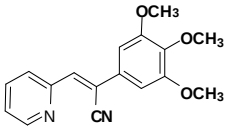 **1p**	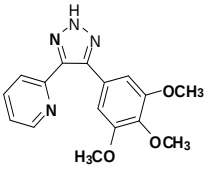 **ST-441**
17	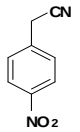	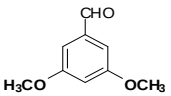	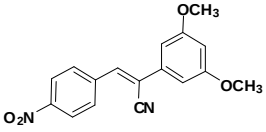 **1q**	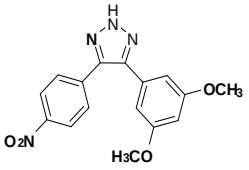

Table 4.2 (continued)

				ST-109
18	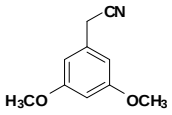	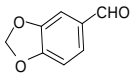	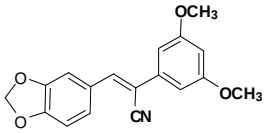 **1r**	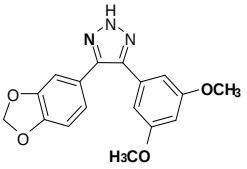 **ST-475**
19	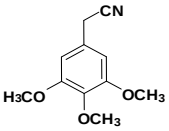	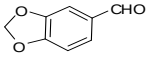	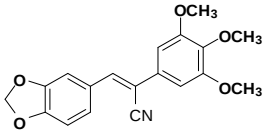 **1s**	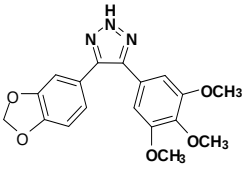 **ST-482**
20	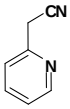	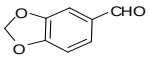	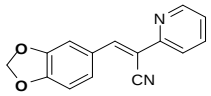 **1t**	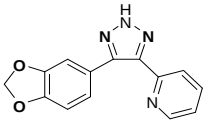 **ST-442**
21	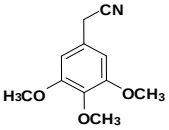	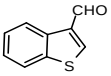	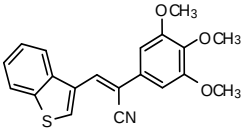 **1u**	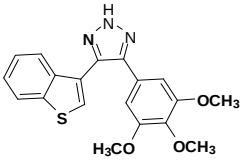 **ST-450**
22	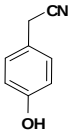	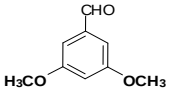	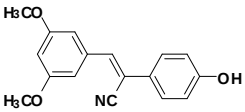 **1v**	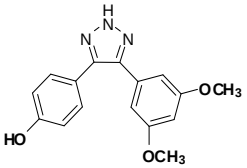 **ST-513**
23	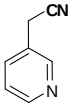	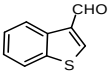	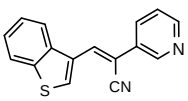	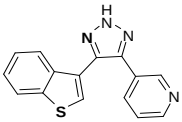

Table 4.2 (continued)

			1w	ST-440
24	-	-	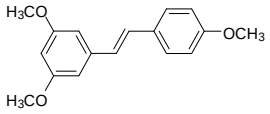 TMR	No reaction

4.4 Analytical Data:

ST-464: ^{1}H NMR (400 MHz, DMSO-d_6): δ 3.77 (s, 12H, -OCH_3), 3.88 (s, 6H, -OCH_2), 6.85 (s, 4H, ArH) ppm. ^{13}C NMR (100 MHz, DMSO-d_6): 56.02, 56.11, 56.19, 60.91, 60.99, 105.47, 125.64, 138.25, 153.27 ppm. HRMS (ESI): *m/z* calcd for C20H23N3O6 [M-H] 402.1665; found 402.1668.

ST-475: ^{1}H NMR (400 MHz, DMSO-d_6): δ 3.75 (s, 6H, -OCH_3), 5.29 (s, 2H, -CH_2), 5.99 (s, 2H, ArH), 6.48 (s, 1H, ArH), 6.72-6.73 (d, *J* =2.4 Hz, 2H, ArH), 6.80-6.83 (d, *J* =8.8 Hz, 1H, ArH), 7.05-7.07 (d, *J* =6.4 Hz, 2H, ArH), 7.26 (S, 1H, ArH) ppm. ^{13}C NMR (100 MHz, DMSO-d_6): 55.42, 55.51, 101.05, 101.25, 106.12, 108.51, 108.80, 122.38, 131.91, 147.81, 147.98, 160.87 ppm. HRMS (ESI): *m/z* calcd for C17H16N3O4 [M-H] 326.1141; found 326.1133.

ST-471: ^{1}H NMR (400 MHz, DMSO-d_6): δ 6.00 (s, 2H, -CH_2), 6.80-6.82 (d, *J* =8.8 Hz, 1H, ArH), 7.03-7.05 (d, *J* =6.8 Hz, 2H, ArH), 7.38-7.40 (t, *J* =5.2 Hz, 3H, ArH),

7.56-7.58 (m, *J* =9.6 Hz, 1H, ArH) ppm. ^{13}C NMR (100 MHz, DMSO-d_6): 101.25, 108.58, 108.70, 122.23, 128.24, 128.70, 147.85 ppm. HRMS (ESI): *m/z* calcd for C15H12N3O2 [M-H] 266.0930; found 266.0928.

ST-466: ^{1}H NMR (400 MHz, DMSO-d_6): δ 3.70-3.72 (d, 9H, -OCH_3), 6.80 (s, 2H, ArH), 7.86 (s, 2H, ArH), 8.29-8.31 (d, *J* =8.4 Hz, 2H, ArH) ppm. ^{13}C NMR (100 MHz, DMSO-d_6): 56.18, 60.81, 124.58, 126.83, 127.84, 137.86, 139.57, 143.83, 149.52, 154.62 ppm. HRMS (ESI): *m/z* calcd for C17H17N4O5 [M-H] 357.1199; found 357.1199.

ST-467: ^{1}H NMR (400 MHz, DMSO-d_6): δ 3.74 (s, 6H, -OCH_3), 3.84 (s, 3H, -OCH_3), 3.89 (s, 3H, -OCH_3), 6.83 (s, 2H, ArH), 6.91-6.93 (d, *J* =8.4 Hz, 2H, ArH), 7.51-7.53 (d, *J* =8.0 Hz, 2H, ArH) ppm. ^{13}C NMR (100 MHz, DMSO-d_6):55.27, 55.36, 55.96, 56.05, 60.90, 60.99, 105.14, 105.18, 114.03, 125.86, 129.79, 138.07, 153.27, 159.97 ppm. HRMS (ESI): *m/z* calcd for C18H20N3O4 [M-H] 342.1454; found 342.1448.

ST-145b: ^{1}H NMR (400 MHz, DMSO-d_6): δ 3.74 (s, 6H, -OCH_3), 3.90 (s, 6H, -OCH_3), 6.84-6.85 (d, *J* =2 Hz, 3H, ArH), 7.05-7.07 (d, *J* =8.4 Hz, 1H, ArH), 7.21 (s, 1H, ArH) ppm. ^{13}C NMR (100 MHz, DMSO-d_6): 55.92, 55.98, 56.07, 60.91, 60.98, 105.23, 110.63, 114.72, 120.61, 123.01, 125.74, 138.09, 145.66, 147.10, 153.23 ppm. HRMS (ESI): *m/z* calcd for C18H20N3O5 [M-H] 358.1403; found 358.1408.

ST-450: ^{1}H NMR (400 MHz, DMSO-d_6): δ 3.57 (s, 6H, -OCH_3), δ 3.84 (s, 3H, -OCH_3), 6.80 (s, *2*H, ArH), 7.34-7.39 (m, *J* =20 Hz, 1H, ArH), 7.61 (s, 1H, ArH), 7.75-7.77 (d, *J* =7.6 Hz, 1H, ArH), 7.90-7.92(d, *J* =8 Hz, 1H, ArH) ppm. ^{13}C NMR (100 MHz, DMSO-d_6):55.72, 55.85, 60.85, 60.99, 104.57, 104.64, 122.61, 122.73, 123.65, 123.77, 124.66, 124.74, 124.83, 124.94, 125.28, 127.21, 127.37, 137.56, 138.12, 139.89, 153.24 ppm. HRMS (ESI): *m/z* calcd for C19H17N3O3S [M-H] 367.0991; found 367.0909.

ST-440: ^{1}H NMR (400 MHz, DMSO-d_6): 7.22-7.36 (m, *J* =54 Hz, 3H, ArH), 7.50 (s, 1H, ArH), 7.68-7.70 (d, *J* =8.0 Hz, 1H, ArH), 7.85-7.87(d, *J* =8 Hz, 2H, ArH), 8.55-8.56 (d, *J* =3.6 Hz, 1H, ArH), 8.94 (s, 1H, ArH) ppm. ^{13}C NMR (100 MHz, DMSO-d_6):122.69, 122.78,123.33, 123.42, 123.72, 123.77, 124.70, 124.72, 124.90, 124.94, 125.35, 126.97, 127.08, 127.42, 135.37, 135.46, 137.31, 140.12, 141.14, 147.94, 148.00, 148.51 ppm.

ST-452: ^{1}H NMR (400 MHz, DMSO-d_6): δ 7.26(s, 1H, ArH), 7.38-7.40(d, *J* =8 Hz, 2H, ArH), 749-7.54 (m, *J* =16.4 Hz, 2H, ArH), 7.66-7.68(d, *J* =6.8 Hz, 1H, ArH), 8.63 (s, 1H, ArH) ppm. ^{13}C NMR (100 MHz, DMSO-d_6):121.33, 123.62, 127.45, 128.96, 129.75, 129.89, 132.95, 134.99, 135.77, 137.04, 149.66 ppm. HRMS (ESI): *m/z* calcd for C13H9Cl2N4 [M-H] 291.0204; found 291.0201.

ST-447: ^{1}H NMR (400 MHz, DMSO-d_6): δ 3.82 (s, 3H, -OCH_3), δ 3.93 (s, 3H, -OCH_3), 6.87-6.89 (d, *J* =8 Hz, 1H, ArH), 7.05-7.07 (d, *J* =12 Hz, 2H, ArH),), 7.42

(s, 2H, ArH), 7.78 (s, 1H, ArH) ppm. ^{13}C NMR (100 MHz, DMSO-d_6):55.87, 55.96, 111.05, 127.31, 129.80, 129.89, 130.54, 132.60, 132.86, 149.15, 149.754 ppm.

ST-441: ^{1}H NMR (400 MHz, DMSO-d_6): δ 3.81 (s, 6H, -OCH_3), δ 3.90 (s, 3H, -OCH_3), 6.9 (s, 2H, ArH), 7.29-7.26 (d, *J* =12.8 Hz, 2H, ArH), 7.70 (s, 2H, ArH), 8.67 (s, 1H, ArH) ppm. ^{13}C NMR (100 MHz, DMSO-d_6): 56.22, 56.33, 61.13, 100.71, 123.62, 124.25, 127.35, 137.22, 139.48, 149.5, 153.1, 154.8 ppm. HRMS (ESI): *m/z* calcd for C16H17N4O3 [M-H] 313.1301; found 313.1298.

ST-445: ^{1}H NMR (400 MHz, DMSO-d_6): δ 7.21-7.22(d, *J* =4.8 Hz, 1H, ArH), 7.31-7.33 (d, *J* =8.4 Hz, 1H, ArH), 7.38-7.41(m, *J* =14.8 Hz, 3H, ArH), 7.49-7.50 (d, *J* =1.2 Hz, 1H, ArH) ppm. ^{13}C NMR (100 MHz, DMSO-d_6):116.17, 116.22, 116.39, 116.44, 121.32, 121.49, 124.56, 126.73, 126.76, 127.01, 129.50, 130.75, 130.83, 130.92, 138.32, 141.30, 156.84, 159.31 ppm. HRMS (ESI): *m/z* calcd for C12H8ClFN3S [M-H] 280.0111; found 280.0118.

ST-442: ^{1}H NMR (400 MHz, DMSO-d_6): δ 5.99 (s, 2H, -CH_2), 6.82-6.84(d, *J* =8.4 Hz, 1H, ArH), 7.13-7.14 (d, *J* =6 Hz, 2H, ArH), 7.26-7.28(d, *J* =8.4 Hz, 1H, ArH), 7.69-7.71 (d, *J* =7.2 Hz, 2H, ArH), 8.69 (s, 1H, ArH) ppm. ^{13}C NMR (100 MHz, DMSO-d_6):101.15, 101.25, 101.35, 108.52, 109.31, 109.34, 122.78, 123.30, 124.04, 137.02, 14777, 148.06, 149.56 ppm. HRMS (ESI): *m/z* calcd for C14H11N4O2 [M-H] 267.0882; found 267.0879.

ST-478: ^{1}H NMR (400 MHz, DMSO-d_6): δ 3.76 (s, 3H, -OCH_3), 7.03-7.04(d, *J* =4.8 Hz, 2H, ArH), 7.39-7.47 (m, *J* =35.2 Hz, 2H, ArH), 7.62-7.63(d, *J* =1.6 Hz, 1H, ArH), 7.71 (s, 2H, ArH) ppm. ^{13}C NMR (100 MHz, DMSO-d_6):55.51, 111.54, 121.21, 122.83, 129.17, 130.48, 131.29, 133.34, 133.42, 134.96, 156.51 ppm. HRMS (ESI): *m/z* calcd for C15H12Br2N3O [M-H] 407.9347; found 407.9327.

ST-489: ^{1}H NMR (400 MHz, DMSO-d_6): δ 3.79 (s, 6H, -OCH_3), 3.91 (s, 3H, -OCH_3), 6.77 (s, 2H, ArH), 7.46 (s, 2H, ArH), 7.82 (s, 1H, ArH) ppm. ^{13}C NMR (100 MHz, DMSO-d_6):56.12, 56.23, 60.96, 61.05, 105.39, 105.45, 127.44, 129.88, 129.97, 130.53, 132.74, 132.84, 138.69, 153.53 ppm. HRMS (ESI): *m/z* calcd for C17H16Cl2N3O3 [M-H] 380.0569; found 380.0564.

ST-492: ^{1}H NMR (400 MHz, DMSO-d_6): δ 3.47 (s, 6H, -OCH_3), 3.81 (s, 3H, -OCH_3), 6.65 (s, 2H, ArH), 7.50-7.52(t, *J* =8 Hz, 1H, ArH), 7.54-7.56(d, *J* =4.4 Hz, 1H, ArH), 7.76-7.77(t, *J* =1.6 Hz, 1H, ArH), 7.82-7.84(d, *J* =8 Hz, 1H, ArH), 8.27-8.29(d, *J* =8.8 Hz, 1H, ArH), 9.03-9.04(d, *J* =4.4 Hz, 1H, ArH) ppm. ^{13}C NMR (100 MHz, DMSO-d_6): 55.70, 55.79, 0.85, 60.95, 104.47, 104.55, 122.68, 122.76, 124.69, 125.95, 126.66, 127.52, 129.42, 130.21, 138.21, 138.45, 148.15, 149.63, 149.69, 153.24 ppm. HRMS (ESI): *m/z* calcd for C20H19N4O3 [M-H] 363.1457; found 363.1460.

ST-491: ^{1}H NMR (400 MHz, DMSO-d_6): δ 3.82 (s, 3H, -OCH_3), 3.92 (s, 3H, -OCH_3), 6.87-6.89(d, *J* =8 Hz, 1H, ArH), 7.04-7.08(m, *J* =14.4 Hz, 2H, ArH), 7.42-

7.42(d, *J* =0.8 Hz, 2H, ArH), 7.78 (s, 1H, ArH) ppm. ^{13}C NMR (100 MHz, DMSO-d_6):55.85, 55.95, 60.47, 111.19, 111.24, 121.00, 127.31, 129.78, 129.87, 130.49, 130.87, 132.41, 132.79, 149.09, 149.62, 171.36 ppm. HRMS (ESI): *m/z* calcd for C16H14Cl2N3O2 [M-H] 350.0463; found 350.0465.

ST-482: Yellow solid; Yield %; ^{1}H NMR (400 MHz, DMSO-d_6): δ 3.77 (s, 6H, -OCH_3), 3.89 (s, 3H, -OCH_3), 4.26-4.29 (q, *J* =12.4 Hz, 4H, ArH), 6.84(s, 2H, ArH), 6.87-6.89(d, *J* =8 Hz, 1H, ArH), 7.04-7.05, 7.04-7.07(dd, *J* =2 Hz, 8 Hz, 1H, ArH), 7.15-7.16(d, *J* =1.6 Hz, 1H, ArH), 7.26(s, 1H, ArH) ppm. ^{13}C NMR (100 MHz, DMSO-d_6):55.99, 56.08, 60.90, 60.99, 64.27, 64.47, 105.24, 105.28, 117.42, 121.80, 138.18, 143.59, 144.09, 153.26 ppm. HRMS (ESI): *m/z* calcd for C19H20N3O5 [M-H] 370.1403; found 370.1398.

ST-497: Yellow solid; Yield %; ^{1}H NMR (400 MHz, DMSO-d_6): δ 3.78 (s, 6H, -OCH_3), 3.91 (s, 3H, -OCH_3), 7.08 (s, 2H, ArH), 7.54-7.58(t, *J* =14.8 Hz, 1H, ArH), 7.70-7.74(t, *J* =14.8 Hz, 1H, ArH), 7.82-7.83(d, *J* =6.4 Hz, 2H, ArH), 8.08-8.10 (d, *J* =8.8 Hz, 1H, ArH), 8.16-8.18(d, *J* =8.4 Hz, 1H, ArH) ppm. ^{13}C NMR (100 MHz, DMSO-d_6):56.08, 56.18, 60.92, 61.01, 106.21, 120.70, 125.57, 127.12, 127.56, 127.73, 127.68, 129.04, 130.20, 136.83, 138.50, 147.76, 153.19 ppm. HRMS (ESI): *m/z* calcd for C20H19N4O3 [M-H] 363.1457; found 363.1456.

ST-494: Yellow solid; Yield %; ^{1}H NMR (400 MHz, DMSO-d_6): δ 3.73 (s, 3H, -OCH_3), 3.80 (s, 6H, -OCH_3), 6.83 (s, 2H, ArH) ppm. ^{13}C NMR (100 MHz, DMSO-d_6):56.48, 56.67, 65.20, 106.29, 116.04, 116.84, 130.15, 139.13, 153.08 ppm.

ST-513: Yellow solid; Yield %; ^{1}H NMR (400 MHz, DMSO-d_6): δ 3.72 (s, 6H, -OCH_3), 5.29 (s, 1H, ArH), 6.73 (s, 2H, ArH), 6.83-6.85 (d, *J* =8.4 Hz, 1H, ArH), 7.42-7.44(d, *J* =8.8 Hz, 1H, ArH) ppm. ^{13}C NMR (100 MHz, DMSO-d_6):56.08, 56.18, 60.92, 61.01, 106.21, 120.70, 125.57, 127.12, 127.56, 127.73, 127.68, 129.04, 130.20, 136.83, 138.50, 147.76, 153.19 ppm.

A mixture of 5-(3,4-dichlorophenyl)-4-(3,4-dimethoxyphenyl)-2*H*-1,2,3-triazole (**ST-447**) (1 mmol), K_2CO_3 (10 mmol) and MeI (2 mmol) in 10 volumes of acetone was refluxed for 5 hrs. 2M aqueous HCl was then added to quench the reaction and the resulting mixture was evaporated to dryness on a rotavaporator. The resulting residue was dissolved in ethyl acetate, filtered, and the filtrate submitted to ethyl acetate/hexane flash column chromatography to yield 4-(3,4-dichlorophenyl)-5-(3,4-dimethoxyphenyl)-2-methyl-2*H*-1,2,3-triazole

(ST-447(a)): Pale yellow solid; ^{1}H NMR (400 MHz, $CDCl_3$-*d*): δ 3.83 (s, 3H, -OCH_3), 3.92 (s, 3H, -OCH_3), 4.25 (s, 3H, -CH_3), 6.86 (d, *J* =8 Hz, 1H, ArH), 7.05 (dd, *J* =15.2 Hz, 2H, ArH), , 7.42 (dd, *J* =16.8 Hz, 2H, ArH), 7.74 (d, *J* =1.6 Hz, 1H, ArH) ppm. ^{13}C NMR (100 MHz, $CDCl_3$-*d*): 41.98, 56.08, 111.40, 121.07, 123.09, 127.45, 129.97, 130.59, 131.376, 132.41, 132.91, 141.99, 144.87, 149.25, 149.63 ppm.

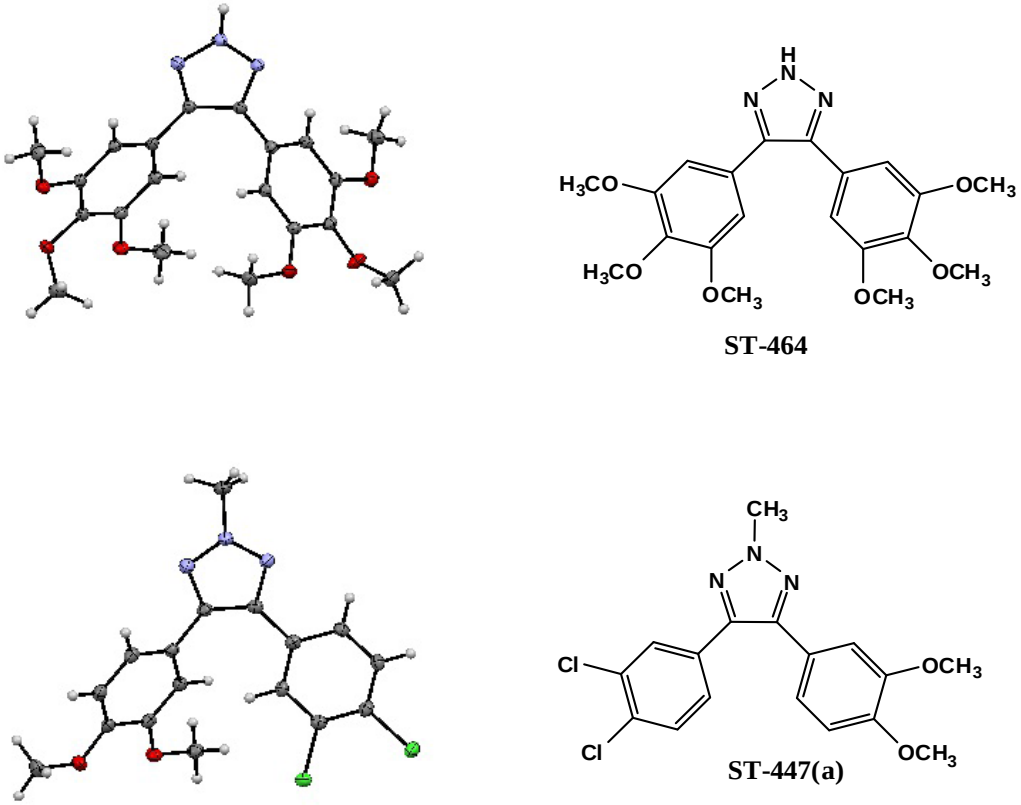

Figure 4.3: X-ray Crystal structures of compounds **ST-464** and **ST-447(a).**

4.5 Biological Evaluation

4.5.1 Anticancer activity of 2*H*-triazole analogs against a panel of NCI 60 human cancer cells

The sulforhodamine B (SRB) assay procedure described in **Chapter 3** was used to screen the synthesized 2*H*-triazole CA-4 analogues against the panel of 60 human tumor cell lines at the NCI (Rubinstein, Shoemaker et al. 1990). The growth inhibitory and cytotoxic properties of a tested compound in our present assay is measured by its percentage growth (PG) which is proportional to optical density (OD) of the tumor (Madadi, Penthala et al. 2014). Optical density (OD) measurements of SRB-derived color just

before exposing the cells to the test compound and after 48hrs exposure to the test compound or the control vehicle are recorded. All the synthesized CA-4 analogues were initially screened at a single dose (10^{-5} M) to determine growth inhibition properties. The NCI screening protocol requires 60% growth inhibition at 10^{-5} M in at least eight cell lines from the panel of 60 cell lines for the compounds to be selected for a complete dose-response study at five different concentrations, viz. 10^{-4} M, 10^{-5} M, 10^{-6} M, 10^{-7} M and 10^{-8} M.

Out of the submitted twenty three triazole derivatives, 12 analogues: **ST-124(a), ST-440, ST-442, ST-452, ST-467, ST-471, ST-475, ST-482, ST-492, ST-497 and ST-145(b)** were selected for single dose screening. The growth percentage values obtained from the initial single dose screens are represented in **Table 4.3** and **Table 4.4**.

Table 4.3: Percentage growth inhibition of NCI 60 human cancer cells by compounds **ST-124(a), ST-440, ST-442, ST-447, ST-452** and **ST-467** at 10µM concentration**.**

Table 4.3 (continued)

Cancer	Cell Type	**ST-124(a)** Growth %	**ST-440** Growth %	**ST-442** Growth %	**ST-447** Growth %	**ST-452** Growth %	**ST-467** Growth %
Leukemia	CCRF-CEM	NA	90.7	97.6	79.5	13.3	3.3
	HL-60(TB)	-12.6	108.8	117.2	80.9	67.8	-3.8
	K-562	10.8	108.2	116.8	57.9	46.6	9.3
	MOLT-4	4.0	106.3	123.2	81.4	53.6	6.2
	RPMI-8226	23.7	92.1	98.3	73.8	55.8	7.1
	SR	5.7	99.9	108.1	79.2	32.4	10.7
Non-Small Cell Lung Cancer	A549/ATCC	15.2	99.3	102.7	92.5	45.4	21.1
	HOP-62	24.2	99.0	106.9	76.5	43.9	24.0
	HOP-92	NA	84.5	95.4	73.9	79.4	26.5
	NCI-H226	46.9	94.0	101.7	96.6	71.7	81.5
	NCI-H23	22.1	96.0	98.1	71.4	55.1	29.0

Table 4.3 (continued)

	NCI-H322M	26.0	92.8	98.7	89.2	22.8	40.2
	NCI-H460	2.4	101.6	102.6	93.1	32.9	4.3
	NCI-H522	-26.6	97.3	105.0	68.0	60.3	-13.8
Colon Cancer	COLO 205	-57.1	105.2	102.9	96.7	64.7	-75.2
	HCC-2998	-5.3	112.1	111.4	90.8	64.0	20.4
	HCT-116	3.7	102.2	96.0	74.0	26.6	9.5
	HCT-15	14.2	91.7	89.8	62.3	23.0	8.9
	HT29	-10.1	105.4	107.8	102.3	44.0	5.8
	KM12	3.0	103.1	104.1	74.3	59.2	5.1
	SW-620	20.5	100.5	102.2	83.8	48.0	21.8
CNS Cancer	SF-268	11.2	107.7	105.0	84.7	56.0	17.6
	SF-295	-10.4	95.4	108.9	76.5	34.1	5.9
	SF-539	-38.7	97.0	96.9	91.0	64.2	-20.3
	SNB-19	108.5	102.3	91.4	93.3	69.5	37.3
	SNB-75	18.1	80.7	73.2	58.5	67.6	25.0
	U251	-5.8	96.4	103.8	84.0	46.1	6.0
Melanoma	LOX IMVI	20.7	NA	NA	NA	NA	21.5
	MALME-3M	53.6	NA	NA	AN	NA	78.7
	M14	5.4	102.0	104.6	82.2	52.1	16.7
	MDA-MB-435	-52.3	102.5	105.5	29.4	68.1	-23.4
	SK-MEL-2	55.3	110.8	118.0	88.2	90.8	45.0
	SK-MEL-28	5.8	105.0	113.8	96.2	86.7	43.9
	SK-MEL-5	58.9	NA				-46.9
	UACC-257	36.6	100.9	101.2	107.0	94.4	72.6
	UACC-62	13.5	92.5	96.1	67.1	38.0	32.6
Ovarian Cancer	IGROV1	-16.2	105.0	104.8	67.4	41.7	22.8
	OVCAR-3	35.1	106.4	109.3	94.6	28.2	-9.6
	OVCAR-4	36.0	97.2	96.8	77.9	39.5	34.0
	OVCAR-5	5.4	103.6	102.4	92.9	88.8	17.5
	OVCAR-8	9.2	101.5	98.7	97.7	44.6	16.3
	NCI/AD	15.9	NA	NA	NA	NA	4.1

Table 4.3 (continued)

	R-RES						
	SK-OV-3	27.8	104.2	108.9	82.4	64.7	18.5
Renal Cancer	786-0	-12.0	111.0	104.2	73.6	51.3	13.8
	A498	33.2	62.9	39.4	66.5	56.3	-14.1
	ACHN	21.8	100.8	99.6	82.9	35.6	15.7
	CAKI-1	45.3	95.4	92.4	66.1	20.5	21.6
	SN12C	25.4	94.0	98.1	93.1	63.7	30.8
	TK-10	43.2	103.2	102.1	64.9	66.8	58.4
	UO-31	20.7	73.5	76.6	47.0	-1.6	24.7
Prostate Cancer	PC-3	10.2	90.5	92.4	79.9	64.1	10.8
	DU-145	-26.2	112.1	111.2	96.2	66.2	4.1
Breast Cancer	MCF7	12.5	85.3	95.6	52.7	40.5	11.9
	MDA-MB-231	-28.4	101.1	85.1	76.7	54.5	16.5
	HS 578T	22.0	102.8	99.7	71.8	76.8	16.0
	BT-549	21.7	108.9	93.7	56.4	66.6	41.5
	T-47D	54.3	92.6	99.5	64.0	35.6	67.9
	MDA-MB-468	47.5	96.4	98.4	55.6	61.9	NA

Table 4.4: Percentage growth inhibition of NCI 60 human cancer cells by compounds **ST-471, ST-475, ST-482, ST-492, ST-497 and ST-145(b)** at 10µM concentration**.**

Cancer	Cell Type	**ST-471** Growth %	**ST-475** Growth %	**ST-482** Growth %	**ST-492** Growth %	**ST-497** Growth %	**ST-145(b)** Growth %
Leukemia	CCRF-CEM	97.8	NA	NA	58.7	11.3	NA
	HL-60(TB)	106.0	NA	NA	60.4	-7.2	NA
	K-562	98.2	NA	NA	62.0	11.3	NA
	MOLT-4	92.3	NA	NA	63.8	7.1	NA
	RPMI-8226	94.0	NA	NA	45.2	14.4	NA
	SR	89.9	NA	NA	25.9	4.2	NA
Non-Small Cell Lung Cancer	A549/ATCC	98.9	NA	NA	87.2	15.1	NA
	HOP-62	91.1	NA	NA	60.1	12.3	NA
	HOP-92	73.2	NA	NA	-11.9	44.3	NA
	NCI-	101.2	NA	NA	80.9	61.6	NA

Table 4.4 (continued)

	H226						
	NCI-H23	111.5	NA	NA	76.6	14.4	NA
	NCI-H322M	106.0	NA	NA	89.2	41.4	NA
	NCI-H460	103.9	NA	NA	89.4	1.2	NA
	NCI-H522	104.2	NA	NA	30.1	-41.5	NA
Colon Cancer	COLO 205	100.7	NA	NA	74.9	-66.0	NA
	HCC-2998	111.7	NA	NA	80.3	6.2	NA
	HCT-116	95.4	NA	NA	71.4	8.7	NA
	HCT-15	104.8	NA	NA	70.2	6.0	NA
	HT29	102.9	NA	NA	74.9	-23.1	NA
	KM12	97.2	NA	NA	71.8	6.1	NA
	SW-620	102.7	NA	NA	83.5	17.9	NA
CNS Cancer	SF-268	98.3	NA	NA	86.1	22.8	NA
	SF-295	95.2	NA	NA	64.5	1.4	NA
	SF-539	100.7	NA	NA	66.0	-43.5	NA
	SNB-19	105.8	NA	NA	84.7	42.8	NA
	SNB-75	83.0	NA	NA	30.9	15.2	NA
	U251	99.2	NA	NA	87.8	-10.5	NA
Melanoma	LOX IMVI	105.0	NA	NA	75.1	13.4	NA
	MALME-3M	102.0	NA	NA	76.0	47.7	NA
	M14	103.8	NA	NA	47.4	15.1	NA
	MDA-MB-435	101.8	NA	NA	41.8	-13.7	NA
	SK-MEL-2	116.0	NA	NA	84.0	15.0	NA
	SK-MEL-28	110.2	NA	NA	72.4	16.8	NA
	SK-MEL-5	94.9	NA	NA	63.1	-38.8	NA
	UACC-257	107.6	NA	NA	76.3	38.1	NA
	UACC-62	104.6	NA	NA	47.4	28.1	NA
Ovarian Cancer	IGROV1	105.6	NA	NA	91.8	17.7	NA
	OVCAR-3	104.9	NA	NA	83.9	-27.0	NA
	OVCAR-4	98.0	NA	NA	71.6	34.4	NA
	OVCAR	110.3	NA	NA	76.2	10.5	NA

Table 4.4 (continued)

	-5						
	OVCAR-8	105.8	NA	NA	85.6	8.1	NA
	NCI/ADR-RES	110.7	NA	NA	78.8	0.8	NA
	SK-OV-3	96.4	NA	NA	80.8	12.4	NA
Renal Cancer	786-0	100.4	NA	NA	58.3	25.0	NA
	A498	84.3	NA	NA	79.3	-17.6	NA
	ACHN	106.0	NA	NA	85.2	6.6	NA
	CAKI-1	87.1	NA	NA	42.1	16.0	NA
	SN12C	101.5	NA	NA	98.0	39.1	NA
	TK-10	100.0	NA	NA	36.5	60.1	NA
	UO-31	93.7	NA	NA	35.9	21.4	NA
Prostate Cancer	PC-3	87.3	NA	NA	39.0	14.5	NA
	DU-145	108.6	NA	NA	99.9	4.9	NA
Breast Cancer	MCF7	106.8	NA	NA	55.9	10.4	NA
	MDA-MB-231	104.2	NA	NA	81.7	22.4	NA
	HS 578T	98.1	NA	NA	65.7	14.8	NA
	BT-549	81.2	NA	NA	NA	17.3	NA
	T-47D	90.5	NA	NA	70.7	64.4	NA
	MDA-MB-468	NA	NA	NA	NA	NA	NA

NA: Not Available

Out of the 12 compounds selected for single dose screening, six compounds were selected for full five dose-response studies; below (**Table 4.5**) are the five dose study results for these six compounds.

Table 4.5: Growth Inhibition **(**GI_{50}/µM) and Total Growth Inhibition (TGI/µM) data for compounds **ST-497, ST-124(a)** and **ST-467** against NCI human cancer cells.

Panel/cell line	**ST-497**		**ST-124(a)**		**ST-467**	
	GI_{50} (nM)	TGI (µM)	GI_{50} (nM)	TGI (µM)	GI_{50} (nM)	TGI (µM)
Leukemia CCRF-CEM	37.3	>100	31.9	21.8	<10	46.3
HL-60(TB)	30.0	5.74	22.7	NA	<10	NA
K-562	25.7	>100	<10	>100	<10	>100
MOLT-4	68.2	>100	48.2	20.0	12.0	16.1

Table 4.5 (continued)

RPMI-8226	36.5	87.6	36.8	21.1	<10	24.6
SR	21.1	>100	<10	16.9	<10	>100
Non-Small Cell Lung Cancer A549/ATCC	54.1	>100	37.4	>100	<10	73.4
HOP-62	46.7	>100	25.0	>100	<10	72.4
HOP-92	98.9	11.3	<10	2.67	<10	0.08
NCI-H23	64.9	>100	37.7	27.9	<10	68.7
NCI-H460	38.1	>100	34.2	>100	<10	10.9
Colon Cancer COLO 205	228	1.16	149	0.64	29.2	0.12
HCC-2998	230	>100	45.9	11.4	24.9	22.4
HCT-116	40.2	NA	<10	1.47	<10	>100
HCT-15	37.3	>100	<10	5.13	<10	>100
HT29	214	14.5	47.6	20.5	<10	10.8
KM12	35.3	>100	29.8	23.8	<10	0.05
SW-620	40.6	>100	29.5	>100	<10	>100
CNS Cancer SF-268	503	>100	177	>100	<10	90.0
SF-295	14.4	>100	10.8	0.15	<10	27.5
SF-539	20.0	0.05	13.8	0.04	<10	<0.01
SNB-19	52.5	>100	36.9	>100	<10	>100
SNB-75	15.7	NA	14.2	>100	<10	NA
U251	37.1	46.9	37.9	>100	<10	16.5
Melanoma LOX IMVI	65.2	>100	75.5	>100	<10	>100
M14	21.5	NA	<10	>100	<10	23.0
MDA-MB-435	<10	NA	<10	0.01	<10	<0.01
SK-MEL-2	26.9	4.24	55.5	>100	<10	30.5
SK-MEL-28	>1000	6.33	NA	NA	NA	60.7
SK-MEL-5	12.6	0.35	26.7	0.32	<10	0.02
UACC-62	157	4.61	<10	>100	>1000	>100
Ovarian Cancer IGROV1	64.8	>100	50.9	>100	<10	21.5
OVCAR-3	10.8	0.04	24.4	>100	<10	<0.01
OVCAR-4	77.4	>100	NA	>100	<10	>100
NCI/ADR-RES	23.1	66.1	<10	0.08	<10	17.5
SK-OV-3	75.0	97.7	45.8	>100	<10	40.3
Renal Cancer 786-0	42.8	>100	15.3	>100	<10	19.4
A498	33.2	6.69	<10	NA	<10	<0.01
ACHN	81.3	>100	145	>100	<10	62.5
CAKI-1	42.6	>100	50.2	>100	<10	>100
UO-31	92.3	>100	20.0	>100	<10	25.1
Prostate Cancer PC-3	45.8	>100	41.5	>100	<10	35.2
DU-145	26.6	NA	44.8	>100	<10	NA
Breast Cancer MCF7	26.9	>100	24.5	>100	<10	>100
MDA-MB-231/ATCC	94.7	>100	46.0	>100	<10	>100
HS 578T	NA	>100	40.9	>100	<10	>100
MDA-MB-468	34.6	26.0	23.3	0.08	<10	22.4

Table 4.6: Growth Inhibition **(**GI_{50}/μM) and Total Growth Inhibition (TGI/μM) data for compounds **ST-282, ST-482, ST-452** against NCI human cancer cells.

Panel/cell line	ST-282		ST-482		ST-452	
	GI_{50} (nM)	TGI (μM)	GI_{50} (nM)	TGI (μM)	GI_{50} (μM)	TGI (μM)
Leukemia CCRF-CEM	33.7	>100	282	>100	3.38	>100
HL-60(TB)	18.9	0.08	201	NA	5.75	>100
K-562	<10	>100	49.6	>100	5.50	>100
MOLT-4	39.9	11.6	572	51.8	4.23	>100
RPMI-8226	32.5	11.0	326	22.1	10.7	>100
SR	<10	24.0	43.6	11.6	5.43	>100
Non-Small Cell Lung Cancer A549/ATCC	22.9	22.6	289	50.9	4.85	>100
HOP-62	18.2	19.3	336	>100	5.32	>100
HOP-92	<10	0.54	122	1.59	3.28	>100
NCI-H23	48.0	41.7	767	>100	9.13	>100
NCI-H460	24.6	20.0	335	28.7	3.67	>100
Colon Cancer COLO 205	26.7	0.07	311	1.30	2.89	>100
HCC-2998	39.4	17.5	>1000	24.6	9.16	>100
HCT-116	<10	0.81	181	15.6	2.89	>100
HCT-15	<10	>100	125	>100	2.93	>100
HT29	25.3	12.3	392	12.5	4.56	>100
KM12	<10	11.2	70.0	11.9	6.87	>100
SW-620	<10	>100	105	>100	4.40	>100
CNS Cancer SF-268	68.5	>100	>1000	>100	7.36	>100
SF-295	<10	42.8	98.9	3.61	3.01	>100
SF-539	<10	NA	181	0.54	NA	>100
SNB-19	29.4	>100	501	>100	7.75	>100
SNB-75	<10	21.9	82.4	NA	1.58	>100
U251	20.1	22.7	302	11.2	5.35	>100
Melanoma LOX IMVI	17.5	37.8	545	87.1	4.83	>100
M14	<10	NA	NA	12.0	14.3	>100
MDA-MB-435	<10	NA	94.8	NA	2.20	>100
SK-MEL-2	<10	18.1	23.6	55.7	6.52	>100
SK-MEL-28	>100	34.8	244	43.5	5.39	>100
SK-MEL-5	<10	0.16	>1000	11.9	7.89	>100
UACC-62	>100	21.2	>1000	30.8	3.35	>100
Ovarian Cancer IGROV1	33.2	30.3	>1000	>100	5.94	>100
OVCAR-3	<10	<0.01	432	0.37	3.38	>100
OVCAR-4	33.6	57.2	76.3	>100	3.04	>100
NCI/ADR-RES	<10	69.7	84.9	24.0	3.92	>100
SK-OV-3	<10	12.7	486	93.2	2.72	>100
Renal Cancer 786-0	<10	13.5	618	63.5	2.75	>100
A498	10.4	1.50	343	9.32	3.18	>100
ACHN	<10	>100	705	>100	1.75	>100
CAKI-1	<10	>100	316	>100	8.42	>100
UO-31	<10	24.6	661	72.7	6.84	>100

Table 4.6 (continued)

Prostate Cancer PC-3	18.4	39.4	255	43.7	4.50	>100
DU-145	25.0	>100	346	>100	1.41	>100
Breast Cancer MCF7	<10	37.9	76.8	>100	2.58	>100
MDA-MB-231/ATCC	44.4	>100	529	31.5	5.89	>100
HS 578T	668	64.2	442	>100	11.6	>100
MDA-MB-468	14.7	30.5	226	25.8	3.20	>100

4.5.2 Anticancer evaluation of ST-145(b) versus 9LSF rat gliosarcoma cells via colony formation assay

9LSF cells were acquired from the laboratory of Dennis Deen, Ph.D. (Brain Tumor Research Center, University of California, San Francisco). Cells were exposed to **ST-145(b)** at concentrations of 1 nM, 3 nM, 10 nM, 30 nM, 100 nM, 1 µM, or 10 µM for 24 hours prior to seeding of the colony formation assay. Cells were then trypsinized, counted, seeded into 25 cm^2 flasks, and incubated at 37°C to form colonies (Borrelli, Stafford et al. 1998). All conditions were seeded in triplicate. Flasks that were plated with less than 50,000 cells were previously plated with 50,000 lethally irradiated A549 cells to serve as feeders (Borrelli, Thompson et al. 1989). Flasks were removed from incubation when colonies were large enough to count (>50 cells). Colonies were then fixed and stained with crystal violet, rinsed, allowed to dry, and counted. LD_{50} was determined as 7.5 nM using SigmaPlot **Figure 4.4**. The colony formation assay was conducted by Kevin Howk at Dr. Borelli's lab.

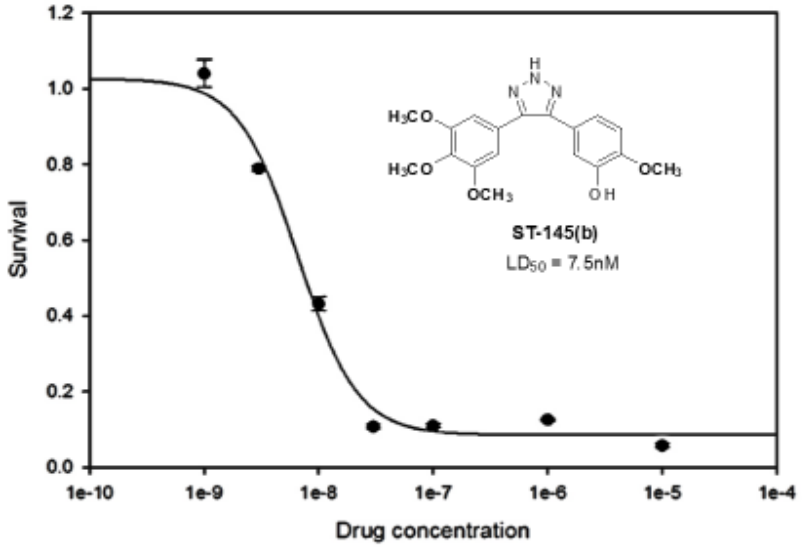

Figure 4.4: Dose response study of **ST-145(b)** against 9LSF cells.

4.6 Conclusion

In summary, we have developed a new facile procedure for the synthesis of 4,5-diaryl-2*H*-1,2,3-triazoles bearing a broad range of aryl moieties from their corresponding (*Z*)-2,3-diarylacrylonitriles. The method does not require an inert atmosphere, is economical, can be applied to a wide range of aryl groups and aromatic ring substitutions, and is a viable alternative to the Huisgen cycloaddition reaction of alkynes with azides.

The 2*H*-triazole CA-4 analogues do not undergo *cis-trans* isomerization and are stable in aqueous solution. They also have a better water-solubility profile compared to the parent CA-4 precursor molecules. With the exception of **ST-452**, all the compounds in this sublibrary had LC_{50} values >100μM against most of the human cancer cell lines in the NCI panel, implying that these compounds are anti-proliferative agents. It is noteworthy

that **ST-467** had impressive GI_{50} values of less than 10nM against almost all the cancer cell lines in the panel, except for melanoma cancer cell line UACC-62, and colon cancer cell lines COLO 205 and HCC-2998. **ST-467** also exhibited potent TGI values of <10nM against CNS cancer cell line SF-539, melanoma cell MDA-MB-435, ovarian cancer cell line OVCAR-3 and renal cancer cell line A498. Analogues **ST-124(a)** and **ST-282** exhibited GI_{50} values of <10nM against leukemia cancer cell lines K-562 and SR, non-small lung cancer cell line HOP-92, colon cancer cell lines HCT-116 and HCT-15, melanoma cancer lines M14 and UACC-62, ovarian cancer cell line NCI/ADR-RES and renal cancer cell line A498. Melanoma cancer cell line MDA-MB-435 and ovarian cancer cell line OVCAR-3 appeared to be the most sensitive to the growth inhibitory effects of **124(a)** and **ST-467**, exhibiting TGI values of <10 nM. Also, analogue **ST-145(b**) was very effective in the colony formation assay against 9LSF rat gliosarcoma cells, exhibiting an LD_{50} value of 7.5 nM.

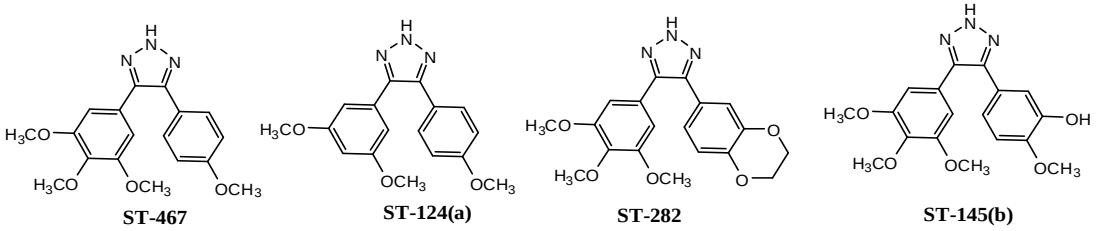

Figure 4.5: Lead 4,5-diaryl-2*H*-1,2,3-triazoles as potent CA-4 analogs.

Thus, analogues **ST-467, ST-124(a)**, **ST-282** and **ST-145(b**) can be considered as lead anticancer agents from the 2*H*-triazole series of compounds and further investigation is warranted to determine their potential as clinically effective therapeutic agents.

Copyright © Nikhil Reddy Madadi 201

Chapter 5

Resveratrol derivatives as selective, high affinity cannabinoid receptor ligands and correlation with their anti-cancer properties

5.1 Introduction

The psychotropic and therapeutic actions of cannabis extracts have been known for centuries. By 1940, the concerns about the danger of abuse has led to the banning of medical marijuana world-wide (Pisanti, Malfitano et al. 2009). However, increasing evidence of biologically beneficial aspects of cannabinoids associated with cancer, inflammation, obesity and brain damage is awakening renewed interest in cannabinoid receptor studies (Munson, Harris et al. 1975, Cridge and Rosengren 2013).

CB1 and CB2 receptors are the two major cannabinoid-specific receptors which have been characterized from mammalian tissues. CB1 receptors (CB1R) are abundantly expressed in the CNS (Pertwee 2006). These receptors are also expressed in peripheral nerve terminals and in many extra-neuronal sites. CB1R activation is responsible for most of the pharmacological effects of cannabinoids in the nervous system. In contrast, CB2 receptors (CB2R) are known to be expressed in other tissues, predominantly in cells of the immune system (Sarfaraz, Adhami et al. 2008). Interestingly, many types of cancer cells express relatively high densities of CB1 and CB2 receptors, and most recent studies report that cannabinoids can reduce tumor growth and progression in several animal models of cancer (Sanchez, de Ceballos et al. 2001, Sarfaraz, Adhami et al. 2008, Wasik, Christensson et al. 2011).

Cannabinoids can be classified into three structurally distinct groups: endocannabinoids, phytocannabinoids, and synthetic cannabinoids (Franks, Ford et al. 2014). Endocannabinoids are endogenous compounds synthesized in the body (example: Anandamide (**Figure 5.1**)). Phytocannabinoids are plant-derived compounds that are often structurally similar to Δ^9-THC (**Figure 5.1**). Lastly, synthetic cannabinoids are compounds specifically designed with high affinity for CB1 and CB2 receptors to alter receptor and/or endocannabinoid function.

To develop cannabinoids with improved therapeutic properties, we synthesized of a novel class of cannabinoid receptor inhibitors, the indolequinuclidines (**Figure 5.1**) that bind with high nanomolar affinity to both types of cannabinoid receptors, and we have characterized the intrinsic activity of such compounds (Madadi, Penthala et al. 2013, Franks, Ford et al. 2014).

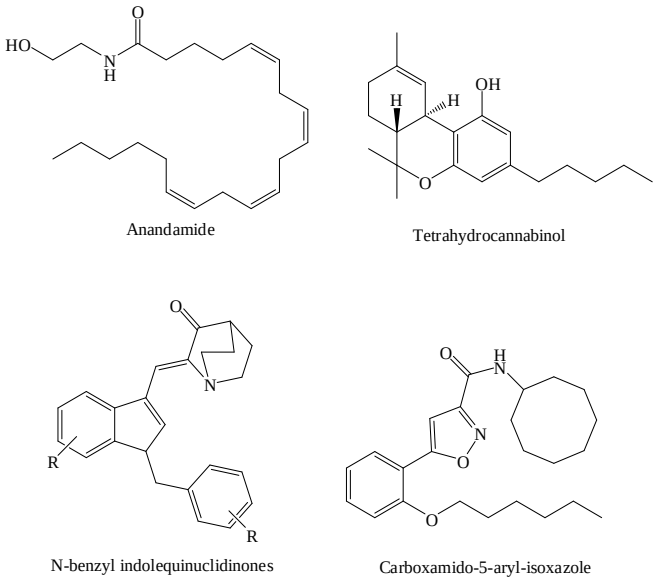

Figure 5.1 Structures of Anandamide, Tetrahydrocannabinol, *N*-benzyl indolequinuclidinones, Carboxamido-5-aryl-isoxazole.

Qamri and co-workers have demonstrated that synthetic cannabinoid receptor agonists JWH-133 and WIN-55 (**Figure 5.2**) inhibit cell proliferation against breast cancer cell lines (MDA-MB231, MDA-MB468). Interestingly, these results were reversed when breast cancer cells were treated with CB1R and CB2R antagonists AM 251 and SR 44528 (**Figure 5.2**), indicating the likely involvement of CB1 and CB2 receptors in tumor growth and metastasis (Qamri, Preet et al. 2009).

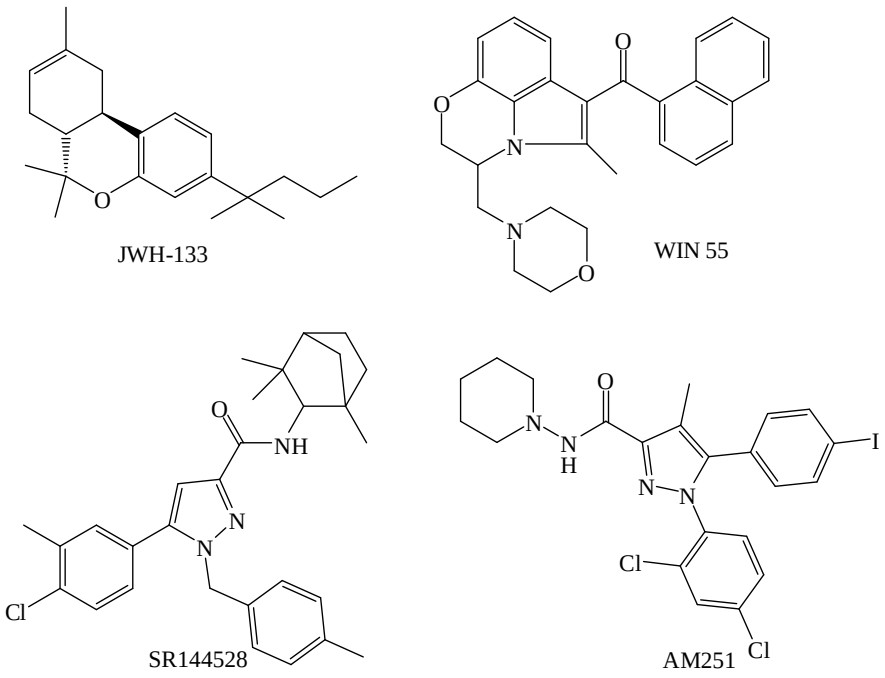

Figure 5.2 Structures of synthetic cannabinoids JWH-133, WIN 55, SR 144528 and AM252.

Recently, much attention has focused on potential chemotherapeutic uses for the naturally occurring plant stilbenoid, resveratrol, and resveratrol analogs such as the prenylated stilbenoids have been reported to have improved affinity for cannabinoid receptors

(Brents, Medina-Bolivar et al. 2012). In this regard, identifying selective and high affinity ligands for both CB1 and CB2 receptors is a worthwhile goal, since most cannabinoid drugs have been associated with potential addictive properties and other unwanted side effects due to their lack of selectivity.

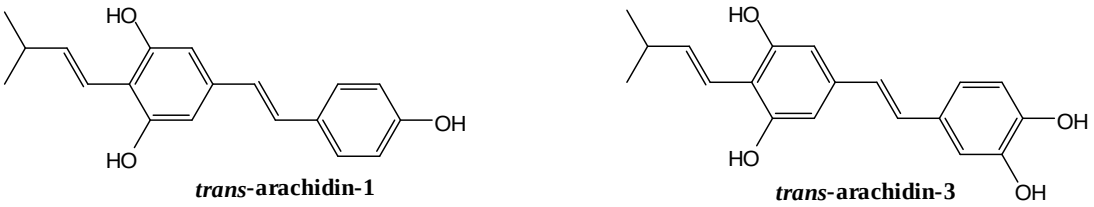

Figure 5.3 Structures of prenylated stilbenoids *trans*-arachidin-1 and *trans*-arachidin-3.

Based on the above mentioned literature review, we hypothesized that the anticancer activity of the synthesized resveratrol analogs may partly be mediated through their interaction with cannabinoid receptors. Thus, we wanted to find a correlation between cannabinoid receptor affinity and anticancer activity for our resveratrol derivatives. We initiated a study to identify selective CB1 and CB2 receptor ligands from the library of novel stilbene scaffolds structurally related to the resveratrol molecule. From our SAR studies we have discovered that incorporating a 3,4-methylenedioxy group into the phenyl moieties and introducing a cyano substituent onto the stilbene double bond not only improved affinity of these novel stilbenes for CB1 and CB2 cannabinoid receptors, but also afforded selectivity at CB1 and CB2 receptors.

5.2 Standard Operating Procedure for cannabinoid affinity screening

Membrane homogenates of either whole mouse brain (50 µg) (CB1R) or Chinese hamster ovary (CHO)-hCB2 cells (25 µg) (CB2R) were incubated for 90 min at room temperature with 0.2 nM [^{3}H]CP-55, 940, 5 mM MgCl2, and either increasing sample concentrations

(10 fM–10 μM), 1 μM WIN 55212-2 (to define non-specific binding) or vehicle (to determine total binding). Each ligand concentration was examined in duplicate, in a final volume of 1 mL of buffer containing 50 mM Tris, 0.05% bovine serum albumin (BSA) and 0.1% ethanol/0.1% dimethyl sulfoxide as vehicle. Reactions were terminated by rapid vacuum filtration through Whatman GF/B glass fiber filters, followed by five washes with ice-cold buffer (50 mM Tris, 0.05% BSA). Filters were immediately placed into 7 mL scintillation vials to which 4 mL of scintillation fluid was added. Bound radioactivity was determined after overnight incubation at room temperature by liquid scintillation spectrophotometry. Specific binding was expressed as total minus nonspecific binding and graphed for each data point as a percentage of specific binding occurring in the absence of any competitor. The affinity of IQDs for CB1Rs and CB2Rs was derived by employing the Cheng–Prusoff (Cheng and Prusoff 1973) equation to convert the observed IC_{50} values to Ki values from 3 to 4 separate competition receptor binding curves for each ligand.

5.3 CB1 and CB2 receptor competitive binding data from screening assay with resveratrol analogs

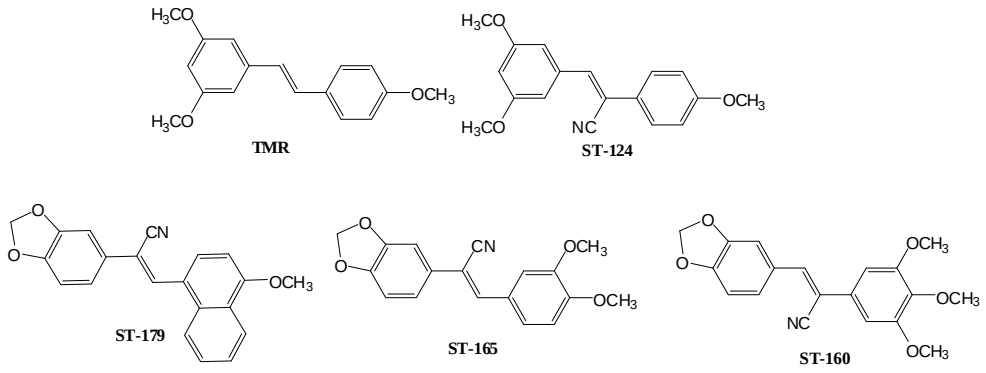

Figure 5.4: Structures of **TMR**, **ST-124**, **ST-179**, **ST-165** and **ST-160.**

By comparing the CB1 and CB2 receptor competitive binding data for **TMR** and **ST-124** (**Figure 6.1**), it was found that incorporating a cyano group into the double bond of the stilbene moiety markedly improved the receptor affinity for both CB1 and CB2 receptors compared to the parent compound. Subsequently, a variety of cyanostilbenes were screened, and it was discovered that 3,4-methylenedioxy cyanostilbenes **ST-179**, **ST-165** and **ST-160 (Figure 6.1**) not only exhibited improved receptor affinity but also afforded compounds that were selective ligands at both CB1 and CB2 receptors.

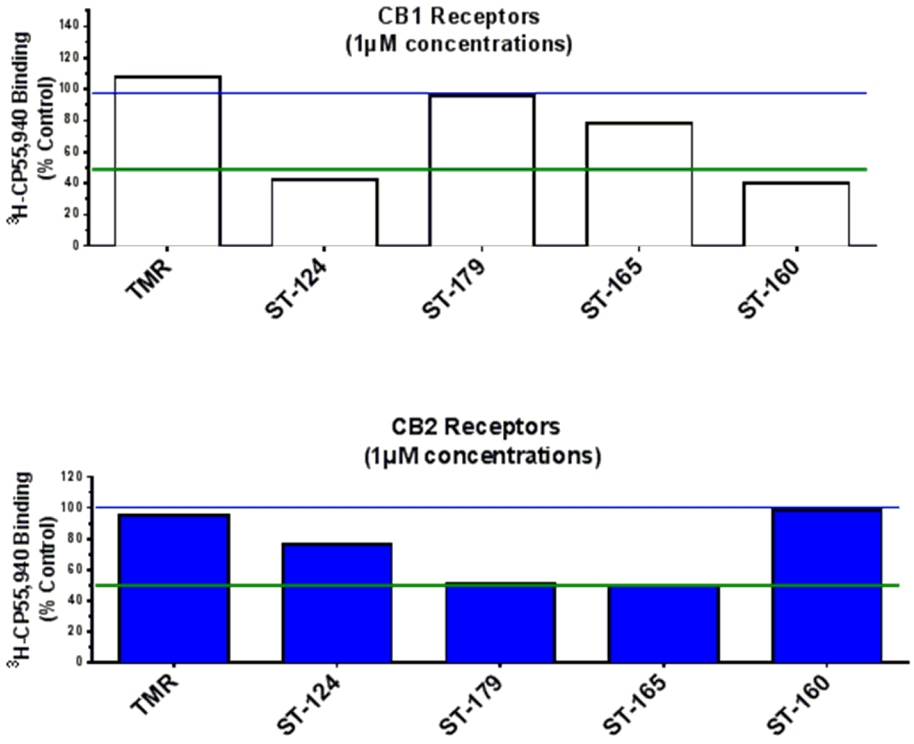

Figure 5.5: CB1 and CB2 competitive binding screen at 1μM concentration with **TMR**, **ST-124**, **ST-179**, **ST-165** and **ST-160**.

Initially, all twenty four 3,4-methylenedioxy cyanostilbenes synthesized were screened at 1μM in CB1 and CB2 competitive receptor binding studies, and several compounds showed promising affinities towards both CB1 and CB2 receptors (full screening results are given in the **Appendix; Figure 8.1-Figure 8.6**). However, only compounds with high affinity and/or selectivity were selected for subsequent evaluation utilizing complete binding curves to derive *Ki* values. Three compounds (**ST-179**, **ST-165** and **ST-160**) were identified as selective for CB1 and CB2 receptors with relatively high affinities (**Table 5.1** and **Figure 5.3**).

Table 5.1: Ki values for compounds **ST-179, ST-165**, and **ST-160** for CB1 and CB2 receptors.

	Ki values (nM)		
Comp.	CB1	CB2	CB1/CB2
ST-179	13290	284	47
ST-165	717	327	2
ST-160	400	780	0.5

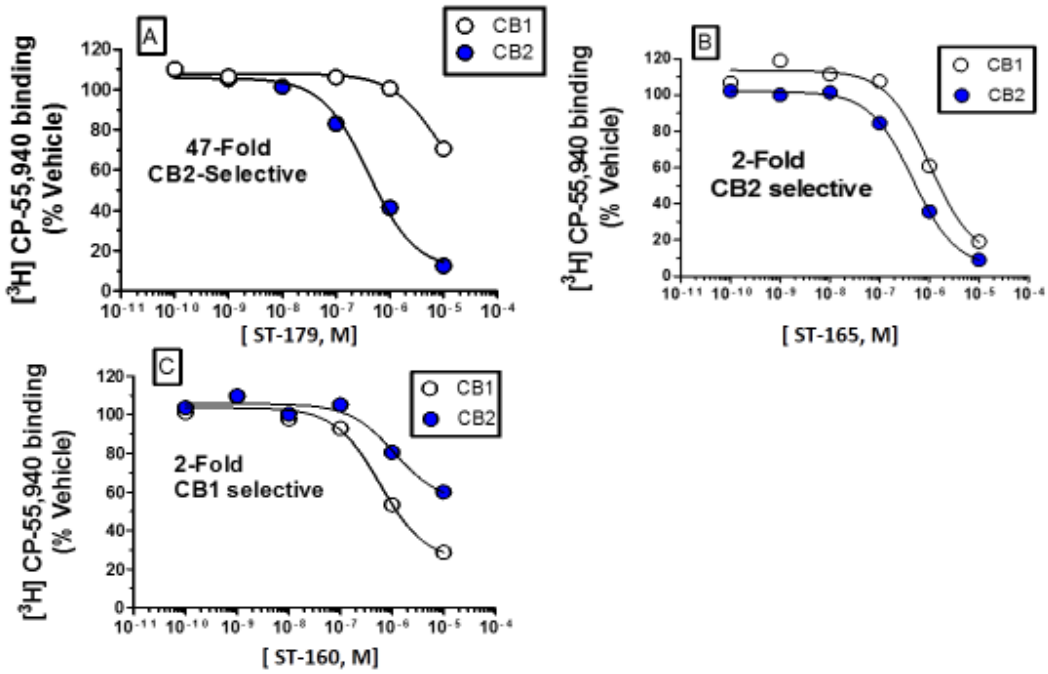

Figure. 5.6: Affinity (*Ki*) of compounds **ST-179**(**A**), **ST-165**(**B**) and **ST-160**(**C**) for mouse brain CB1Rs (mCB1) and human CB2Rs (hCB2).

5.4 Discussion and Conclusion

Twenty four novel 3,4-methylenedioxy substituted stilbene analogs were synthesized (**Chapter 2**). Several showed promising affinities in cannabinoid receptor binding assays, and some were selective for both CB1 and CB2 cannabinoid receptors. Two compounds were identified as selective receptor ligands. Compound **ST-179** had 47-fold selectivity for CB2 receptors (*Ki* = 284 nM) compared to CB1 receptors, while compound **ST-160** was 2-fold selective for CB1 receptors (*Ki* = 400 nM) compared to the CB2 receptors. Current studies are ongoing to determine the intrinsic activity of these high affinity cannabinoid ligands.

Compounds **ST-179** and **ST-165** were screened at a single dose (10^{-5} M) at NCI to determine their growth inhibition properties against various cancer cell lines. To our dissapointment compound **ST-160** was not selected for single dose screening in the NCI panel of human cancer cell lines. Based on the single dose screening results, Compound **ST-179** was selected for full five dose response study against the NCI 60 cell panel of human tumor cell lines. The anticancer study results are presented in **Chapter 3**. Unfortunately, no direct correlation could be derived between the anticancer activity and the cannabinoid affinity results for **ST-179**, **ST-165** and **ST-160**. Thus, further studies need to be conducted on these resveratrol analogs to establish if any correlation between cannabinoid affinities and anticancer activities exists.

In conclusion, we have identified 3,4-methylenedioxy cyanostilbenes as a novel class of selective cannabinoid ligands that have the potential for development as novel cannabinoid therapeutics for treatment of obesity and/or drug dependency. The cannabinoid receptor activities of the molecules does not appear to correlate with their anticancer activities against human cancer cell lines.

Chapter 6

Summary

Herein, two medicinal chemistry projects related to the natural products resveratrol and combretastatin-A4, which possess anticancer properties, are presented. Resveratrol (3,5,4-trihydroxystilbene) is a well-known phytoalexin found in grapes, peanuts, red wine and other foods. It has been reported as a potential chemotherapeutic agent due to its striking inhibitory effects on cellular events associated with cancer initiation, promotion, and progression. However, resveratrol has some limitations which preclude its use in cancer treatment. It cannot be used as an antitumor drug due to its low bioavailability caused by rapid metabolism.

We have synthesized 184 compounds related to resveratrol with chemical alterations designed to make the molecule more potent and drug-like (presented in **Chapter 2**). Thus, the majority of the aromatic hydroxyl groups were defunctionalized by O-methylation and novel functional groups where added to the stilbene scaffold to improve anticancer potency. The resulting resveratrol analogs were divided into four groups based on the nature and position of the functional group introduced into the stilbene skeleton, i.e. simple stilbenes, C2-substituted stilbenes, cyanostilbenes and tetrazole stilbenes. All 184 resveratrol analogues were submitted to the NCI anticancer screening program and evaluated against a panel of 60 human tumor cells. Eighty five of these analogues were selected for single dose screening at 10μM concentration. NCI selects compounds based on drug-likeliness of the structures analyzed by the algorithm software COMPARE, and does not accept compounds which have been previously submitted. From the 85

compounds selected for single dose screening, 25 resveratrol analogs showed promising anticancer activity and were selected for full five-dose studies. We have identified a tetrazole resveratrol analog **ST-145(a)** [(*Z*)-5-(2-(1*H*-tetrazol-5-yl)-2-(3,4,5trimethoxyphenyl)vinyl)-2-methoxyphenol] as a lead anticancer agent from the resveratrol analog series. **ST-145(a)** had impressive GI_{50} values of less than 10nM against almost all 60 cell lines in the NCI panel of human cancer cells, except for colon cancer cell lines HT29 and COLO 205. **ST-14**5 also showed potent TGI (Total Growth Inhibition) values of <10nM against Non-small cell lung cancer cell line NCI-H522, CNS cancer cell line SF-539, Melanoma cell line MDA-MB-435 and renal cancer cell line A498. The full anticancer activitiesof the synthesized resveratrol analogs are presented in **Chapter 3**.

In a separate study we aimed to test the hypothesis that the limited bioavailability of resveratrol, can be improved by synthesizing analogs which would be glucuronidated at a lower rate than resveratrol itself. From our library of resveratrol analogs we have selected three compounds (**ST-05**, **ST-12(a)** and **DNR-1**) hypothesizing that the functional moieties that were introduced into the molecule would slow the rate of glucuronidation and could constitute useful scaffolds for the subsequent design of resveratrol analogs with improved bioavailability. In the current study we demonstrated that **ST-05 [**(*E*)-2,4-dimethoxy-6-(4-methoxystyryl)benzaldehyde oxime) and **ST-12(a)** [(*E*)-3-(3-hydroxy-4-methoxyphenyl)-2-(3,4,5-trimethoxyphenyl)acrylic acid] were substrates for recombinant UGT enzymes and human hepatic and intestinal microsomes. In conclusion, the glucuronidation of the novel stilbenoids studied in this study revealed that these compounds exhibit lower glucuronidation profiles when compared to resveratrol, and

likely represent useful scaffolds for the design of efficacious resveratrol analogs with improved bioavailability. The glucuronidation study results are discussed in **Data set 1** (Appendices).

Recently, resveratrol analogs such as prenylated stilbenoids have been reported to have improved affinity for cannabinoid receptors. In this regard, identifying selective and high affinity ligands for both CB1 and CB2 cannabinoid receptors is a worthwhile goal, since most cannabinoid drugs have been associated with potential addictive properties and other unwanted side effects due to their lack of selectivity. We initiated a new discovery program at UAMS to identify selective CB1 and CB2 receptor ligands from the library of novel stilbene scaffolds structurally related to the resveratrol molecule. Several of these compounds showed promising affinities in cannabinoid receptor binding assays, and some were selective for both CB1 and CB2 cannabinoid receptors. From the screened resveratrol analogs, two compounds were identified as selective CB2 and CB1 ligands, compound **ST-179** exhibited 47-fold selectivity for CB2 (*Ki* = 284 nM) compared to CB1 receptors. Compound **ST-160** was 2-fold selective for CB1 receptors (Ki = 400 nM) compared to the CB2 receptors. These structural analogs may have potential for the development as novel cannabinoid therapeutics for treatment of obesity and/or drug dependency. The cannabinoid receptor affinity studies with the stilbenes are presented in **Chapter 5**)

Combretastatin A4 (CA-4) is a *cis*-stilbene originating from the South African willow tree *Combretum caffrum.* It is one of the most potent antiangiogenic and antimitotic agents of natural origin. Its O-phosphate prodrug (CA-4P) is currently in phase 3 clinical

trial for the treatment of anaplastic thyroid cancer, and successfully retards tumor growth in wide spectrum of solid tumor models. However, recent studies have reported the chemical instability of CA-4 in solution due to *cis*- *trans* isomerization to the more thermodynamically stable, but less potent *trans*-CA-4 isomer. To circumvent this problem, introduced an aromatic triazole ring in place of the double bond of the cis-stilbene moiety of CA-4 to constrain molecule to the *cis*-configuration and to make moecule more stable more water-soluble. We have developed a facile procedure for the general synthesis of 4,5-diaryl-2*H*-1,2,3-triazoles as CA-4 analogs that incorporate a broad range of aryl moieties from their corresponding (*Z*)-2,3-diarylacrylonitriles. This method does not require an inert atmosphere, is economical, can be applied to a wide range of aryl groups and aromatic ring substitutions, and is a viable alternative to the Huisgen cycloaddition reaction of alkynes with azides. The methodology, development and design of these 4,5 disubstitutes-2*H*-1,2,3-triazoles is discussed in **Chapter 4**.

A total of twenty three 4,5-diaryl-2*H*-1,2,3-triazoles as CA-4 analogs were synthesized and submitted to the NCI panel of 60 human tumor cells for anticancer screening. Of these, twelve analogs were selected for single dose screening at 10μM concentration. From the 12 compounds selected for single dose screening, six of these CA-4 analogs showed promising anticancer activity and were selected for full five dose-studies. From these CA-4 analogs, **ST-467** (4-(4-methoxyphenyl)-5-(3,4,5-trimethoxyphenyl)-2H-1,2,3-triazole) had impressive GI_{50} values of less than 10nM against almost all the cell lines in the panel, except for melanoma cancer cell line UACC-62, and colon cancer cell lines COLO 205 and HCC-2998. Compound **ST-467** also showed potent TGI values of <10nM against CNS cancer cell line SF-539, melanoma cell line MDA-MB-435, ovarian

cancer cell line OVCAR-3, and renal cancer cell line A498. Also, compound **ST-145(b**) (2-methoxy-5-(5-(3,4,5-trimethoxyphenyl)-2*H*-1,2,3-triazol-4-yl)phenol), another triazole CA-4 analogue, was very effective in the colony formation assay against 9LSF rat gliosarcoma cells, exhibiting an LD_{50} of 7.5 nM. Both **ST-467** and **ST-145(b**) can be considered as lead anticancer agents from the triazole CA-4 series and further investigation into their in vivo effects in various solid tumor xenograph models in nude mice may provide additional data on their potential as therapeutic agents for treatment of a variety of solid tumors. The anticancer activity results of the triazole CA4 analogs are presented in **Chapter 4**.

Copyright © Nikhil Reddy Madadi 2014

Appendices

Data set 1

Novel Resveratrol-Based Substrates for Human Hepatic, Renal, and Intestinal UDP-Glucuronosyltransferases

7.1 Introduction

Resveratrol is a well-known, natural polyphenol known to be a potent antioxidant, coronary protective, hepatic protective, neuroprotective, cardiovascular protective, anti-inflammatory and anti-carcinogenic agent (Pace-Asciak, Rounova et al. 1996, Jang, Kang et al. 1999, Aggarwal, Bhardwaj et al. 2004, Kim, Zhu et al. 2006). Although initial preclinical data was encouraging, resveratrol could not be used as a drug because of its low bioavailability. Resveratrol was found to have a short half-life of 8-10 min after oral administration and was extensively metabolized to both O-sulfate and O-glucuronide conjugates (Marier, Vachon et al. 2002).

The human hepatic and intestinal UDP-glucuronosyltransferases (UGTs) actively transform resveratrol to its O-glucuronide conjugate (Sabolovic, Humbert et al. 2006). To circumvent this unfavorable metabolism of resveratrol, the search for resveratrol analogs with chemical stability, enhanced bioavailability and more promising metabolic stability, is of great importance.

Recently, Dr. Radominska's group at UAMS have discovered that prenylated resveratrol analogues, *trans*-arachidin-1 and *trans*-arachidin-3 (**Figure 7.1**) had O-glucuronidation rates that were slower in comparison to resveratrol (Brents, Medina-Bolivar et al. 2012). From our library of resveratrol analogs, three compounds were selected (**ST-05**, **ST-12(a)** and **DNR-1, Figure 5.1**) that were hypothesized to have a slow rate of O-glucuronidation and might represent a useful scaffold for the design of potent resveratrol analogs with improved bioavailability and which could be developed as chemotherapeutic agents with clinical potential. The glucoronate studies were carried out by members of Dr. Radominska's research group.

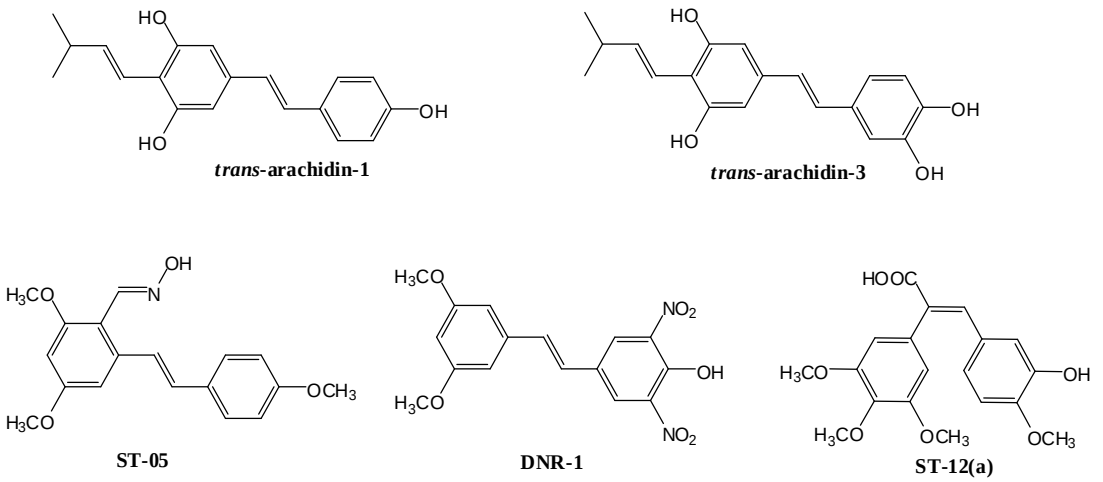

Figure 7.1: Structures of resveratrol analogs ***trans*-arachidin-1**, ***trans*-arachidin-3**, **ST-05**, **DNR-1** and **ST-12(a)**.

The three compounds selected for the study had the majority phenolic groups blocked by O-methylation or incorporated a hydroxylamine, carboxylic acid or aromatic nitro group on the stilbene scaffold.

The study was designed to elucidate:

1) If the above three chemically synthesized stilbene derivatives are substrates for human recombinant UGTs.

2) If the rate of glucuronidation of the three analogues was comparable to resveratrol itself.

Twelve major recombinant human UGT1A and UGT2B enzymes were utilized to determine their capability to metabolize these three reseveratrol analogs. HPLC−UV−VIS analysis was used to identify the formation of glucuronide conjugates. LC−MS/MS and β-glucuronidase hydrolysis was used to elucidate the structures of the metabolites.

7.2 Source of Human Microsomes and Recombinant UGTs.

Human hepatic microsomes were acquired from ten contributors, and human intestinal microsomes were acquired from thirteen contributors. Recombinant proteins UGT1A1, 1A3, 1A4, and 1A6−1A10 were cloned and expressed in baculovirus-infected insect cells (Kurkela, Garcia-Horsman et al. 2003, Kuuranne, Kurkela et al. 2003). Human UGT2B4, 2B7, 2B15, and 2B17 were purchased from BD Biosciences (Woburn, MA) and the manufacturer's protocols were used to carry out the assays.

7.3 Screening of Human Microsomes and Recombinant UGTs

Screening trials for glucuronidation were conducted with human hepatic and intestinal microsomes from 10 and 13 donors, respectively, one pooled liver sample, and commercially available hepatosomes. A 250 μL aliquot of substrate was dissolved in

ethanol solution and added to the incubation tube. The resveratrol analogs were sonicated to ensure solubilization. Reaction buffer and human microsomes (50 mg of total protein) or recombinant UGT membranes (5 mg of total protein) were then added. UDP-GlcUA in molar excess was added, and the samples containing the analogs were incubated at 37 °C for one hour. Final reaction concentrations were as follows: 100 μM Tris−HCl (pH 7.4)/5 mM $MgCl_2$/5 mM saccharolactone/2% DMSO/250 μM substrate/2 micromolar UDPGA/50 or 5 μg of total protein, respectively. The total reaction volume was 30 μL. Controls were run under the same reaction conditions in the absence of substrate molecules. The glucuronidation rate with these enzymes has been shown to be linear for a maximum of 3 hours. The reactions were finally stopped by addition of 30 μL of ethanol. Later, centrifugation of the samples was carried out at 14 000 rpm for 8 min to collect the protein. The supernatants were investigated by HPLC using an HP1050 HPLC system equipped with a UV−VIS diode array detector. Instrument function and data acquisition were assessed using Agilent ChemStation software.

7.4 Enzyme Kinetics Assays.

Kinetic parameters were calculated by incubating recombinant UGT protein with different concentrations of ST-12a (10−1000 μM) or ST-05 (1−1000 μM) with a molar excess of UDP-GlcUA for 1 hour. All kinetic assays were conducted in duplicate under conditions identical to those employed for screening assays.

7.5 Data Analysis.

Kinetic data analysis for the glucuronidation of ST-12(a) and ST-05 by UGTs were estimated by plotting the measured initial reaction velocity values as a function of substrate concentration. Graph-Pad Prism v4.0b (GraphPad Software, Inc., San Diego, CA) was utilized for conducting curve-fitting and statistical analyses. Kinetic constants were obtained by fitting the experimental data to the following kinetic models using the nonlinear regression (Curve Fit) function.

1. Michaelis−Menten (M−M) equation used for the one-enzyme model.

$$v = \frac{V_{max} \times [S]}{K_m + [S]}$$

2. Hill equation reflects the extent of cooperativity among multiple binding sites (Weiss 1997).

$$v = \frac{V_{max} \times [S]^n}{{S_{50}}^n + [S]^n}$$

3. Uncompetitive substrate inhibition (USI) model, where Ki is the inhibition constant describing the rate reduction.

$$v = \frac{V_{max}}{1 + \frac{K_m}{[S]} + \frac{[S]}{K_i}}$$

7.6 Glucuronide Product Analysis

A HP1050 LC system equipped with a variable wavelength UV-DAD detector was used for HPLC-UV analyses of supernatants. Agilent ChemStation software was used for instrument control and data collection. A reversed-phase 5 μm Suplex pKb-100 analytical column (0.46 cm x 25 cm, C18) was used for HPLC separations. The temperature was maintained at 25 ˚C. A flow rate of 1 ml/min with a linear gradient from 15-80% methanol in ammonium formate buffer (0.05 M, pH 3.4) for 25 min, followed by a linear gradient from 80-100% methanol in ammonium formate for 3 min was utilized. The elution of each metabolite of ST-12(a) was monitored at 335 nm, whereas the elution of the metabolite of ST-05 was monitored at 325 nm.

7.7 Analysis of Glucuronide Product Structures by ESI-HPLC-MS

An Acquity uHPLC system interfaced to a Quattro Premier triple quadrupole mass analyzer (Waters Corporation, Beverly, MA) with an electrospray probe operating in the positive ion mode was used for HPLC-MS analysis of the glucuronide and structural identification of glucuronide products. Liquid chromatography settings were identical to those used for LC-UV analysis, and 10 μL of sample was injected onto the column. The nitrogen flow rate was 600 L/h and was maintained at 500°C. The source temperature was 150°C.

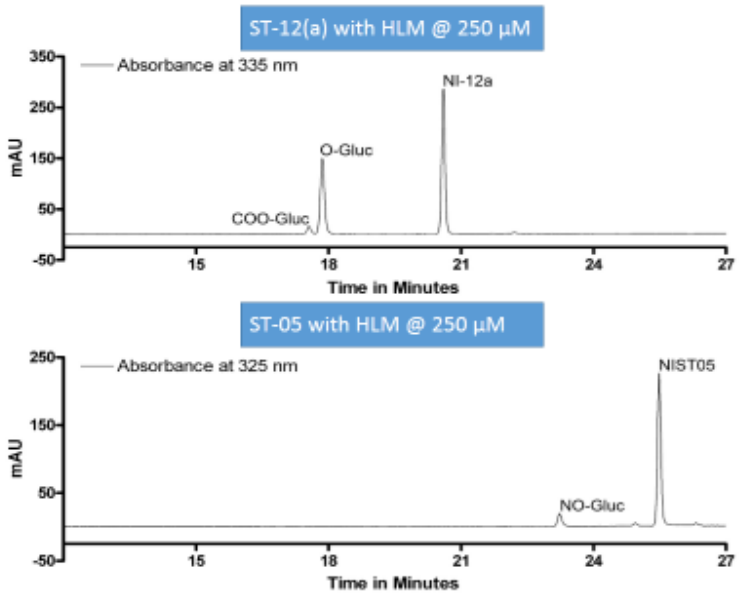

Figure 7.2. Metabolism of **ST-12(a)** and **ST-05** with human liver microsomes. Representative HPLC analyses are shown from 60 min incubations of 50 µg of human liver proteins with 0.25 mM substrate and 3 mM UDP-GlcUA. **DNR-1** was not metabolized under the similar conditions.

7.8 Glucuronide Metabolite Analysis by HPLC−UV−VIS and HPLC−MS/MS

UGT1A and UGT2B enzymes were used for preliminary studies on the glucuronidation of **ST-05**, **DNR-1**, and **ST-12(a)**. Glucuronidation products for **ST-05** and **ST-12(a)** were detected, identified and quantitated, but no glucuronidation product of **DNR-1** was formed. Two metabolites at tR = 17.6 and tR = 17.8 min for **ST-12(a)** and one metabolic product at tR 23.2 min for **ST-05** were identified (**Figure 7.3**).

LC− (+)-ESI−MS analysis (Figure 5.4), indicated that the two glucuronides of **ST-12(a)** (tR = 16.0 and 16.3 min) had an $[M + NH_4]$ + peak m/z 554, and suspected to be COO- and O-conjugated glucuronides. The enzyme β-glucuronidase selectively hydrolyzes only

O-glucuronides, and this enzyme was used to identify which of the two possible glucuronide metabolites were present. It was determined that the peak at tR = 16.0 min in the HPLC chromatogram was an acyl glucuronide.

In **Figure 7.4**, ammonium adducts of **ST-05** glucuronides were not observed; however, the proton adduct [M + H]+) was observed with a retention time of 23.2 min and an m/z 490. We suspected the glucuronide product to be a C=N-O-glucuronide. The different LC systems with unique system dead volumes can be attributed to the different retention times on LC-MS and LC-UV runs.

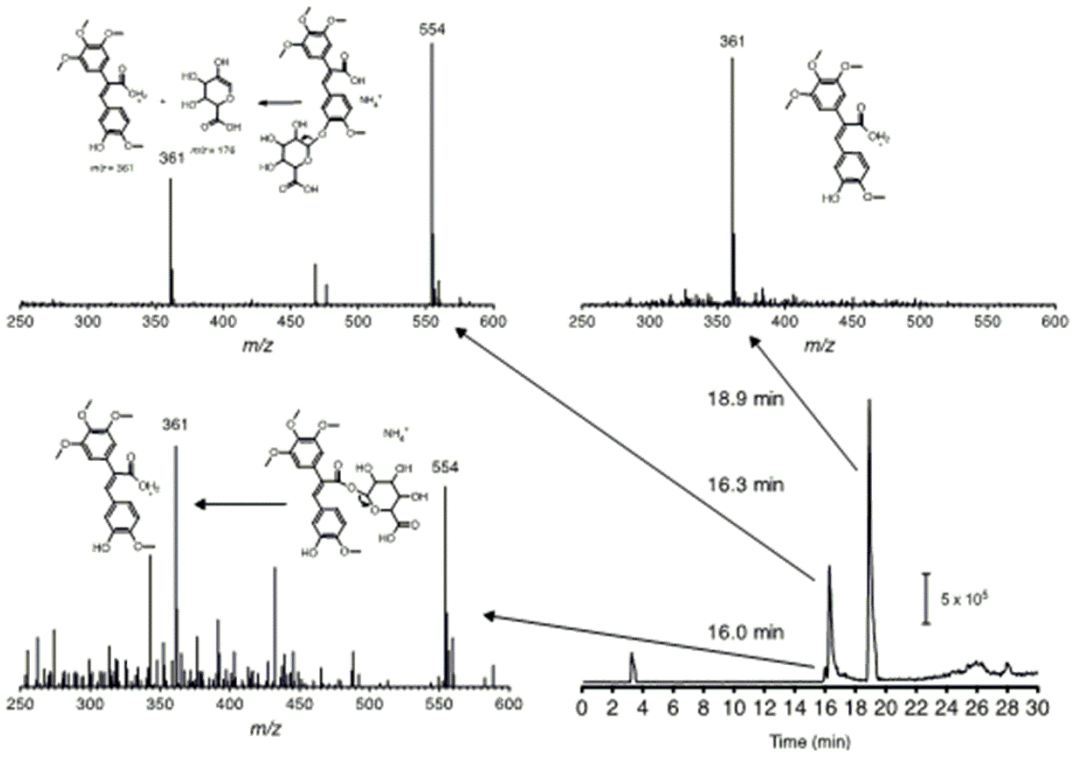

Figure 7.3. Extracted ion chromatogram (m/z 361) and (+)-ESI mass spectra of **ST-12(a)** and its glucuronide conjugate NH_4+ adducts. Spectra of **ST-12(a)** glucuronides (two isomers of tR = 16.0 and 16.3 min) showed an [M + NH_4] + peak (m/z 554) plus a fragment ion resulting from neutral loss of the glucuronide moiety (m/z 361).

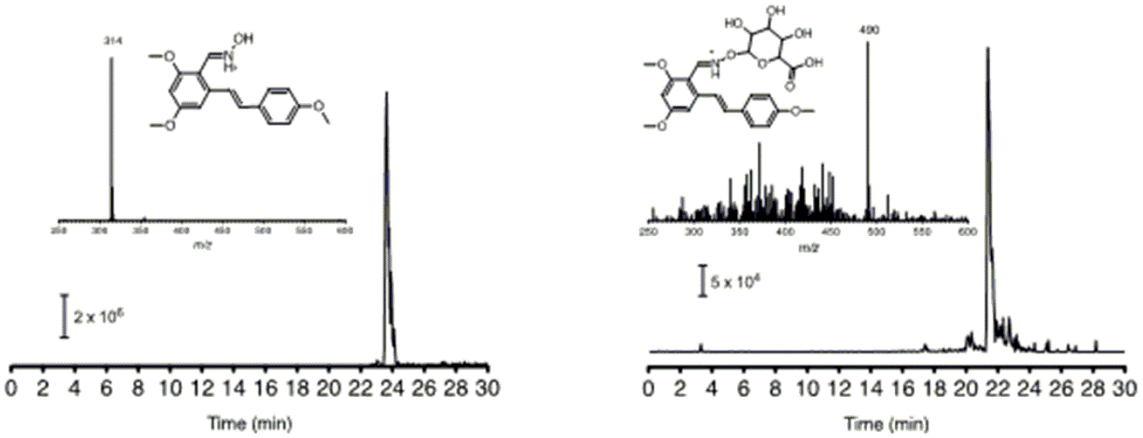

Figure 7.4. Structures and Mass spectra of **ST-05** and its glucuronide conjugates. Spectrum of **ST-05** glucuronide (tR = 21.4 min) showed an [M+ H]+ peak (m/z 490) plus a major peak corresponding to the **ST-05** substrate (m/z 314).

7.9 Screening of Recombinant UGTs for glucuronidation of ST-12a and ST-05.

Eight human recombinant UGT1 enzymes and UGT2B4, 2B7, 2B15, and 2B17 were acquired from BD Biosciences and were evaluated for their ability to glucuronidate **ST-12a** and **ST-05**. β-Glucuronidase hydrolysis was used to differentiate between COO- and O-glucuronides in **ST-12(a) (Figure 7.5)**.

For **ST-12(a)**, treatment with human recombinant UGT1A3 led to both COO- and O-glucuronide formation. When UGT1A1 was utilized only the carboxyl metabolite was produced, whereas UGTs 1A7−1A10 formed only the O-glucuronide. None of the UGT2B enzymes, UGT1A4 and 1A6 were active toward this compound.

For compound **ST-05**, treatment with human recombinant UGT1A1, 1A9, and 1A10 resulted in the formation of the C=N−O-glucuronide. All of the other UGTs remained inactive.

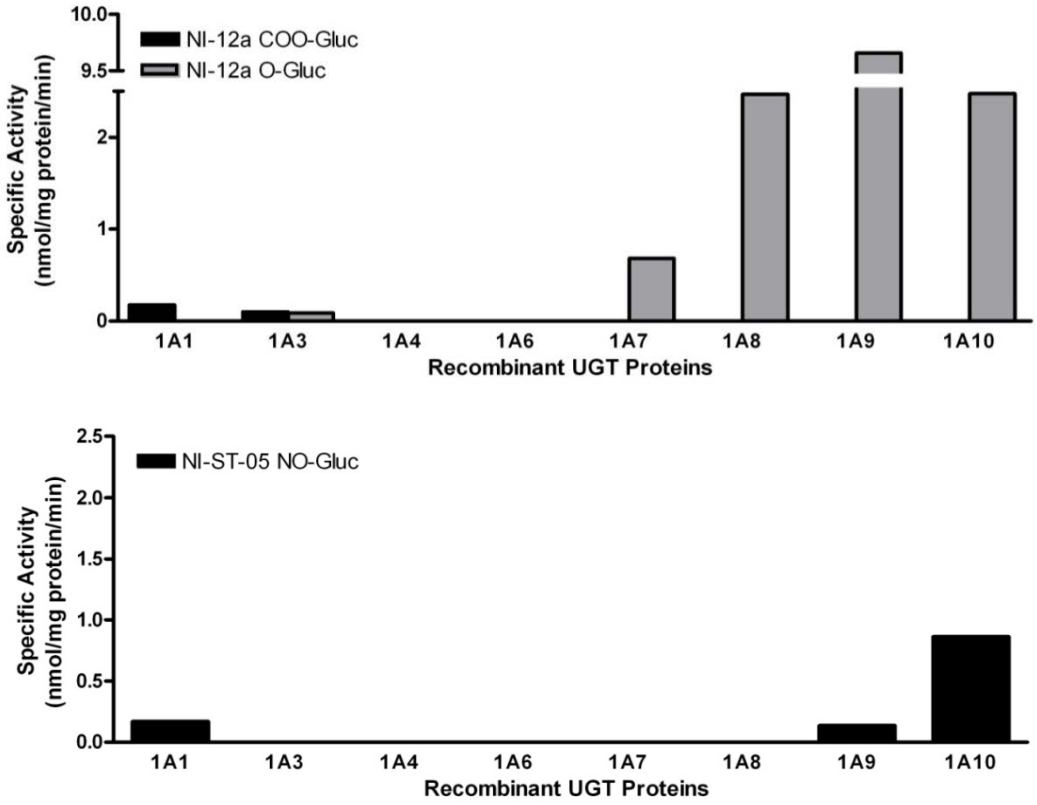

Figure 7.5. Glucuronidation of **NI-12a** and **ST-05** by human recombinant UGTs. UGT1A1, 1A3, 1A4, 1A6, 1A7, 1A8, 1A9, 1A10, 2B4, 2B7, 2B15, 2B17 (5 μg of protein) were evaluated for their ability to glucuronidate **DNR-1**, **ST-12(a)**, and **ST-05**. No activity was observed toward **DNR-1**, and UGT2B7, 2B4, 2B15, and 2B17 were not active toward any compound. Activities are expressed in nanomoles per milligram of protein per minute.

7.10 Glucuronidation of ST-12(a) and ST-05 by Human Hepatic and Intestinal Microsomes.

Screening assays for glucuronidation activity were conducted with HLM (Human Liver Microsomes) and HIM (Human Intestine Microsomes) from 10 and 13 contributors, one pooled liver sample, and commercial hepatosomes (**Figure 7.6**). Both **ST-12(a)** and **ST-05** were shown to be glucuronidated with all the hepatic samples utilized, producing two metabolites of **ST-12(a)** and one metabolic product from **ST-05**.

Intestinal samples HI27, HI28, HI29 and HI54 failed to display glucuronidation activity toward **ST-12(a)**. Contributors HI34, HI36, HI40 and HI41 produced only the O-glucuronide. The remaining contributors with activity produced both COO- and O-glucuronide metabolites. In the case of **ST-05**, donors HI27, HI29, and HI30 did not display any glucuronidation activity, but all other donors produced the C=N−O-glucuronide.

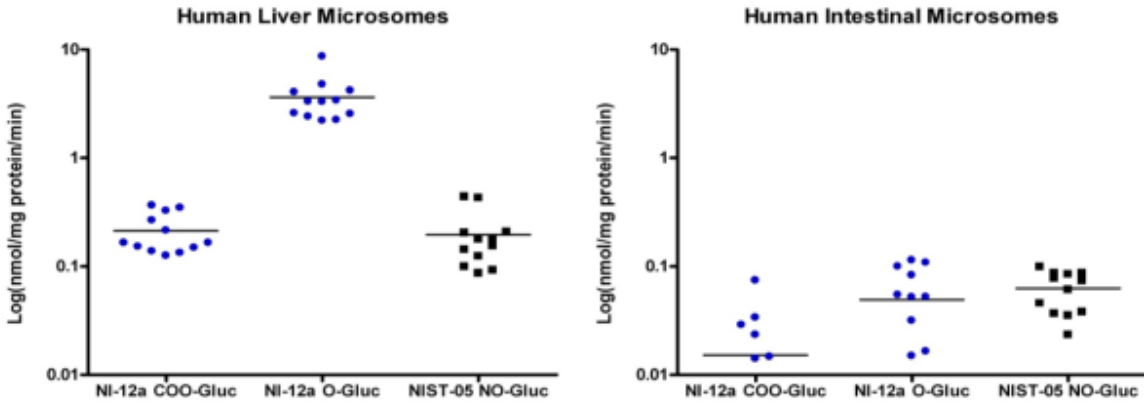

Figure 7.6. Glucuronidation activities of Human Liver Microsomes and Human Intestinal Microsomes toward **NI-12a** and **NI-ST-05.** Human liver microsomes from 10 different donors, a pooled liver sample, and hepatosomes and human intestine microsomes from 13 different donors were analyzed. Each substrate concentration was 0.25 mM for HIM, with a molar excess of UDP-GlcUA; the reactions were incubated for 60 minutes. Activities are expressed in nmol/mg protein/min.

7.11 Kinetic Analysis of NI-12a and NI-ST-05 with selected recombinant UGTs

Based on the activity screening data human recombinant UGT isoforms (UGT 1A7 to 1A10 for **ST-12(a)** and UGT1A1, 1A9, and 1A10 for **ST-05**) were subjected to kinetic analysis and the results presented in **Table 1** and **Figure 7.8,7.9** In the case of **ST-12(a)**,

human recombinant isoform UGT1A9 was the most active with V_{max} = 8.3 nm /mg protein/min. UGT1A7 showed the greatest affinity for **ST-12(a)** with Km = 62 μM, and UGT1A10 had the lowest affinity with Km = 500 μM. Because of the high V_{max}, the catalytic efficiency of UGT1A9 toward **ST-12(a)**, measured by the ratio Vmax/Km (35 μL/min/mg), was also the highest. Data generated for UGT1A7 and 1A8 fits an uncompetitive substrate inhibition kinetic model, which suggests the existence of multiple binding sites on these UGT isoforms.

For **ST-05**, because of the very small amount of product formation (C=N-O-glucuronidation) and the low sensitivity of our HPLC-UV/VIS detection capabilities, our ability to perform kinetic analyses was limited. Assuming michaelis–menten kinetics UGT1A1 activities at concentrations above 5 μM were used to estimate a V_{max} value of 0.2 nmol/mg/min. Cooperative binding was indicated for UGT1A10 which fit to the Hill equation. Also, data generated with isoform UGT1A9 did not fit any of the kinetic models tested.

Table 7.1. Glucuronidation Kinetics for **NI-12(a)** and **NI-ST-05** Metabolites. Glucuronidation activities of selected recombinant UGTs were measured by incubating membrane fractions with increasing concentrations of substrate (see **Figures 7.7** and **7.8**) at a constant concentration of UDP-GlcUA (3 mM). Reactions were centrifuged, supernatants separated by HPLC, and curve fits and kinetic constants determined using GraphPad Prism 4 software. *Values estimated based on an incomplete data set.

	UGT1A1	UGT1A7	UGT1A8	UGT1A9	UGT1A10
ST-12(a)					
ST-12a-O-Gluc	Not Produced				
K_m (μM)		62 ± 43	240 ± 76	240 ± 40	500 ± 75
V_{max} (nmol/mg/min)		2.2 ± 0.77	6.0 ± 1.3	8.3 ± 0.52	3.5 ± 0.24
K_s (μM)		242 ± 133	950 ± 449		
CL_{int} or CL_{max} (μL/mg/min)		35	25	35	7
Kinetic Model		USI	USI	M-M	M-M
R^2		0.82	0.98	0.97	0.98
ST-12a-COO-Gluc	Too low to be assessed	Not Produced	Not Produced	Not Produced	Not Produced
ST-05					
ST-05-N-O-Gluc		Not Produced	Not Produced		
K_m or S_{50} (μM)	<5*			<5*	6.2 ± 0.35
V_{max} (nmol/mg/min)	0.21 ± 0.02*			Undetermined	0.65 ± 0.017
n					3.4
CL_{int} or CL_{max} (μL/mg/min)					105
Kinetic Model	M-M*			Undetermined	Hill
R^2	0.61*				0.87

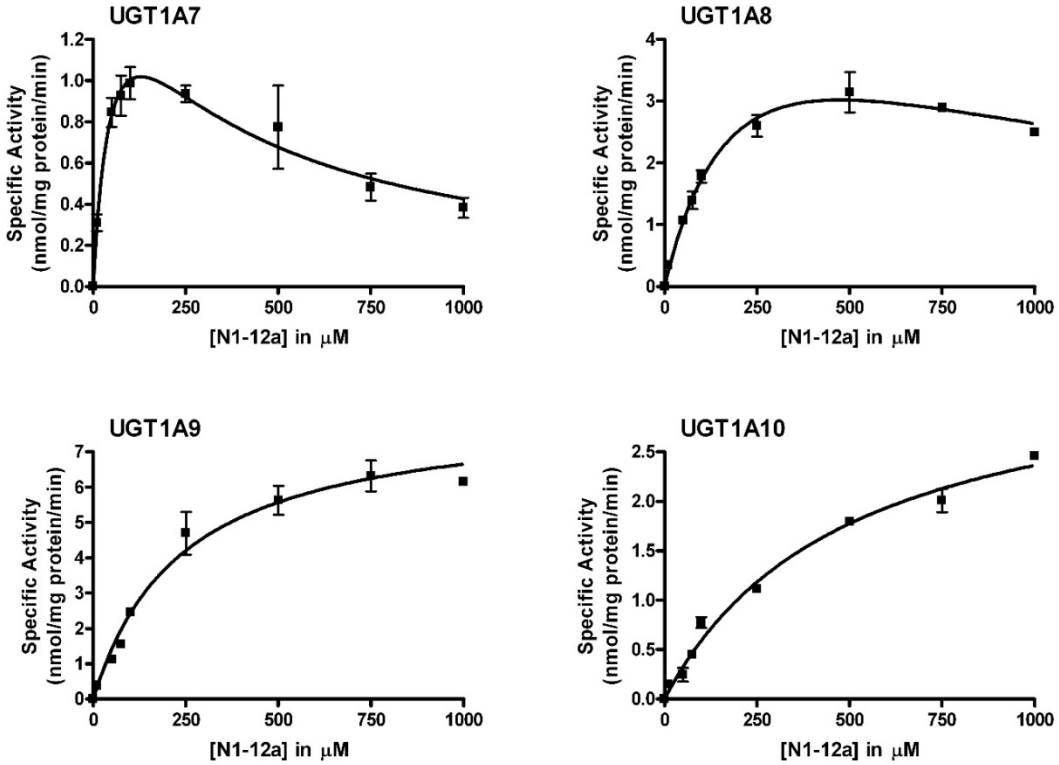

Figure 7.7. Steady state kinetic curves for the glucuronidation of **NI-12a** by selected human recombinant UGTs. Glucuronidation activities for wildtype UGT1A7, 1A8, 1A9, and 1A10 were measured by incubating membrane fractions containing recombinant UGTs with increasing concentrations (shown in figure) of the substrates at a constant concentration of UDP-GlcUA (3 mM) for 60 min at 37 °C. Curve fits and kinetic constants were determined using GraphPad Prism 4 software. The graphical fits of the data (mean ± SD) are shown.

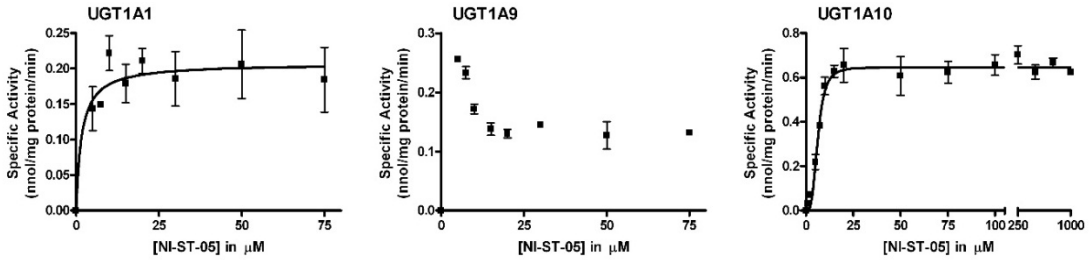

Figure 7.8. Steady state kinetic curves for the glucuronidation of **ST-05** by selected human recombinant UGTs. Glucuronidation activities for wildtype UGT1A1, 1A9, and 1A10 were measured by incubating membrane fractions containing recombinant UGTs with increasing concentrations (shown in figure) of the substrates at a constant concentration of UDP-GlcUA (3 mM) for 60 min at 37 °C. Curve fits and kinetic constants were determined using GraphPad Prism 4 software. The graphical fits of the data (mean ± SD) are shown.

5.12 Conclusion

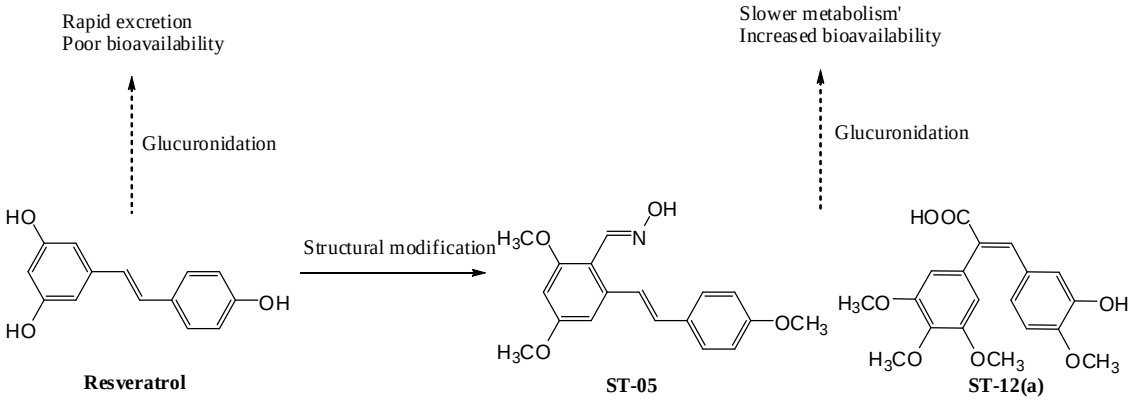

Figure 7.9. Glucuronidation rates of resveratrol, **ST-05** and **ST-12(a)**.

The current study was designed to test the hypothesis that the limited bioavailability of resveratrol can be improved by synthesizing analogs that will be glucuronidated at a lower rate than resveratrol itself. The analogs selected for the study: **ST-05**, **DNR-1**, and **ST-12(a)**, had aromatic hydroxylamine, hydroxyl, nitro and carboxylic acid moieties incorporated into their structures and were assumed to be less susceptible to glucuronidation, thereby improving their bioavailability. In the current study we

demonstrated that **ST-05** and **ST-12(a)** were substrates for recombinant UGT enzymes and human hepatic and intestinal microsomes. Because of the presence of sterically hindering aromatic nitro groups in the molecule, O-glucuronidation of **DNR-1** was not observed. Glucuronidation experiments with **ST-12(a)** resulted in different products and atypical reaction kinetics specific for each enzyme (Table 1), which indicates a complex mechanism of metabolism for this analog. The results from the kinetic parameters discussed earlier indicate that **ST-12(a)** will have improved bioavailability compared to that of resveratrol. Glucuronidation experiments with **ST-05** resulted in the formation of a rare C=N−O -glucuronide, and the rate of this reaction was significantly lower than that for O-glucuronidation of resveratrol.

In conclusion, the glucuronidation of the novel stilbenoids utilized in this study revealed that these compounds exhibit lower glucuronidation profiles as compared to resveratrol. Compound **ST-12(a)** and related stilbenes have been reported to be effective antitubulin agents (Borrel, Thoret et al. 2005), and based of these data, the synthesized stilbenoids likely represent a useful scaffold for the design of efficacious resveratrol analogs with improved bioavailability over resveratrol.

This data set has been reproduced with permission from the following publication: copyright ACS publications: Greer, A. K., N. R. Madadi, S. M. Bratton, S. D. Eddy, Z. Mazerska, H. Hendrickson, P. A. Crooks and A. Radominska-Pandya (2014). "Novel Resveratrol-Based Substrates for Human Hepatic, Renal and Intestinal UDP-Glucuronosyltransferases." *Chem. Res. Toxicol.*, **2014**, *27* (4), pp 536–545.

Copyright © Nikhil Reddy Madadi 2014

Data Set 2

NCI single dose percentage growth results for the simple stilbene analogues.

Table 8.1. Percentage growth inhibition of NCI 60 human cancer cells by compounds **ST-191, ST-192, ST-193, ST-194, ST-197, ST-198 and ST-209** at 10μM concentration**.**

Cancer	cell type	ST-191	ST-192	ST-193	ST-194	ST-197	ST-198	ST-209
Leukemia	CCRF-CEM	96.6	86.2	NA	82.9	NA	NA	NA
	HL-60(TB)	119.6	89.2	101.1	47.0	91.7	-18.8	88.1
	K-562	129.1	150.9	146.2	21.8	105.5	17.6	NA
	MOLT-4	108.6	92.0	82.8	50.4	114.1	16.1	118.8
	RPMI-8226	95.3	75.2	NA	44.6	92.9	49.8	95.6
	SR	103.6	100.4	108.4	40.8	91.1	9.6	94.9
Non-Small Cell Lung Cancer	A549/ATCC	122.8	88.4	98.0	67.6	108.7	32.5	116.6
	HOP-62	99.9	97.8	99.9	80.6	88.6	46.6	92.3
	HOP-92	120.6	114.2	NA	NA	NA	NA	NA
	NCI-H226	95.2	92.8	94.6	74.3	89.9	34.5	123.9
	NCI-H23	96.5	89.2	101.9	74.0	86.8	40.0	97.5
	NCI-H322M	83.1	95.6	94.1	87.0	85.7	52.7	97.2
	NCI-H460	104.4	103.7	97.9	93.7	102.2	14.1	99.8
	NCI-H522	95.6	98.0	102.9	59.8	98.6	32.5	103.3
Colon Cancer	COLO 205	104.6	85.9	99.7	71.5	89.6	0.6	98.7
	HCC-2998	99.6	97.4	106.0	90.7	111.6	9.8	105.5
	HCT-116	97.0	97.3	101.3	68.7	95.4	9.9	103.0
	HCT-15	102.7	99.5	96.4	63.1	85.4	20.2	102.3
	HT29	98.7	92.7	109.2	60.0	98.1	12.6	104.8
	KM12	99.9	91.2	98.5	64.0	100.2	16.1	103.7
	SW-620	100.6	104.9	91.9	64.7	99.3	28.2	100.9
CNS Cancer	SF-268	103.3	94.7	101.9	81.3	96.9	39.0	107.8
	SF-295	97.3	104.2	106.3	78.9	93.7	6.6	101.1
	SF-539	102.0	97.9	94.2	83.2	100.5	-2.9	108.8
	SNB-19	98.4	85.4	94.5	70.0	74.0	54.3	104.9
	SNB-75	56.0	100.7	NA	57.8	103.6	NA	NA
	U251	108.6	97.1	98.2	76.7	98.3	29.0	121.9
Melanoma	LOX IMVI	106.1	124.4	115.0	77.6	95.4	35.1	109.3
	MALME-3M	100.8	93.3	102.7	59.3	96.2	61.9	99.8
	M14	102.2	88.5	96.5	64.4	91.9	20.4	94.3
	MDA-MB-435	103.4	115.6	105.0	2.4	103.7	-26.4	90.6
	SK-MEL-2	123.2	94.7	115.0	69.6	90.4	62.5	112.8

Table 8.1 (continued)

	SK-MEL-28	104.8	98.3	101.9	74.5	87.8	55.7	94.7
	SK-MEL-5	96.9	92.9	96.9	57.0	114.9	27.0	101.3
	UACC-257	NA	NA	NA	49.3	72.6	NA	78.1
	UACC-62	95.7	74.2	115.8	51.6	93.6	28.3	104.3
Ovarian Cancer	IGROV1	91.1	96.0	91.1	85.0	101.1	43.5	104.1
	OVCAR-3	104.5	103.9	91.5	NA	NA	-13.4	NA
	OVCAR-4	85.8	93.7	98.5	75.5	80.0	45.9	90.1
	OVCAR-5	97.9	103.2	90.2	87.1	91.4	50.9	97.5
	OVCAR-8	104.2	103.0	94.7	85.3	NA	28.0	NA
	NCI/ADR-RES	107.1	95.0	107.7	63.3	86.9	12.7	109.0
	SK-OV-3	104.0	95.7	108.5	84.3	98.5	26.8	97.1
Renal Cancer	786-0	102.8	105.0	97.5	88.1	101.6	51.2	106.4
	A498	90.6	80.5	102.1	56.4	83.3	-4.3	80.7
	ACHN	110.9	105.6	72.8	84.0	101.1	46.0	106.2
	CAKI-1	94.7	94.3	99.0	62.6	92.4	43.8	100.7
	RXF 393	104.1	112.2	92.7	89.5	95.0	-7.0	116.6
	SN12C	99.0	91.4	103.0	78.9	85.5	23.9	100.8
	TK-10	132.4	90.9	89.9	74.1	115.6	76.2	104.1
	UO-31	89.7	79.8	147.5	51.2	71.8	42.6	92.2
Prostate Cancer	PC-3	98.6	83.4	67.0	59.6	93.4	49.2	103.1
	DU-145	105.2	100.3	110.7	90.7	94.8	12.1	109.6
Breast Cancer	MCF7	88.8	89.3	80.9	42.2	96.9	1.8	90.2
	MDA-MB-231	99.4	102.6	87.4	66.9	94.1	18.2	129.3
	HS 578T	119.2	94.3	109.0	76.4	98.6	12.0	131.0
	BT-549	92.5	91.2	81.4	69.0	85.8	38.9	100.3
	T-47D	86.2	87.2	84.0	64.1	101.3	56.3	94.6
	MDA-MB-468	100.6	90.4	101.5	NA	NA	16.7	NA

Table 8.2. Percentage growth inhibition of NCI 60 human cancer cells by compounds **ST-212, ST-220, ST-226, ST-227, ST-233, ST-234 and ST-236** at 10μM concentration**.**

Cancer	**cell type**	**ST-212**	**ST-220**	**ST-226**	**ST-227**	**ST-233**	**ST-234**	**ST-236**
Leukemia	CCRF-CEM	93.6	88.5	98.9	106.5	89.5	98.8	85.4
	HL-60(TB)	73.1	78.2	NA	NA	79.2	96.6	86.2
	K-562	92.2	101.0	98.9	114.2	89.3	99.4	30.6
	MOLT-4	82.6	79.8	89.5	91.7	74.0	84.1	79.5
	RPMI-8226	86.2	74.4	109.7	102.1	103.0	100.7	99.1
	SR	84.9	95.9	91.8	108.0	69.5	77.4	44.8
Non-Small	A549/ATCC	83.7	87.7	96.4	100.3	97.0	102.0	85.2

Table 8.2 (continued)

Cell Lung Cancer	HOP-62	83.5	100.8	118.1	92.1	84.4	90.4	85.0
	HOP-92	NA	NA	90.6	94.6	86.1	NA	79.7
	NCI-H226	104.5	97.7	103.7	110.0	85.8	101.5	100.3
	NCI-H23	98.6	94.4	95.4	104.4	95.3	90.5	92.0
	NCI-H322M	95.1	100.4	104.5	98.7	103.1	108.9	112.6
	NCI-H460	97.4	99.9	106.2	125.3	103.7	105.4	104.1
	NCI-H522	74.3	77.4	76.5	106.7	67.0	72.8	29.1
Colon Cancer	COLO 205	100.3	107.4	98.6	91.9	97.4	100.7	98.6
	HCC-2998	103.4	111.0	103.3	100.2	95.3	96.7	92.4
	HCT-116	98.4	91.9	99.4	111.1	98.7	91.8	79.3
	HCT-15	91.9	90.1	95.0	94.7	92.6	96.0	74.6
	HT29	79.9	88.7	90.7	102.3	88.3	86.2	75.2
	KM12	99.5	91.5	97.5	94.1	93.8	91.4	75.3
	SW-620	93.3	97.2	106.3	116.0	100.5	103.3	80.2
CNS Cancer	SF-268	106.0	104.3	110.7	116.0	83.2	99.8	90.7
	SF-295	91.1	98.8	111.5	107.1	94.2	101.5	74.6
	SF-539	99.0	99.5	100.0	98.4	97.1	97.6	94.9
	SNB-19	99.8	97.3	107.1	96.5	98.3	109.9	92.9
	SNB-75	94.1	89.0	88.3	111.0	80.2	84.2	87.8
	U251	95.2	95.6	109.6	95.6	90.5	103.0	79.8
Melanoma	LOX IMVI	100.9	103.3	98.0	98.7	88.6	90.3	84.4
	MALME-3M	100.9	109.6	114.0	101.4	97.1	99.8	56.0
	M14	99.0	97.2	108.4	120.1	92.3	93.6	73.1
	MDA-MB-435	92.5	96.1	102.9	103.6	95.9	103.0	3.6
	SK-MEL-2	97.8	98.8	101.4	105.5	85.8	83.0	81.7
	SK-MEL-28	97.6	100.3	100.6	99.8	95.5	98.8	79.1
	SK-MEL-5	96.9	99.1	104.0	111.4	90.9	96.4	85.8
	UACC-257	72.0	71.7	117.9	105.5	101.0	105.1	88.5
	UACC-62	94.9	104.5	78.2	94.6	63.9	67.1	58.5
Ovarian Cancer	IGROV1	104.4	104.6	109.0	102.5	98.2	101.8	94.0
	OVCAR-3	NA	NA	NA	NA	NA	NA	NA
	OVCAR-4	83.7	88.7	94.6	115.5	100.6	102.3	102.2
	OVCAR-5	82.5	95.1	100.0	99.9	93.1	95.2	95.2
	OVCAR-8	101.2	101.8	113.3	115.5	93.0	101.9	101.6
	NCI/ADR-RES	99.7	109.5	106.8	109.5	89.4	101.2	63.7
	SK-OV-3	99.9	99.4	101.3	103.8	96.5	93.1	95.7
Renal Cancer	786-0	97.0	104.0	100.4	98.4	90.9	104.1	90.9
	A498	83.2	80.7	106.0	104.8	74.1	92.6	66.7
	ACHN	92.1	97.0	105.4	106.0	94.9	102.1	94.8
	CAKI-1	92.1	91.7	99.5	98.6	94.5	106.5	71.7
	RXF 393	108.5	110.1	118.9	111.5	100.4	104.4	87.3

Table 8.2 (continued)

	SN12C	95.4	98.7	102.0	110.6	81.8	98.3	87.8
	TK-10	78.6	110.4	95.0	95.9	88.3	100.5	78.1
	UO-31	82.9	86.6	93.5	94.7	71.6	107.1	87.9
Prostate Cancer	PC-3	93.2	93.2	87.5	103.6	87.3	90.8	90.2
	DU-145	93.2	97.6	101.4	102.2	90.6	101.3	98.6
Breast Cancer	MCF7	87.0	87.0	60.6	100.4	98.0	105.4	58.0
	MDA-MB-231	108.8	94.4	120.3	118.9	89.9	95.4	88.5
	HS 578T	103.8	104.7	118.2	117.6	100.3	106.6	92.4
	BT-549	94.6	98.9	104.0	98.2	82.1	82.3	106.6
	T-47D	82.3	84.6	73.8	103.1	86.5	64.4	81.2
	MDA-MB-468	NA	NA	98.7	109.8	96.5	100.4	92.6

Table 8.3. Percentage growth inhibition of NCI 60 human cancer cells by compounds **ST-239, ST-247, ST-294, ST-297, ST-309, ST-315 and ST-320** at 10μM concentration**.**

Cancer	**cell type**	**ST-239**	**ST-247**	**ST-294**	**ST-297**	**ST-309**	**ST-315**	**ST-320**
Leukemia	CCRF-CEM	95.1	91.5	97.6	99.6	97.0	99.7	71.4
	HL-60(TB)	100.5	98.8	NA	NA	NA	NA	NA
	K-562	107.5	94.8	95.6	68.9	73.0	81.0	22.3
	MOLT-4	90.8	79.2	89.6	60.2	74.2	90.7	71.1
	RPMI-8226	92.1	102.0	92.9	71.9	83.8	81.3	84.4
	SR	88.3	73.3	95.9	64.8	77.9	79.6	43.0
Non-Small Cell Lung Cancer	A549/ATCC	95.7	94.7	88.2	79.0	79.5	92.0	91.4
	HOP-62	95.0	89.4	86.2	93.3	96.6	97.3	97.6
	HOP-92	101.3	NA	122.6	90.4	73.7	82.8	80.2
	NCI-H226	96.8	89.7	74.6	95.8	98.4	103.3	98.1
	NCI-H23	101.2	90.1	83.3	104.4	91.7	97.5	91.7
	NCI-H322M	104.1	88.2	95.3	100.9	78.7	91.5	88.9
	NCI-H460	103.6	87.0	98.3	100.4	104.7	104.3	99.3
	NCI-H522	84.2	76.0	81.1	59.9	59.8	76.3	76.1
Colon Cancer	COLO 205	100.5	96.4	98.2	88.6	91.4	91.5	98.3
	HCC-2998	101.3	84.8	102.7	92.7	89.7	103.7	99.8
	HCT-116	97.0	86.9	91.7	89.3	87.2	93.5	88.2
	HCT-15	101.8	90.7	83.4	76.0	66.1	89.4	62.2
	HT29	101.2	85.5	89.1	68.3	77.6	79.5	73.2
	KM12	101.2	81.7	87.2	100.0	89.2	94.1	79.0
	SW-620	106.1	98.8	95.5	99.7	91.9	105.1	81.4
CNS	SF-268	102.7	101.7	98.7	85.2	81.3	94.8	91.9

Table 8.3 (continued)

Cancer	SF-295	NA	102.1	105.8	96.6	90.0	89.3	95.4
	SF-539	99.9	98.0	89.9	94.2	96.6	93.7	86.3
	SNB-19	111.4	105.0	103.2	77.1	74.9	79.6	84.1
	SNB-75	99.4	80.2	84.9	91.8	72.0	81.9	92.3
	U251	97.0	91.9	87.9	88.7	81.4	96.2	87.0
Melanoma	LOX IMVI	99.9	93.8	89.1	101.4	97.6	97.9	91.0
	MALME-3M	93.1	83.0	91.0	83.6	120.3	97.7	75.4
	M14	99.4	88.4	86.6	86.7	92.7	91.0	80.1
	MDA-MB-435	109.9	100.6	102.1	86.3	92.1	85.9	28.9
	SK-MEL-2	101.0	95.6	99.7	94.1	79.4	90.2	89.2
	SK-MEL-28	107.2	103.1	111.1	95.3	92.5	99.7	93.8
	SK-MEL-5	101.7	93.8	93.9	87.8	87.1	93.0	90.5
	UACC-257	118.0	103.5	116.5	95.4	95.9	102.8	93.4
	UACC-62	101.2	82.4	91.9	80.3	70.5	74.7	75.3
Ovarian Cancer	IGROV1	97.0	88.8	77.6	96.5	87.1	101.5	86.1
	OVCAR-3	NA	NA	NA	NA	NA	NA	NA
	OVCAR-4	102.5	82.4	78.2	97.1	89.4	83.6	84.9
	OVCAR-5	103.4	96.0	109.1	91.0	91.4	91.4	94.2
	OVCAR-8	105.4	99.8	103.7	95.6	93.5	96.0	96.5
	NCI/ADR-RES	113.6	106.6	104.7	90.7	73.5	94.5	89.0
	SK-OV-3	102.2	88.4	99.9	101.0	106.8	104.3	90.9
Renal Cancer	786-0	97.1	100.2	97.0	89.8	82.4	94.1	91.8
	A498	111.5	97.8	86.2	69.3	81.0	67.8	66.8
	ACHN	108.9	96.5	94.2	89.4	79.1	93.9	98.8
	CAKI-1	NA	98.0	85.1	88.9	71.6	100.6	86.3
	RXF 393	114.0	110.2	NA	98.3	88.5	107.2	87.4
	SN12C	105.5	98.1	101.9	80.9	75.8	87.1	91.8
	TK-10	114.1	103.9	131.1	74.8	61.2	65.0	82.6
	UO-31	92.2	81.6	69.5	65.2	59.1	63.5	74.8
Prostate Cancer	PC-3	100.8	94.2	92.4	64.4	61.5	77.3	80.8
	DU-145	104.1	105.9	99.2	92.7	87.9	94.0	99.2
Breast Cancer	MCF7	83.6	15.8	66.7	88.2	84.5	89.6	65.3
	MDA-MB-231	102.0	95.9	77.5	102.8	90.7	93.9	84.6
	HS 578T	111.6	101.8	102.0	112.7	100.5	112.1	118.1
	BT-549	97.1	86.6	89.1	83.3	73.3	82.7	92.9
	T-47D	87.9	58.6	56.3	69.0	62.5	86.2	82.0
	MDA-MB-468	108.4	7.7	78.6	94.5	85.2	101.7	90.3

Table 8.4. Percentage growth inhibition of NCI 60 human cancer cells by compound **ST-321** a 10μM concentration**.**

Cancer	Cell type	ST-321
Leukemia	CCRF-CEM	95.2
	HL-60(TB)	NA
	K-562	NA
	MOLT-4	83.2
	RPMI-8226	88.8
	SR	107.9
Non-Small Cell Lung Cancer	A549/ATCC	95.0
	HOP-62	93.2
	HOP-92	84.5
	NCI-H226	87.0
	NCI-H23	95.3
	NCI-H322M	94.1
	NCI-H460	102.8
	NCI-H522	75.2
Colon Cancer	COLO 205	91.8
	HCC-2998	NA
	HCT-116	92.3
	HCT-15	91.5
	HT29	85.6
	KM12	96.2
	SW-620	97.5
CNS Cancer	SF-268	101.3
	SF-295	102.7
	SF-539	92.6
	SNB-19	92.8
	SNB-75	84.4
	U251	92.0
Melanoma	LOX IMVI	93.2
	MALME-3M	83.1
	M14	90.0
	MDA-MB-435	97.9
	SK-MEL-2	93.8
	SK-MEL-28	97.8
	SK-MEL-5	91.2

Table 8.4 (continued)

	UACC-257	91.8
	UACC-62	72.7
Ovarian Cancer	IGROV1	96.7
	OVCAR-3	NA
	OVCAR-4	96.5
	OVCAR-5	95.5
	OVCAR-8	93.9
	NCI/ADR-RES	106.0
	SK-OV-3	92.3
Renal Cancer	786-0	102.0
	A498	102.8
	ACHN	92.2
	CAKI-1	87.8
	RXF 393	94.2
	SN12C	94.0
	TK-10	114.2
	UO-31	82.2
Prostate Cancer	PC-3	86.6
	DU-145	104.0
Breast Cancer	MCF7	70.1
	MDA-MB-231	88.4
	HS 578T	106.1
	BT-549	105.6
	T-47D	83.0
	MDA-MB-468	101.2

NCI single dose percentage growth results for the resveratrol analogues with substitutions at the C2 position on the stilbene.

Table 8.5. Percentage growth inhibition of NCI 60 human cancer cells by compounds **RES-14, RES-17, RES-18, RES-27, RES-16 and RES-54** at 10μM concentration**.**

Cancer	Cell line	RES-14	RES-17	RES-18	RES-27	RES-16	RES-54
Leukemia	CCRF-CEM	82.6	-36.0	74.0	91.8	81.2	NA
	HL-60(TB)	100.5	-12.4	79.8	93.0	104.4	94.2
	MOLT-4	84.6	-66.5	77.5	82.5	87.8	95.8
	RPMI-8226	83.3	40.1	75.4	87.4	77.5	NA

Table 8.5 (continued)

	SR	88.6	27.9	70.8	71.7	74.3	NA
Non-Small Cell Lung Cancer	A549/ATCC	99.0	63.9	94.2	104.7	104.0	100.2
	EKVX	101.8	59.0	79.9	75.5	92.1	105.1
	HOP-62	97.5	85.9	103.1	113.4	121.5	104.4
	NCI-H226	109.6	76.5	93.5	98.5	103.0	104.6
	NCI-H23	93.9	55.1	87.4	93.9	91.0	103.9
	NCI-H322M	NA	41.5	108.7	116.1	109.4	108.4
	NCI-H460	105.3	76.1	88.6	99.3	110.8	112.5
	NCI-H522	86.5	25.3	64.3	74.0	78.2	98.5
Colon Cancer	HCC-2998	100.9	-100.0	98.1	108.0	111.6	103.6
	HCT-116	102.6	12.7	75.6	91.8	107.8	103.0
	HCT-15	96.4	8.4	93.5	97.9	91.7	100.6
	HT29	104.4	27.9	86.5	106.1	107.2	107.3
	KM12	109.3	25.7	94.5	104.3	106.7	101.5
	SW-620	97.1	-23.5	86.8	93.7	108.0	107.7
CNS Cancer	SF-268	99.0	-29.5	89.5	96.5	103.9	109.2
	SF-295	100.0	53.7	84.8	88.4	87.1	103.4
	SF-539	101.4	95.2	96.5	101.2	102.9	113.3
	SNB-19	89.8	71.6	81.7	103.2	96.0	107.9
	SNB-75	79.0	83.5	72.7	78.6	96.5	91.3
	U251	100.4	86.0	79.4	99.2	104.1	111.1
Melanoma	MALME-3M	NA	126.2	134.1	120.3	123.7	100.6
	M14	108.5	82.6	99.6	107.1	106.1	123.7
	MDA-MB-435	93.9	84.9	67.6	75.3	99.3	107.9
	SK-MEL-2	121.2	74.1	102.4	105.9	100.3	99.7
	SK-MEL-28	103.0	91.3	96.6	103.0	107.6	112.5
	SK-MEL-5	114.5	85.2	86.2	103.0	94.0	109.2
	UACC-257	104.1	86.9	113.3	114.8	141.5	106.3
	UACC-62	88.3	48.1	86.0	88.4	87.2	104.8
Ovarian Cancer	IGROV1	NA	84.4	105.7	110.6	123.3	102.7
	OVCAR-3	106.2	93.6	95.1	110.2	113.2	115.1
	OVCAR-4	136.7	93.8	90.4	86.1	110.5	105.0
	OVCAR-5	107.2	91.9	99.2	95.0	115.2	103.3
	OVCAR-8	102.7	74.2	95.8	99.9	122.9	111.8
	NCI/ADR-RES	99.6	67.0	96.2	98.9	98.9	105.5
	SK-OV-3	108.0	19.2	106.4	125.6	118.9	109.0
Renal Cancer	786-0	99.8	89.6	94.6	103.0	93.1	100.7
	A498	90.8	94.0	68.7	87.8	90.1	103.0
	ACHN	108.3	52.1	97.4	100.1	107.6	106.5
	CAKI-1	NA	81.2	115.2	120.5	125.3	106.3
	RXF 393	109.3	90.0	104.2	99.4	106.1	99.9

Table 8.5 (continued)

	SN12C	93.3	15.3	86.8	104.4	99.4	102.4
	TK-10	128.9	70.6	93.1	131.7	92.3	112.2
	UO-31	NA	76.8	79.9	97.4	93.5	95.8
Prostate Cancer	PC-3	97.3	45.4	76.0	93.8	119.7	100.2
	DU-145	115.7	53.7	113.1	116.1	115.6	109.0
Breast Cancer	MCF7	74.8	15.4	72.3	78.2	91.8	100.7
	MDA-MB-231/ATCC	97.6	67.5	86.0	100.8	88.6	112.9
	HS 578T	106.4	78.4	89.8	93.1	106.9	108.3
	BT-549	89.4	96.0	89.4	86.4	96.1	112.3
	T-47D	83.7	35.0	85.8	91.8	95.6	102.8
	MDA-MB-468	107.2	55.6	91.0	111.9	115.2	110.8

Table 8.6. Percentage growth inhibition of NCI 60 human cancer cells by compounds **RES-57, RES-11, RES-75, RES-59, RES-80 and RES-62** at 10μM concentration**.**

Cancer	**Cell line**	**RES-57**	**RES-11**	**RES-75**	**RES-59**	**RES-80**	**RES-62**
Leukemia	CCRF-CEM	NA	NA	NA	NA	NA	NA
	HL-60(TB)	85.8	NA	NA	NA	95.2	NA
	MOLT-4	101.9	NA	NA	NA	100.4	NA
	RPMI-8226	NA	NA	NA	NA	NA	NA
	SR	NA	NA	NA	NA	NA	NA
Non-Small Cell Lung Cancer	A549/ATCC	110.4	33.9	87.5	51.9	100.6	89.4
	EKVX	111.5	64.5	95.0	82.9	103.5	76.3
	HOP-62	118.3	31.5	95.7	51.9	104.1	88.5
	NCI-H226	108.8	50.1	104.6	83.4	107.9	91.7
	NCI-H23	106.6	41.2	91.0	52.3	104.9	83.7
	NCI-H322M	102.4	69.5	98.0	88.4	105.7	97.0
	NCI-H460	108.8	17.5	97.1	21.4	110.0	101.6
	NCI-H522	96.6	-18.5	78.0	-11.8	107.6	67.0
Colon Cancer	HCC-2998	105.4	53.1	98.8	65.4	105.3	89.3
	HCT-116	103.4	31.1	93.0	19.7	106.2	81.1
	HCT-15	106.5	38.4	86.9	45.6	100.4	86.1
	HT29	108.9	6.0	101.2	9.9	112.9	89.7
	KM12	105.7	26.0	86.6	19.7	105.4	65.7
	SW-620	103.7	28.8	91.4	26.0	105.8	84.7
CNS Cancer	SF-268	109.7	53.7	82.6	44.6	112.6	89.6
	SF-295	102.9	6.6	89.9	23.6	98.8	68.0
	SF-539	113.1	4.5	88.6	36.4	110.7	85.8
	SNB-19	103.9	48.2	89.0	54.4	108.5	87.2

Table 8.6 (continued)

	SNB-75	103.7	-13.5	77.5	6.4	101.3	73.7
	U251	105.1	21.2	86.0	29.2	104.0	88.0
Melanoma	MALME-3M	98.1	39.0	89.1	39.7	99.6	81.5
	M14	99.0	NA	NA	NA	NA	NA
	MDA-MB-435	115.5	26.1	84.6	27.1	110.2	69.3
	SK-MEL-2	99.5	-27.7	79.3	-6.3	99.0	13.1
	SK-MEL-28	107.7	39.2	102.6	25.7	112.2	108.7
	SK-MEL-5	110.4	67.1	102.1	58.0	117.6	83.5
	UACC-257	109.3	14.2	74.3	25.6	106.5	60.5
	UACC-62	95.2	51.1	75.8	71.8	105.8	83.9
Ovarian Cancer	IGROV1	99.1	39.2	62.8	40.1	99.9	61.3
	OVCAR-3	109.3	55.4	107.3	62.7	111.1	73.0
	OVCAR-4	113.6	-23.0	90.4	-12.4	116.2	93.5
	OVCAR-5	111.1	54.2	90.8	76.7	114.8	97.6
	OVCAR-8	111.4	60.6	102.9	84.6	114.7	96.8
	NCI/ADR-RES	101.3	34.0	86.2	60.6	106.4	94.4
	SK-OV-3	112.4	24.2	86.3	7.6	107.9	76.2
Renal Cancer	786-0	104.1	17.2	92.9	51.8	100.4	88.7
	A498	104.0	44.0	82.7	42.0	107.5	101.6
	ACHN	103.3	19.1	66.9	43.7	98.1	61.8
	CAKI-1	101.6	58.4	73.1	60.4	105.4	90.2
	RXF 393	97.6	33.5	92.2	57.7	94.1	61.7
	SN12C	101.4	47.6	83.1	62.2	108.2	85.8
	TK-10	112.1	50.6	103.5	71.9	115.0	110.8
	UO-31	90.3	50.7	72.8	62.3	97.8	74.8
Prostate Cancer	PC-3	102.9	29.5	93.7	54.1	99.2	78.1
	DU-145	110.9	24.8	86.2	66.7	114.0	102.0
Breast Cancer	MCF7	100.6	34.9	130.0	34.6	97.7	67.1
	MDA-MB-231/ATCC	104.4	33.4	77.1	43.4	106.8	65.2
	HS 578T	112.6	45.6	86.9	51.9	106.2	74.4
	BT-549	104.2	33.5	77.4	52.2	104.6	95.2
	T-47D	103.8	36.2	82.5	58.4	103.2	73.9
	MDA-MB-468	108.3	-3.6	80.1	6.2	100.2	71.4

Table 8.7. Percentage growth inhibition of NCI 60 human cancer cells by compounds **ST-132(a), ST-127, ST-128 and ST-138** at 10μM concentration**.**

Cancer	**cell type**	**ST-132(a)**	**ST-127**	**ST-128**	**ST-138**
Leukemia	CCRF-CEM	40.1	NA	NA	NA

Table 8.7 (continued)

	HL-60(TB)	86.0	24.2	100.6	90.1
	K-562	86.9	15.8	86.8	95.0
	MOLT-4	62.7	44.7	86.0	92.2
	RPMI-8226	89.8	54.2	72.6	74.5
	SR	74.7	15.7	84.1	86.1
Non-Small Cell Lung Cancer	A549/ATCC	98.1	NA	NA	NA
	HOP-62	93.6	59.7	97.7	101.8
	HOP-92	61.1	48.7	76.9	73.3
	NCI-H226	87.1	87.2	78.8	97.8
	NCI-H23	84.9	82.1	79.9	92.2
	NCI-H322M	110.7	92.2	97.6	99.7
	NCI-H460	96.1	75.1	101.4	101.6
	NCI-H522	68.3	NA	NA	NA
Colon Cancer	COLO 205	118.2	72.9	89.0	101.8
	HCC-2998	95.1	76.2	107.3	107.4
	HCT-116	90.0	36.3	76.1	92.8
	HCT-15	90.3	31.7	87.3	86.7
	HT29	94.3	15.0	87.0	102.6
	KM12	88.1	34.0	86.2	88.2
	SW-620	96.5	42.3	100.3	109.8
CNS Cancer	SF-268	101.9	66.6	94.4	90.5
	SF-295	94.1	57.1	103.8	94.0
	SF-539	88.1	55.3	98.2	92.6
	SNB-19	89.3	80.1	99.6	91.5
	SNB-75	92.2	49.9	78.7	70.0
	U251	94.1	47.5	96.1	91.0
Melanoma	LOX IMVI	98.1	52.7	86.8	87.0
	MALME-3M	85.2	45.6	90.9	80.1
	M14	84.4	42.4	81.5	81.8
	MDA-MB-435	59.2	-18.1	100.6	89.4
	SK-MEL-2	86.0	30.1	83.6	73.5
	SK-MEL-28	92.6	60.4	101.2	97.4
	SK-MEL-5	97.6	50.3	95.3	90.8
	UACC-257	96.4	NA	NA	NA
	UACC-62	61.7	66.7	84.5	84.5
Ovarian Cancer	IGROV1	95.4	51.7	79.6	104.3
	OVCAR-3	108.6	50.7	95.6	98.9
	OVCAR-4	95.4	88.1	95.0	88.4
	OVCAR-5	84.5	82.0	98.4	111.0

Table 8.7 (continued)

	OVCAR-8	102.0	74.5	97.8	85.9
	NCI/ADR-RES	89.0	24.3	83.5	86.2
	SK-OV-3	92.0	65.0	85.7	97.4
Renal Cancer	786-0	98.5	68.4	93.5	92.4
	A498	76.3	51.5	112.5	83.1
	ACHN	89.8	59.8	92.3	68.8
	CAKI-1	91.8	52.3	71.2	91.3
	RXF 393	95.7	58.8	101.8	81.6
	SN12C	90.7	80.4	97.2	96.2
	TK-10	116.7	68.6	135.2	104.4
	UO-31	84.6	68.5	76.0	77.3
Prostate Cancer	PC-3	86.6	57.8	84.5	90.2
	DU-145	102.4	80.6	104.5	95.9
Breast Cancer	MCF7	94.8	25.0	72.8	103.2
	MDA-MB-231	82.0	64.0	100.6	93.6
	HS 578T	88.8	74.7	98.8	105.3
	BT-549	100.1	37.7	83.4	73.6
	T-47D	86.5	43.7	56.4	83.7
	MDA-MB-468	NA	61.3	107.0	85.4

Table 8.8. Percentage growth inhibition of NCI 60 human cancer cells by compounds **ST-139, ST-98, ST-100 and ST-89** at 10µM concentration**.**

Cancer	cell type	**ST-139**	**ST-98**	**ST-100**	**ST-89**
Leukemia	CCRF-CEM	NA	85.5	3.0	68.9
	HL-60(TB)	99.9	99.8	5.7	58.1
	K-562	87.5	77.0	13.4	45.5
	MOLT-4	73.2	64.5	1.9	54.5
	RPMI-8226	72.5	81.9	7.7	53.9
	SR	79.7	62.5	2.7	59.2
Non-Small Cell Lung Cancer	A549/ATCC	NA	103.9	20.1	78.9
	HOP-62	103.1	117.3	26.9	85.1
	HOP-92	73.0	73.4	58.3	64.7
	NCI-H226	92.3	83.4	65.7	80.3
	NCI-H23	84.3	91.2	31.1	79.5

Table 8.8 (continued)

	NCI-H322M	98.4	92.4	42.1	93.5
	NCI-H460	94.2	98.5	11.5	86.4
	NCI-H522	NA	75.5	-28.8	55.9
Colon Cancer	COLO 205	87.0	121.8	-24.6	101.3
	HCC-2998	96.3	99.0	40.6	72.0
	HCT-116	79.1	90.5	14.3	61.3
	HCT-15	82.1	91.4	24.6	74.1
	HT29	78.3	94.8	5.1	63.3
	KM12	88.9	93.9	25.3	82.4
	SW-620	95.7	96.9	26.9	87.6
CNS Cancer	SF-268	92.2	90.2	41.9	94.7
	SF-295	101.6	88.9	36.8	83.1
	SF-539	96.8	NA	NA	NA
	SNB-19	101.8	99.1	49.5	79.6
	SNB-75	74.0	87.6	-1.9	77.5
	U251	84.3	94.3	17.1	67.7
Melanoma	LOX IMVI	88.9	67.2	42.6	59.5
	MALME-3M	88.2	101.4	24.9	63.7
	M14	90.6	103.6	16.8	84.9
	MDA-MB-435	93.2	94.1	-19.6	81.0
	SK-MEL-2	83.6	98.9	25.3	86.0
	SK-MEL-28	91.1	107.6	42.4	95.3
	SK-MEL-5	102.6	92.5	6.9	75.7
	UACC-257	NA	105.6	41.7	85.1
	UACC-62	88.3	75.0	31.8	81.3
Ovarian Cancer	IGROV1	84.5	100.3	53.4	66.7
	OVCAR-3	99.1	97.9	-21.6	76.3
	OVCAR-4	93.7	102.4	58.0	95.5
	OVCAR-5	95.3	104.5	61.8	90.4
	OVCAR-8	92.4	103.8	21.6	75.8
	NCI/ADR-RES	89.1	90.1	11.7	66.9
	SK-OV-3	93.1	101.8	6.3	88.8
Renal Cancer	786-0	96.6	90.2	48.3	86.4
	A498	92.3	88.6	5.6	66.9
	ACHN	90.0	87.2	54.6	74.1
	CAKI-1	91.2	80.6	43.9	79.7
	RXF 393	107.6	84.2	-29.6	85.6
	SN12C	99.1	95.7	47.3	81.0
	TK-10	112.6	86.4	57.2	94.5
	UO-31	80.3	71.2	35.7	49.3

Table 8.8 (continued)

Prostate Cancer	PC-3	84.5	81.0	35.7	66.3
	DU-145	97.2	99.0	14.7	100.2
Breast Cancer	MCF7	74.0	84.6	14.7	69.6
	MDA-MB-231	95.0	89.7	36.5	73.4
	HS 578T	99.4	92.8	19.4	86.7
	BT-549	85.6	96.2	57.2	67.1
	T-47D	65.1	79.7	37.4	64.1
	MDA-MB-468	106.8	80.7	16.0	64.3

NCI single dose percentage growth results for (*E/Z*)-2,3-diaryl substituted acrylonitriles

Table 8.9. Percentage growth inhibition of NCI 60 human cancer cells by compounds **ST-101, ST-113, ST-148, ST-147, ST-145, ST-145(a) and ST-161** at 10μM concentration**.**

Cancer	cell type	ST-101	ST-113	ST-148	ST-147	ST-145	ST-145(a)	ST-161
Leukemia	CCRF-CEM	107.4	3.3	7.9	25.2	6.4	10.8	73.2
	HL-60(TB)	104.5	-33.3	-44.8	-4.3	-25.1	105.5	57.9
	K-562	89.4	9.9	3.9	8.1	11.9	99.3	24.9
	MOLT-4	105.1	-1.0	-12.4	64.5	2.0	94.9	67.7
	RPMI-8226	107.7	-7.6	6.2	60.4	5.2	8.5	75.2
	SR	93.7	1.4	7.5	11.1	1.3	NA	26.2
Non-Small Cell Lung Cancer	A549/ATCC	93.7	10.1	28.0	37.9	15.3	25.9	59.5
	HOP-62	113.2	21.8	27.0	42.1	30.2	19.5	76.7
	HOP-92	103.0	-1.1	17.0	57.0	NA	17.2	94.2
	NCI-H226	99.7	21.5	33.8	73.8	48.4	33.0	94.9
	NCI-H23	113.5	12.1	22.6	84.1	24.9	21.8	83.2
	NCI-H322M	98.8	10.6	37.6	80.0	21.6	48.4	106.1
	NCI-H460	101.9	4.0	4.9	79.5	6.4	2.7	83.6
	NCI-H522	87.6	-45.4	-21.9	17.3	-22.1	-6.3	76.4
Colon Cancer	COLO 205	112.1	-57.3	-67.3	27.3	52.7	33.1	59.8
	HCC-2998	102.5	14.2	6.2	66.9	5.1	20.3	72.3
	HCT-116	104.3	4.6	3.6	24.1	5.5	5.3	57.5
	HCT-15	98.0	14.1	7.0	33.0	15.9	15.1	43.9
	HT29	107.9	-12.6	0.7	11.9	24.2	38.8	39.6
	KM12	105.6	8.1	4.2	NA	2.1	-1.7	42.2
	SW-620	105.9	22.7	26.2	33.4	27.8	26.1	42.9

Table 8.9 (continued)

CNS Cancer	SF-268	103.3	32.8	19.7	63.9	31.9	15.2	81.2
	SF-295	95.3	-12.5	14.2	NA	-0.2	4.5	76.5
	SF-539	110.9	-5.6	-32.7	28.9	-17.7	-2.0	79.4
	SNB-19	101.3	47.9	56.3	75.8	116.9	70.7	95.9
	SNB-75	102.3	13.0	45.5	41.2	27.2	54.9	94.3
	U251	105.5	5.4	11.5	56.4	-26.9	10.5	77.2
Melanoma	LOX IMVI	97.5	7.4	22.6	34.4	31.3	24.9	65.1
	MALME-3M	96.1	23.3	85.6	66.5	67.0	123.7	69.0
	M14	110.0	21.3	19.9	29.1	18.1	18.6	50.8
	MDA-MB-435	105.8	-44.1	-13.0	-35.9	-43.3	-8.4	-5.7
	SK-MEL-2	110.4	-2.3	20.8	31.4	NA	26.2	63.5
	SK-MEL-28	113.9	52.2	74.3	66.4	56.9	74.4	88.5
	SK-MEL-5	101.3	-5.9	-49.8	28.1	0.6	-54.1	75.9
	UACC-257	105.4	58.8	80.9	70.7	62.1	72.8	80.2
	UACC-62	99.0	27.7	36.6	47.8	44.9	44.2	69.4
Ovarian Cancer	IGROV1	111.0	-45.2	34.5	59.9	12.5	37.5	66.1
	OVCAR-3	111.1	-12.9	-21.7	29.3	0.8	-8.5	71.7
	OVCAR-4	119.4	40.4	61.2	84.2	47.5	68.4	89.7
	OVCAR-5	104.4	37.8	34.3	91.2	51.9	55.9	97.9
	OVCAR-8	103.8	-3.4	24.7	68.2	8.6	21.2	83.8
	NCI/ADR-RES	107.3	9.8	12.8	29.5	11.1	11.9	41.0
	SK-OV-3	104.6	11.8	22.6	46.9	19.4	16.3	85.5
Renal Cancer	786-0	100.0	14.9	24.6	46.0	24.2	21.9	90.0
	A498	88.3	-17.0	-7.1	57.5	-6.5	-3.5	73.7
	ACHN	129.3	28.4	21.5	53.9	23.7	24.9	96.2
	CAKI-1	92.4	7.1	28.6	NA	17.0	33.0	66.8
	RXF 393	92.8	13.3	41.2	69.3	62.7	43.7	94.7
	SN12C	96.7	21.4	22.0	56.9	27.2	31.6	90.7
	TK-10	NA	NA	53.8	65.0	47.4	73.4	91.0
	UO-31	100.3	19.0	32.1	41.1	21.1	32.8	86.7
Prostate Cancer	PC-3	108.8	5.6	25.5	58.0	16.3	33.5	70.2
	DU-145	103.6	-14.0	-9.3	94.7	-8.4	3.4	92.5
Breast Cancer	MCF7	95.4	10.8	14.7	25.5	8.8	10.7	23.9
	MDA-MB-231	111.4	2.0	7.3	80.3	6.5	27.0	66.8
	HS 578T	94.0	26.7	32.2	69.3	41.0	34.4	89.7
	BT-549	96.2	52.4	24.9	45.2	21.3	39.8	49.6
	T-47D	99.5	7.5	73.7	32.1	58.2	53.8	67.7
	MDA-MB-468	NA	NA	8.9	37.2	29.6	6.1	54.9

Table 8.10. Percentage growth inhibition of NCI 60 human cancer cells by compounds **ST-162, ST-163, ST-164, ST-165, ST-168, ST-169 and ST-170** at 10μM concentration**.**

Cancer	cell type	ST-162	ST-163	ST-164	ST-165	ST-168	ST-169	ST-170
Leukemia	CCRF-CEM	96.5	21.6	83.4	89.4	75.4	86.7	91.9
	HL-60(TB)	88.6	0.1	64.5	72.0	62.9	75.0	83.1
	K-562	80.4	15.8	98.7	94.8	96.2	77.5	94.8
	MOLT-4	87.2	19.5	67.2	85.2	66.6	61.2	72.2
	RPMI-8226	88.5	18.9	89.4	96.9	76.6	84.4	80.1
	SR	83.5	11.8	82.0	83.0	79.0	77.0	77.7
Non-Small Cell Lung Cancer	A549/ATCC	93.6	32.3	84.6	96.6	79.9	79.9	70.0
	HOP-62	92.2	43.8	92.3	97.6	103.6	90.6	88.0
	HOP-92	NA	40.4	NA	110.2	112.6	NA	NA
	NCI-H226	100.9	71.8	99.8	114.5	114.9	111.0	98.9
	NCI-H23	94.5	43.2	96.6	97.1	91.5	93.7	88.0
	NCI-H322M	103.8	35.7	89.5	96.8	91.4	102.2	74.1
	NCI-H460	107.1	15.5	101.8	105.7	99.4	101.5	84.7
	NCI-H522	85.8	-2.4	87.9	94.5	76.3	65.4	82.7
Colon Cancer	COLO 205	103.6	11.9	97.7	106.0	105.6	99.6	93.2
	HCC-2998	91.3	49.4	102.3	106.1	90.7	89.9	92.1
	HCT-116	99.4	17.4	96.3	104.6	82.1	89.7	70.1
	HCT-15	85.7	17.8	102.4	99.8	92.6	92.6	88.7
	HT29	88.8	6.0	92.4	106.1	91.1	93.7	101.6
	KM12	93.8	30.0	94.6	96.2	92.4	95.2	91.7
	SW-620	98.9	19.6	102.1	107.2	100.9	99.9	89.8
CNS Cancer	SF-268	94.4	38.5	95.5	99.5	93.5	101.5	80.9
	SF-295	96.1	11.2	99.2	105.0	96.4	95.6	77.0
	SF-539	92.4	-13.8	103.8	102.6	94.4	97.9	86.9
	SNB-19	93.8	46.0	100.7	105.1	108.8	106.3	105.3
	SNB-75	114.5	2.2	68.9	87.5	77.3	51.5	20.3
	U251	96.6	16.5	93.7	102.3	99.9	89.0	86.3
Melanoma	LOX IMVI	108.9	33.3	103.2	100.9	97.1	98.9	62.7
	MALME-3M	98.9	24.3	95.7	103.0	84.0	56.1	NA
	M14	95.0	10.5	99.5	106.1	92.8	89.7	96.5
	MDA-MB-435	74.7	-29.1	100.2	96.1	98.7	63.5	93.7
	SK-MEL-2	90.2	-17.7	94.4	102.1	88.7	90.6	89.7
	SK-MEL-28	97.6	40.7	105.9	115.8	98.9	104.2	105.1
	SK-MEL-5	92.2	16.4	97.3	102.6	95.4	93.5	98.4
	UACC-257	97.5	23.0	97.0	118.3	100.0	99.8	86.3

Table 8.10 (continued)

	UACC-62	87.6	37.5	86.4	113.5	85.4	86.4	108.3
Ovarian Cancer	IGROV1	95.3	46.3	87.1	96.9	85.1	85.6	67.2
	OVCAR-3	108.3	4.9	102.6	108.7	102.6	97.7	97.7
	OVCAR-4	89.2	67.3	82.9	109.6	81.3	79.9	26.1
	OVCAR-5	99.7	49.6	111.4	104.2	100.1	103.2	99.3
	OVCAR-8	96.3	26.7	92.3	103.8	107.7	92.6	70.9
	NCI/ADR-RES	93.9	11.6	99.7	101.7	94.9	103.1	79.3
	SK-OV-3	102.7	28.8	101.3	104.8	94.4	97.9	70.6
Renal Cancer	786-0	96.5	50.3	94.5	103.2	98.2	95.6	72.4
	A498	81.8	-6.2	88.9	96.5	90.4	82.7	94.3
	ACHN	96.0	45.7	107.7	110.8	96.1	103.4	49.1
	CAKI-1	86.6	24.8	96.5	101.6	88.1	83.2	87.4
	RXF 393	100.0	23.3	106.2	111.0	95.5	96.1	94.4
	SN12C	95.4	37.2	95.3	103.2	94.7	95.9	93.5
	TK-10	98.1	32.2	95.6	96.5	96.1	81.0	90.2
	UO-31	67.1	28.0	78.6	88.0	76.5	80.1	73.7
Prostate Cancer	PC-3	88.7	21.2	97.3	100.4	89.2	94.3	91.5
	DU-145	107.2	28.3	94.4	104.2	94.2	99.3	94.1
Breast Cancer	MCF7	NA	20.7	85.5	87.2	82.3	93.7	79.9
	MDA-MB-231	88.2	49.6	92.5	106.5	89.9	95.8	80.5
	HS 578T	100.2	27.2	115.1	114.1	112.0	101.0	81.3
	BT-549	82.1	30.3	86.4	91.8	91.4	100.4	94.1
	T-47D	70.7	35.8	75.6	88.7	82.0	83.8	74.7
	MDA-MB-468	99.6	1.2	98.7	104.0	103.3	84.9	101.0

Table 8.11. Percentage growth inhibition of NCI 60 human cancer cells by compounds **ST-171, ST-173, ST-174, ST-175, ST-176, ST-177 and ST-178** at 10μM concentration**.**

Cancer	**cell type**	**ST-171**	**ST-173**	**ST-174**	**ST-175**	**ST-176**	**ST-177**	**ST-178**
Leukemia	CCRF-CEM	97.7	27.0	93.3	104.5	93.7	NA	52.3
	HL-60(TB)	108.4	7.1	87.3	83.5	83.8	NA	NA
	K-562	105.7	15.9	76.2	105.2	112.9	39.2	21.7
	MOLT-4	83.1	22.7	79.2	79.7	NA	NA	NA
	RPMI-8226	94.7	58.1	84.6	103.5	89.3	NA	77.0
	SR	84.6	15.5	68.7	86.5	92.8	51.1	23.8
Non-Small Cell Lung Cancer	A549/ATCC	100.5	36.4	92.3	92.1	102.6	84.7	55.9
	HOP-62	91.9	54.0	88.0	94.5	102.9	87.2	75.9
	HOP-92	124.6	NA	99.9	NA	NA	NA	NA

Table 8.11 (continued)

	NCI-H226	102.1	73.8	113.1	101.0	98.9	85.0	83.0
	NCI-H23	102.8	59.1	96.3	106.0	97.2	85.0	77.7
	NCI-H322M	121.0	67.6	86.4	90.6	97.0	97.8	90.5
	NCI-H460	102.7	36.0	103.4	104.3	101.6	92.6	77.8
	NCI-H522	132.5	43.3	75.8	95.4	71.7	66.0	47.6
Colon Cancer	COLO 205	105.3	25.4	99.0	101.1	112.0	85.0	56.0
	HCC-2998	94.6	60.5	94.8	106.1	107.0	76.9	68.8
	HCT-116	97.1	19.3	99.5	102.2	94.0	71.4	32.7
	HCT-15	99.4	24.4	82.9	106.6	98.8	63.9	40.6
	HT29	108.6	10.0	89.7	102.2	106.1	70.3	23.5
	KM12	97.6	28.1	76.0	94.6	108.8	69.2	39.2
	SW-620	104.8	31.9	105.8	108.7	94.8	62.3	35.2
CNS Cancer	SF-268	101.1	53.1	94.4	101.5	108.9	98.2	71.0
	SF-295	98.5	27.1	97.5	100.9	109.6	91.1	68.2
	SF-539	97.8	19.0	93.8	105.4	99.8	91.8	67.9
	SNB-19	109.7	55.6	99.8	101.1	101.3	89.6	82.1
	SNB-75	111.8	12.8	76.2	67.7	102.3	73.5	61.6
	U251	107.8	29.2	91.1	93.7	95.8	95.5	47.3
Melanoma	LOX IMVI	104.6	41.0	102.9	111.6	103.1	77.3	65.2
	MALME-3M	116.4	49.3	76.4	113.5	106.8	79.1	73.3
	M14	99.0	16.4	88.7	105.3	94.9	72.4	37.9
	MDA-MB-435	98.2	-28.6	50.7	107.4	97.1	15.3	-28.5
	SK-MEL-2	119.3	2.7	98.9	106.2	98.9	80.1	59.8
	SK-MEL-28	115.1	50.2	98.3	113.0	113.1	91.0	64.6
	SK-MEL-5	104.7	31.7	98.9	102.4	92.2	85.0	66.2
	UACC-257	104.5	44.7	93.8	110.5	111.9	106.5	103.0
	UACC-62	105.7	39.7	81.9	106.5	85.7	56.6	44.7
Ovarian Cancer	IGROV1	121.0	45.1	97.9	96.4	113.4	77.1	68.8
	OVCAR-3	109.4	15.3	98.4	103.4	115.4	100.5	46.8
	OVCAR-4	106.6	73.7	88.7	91.0	100.0	98.6	68.9
	OVCAR-5	102.9	81.6	105.9	115.2	105.9	92.8	98.2
	OVCAR-8	96.7	63.1	104.0	90.8	56.2	100.1	99.0
	NCI/ADR-RES	105.6	20.3	100.5	113.4	100.6	60.5	36.5
	SK-OV-3	102.3	33.2	97.3	102.2	103.2	89.2	61.9
Renal Cancer	786-0	94.6	52.1	91.4	96.7	94.0	84.8	77.1
	A498	111.3	26.5	100.9	103.3	90.7	72.5	35.7
	ACHN	109.3	59.1	101.5	112.1	108.7	92.3	79.3
	CAKI-1	94.2	40.0	86.9	97.3	102.6	79.3	61.2
	RXF 393	98.5	40.3	100.6	101.2	98.3	78.3	64.3

Table 8.11 (continued)

	SN12C	106.5	53.3	101.8	103.5	91.7	83.5	75.9
	TK-10	118.9	49.7	90.7	104.1	105.6	87.6	78.2
	UO-31	104.1	46.7	75.1	84.6	87.6	74.9	80.3
Prostate Cancer	PC-3	101.2	47.0	93.4	110.2	100.9	NA	80.1
	DU-145	109.0	63.9	99.3	98.5	114.6	103.9	77.7
Breast Cancer	MCF7	88.4	NA	109.5	87.1	112.1	71.6	26.1
	MDA-MB-231	102.2	48.9	119.0	102.8	99.8	82.3	48.3
	HS 578T	121.7	43.8	135.0	118.8	128.9	81.9	65.5
	BT-549	94.5	35.3	86.4	96.5	88.5	64.1	51.8
	T-47D	102.0	43.5	76.3	90.7	93.4	65.1	67.9
	MDA-MB-468	102.5	8.3	82.1	105.1	93.7	48.8	25.9

Table 8.12. Percentage growth inhibition of NCI 60 human cancer cells by compounds **ST-179, ST-180, ST-181, ST-183, ST-152, ST-153 and ST-112** at 10μM concentration**.**

Cancer	**cell type**	**ST-179**	**ST-180**	**ST-181**	**ST-183**	**ST-152**	**ST-153**	**ST-112**
Leukemia	CCRF-CEM	21.6	16.8	87.7	89.7	90.1	72.1	79.8
	HL-60(TB)	7.8	0.5	70.8	87.1	93.7	66.6	82.0
	K-562	19.1	18.8	64.2	70.3	89.9	37.9	41.3
	MOLT-4	26.8	17.4	71.5	78.5	73.0	70.4	70.2
	RPMI-8226	5.3	9.3	73.2	84.9	81.0	64.7	81.8
	SR	18.4	13.5	50.1	60.5	81.2	39.3	28.3
Non-Small Cell Lung Cancer	A549/ATCC	31.7	17.2	77.4	56.8	88.9	71.2	87.4
	HOP-62	44.4	58.5	88.1	69.7	97.4	86.6	105.2
	HOP-92	NA	60.8	64.9	90.2	54.1	93.0	83.5
	NCI-H226	38.5	28.7	93.3	70.8	72.5	86.6	91.8
	NCI-H23	49.9	31.1	93.7	58.8	77.3	96.1	89.2
	NCI-H322M	34.3	40.9	98.3	66.6	94.3	94.7	99.6
	NCI-H460	13.2	9.7	95.2	24.7	96.8	64.3	98.3
	NCI-H522	1.4	-20.5	79.8	58.8	58.7	90.5	56.7
Colon Cancer	COLO 205	7.6	-33.9	97.6	103.5	103.9	76.2	114.2
	HCC-2998	45.7	6.4	93.2	95.1	101.8	80.0	79.1
	HCT-116	21.1	11.6	82.6	20.5	70.3	64.9	86.1
	HCT-15	21.4	20.4	78.0	79.7	74.9	59.0	76.2
	HT29	10.0	5.0	63.8	71.9	84.8	64.5	85.6
	KM12	21.0	6.0	63.9	86.8	89.0	63.6	63.0
	SW-620	10.6	21.0	86.1	89.9	73.1	84.9	83.5
CNS	SF-268	34.0	23.8	91.0	62.5	98.4	92.0	96.9

Table 8.12 (continued)

Cancer	SF-295	5.6	2.9	89.3	64.0	95.6	80.8	94.7
	SF-539	-42.9	-10.1	83.1	69.6	90.8	83.7	NA
	SNB-19	36.1	46.4	96.4	34.7	96.4	49.4	93.0
	SNB-75	-3.1	0.5	57.0	5.4	32.2	80.8	85.0
	U251	18.7	18.4	84.5	26.7	69.6	80.9	88.5
Melanoma	LOX IMVI	35.2	19.9	95.6	59.5	99.8	101.9	77.0
	MALME-3M	37.9	55.1	90.6	68.3	90.6	79.9	85.1
	M14	16.2	20.6	91.1	90.3	88.4	10.4	88.7
	MDA-MB-435	-26.3	-37.2	37.2	48.3	97.8	77.9	22.7
	SK-MEL-2	13.1	29.2	93.2	87.1	83.2	90.1	84.1
	SK-MEL-28	43.6	60.6	95.1	88.6	104.6	81.4	84.0
	SK-MEL-5	19.1	16.6	84.1	95.3	88.7	91.4	88.5
	UACC-257	41.0	72.8	89.4	NA	NA	NA	103.5
	UACC-62	25.1	24.0	79.9	86.8	64.2	69.2	76.0
Ovarian Cancer	IGROV1	36.3	34.3	90.6	55.1	70.5	84.6	84.0
	OVCAR-3	-21.2	-29.5	100.0	63.0	82.3	88.7	101.7
	OVCAR-4	49.7	60.2	81.6	45.0	65.6	76.4	106.1
	OVCAR-5	55.7	50.4	95.0	81.1	98.7	93.9	112.6
	OVCAR-8	29.0	14.0	90.1	60.8	92.8	94.7	86.2
	NCI/ADR-RES	10.5	-1.9	86.0	64.3	89.0	75.3	72.1
	SK-OV-3	26.9	20.7	83.1	25.8	91.1	88.6	91.3
Renal Cancer	786-0	40.2	44.7	106.6	51.9	99.9	95.4	98.2
	A498	-8.4	-7.5	70.8	54.1	83.7	63.3	91.0
	ACHN	44.7	38.8	93.4	41.4	86.5	95.3	86.5
	CAKI-1	30.8	41.2	75.3	76.0	71.8	78.2	88.8
	RXF 393	-17.7	-2.6	86.5	80.0	84.1	91.4	92.7
	SN12C	38.6	25.3	92.6	73.0	89.6	84.3	93.7
	TK-10	43.8	42.7	80.4	45.0	122.7	85.7	103.8
	UO-31	42.1	34.9	82.3	72.8	70.1	72.8	79.6
Prostate Cancer	PC-3	36.1	25.8	77.9	77.5	79.2	81.0	82.9
	DU-145	14.9	5.1	97.4	81.3	100.0	95.0	102.9
Breast Cancer	MCF7	12.1	16.3	83.5	84.6	49.6	60.8	71.4
	MDA-MB-231	39.4	24.3	75.6	50.2	69.5	68.7	87.5
	HS 578T	-14.1	-5.4	100.7	34.8	105.2	92.4	97.1
	BT-549	26.6	56.4	81.0	86.1	80.0	74.7	84.0
	T-47D	38.2	70.4	81.0	69.4	45.4	70.0	82.5
	MDA-MB-468	-14.5	14.1	60.8	77.8	64.6	48.6	81.6

Table 8.13. Percentage growth inhibition of NCI 60 human cancer cells by compounds **TMR-03, TMR-01, ST-252, ST-253, ST-257, ST-260 and ST-261** at 10μM concentration**.**

Cancer	cell type	TMR-03	TMR-01	ST-252	ST-253	ST-257	ST-260	ST-261
Leukemia	CCRF-CEM	NA	NA	58.7	0.4	6.4	3.7	1.3
	HL-60(TB)	97.4	33.1	38.0	-46.3	-15.7	-41.3	-47.7
	K-562	93.9	14.3	18.7	7.5	11.6	5.3	3.4
	MOLT-4	98.9	65.1	32.2	-14.3	19.6	-15.8	-12.8
	RPMI-8226	86.2	63.4	80.8	39.2	57.1	67.1	50.3
	SR	80.0	10.9	-1.3	-11.0	1.8	-9.0	-16.5
Non-Small Cell Lung Cancer	A549/ATCC	86.5	38.0	41.5	21.1	40.0	18.1	19.1
	HOP-62	56.3	82.7	68.3	40.8	36.9	38.5	30.6
	HOP-92	NA	NA	89.0	-1.7	39.3	6.5	NA
	NCI-H226	88.2	78.2	81.2	43.9	71.1	47.4	42.9
	NCI-H23	74.9	64.1	78.3	20.7	46.8	22.3	21.1
	NCI-H322M	94.6	95.7	77.5	24.2	34.5	19.5	27.1
	NCI-H460	81.8	49.6	33.4	5.2	12.4	4.5	3.3
	NCI-H522	62.8	55.5	39.3	-27.0	-30.1	-42.2	-44.8
Colon Cancer	COLO 205	112.8	67.9	50.5	-74.4	-1.3	-51.6	-70.0
	HCC-2998	107.1	69.8	55.7	14.9	60.1	14.9	14.6
	HCT-116	83.2	74.1	38.8	-12.3	22.3	-12.6	-31.0
	HCT-15	95.1	47.4	43.4	16.5	31.6	14.3	10.5
	HT29	103.2	48.2	21.8	0.4	6.6	-17.8	-17.8
	KM12	99.5	54.6	27.8	2.0	30.6	0.7	-10.7
	SW-620	95.4	60.2	28.8	25.2	15.5	22.8	21.6
CNS Cancer	SF-268	74.6	82.5	71.9	24.6	53.2	26.8	20.5
	SF-295	91.5	66.3	66.7	-8.0	-14.0	-20.2	-21.2
	SF-539	NA	NA	63.7	2.5	5.6	-2.4	-19.9
	SNB-19	101.3	80.9	83.3	51.2	53.2	55.4	50.2
	SNB-75	72.3	85.0	61.1	17.1	2.2	5.8	15.2
	U251	88.7	71.0	36.3	8.1	19.9	5.6	4.7
Melanoma	LOX IMVI	NA	NA	56.7	24.7	44.9	21.3	25.3
	MALME-3M	91.2	66.1	64.6	64.3	51.8	45.2	64.2
	M14	94.7	12.6	38.5	5.7	19.7	1.2	-15.0
	MDA-MB-435	97.5	53.0	-29.8	-22.2	-17.6	-34.5	-26.3

Table 8.13 (continued)

	SK-MEL-2	88.4	66.3	36.0	24.1	19.4	10.5	2.2
	SK-MEL-28	86.7	43.8	75.3	63.0	61.7	64.1	62.0
	SK-MEL-5	81.4	79.8	45.0	-38.0	16.8	-1.5	-31.8
	UACC-257	91.3	50.8	76.7	76.0	66.7	72.8	76.7
	UACC-62	77.2	68.3	53.7	45.4	43.7	38.2	42.3
Ovarian Cancer	IGROV1	98.3	95.1	71.3	25.5	49.5	26.2	31.4
	OVCAR-3	103.1	64.8	NA	NA	NA	NA	NA
	OVCAR-4	63.2	86.4	94.6	44.9	69.3	40.9	33.2
	OVCAR-5	105.4	82.4	88.0	49.1	73.5	42.5	43.5
	OVCAR-8	69.1	48.1	77.1	10.4	30.1	6.2	2.4
	NCI/ADR-RES	81.0	76.0	34.4	17.0	24.5	2.5	15.2
	SK-OV-3	69.8	82.5	81.0	17.6	20.0	15.9	3.5
Renal Cancer	786-0	95.0	-10.6	80.2	14.8	39.3	17.2	10.7
	A498	87.8	74.9	70.9	-11.0	-4.1	-1.3	-10.1
	ACHN	83.5	62.9	87.7	34.4	51.3	34.8	27.1
	CAKI-1	88.2	60.4	64.2	20.0	17.6	8.5	0.5
	RXF 393	96.3	82.2	77.3	41.8	14.9	19.2	27.1
	SN12C	87.5	83.5	72.1	34.5	56.7	34.1	27.1
	TK-10	124.6	66.7	65.2	48.5	45.7	41.7	50.2
	UO-31	83.8	63.6	73.2	23.9	41.8	26.9	31.4
Prostate Cancer	PC-3	80.9	91.8	70.9	26.5	21.3	16.5	16.3
	DU-145	100.0	63.4	84.7	6.7	20.7	6.5	0.3
Breast Cancer	MCF7	63.3	40.3	24.4	14.6	20.1	13.8	11.5
	MDA-MB-231	74.2	73.0	68.4	13.7	63.0	16.9	13.7
	HS 578T	72.9	63.2	79.6	18.7	16.3	17.2	11.0
	BT-549	70.9	82.6	56.6	-17.2	19.2	-16.9	-37.9
	T-47D	NA	NA	40.4	84.4	31.0	79.3	83.1
	MDA-MB-468	51.7	50.1	14.8	-15.1	-11.4	2.0	0.3

Table 8.14. Percentage growth inhibition of NCI 60 human cancer cells by compounds **ST-287, ST-288, ST-507, ST-507(A), ST-509, ST-510 and ST-124** at 10μM concentration**.**

Cancer	**cell type**	**ST-287**	**ST-288**	**ST-507**	**ST-507(A)**	**ST-509**	**ST-510**	**ST-124**
Leukemia	CCRF-CEM	83.4	88.3	14.5	18.1	17.6	7.9	NA
	HL-60(TB)	41.8	92.3	-3.9	2.5	5.4	5.4	NA
	K-562	NA	NA	12.3	14.5	11.7	14.3	NA

Table 8.14 (continued)

	MOLT-4	84.3	83.5	15.1	19.9	15.9	8.0	NA
	RPMI-8226	87.1	79.9	37.1	38.3	25.1	12.8	NA
	SR	37.5	88.7	7.1	8.9	9.6	19.0	NA
Non-Small Cell Lung Cancer	A549/ATCC	44.7	86.9	19.4	25.2	22.4	35.8	88.7
	HOP-62	84.5	94.1	41.5	48.2	33.4	49.2	89.8
	HOP-92	55.8	64.1	77.9	47.9	35.4	15.3	111.5
	NCI-H226	94.2	83.4	77.3	72.0	67.7	33.3	100.3
	NCI-H23	89.1	88.7	27.8	28.0	20.1	4.1	101.6
	NCI-H322M	91.7	93.9	49.9	49.0	40.2	-35.6	95.5
	NCI-H460	79.7	99.0	6.6	8.3	9.5	6.1	100.5
	NCI-H522	66.8	71.8	-24.2	-8.3	-30.6	14.1	92.1
Colon Cancer	COLO 205	79.3	103.2	97.9	92.3	57.2	6.0	NA
	HCC-2998	93.6	102.3	23.9	26.7	22.6	8.4	97.8
	HCT-116	92.4	97.5	6.3	2.5	2.8	8.9	103.2
	HCT-15	67.8	81.1	13.8	13.6	13.6	10.0	98.3
	HT29	72.4	87.7	81.6	87.9	58.0	22.5	101.8
	KM12	68.4	109.8	16.6	16.1	16.0	22.5	103.5
	SW-620	80.9	102.0	28.5	35.3	36.1	6.2	104.5
CNS Cancer	SF-268	95.4	94.3	41.7	42.6	36.1	-24.8	108.1
	SF-295	87.6	98.7	19.6	28.1	18.6	22.7	96.8
	SF-539	93.7	101.4	8.4	-1.2	-6.0	61.0	96.2
	SNB-19	90.3	90.0	55.7	62.8	56.8	4.9	108.2
	SNB-75	67.2	89.5	49.2	59.0	70.1	19.2	106.4
	U251	82.1	79.4	13.4	9.6	1.0	70.5	92.8
Melanoma	LOX IMVI	93.0	102.0	29.6	33.7	34.2	11.2	NA
	MALME-3M	78.4	103.7	85.4	80.4	74.5	-13.4	113.7
	M14	91.8	104.6	19.3	13.3	11.4	25.0	NA
	MDA-MB-435	19.5	96.2	1.9	7.8	5.2	53.7	99.0
	SK-MEL-2	86.9	97.8	28.7	48.5	27.9	-47.2	90.4
	SK-MEL-28	86.8	99.0	47.9	47.4	58.6	46.9	107.2
	SK-MEL-5	66.5	94.6	-20.8	-51.9	-64.1	10.5	116.1
	UACC-257	82.8	91.6	82.6	91.4	63.3	27.0	105.1
	UACC-62	68.7	81.4	47.8	54.6	44.9	1.5	106.7
Ovarian Cancer	IGROV1	87.5	99.6	41.4	37.6	33.6	38.4	81.4
	OVCAR-3	NA	NA	NA	NA	NA	NA	104.6
	OVCAR-4	75.0	76.0	10.4	15.0	14.6	7.4	118.2
	OVCAR-5	83.6	97.1	66.4	67.0	55.9	0.7	111.9
	OVCAR-8	85.8	93.6	42.9	50.4	34.8	2.0	102.9
	NCI/ADR-RES	76.6	99.7	19.7	19.3	12.9	19.2	98.7

Table 8.14 (continued)

	SK-OV-3	86.7	105.3	22.2	25.2	24.9	-15.2	89.7
Renal Cancer	786-0	92.7	97.1	33.5	40.8	23.0	22.7	107.7
	A498	14.4	74.0	30.0	21.4	15.5	22.9	108.0
	ACHN	76.0	88.5	36.2	36.4	8.1	22.2	89.1
	CAKI-1	73.6	92.8	27.7	26.7	29.6	24.6	97.2
	RXF 393	NA	NA	41.6	39.5	33.7	55.0	78.5
	SN12C	86.1	91.7	45.5	41.2	42.9	34.1	96.3
	TK-10	78.6	89.0	86.4	87.9	78.2	29.0	116.6
	UO-31	72.5	84.3	47.0	45.4	35.2	10.4	83.2
Prostate Cancer	PC-3	87.9	86.5	26.4	29.2	35.5	10.5	97.3
	DU-145	101.3	NA	15.5	14.9	16.2	5.9	111.7
Breast Cancer	MCF7	77.9	103.1	19.4	24.2	22.1	40.1	89.7
	MDA-MB-231	76.9	98.4	25.8	27.4	33.9	3.5	80.3
	HS 578T	88.7	101.2	44.0	59.7	49.3	61.6	94.6
	BT-549	84.0	93.6	NA	NA	NA	NA	120.2
	T-47D	75.2	80.1	NA	NA	NA	NA	92.7
	MDA-MB-468	64.6	89.1	32.5	38.5	8.3	-5.9	65.1

Data Set 3

CB1 and CB2 competitive binding screening at 1µM concentration.

Figure 8.1: CB1 and CB2 competitive binding screen at 1µM concentration with **ST-179, ST-173, ST-165, ST-172, ST-171** and **ST-167**.

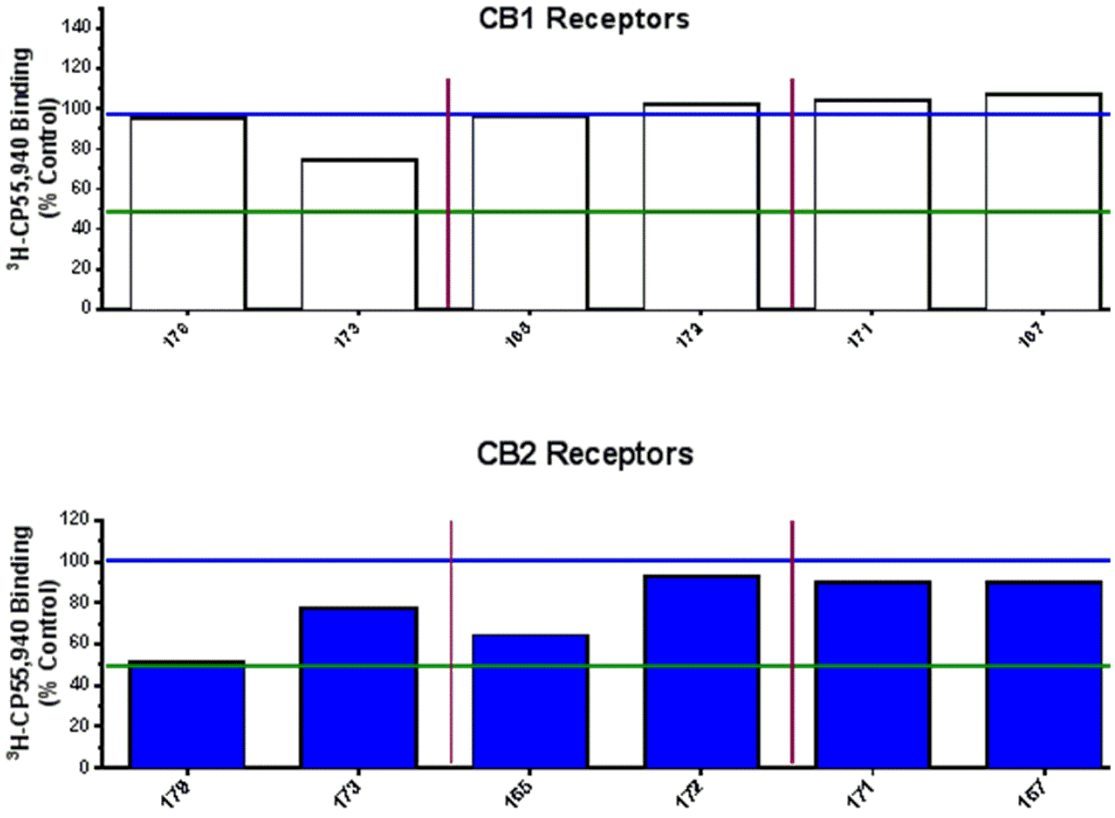

Figure 8.2: CB1 and CB2 competitive binding screen at 1µM concentration with **ST-177, ST-162, ST-164, ST-184, ST-178 and ST-161**

.

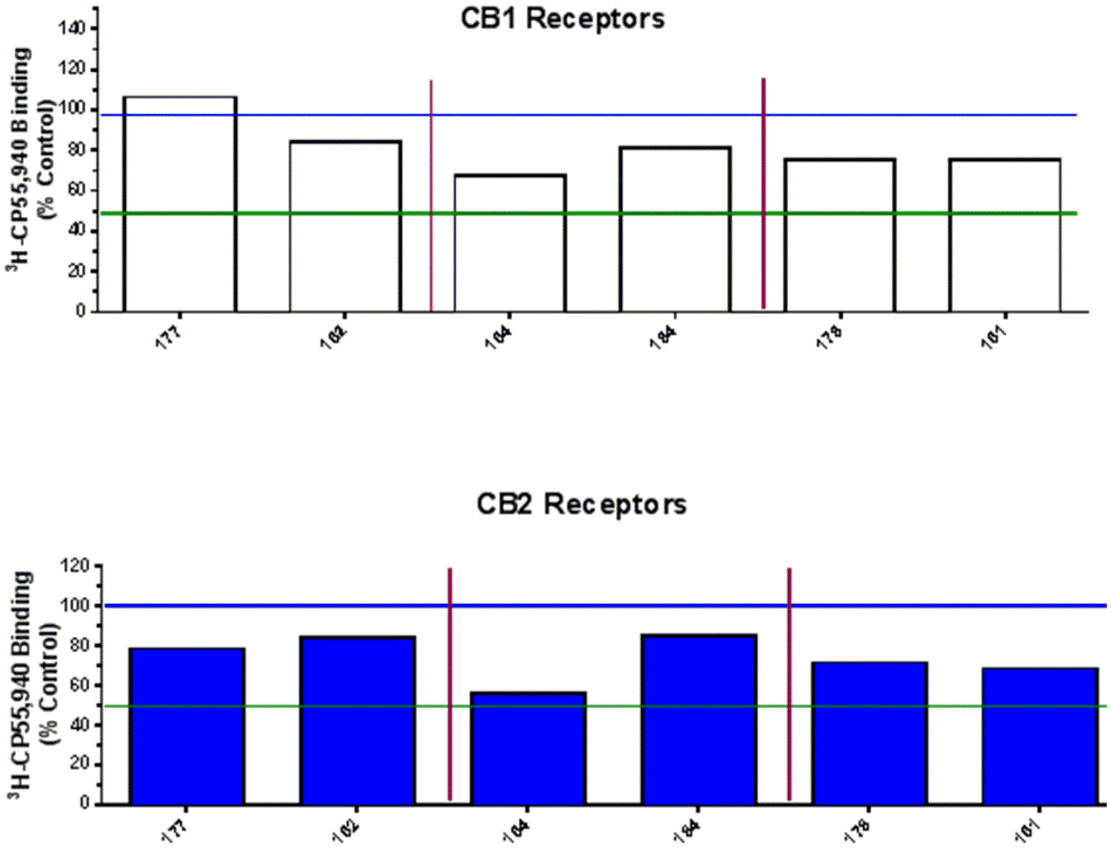

Figure 8.3: CB1 and CB2 competitive binding screen at 1µM concentration with **ST-190, ST-175, ST-181, ST-185, ST-169** and **ST-183**.

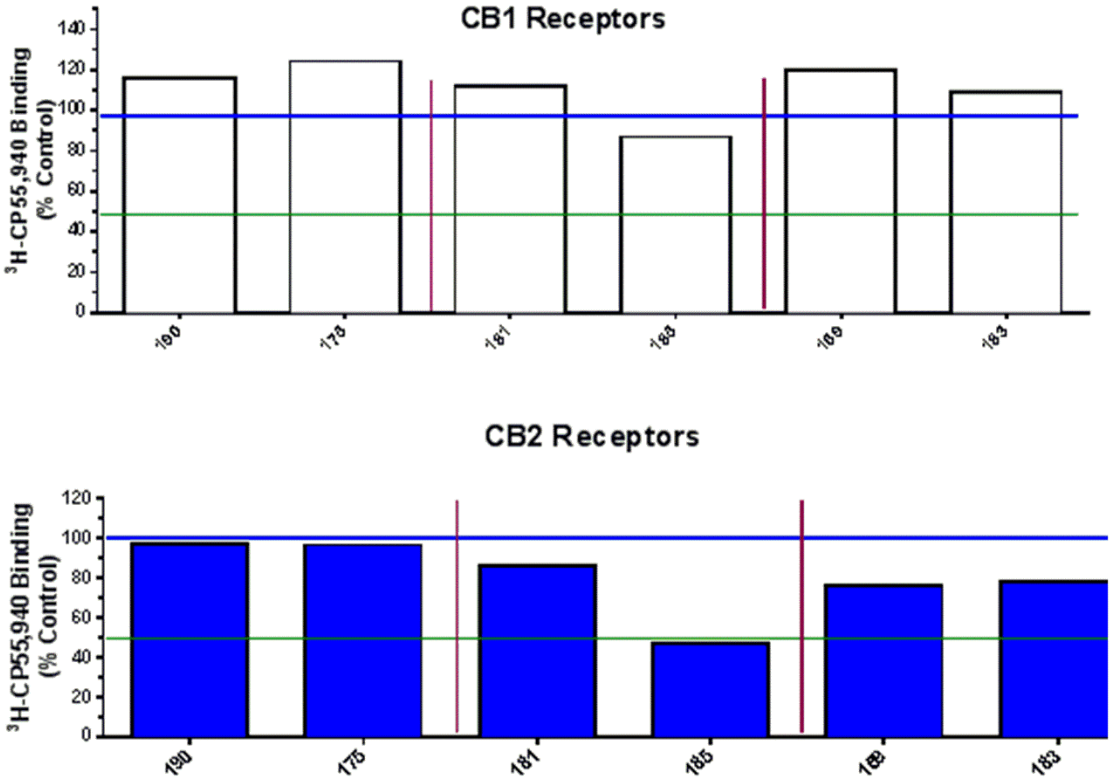

Figure 8.4: CB1 and CB2 competitive binding screen at 1μM concentration with **ST-192, ST-193, ST-194, ST-195, ST-196** and **ST-197**.

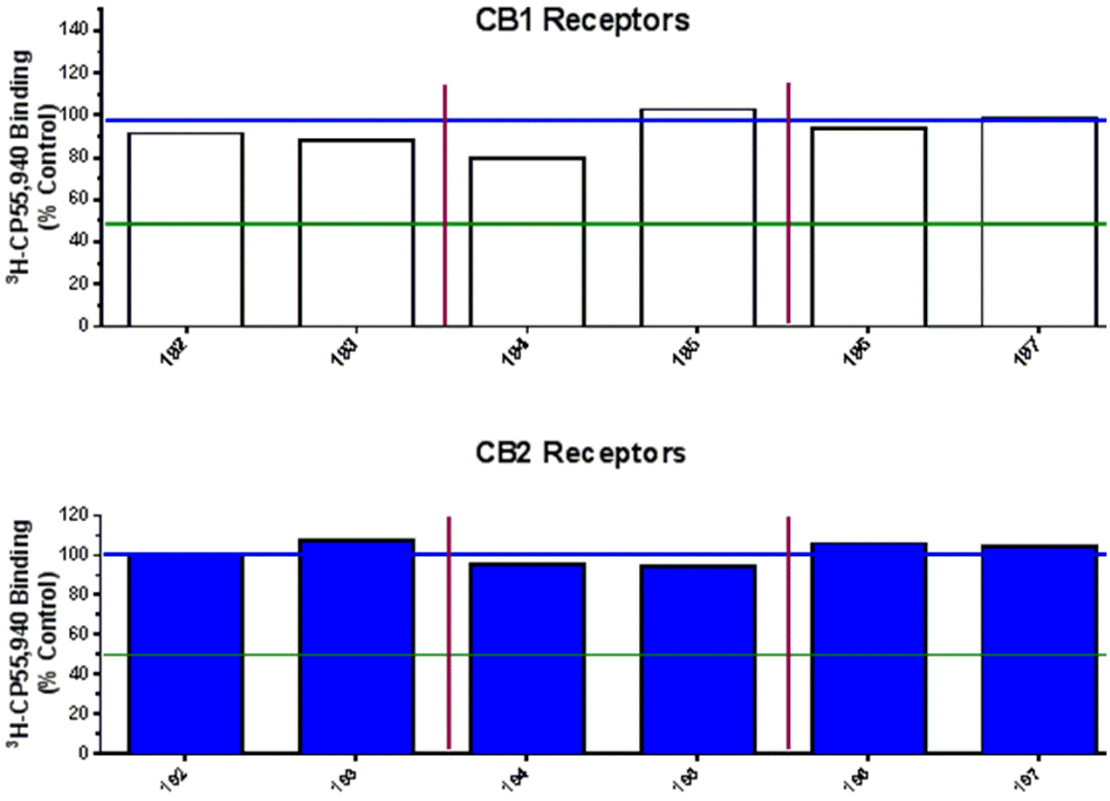

Figure 8.5: CB1 and CB2 competitive binding screen at 1µM concentration with **ST-198, ST-179(repeat), ST-188, ST-166, ST-176** and **ST-191**

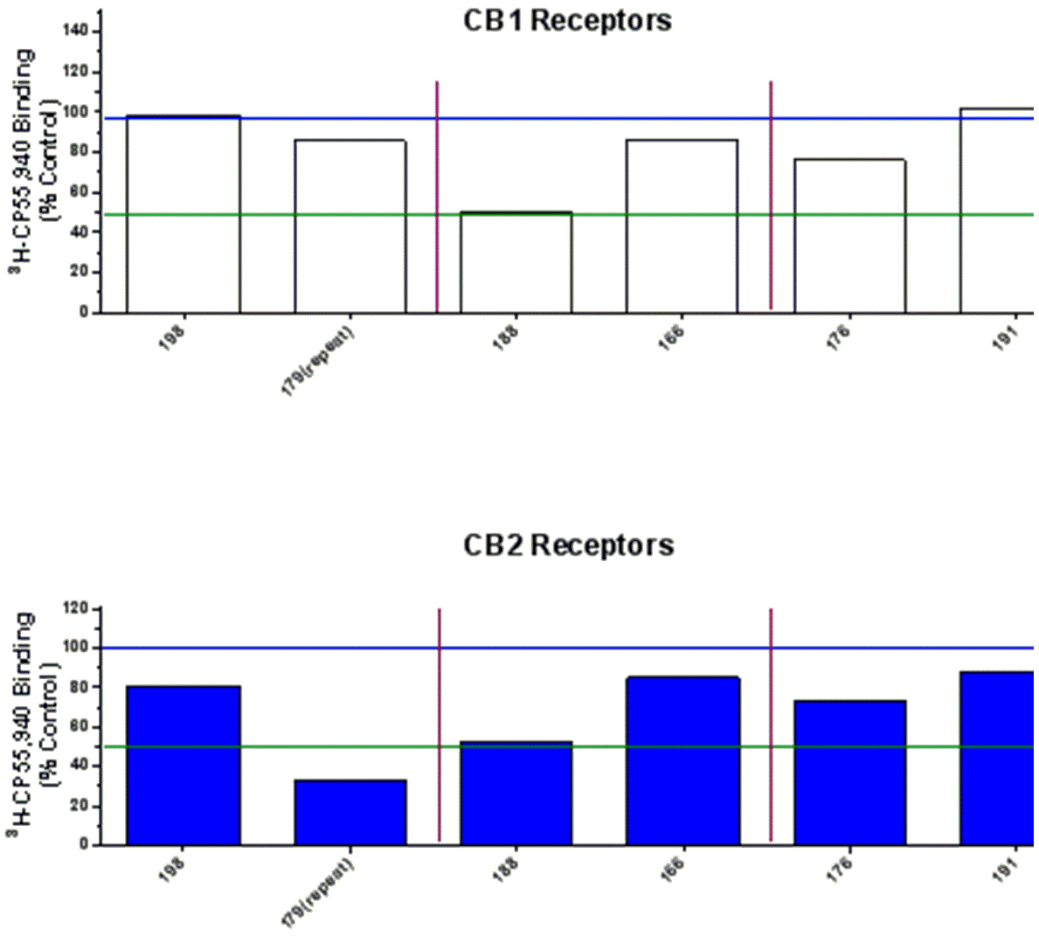

Figure 8.6: CB1 and CB2 competitive binding screen at 1μM concentration with **ST-153, ST-155, ST-147(a)** and **ST-156**.

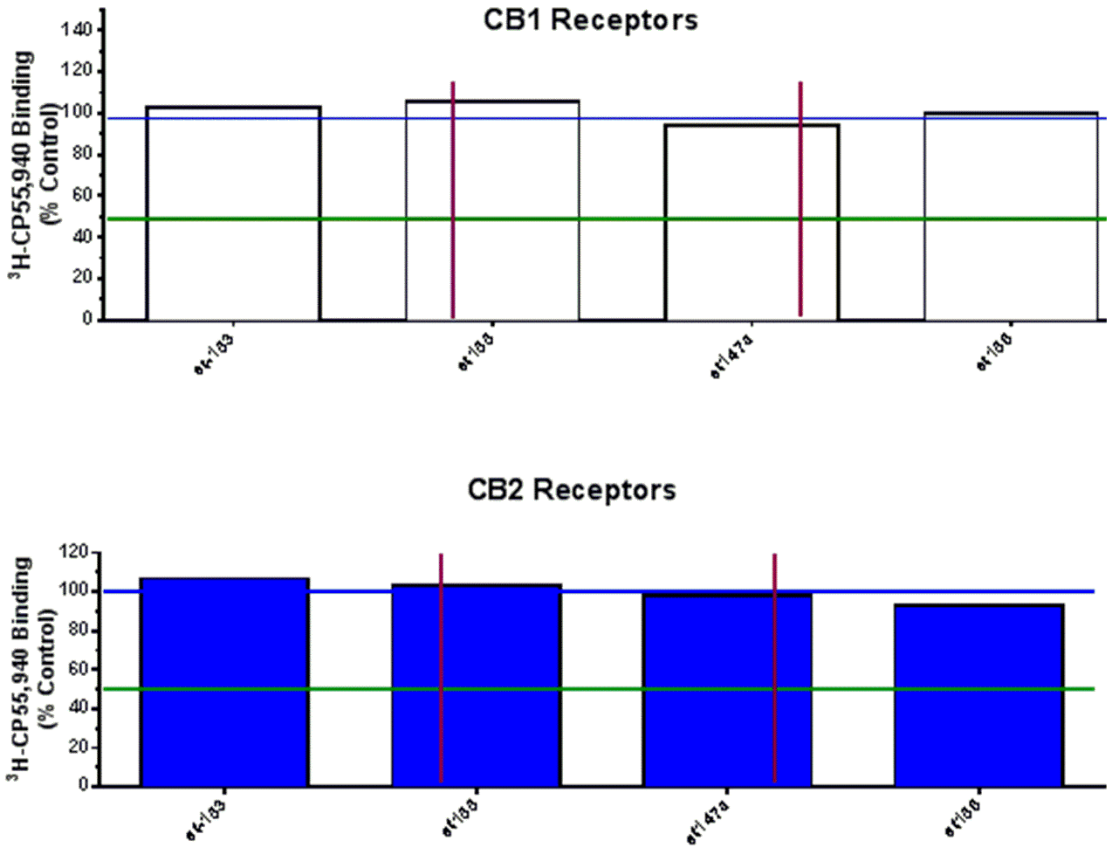

Data Set 4

NMR spectral data of selected compounds.

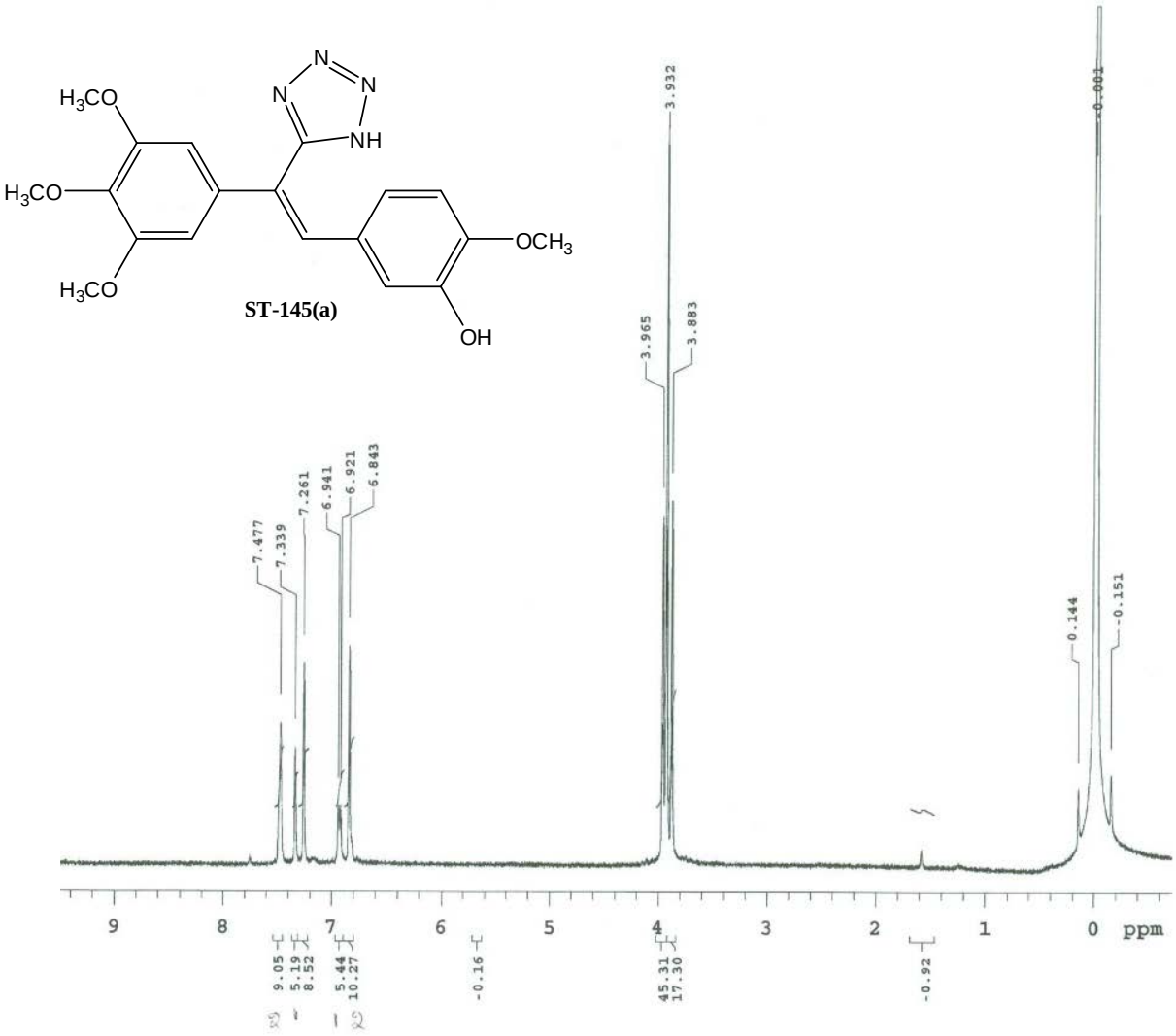

Figure 8.7 ^{1}H NMR spectral data of compound **ST-145(a)**

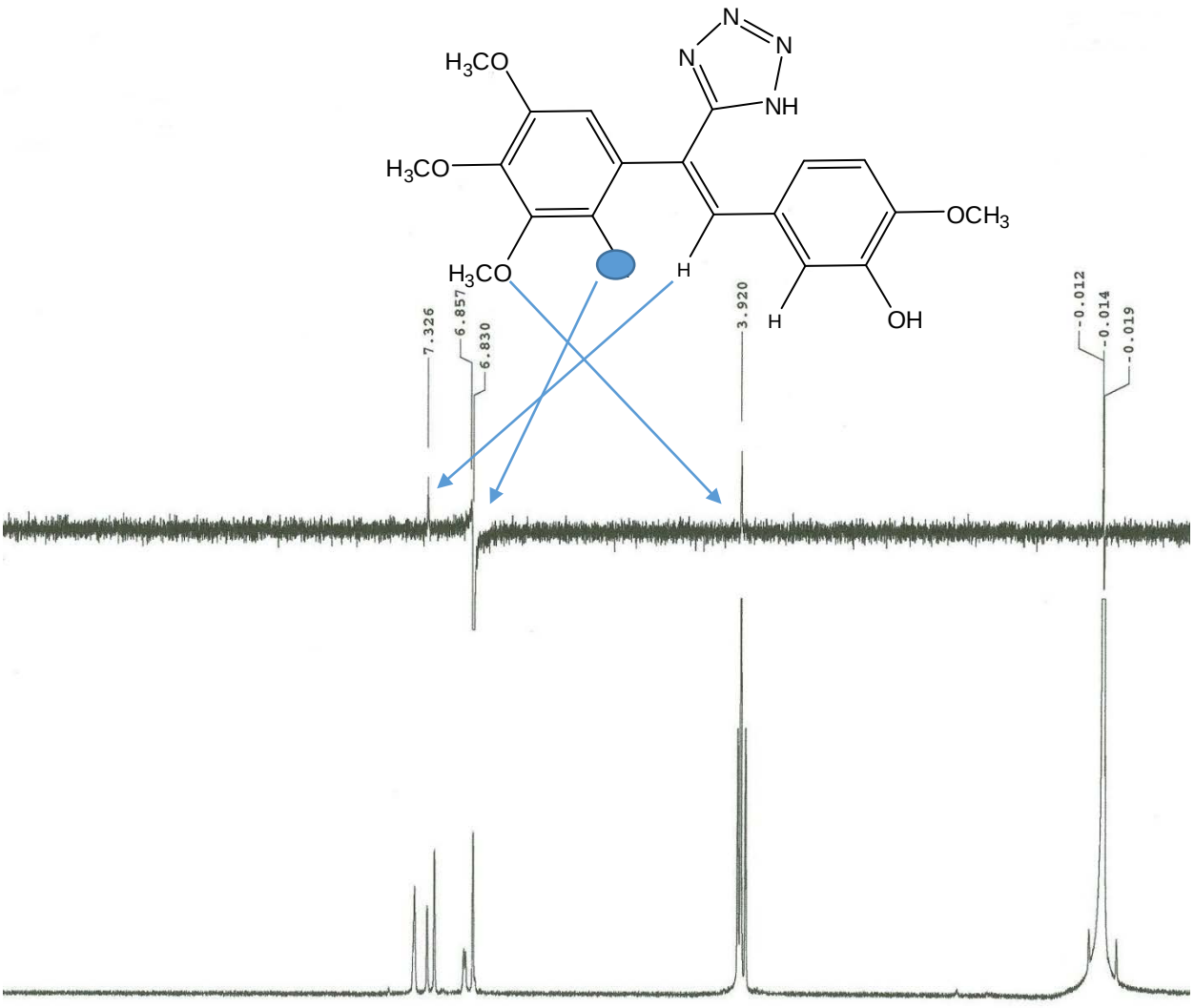

Figure 8.8 1D NOE spectral data of compound **ST-145(a).** Blue circled hydrogen is excited.

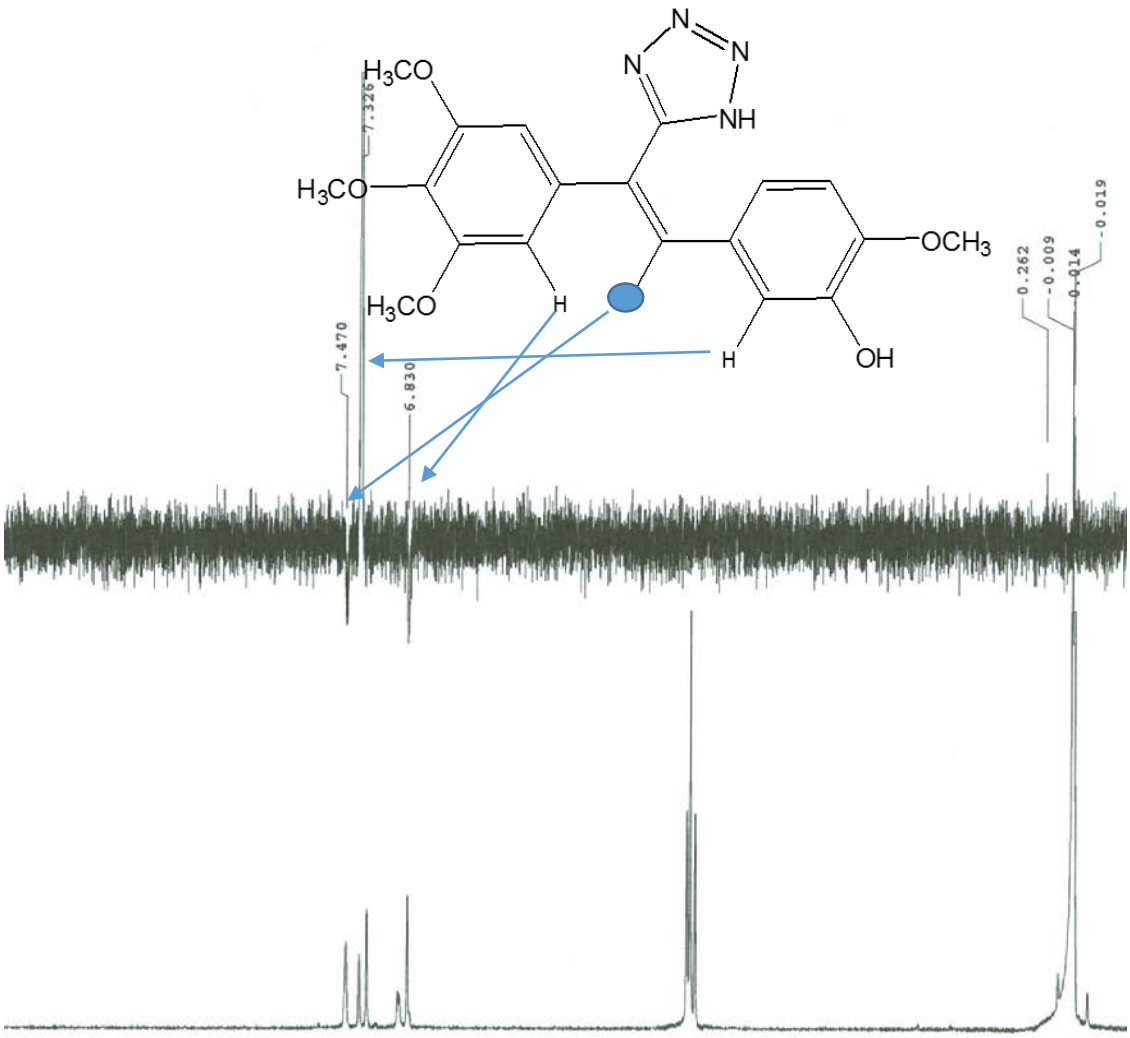

Figure 8.9 1D NOE spectral data of compound **ST-145(a).** Blue circled hydrogen is excited.

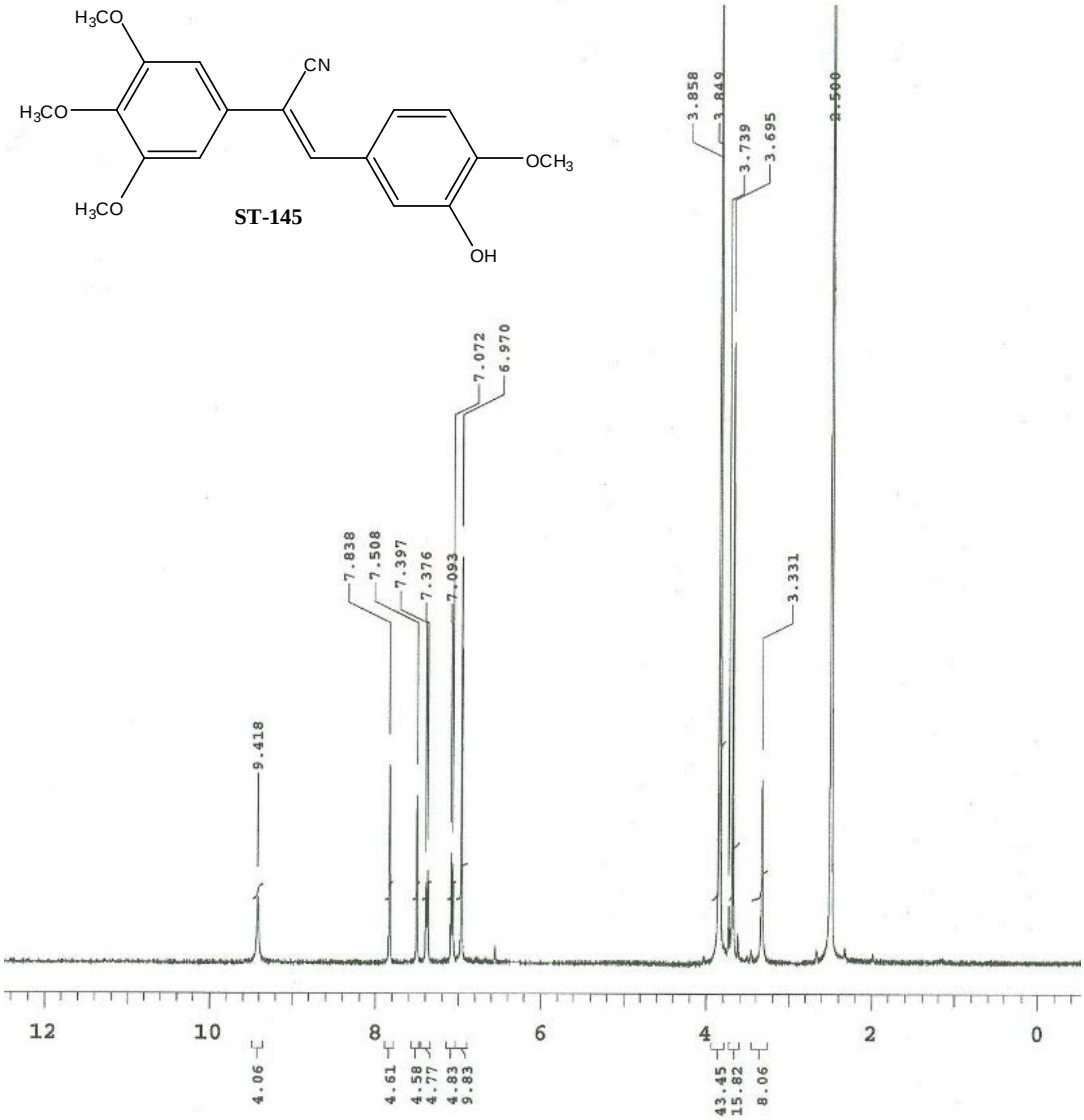

Figure 8.10 [1]H NMR spectral data of compound **ST-145**

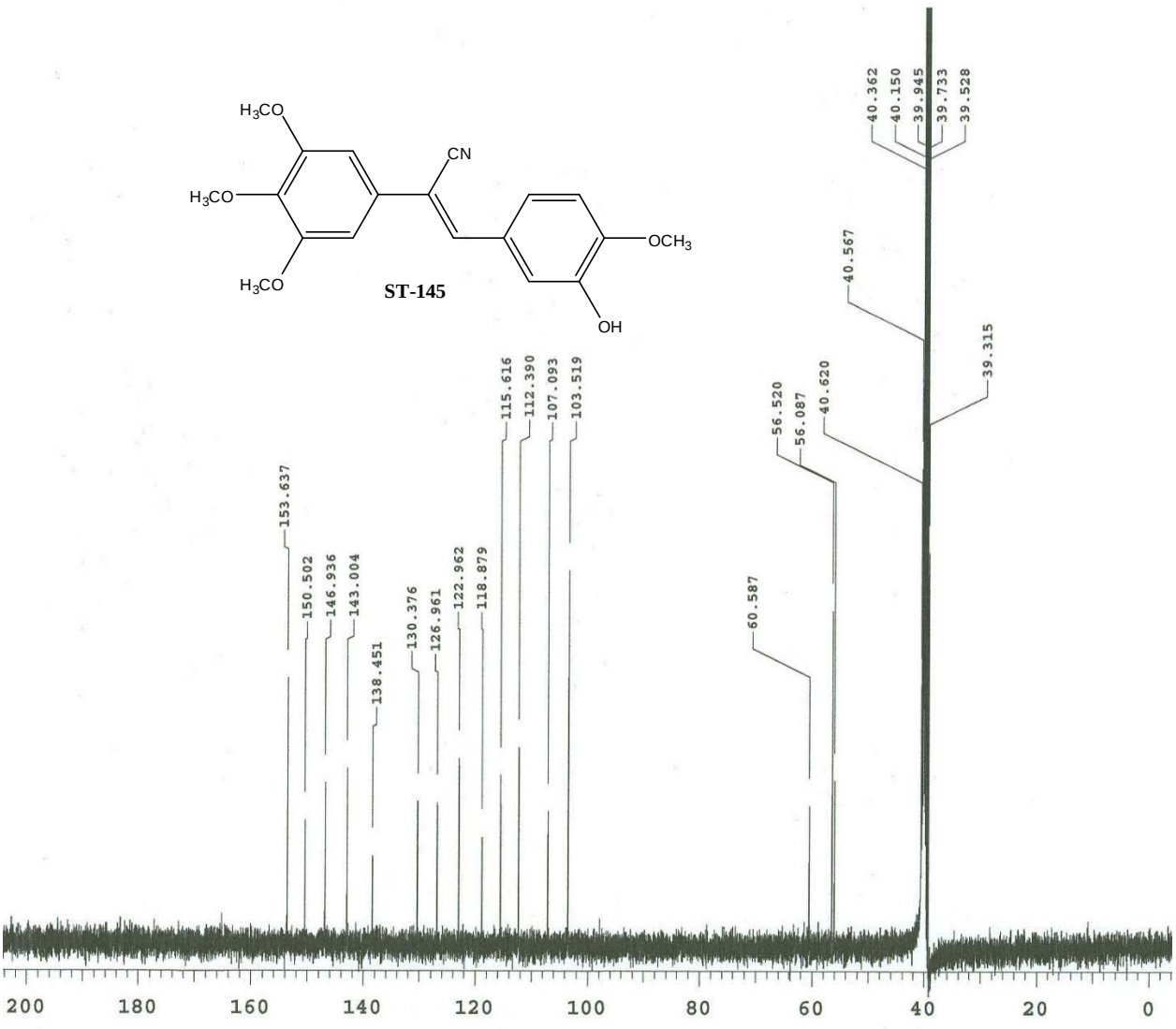

Figure 8.11 ^{13}C NMR spectral data of compound **ST-145**

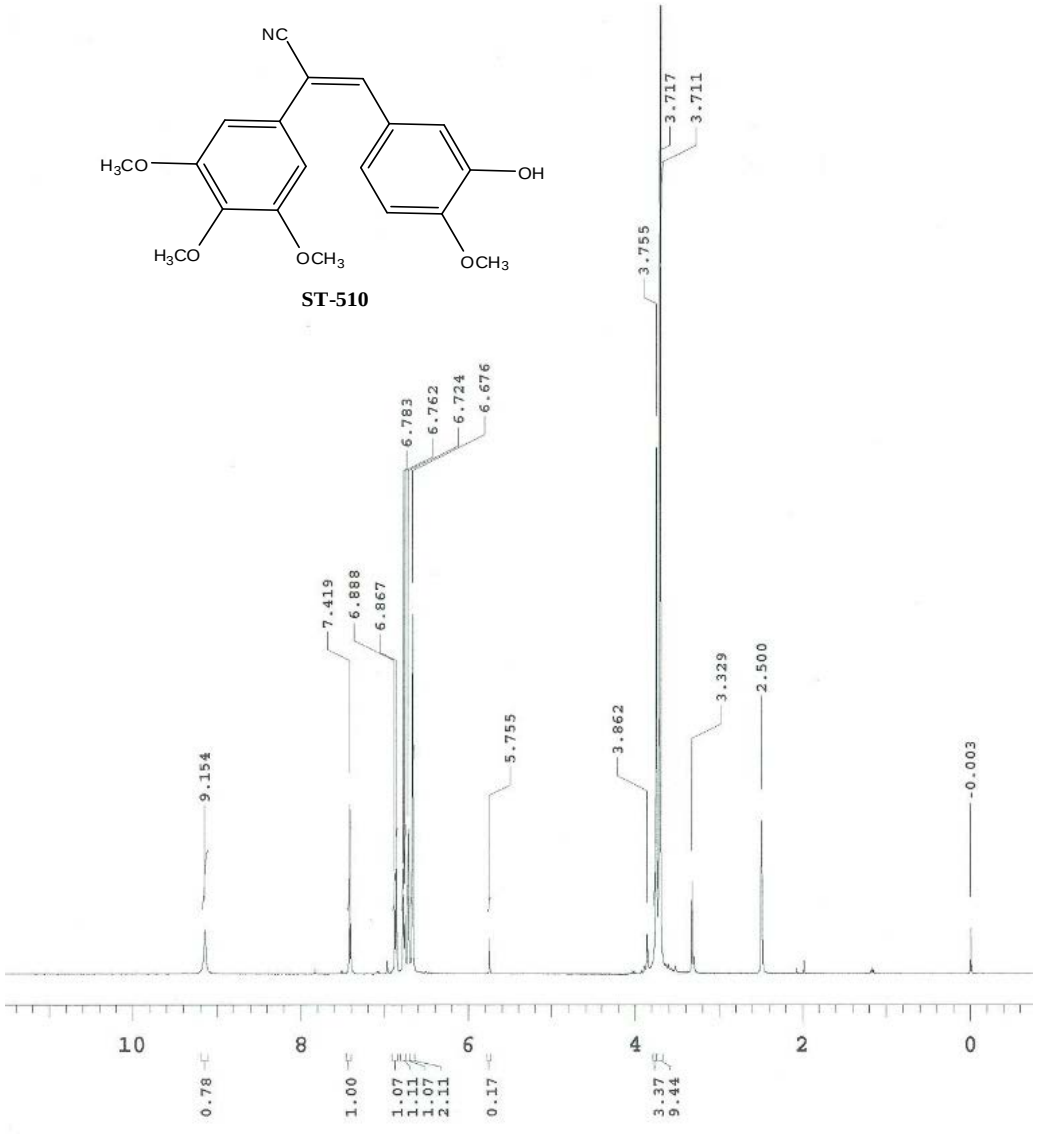

Figure 8.12 [1]H NMR spectral data of compound **ST-510**

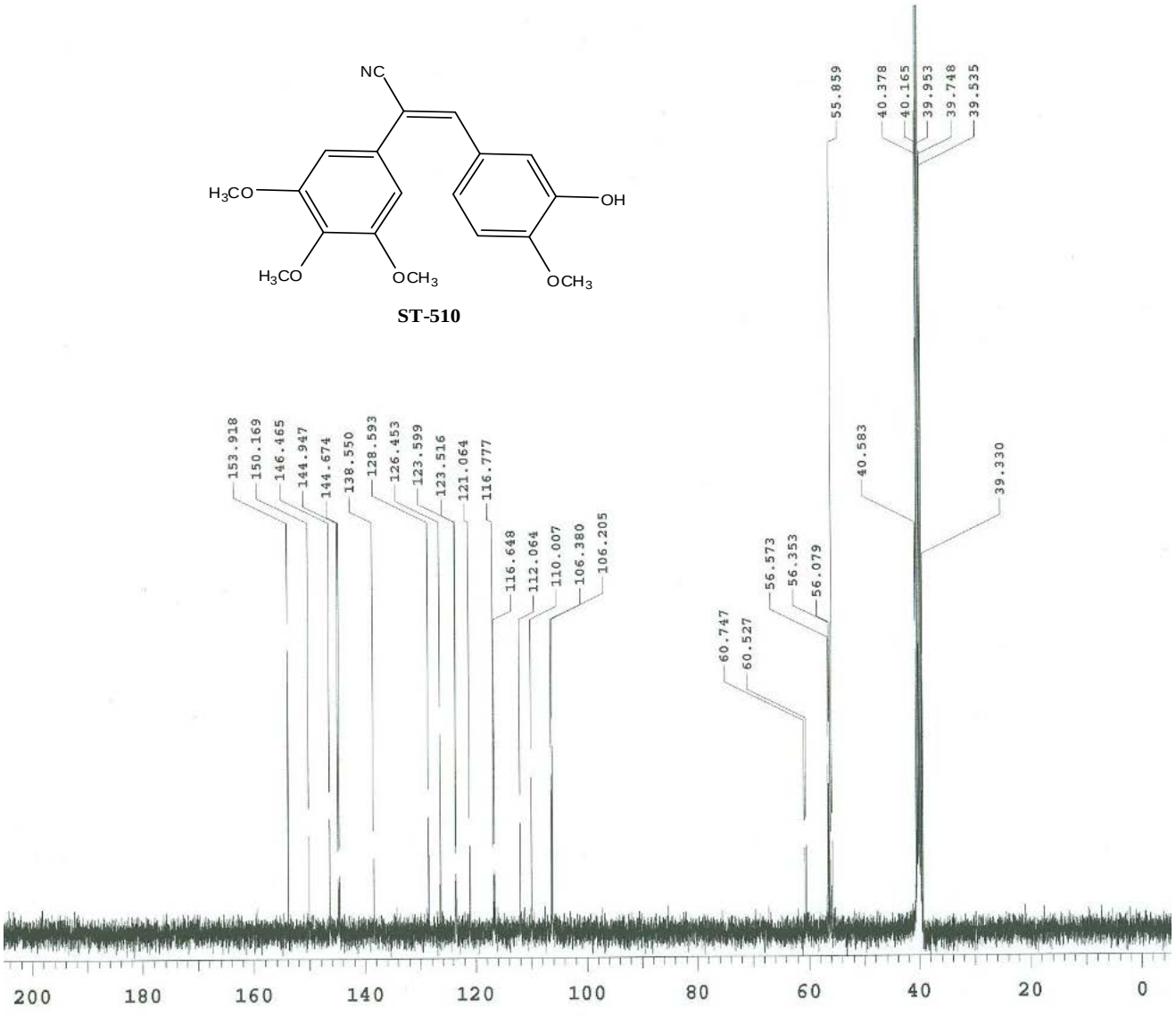

Figure 8.13 ^{13}C NMR spectral data of compound **ST-510**

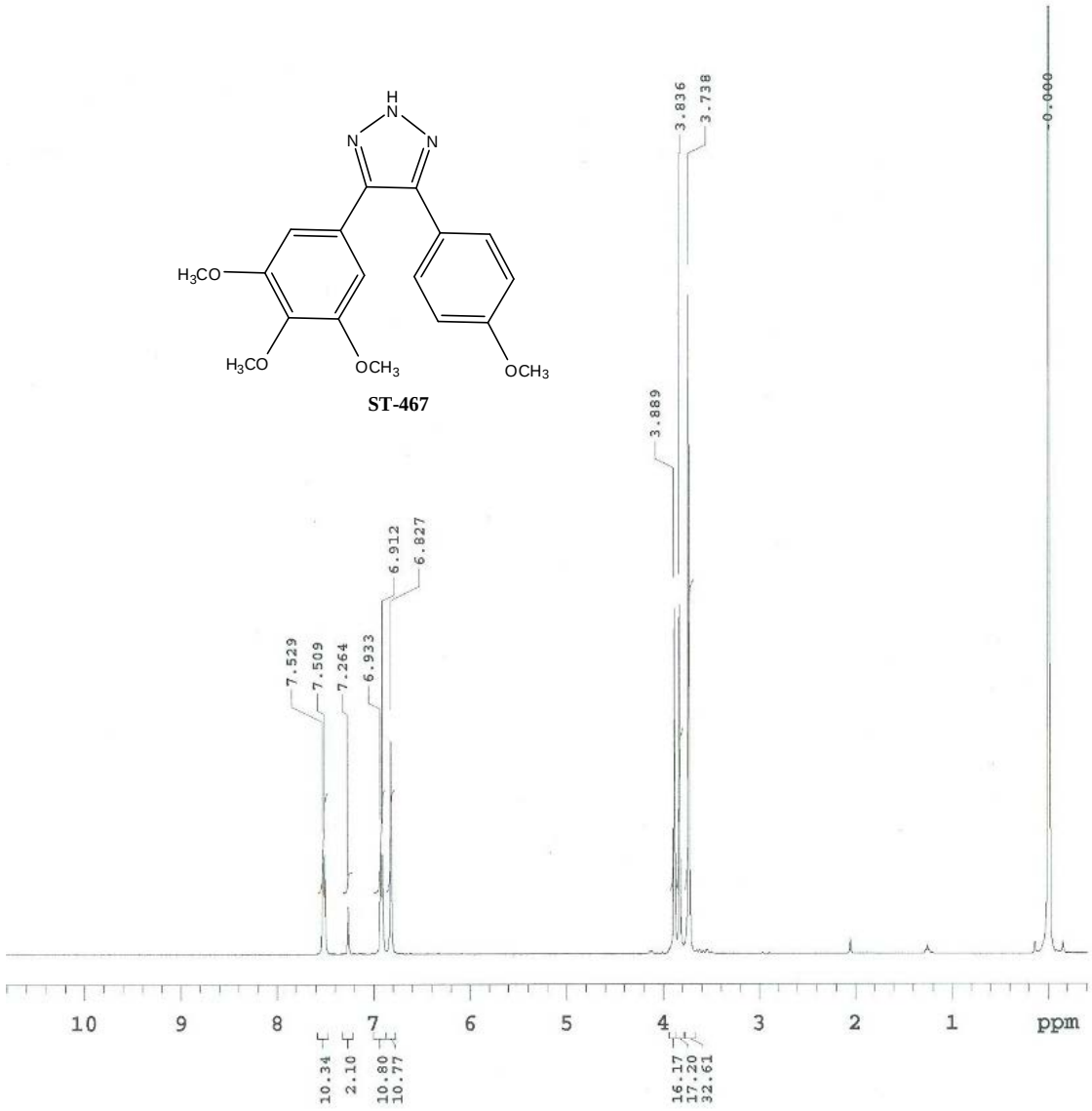

Figure 8.14 ^{1}H NMR spectral data of compound **ST-467**

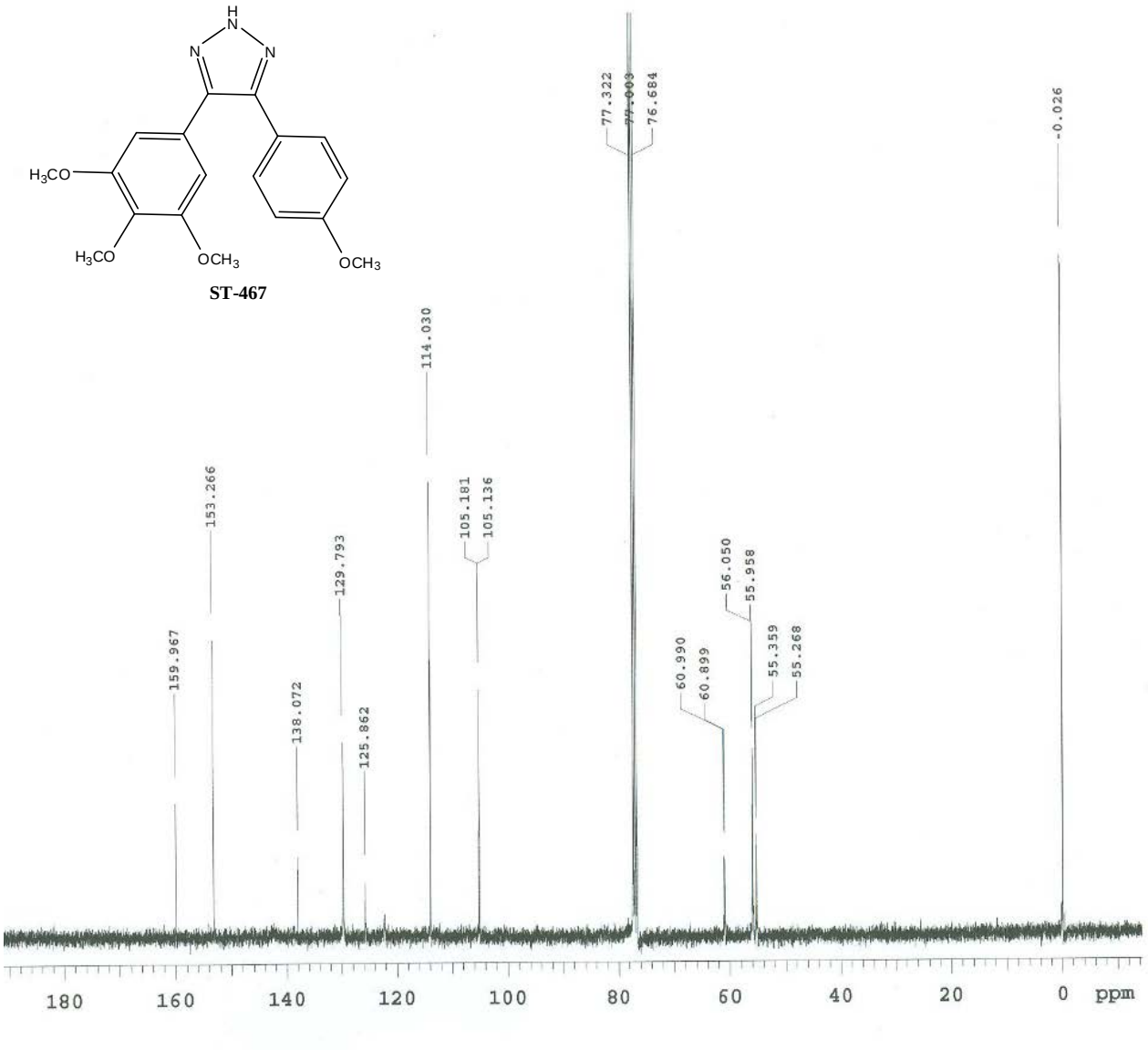

Figure 8.15 ^{13}C NMR spectral data of compound **ST-467**

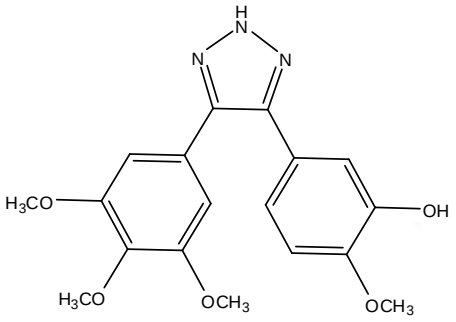

ST-145(b)

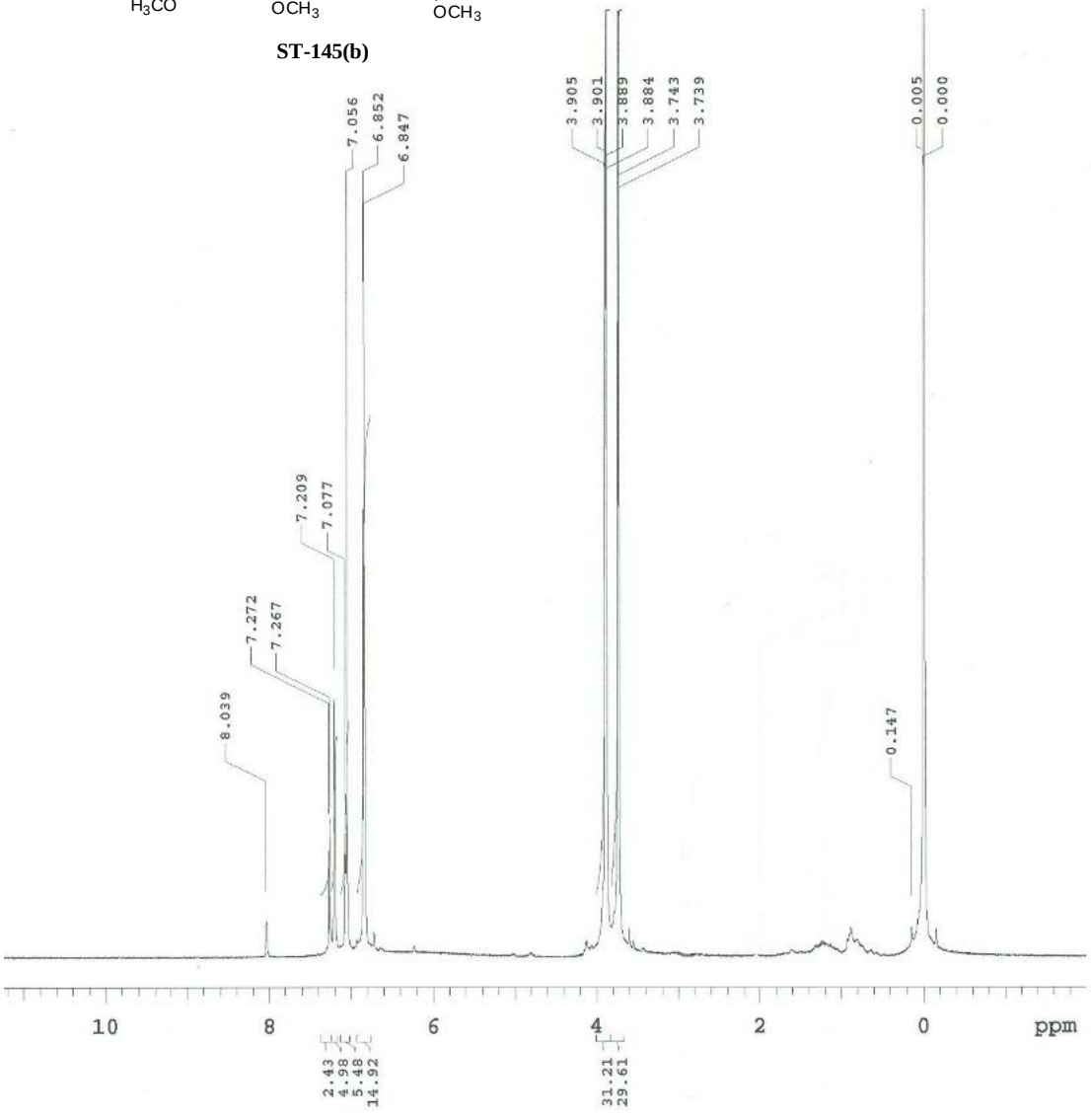

Figure 8.16 ^{1}H NMR spectral data of compound **ST-145(b)**

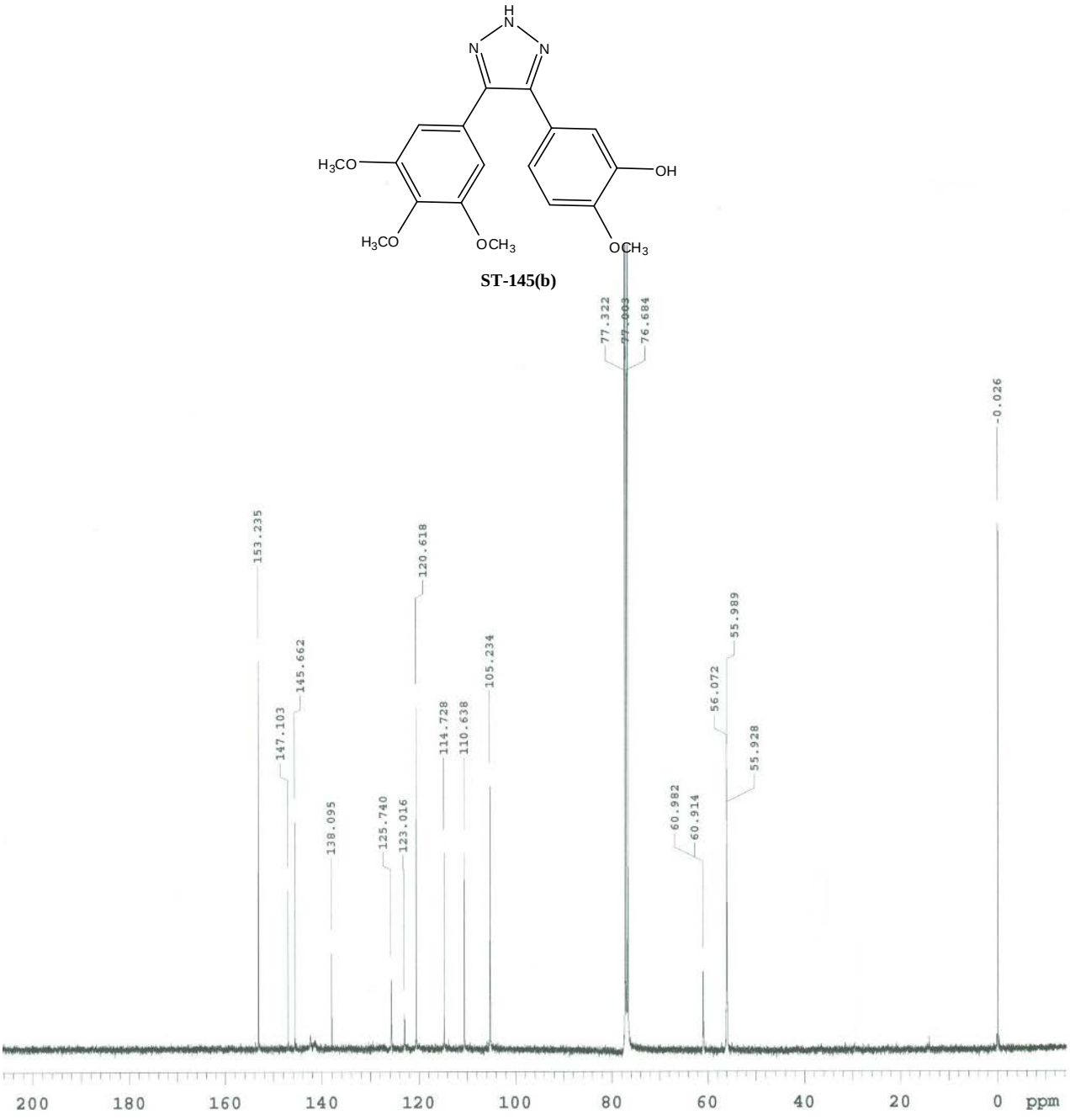

Figure 8.17 ^{13}C NMR spectral data of compound **ST-145(b)**

References:

Aggarwal, B. B., A. Bhardwaj, R. S. Aggarwal, N. P. Seeram, S. Shishodia and Y. Takada (2004). "Role of resveratrol in prevention and therapy of cancer: preclinical and clinical studies." Anticancer Res **24**(5A): 2783-2840.

Aggarwal, B. B., Y. Takada and O. V. Oommen (2004). "From chemoprevention to chemotherapy: common targets and common goals." Expert Opinion on Investigational Drugs **13**(10): 1327-1338.

Akhmanova, A. and M. O. Steinmetz (2008). "Tracking the ends: a dynamic protein network controls the fate of microtubule tips." Nat Rev Mol Cell Biol **9**(4): 309-322.

Alkhalaf, M. (2007). "Resveratrol-induced apoptosis is associated with activation of p53 and inhibition of protein translation in T47D human breast cancer cells." Pharmacology **80**(2-3): 134-143.

Alvarez, R., S. Velazquez, A. San-Felix, S. Aquaro, E. D. Clercq, C.-F. Perno, A. Karlsson, J. Balzarini and M. J. Camarasa (1994). "1,2,3-Triazole-[2,5-Bis-O-(tert-butyldimethylsilyl)-.beta.-D-ribofuranosyl]-3'-spiro-5"-(4"-amino-1",2"-oxathiole 2",2"-dioxide) (TSAO) Analogs: Synthesis and Anti-HIV-1 Activity." Journal of Medicinal Chemistry **37**(24): 4185-4194.

Arcamone, F., G. Franceschi, P. Orezzi, G. Cassinelli, W. Barbieri and R. Mondelli (1964). "Daunomycin. I. The Structure of Daunomycinone." Journal of the American Chemical Society **86**(23): 5334-5335.

Athar, M., J. H. Back, L. Kopelovich, D. R. Bickers and A. L. Kim (2009). "Multiple molecular targets of resveratrol: Anti-carcinogenic mechanisms." Archives of Biochemistry and Biophysics **486**(2): 95-102.

Atten, M. J., B. M. Attar, T. Milson and O. Holian (2001). "Resveratrol-induced inactivation of human gastric adenocarcinoma cells through a protein kinase C-mediated mechanism." Biochemical Pharmacology **62**(10): 1423-1432.

Awad, A. B., A. T. Burr and C. S. Fink (2005). "Effect of resveratrol and beta-sitosterol in combination on reactive oxygen species and prostaglandin release by PC-3 cells." Prostaglandins Leukot Essent Fatty Acids **72**(3): 219-226.

Aziz, M. H., M. Nihal, V. X. Fu, D. F. Jarrard and N. Ahmad (2006). "Resveratrol-caused apoptosis of human prostate carcinoma LNCaP cells is mediated via modulation

of phosphatidylinositol 3'-kinase/Akt pathway and Bcl-2 family proteins." Mol Cancer Ther **5**(5): 1335-1341.

Baas, P. W. and M. M. Black (1990). "Individual microtubules in the axon consist of domains that differ in both composition and stability." J Cell Biol **111**(2): 495-509.

Banimustafa, M., A. Kheirollahi, M. Safavi, S. Kabudanian Ardestani, H. Aryapour, A. Foroumadi and S. Emami (2013). "Synthesis and biological evaluation of 3-(trimethoxyphenyl)-2(3H)-thiazole thiones as combretastatin analogs." European Journal of Medicinal Chemistry **70**(0): 692-702.

Baur, J. A., K. J. Pearson, N. L. Price, H. A. Jamieson, C. Lerin, A. Kalra, V. V. Prabhu, J. S. Allard, G. Lopez-Lluch, K. Lewis, P. J. Pistell, S. Poosala, K. G. Becker, O. Boss, D. Gwinn, M. Wang, S. Ramaswamy, K. W. Fishbein, R. G. Spencer, E. G. Lakatta, D. Le Couteur, R. J. Shaw, P. Navas, P. Puigserver, D. K. Ingram, R. de Cabo and D. A. Sinclair (2006). "Resveratrol improves health and survival of mice on a high-calorie diet." Nature **444**(7117): 337-342.

Baur, J. A. and D. A. Sinclair (2006). "Therapeutic potential of resveratrol: the in vivo evidence." Nat Rev Drug Discov **5**(6): 493-506.

Beale, T. M., P. J. Bond, J. D. Brenton, D. S. Charnock-Jones, S. V. Ley and R. M. Myers (2012). "Increased endothelial cell selectivity of triazole-bridged dihalogenated A-ring analogues of combretastatin A–1." Bioorganic & Medicinal Chemistry **20**(5): 1749-1759.

Belleri, M., D. Ribatti, S. Nicoli, F. Cotelli, L. Forti, V. Vannini, L. A. Stivala and M. Presta (2005). "Antiangiogenic and vascular-targeting activity of the microtubule-destabilizing trans-resveratrol derivative 3,5,4'-trimethoxystilbene." Mol Pharmacol **67**(5): 1451-1459.

Benitez, D. A., E. Pozo-Guisado, A. Alvarez-Barrientos, P. M. Fernandez-Salguero and E. A. Castellon (2007). "Mechanisms involved in resveratrol-induced apoptosis and cell cycle arrest in prostate cancer-derived cell lines." J Androl **28**(2): 282-293.

Borrel, C., S. Thoret, X. Cachet, D. Guenard, F. Tillequin, M. Koch and S. Michel (2005). "New antitubulin derivatives in the combretastatin A4 series: synthesis and biological evaluation." Bioorg Med Chem **13**(11): 3853-3864.

Borrelli, M. J., D. M. Stafford, C. M. Rausch, L. J. Bernock, M. L. Freeman, J. R. Lepock and P. M. Corry (1998). "Diamide-induced cytotoxicity and thermotolerance in CHO cells." J Cell Physiol **177**(3): 483-492.

Borrelli, M. J., L. L. Thompson and W. C. Dewey (1989). "Evidence that the feeder effect in mammalian cells is mediated by a diffusible substance." Int J Hyperthermia **5**(1): 99-103.

Bove, K., D. W. Lincoln and M. F. Tsan (2002). "Effect of resveratrol on growth of 4T1 breast cancer cells in vitro and in vivo." Biochem Biophys Res Commun **291**(4): 1001-1005.

Boyd, M. R. and K. D. Paull (1995). "Some practical considerations and applications of the national cancer institute in vitro anticancer drug discovery screen." Drug Development Research **34**(2): 91-109.

Brents, L. K., F. Medina-Bolivar, K. A. Seely, V. Nair, S. M. Bratton, L. Nopo-Olazabal, R. Y. Patel, H. Liu, R. J. Doerksen, P. L. Prather and A. Radominska-Pandya (2012). "Natural prenylated resveratrol analogs arachidin-1 and -3 demonstrate improved glucuronidation profiles and have affinity for cannabinoid receptors." Xenobiotica **42**(2): 139-156.

Butler, M. S. (2008). "Natural products to drugs: natural product-derived compounds in clinical trials." Nat Prod Rep **25**(3): 475-516.

Calligaris, D., P. Verdier-Pinard, F. Devred, C. Villard, D. Braguer and D. Lafitte (2010). "Microtubule targeting agents: from biophysics to proteomics." Cell Mol Life Sci **67**(7): 1089-1104.

Capdeville, R., E. Buchdunger, J. Zimmermann and A. Matter (2002). "Glivec (STI571, imatinib), a rationally developed, targeted anticancer drug." Nat Rev Drug Discov **1**(7): 493-502.

Carr, M., L. M. Greene, A. J. S. Knox, D. G. Lloyd, D. M. Zisterer and M. J. Meegan (2010). "Lead identification of conformationally restricted β-lactam type combretastatin analogues: Synthesis, antiproliferative activity and tubulin targeting effects." European Journal of Medicinal Chemistry **45**(12): 5752-5766.

Chakraborti, S., L. Das, N. Kapoor, A. Das, V. Dwivedi, A. Poddar, G. Chakraborti, M. Janik, G. Basu, D. Panda, P. Chakrabarti, A. Surolia and B. Bhattacharyya (2011). "Curcumin recognizes a unique binding site of tubulin." J Med Chem **54**(18): 6183-6196.

Chaudhary, A., S. N. Pandeya, P. Kumar, P. P. Sharma, S. Gupta, N. Soni, K. K. Verma and G. Bhardwaj (2007). "Combretastatin a-4 analogs as anticancer agents." Mini Rev Med Chem **7**(12): 1186-1205.

Chen, Y., F. Hu, Y. Gao, S. Jia, N. Ji and E. Hua (2013). "Design, synthesis, and evaluation of methoxylated resveratrol derivatives as potential antitumor agents." Research on Chemical Intermediates: 1-14.

Chen, Y., S. H. Tseng, H. S. Lai and W. J. Chen (2004). "Resveratrol-induced cellular apoptosis and cell cycle arrest in neuroblastoma cells and antitumor effects on neuroblastoma in mice." Surgery **136**(1): 57-66.

Cheng, Y. and W. H. Prusoff (1973). "Relationship between the inhibition constant (K1) and the concentration of inhibitor which causes 50 per cent inhibition (I50) of an enzymatic reaction." Biochem Pharmacol **22**(23): 3099-3108.

Cooney, M. M., J. Ortiz, R. M. Bukowski and S. C. Remick (2005). "Novel vascular targeting/disrupting agents: combretastatin A4 phosphate and related compounds." Curr Oncol Rep **7**(2): 90-95.

Cridge, B. J. and R. J. Rosengren (2013). "Critical appraisal of the potential use of cannabinoids in cancer management." Cancer Manag Res **5**: 301-313.

Crowell, J. A., P. J. Korytko, R. L. Morrissey, T. D. Booth and B. S. Levine (2004). "Resveratrol-associated renal toxicity." Toxicol Sci **82**(2): 614-619.

Demchuk, D. V., A. V. Samet, N. B. Chernysheva, V. I. Ushkarov, G. A. Stashina, L. D. Konyushkin, M. M. Raihstat, S. I. Firgang, A. A. Philchenkov, M. P. Zavelevich, L. M. Kuiava, V. F. Chekhun, D. Y. Blokhin, A. S. Kiselyov, M. N. Semenova and V. V. Semenov (2014). "Synthesis and antiproliferative activity of conformationally restricted 1,2,3-triazole analogues of combretastatins in the sea urchin embryo model and against human cancer cell lines." Bioorganic & Medicinal Chemistry **22**(2): 738-755.

Dias, S. J., K. Li, A. M. Rimando, S. Dhar, C. S. Mizuno, A. D. Penman and A. S. Levenson (2013). "Trimethoxy-resveratrol and piceatannol administered orally suppress and inhibit tumor formation and growth in prostate cancer xenografts." Prostate **73**(11): 1135-1146.

Docherty, J. J., M. M. H. Fu, B. S. Stiffler, R. J. Limperos, C. M. Pokabla and A. L. DeLucia (1999). "Resveratrol inhibition of herpes simplex virus replication." Antiviral Research **43**(3): 145-155.

Early Breast Cancer Trialists' Collaborative, G. (1992). "Systemic treatment of early breast cancer by hormonal, cytotoxic, or immune therapy: 133 randomised trials involving 31 000 recurrences and 24 000 deaths among 75 000 women." The Lancet **339**(8784): 1-15.

Estrov, Z., S. Shishodia, S. Faderl, D. Harris, Q. Van, H. M. Kantarjian, M. Talpaz and B. B. Aggarwal (2003). "Resveratrol blocks interleukin-1beta-induced activation of the nuclear transcription factor NF-kappaB, inhibits proliferation, causes S-phase arrest, and induces apoptosis of acute myeloid leukemia cells." Blood **102**(3): 987-995.

Faber, A. C. and T. C. Chiles (2006). "Resveratrol induces apoptosis in transformed follicular lymphoma OCI-LY8 cells: evidence for a novel mechanism involving inhibition of BCL6 signaling." International Journal of Oncology **29**(6): 1561-1566.

Faber, A. C., F. J. Dufort, D. Blair, D. Wagner, M. F. Roberts and T. C. Chiles (2006). "Inhibition of phosphatidylinositol 3-kinase-mediated glucose metabolism coincides with

resveratrol-induced cell cycle arrest in human diffuse large B-cell lymphomas." Biochemical Pharmacology **72**(10): 1246-1256.

Farber, S., G. D'Angio, A. Evans and A. Mitus (1960). "CLINICAL STUDIES OF ACTINOMYCIN D WITH SPECIAL REFERENCE TO WILMS' TUMOR IN CHILDREN*." Annals of the New York Academy of Sciences **89**(2): 421-424.

Fauconneau, B., P. Waffo-Teguo, F. Huguet, L. Barrier, A. Decendit and J. M. Merillon (1997). "Comparative study of radical scavenger and antioxidant properties of phenolic compounds from Vitis vinifera cell cultures using in vitro tests." Life Sci **61**(21): 2103-2110.

Frankel, E. N., A. L. Waterhouse and J. E. Kinsella (1993). "Inhibition of human LDL oxidation by resveratrol." The Lancet **341**(8852): 1103-1104.

Franks, L. N., B. M. Ford, N. R. Madadi, N. R. Penthala, P. A. Crooks and P. L. Prather (2014). "Characterization of the intrinsic activity for a novel class of cannabinoid receptor ligands: Indole quinuclidine analogues." European Journal of Pharmacology, **737**: 140-148.

Gigant, B., C. Wang, R. B. Ravelli, F. Roussi, M. O. Steinmetz, P. A. Curmi, A. Sobel and M. Knossow (2005). "Structural basis for the regulation of tubulin by vinblastine." Nature **435**(7041): 519-522.

Gobbi, P. G., C. Broglia, F. Merli, M. Dell'Olio, C. Stelitano, E. Iannitto, M. Federico, R. Berte, D. Luisi, S. Molica, C. Cavalli, L. Dezza and E. Ascari (2003). "Vinblastine, bleomycin, and methotrexate chemotherapy plus irradiation for patients with early-stage, favorable Hodgkin lymphoma: the experience of the Gruppo Italiano Studio Linfomi." Cancer **98**(11): 2393-2401.

Goldberg, D. M., E. Ng, A. Karumanchiri, J. Yan, E. P. Diamandis and G. J. Soleas (1995). "Assay of resveratrol glucosides and isomers in wine by direct-injection high-performance liquid chromatography." Journal of Chromatography A **708**(1): 89-98.

Golkar, L., X. Z. Ding, M. B. Ujiki, M. R. Salabat, D. L. Kelly, D. Scholtens, A. J. Fought, D. J. Bentrem, M. S. Talamonti, R. H. Bell and T. E. Adrian (2007). "Resveratrol inhibits pancreatic cancer cell proliferation through transcriptional induction of macrophage inhibitory cytokine-1." J Surg Res **138**(2): 163-169.

Goncalves, A., D. Braguer, G. Carles, N. Andre, C. Prevot and C. Briand (2000). "Caspase-8 activation independent of CD95/CD95-L interaction during paclitaxel-induced apoptosis in human colon cancer cells (HT29-D4)." Biochem Pharmacol **60**(11): 1579-1584.

Gordaliza, M. (2007). "Natural products as leads to anticancer drugs." Clin Transl Oncol **9**(12): 767-776.

Gosslau, A., S. Pabbaraja, S. Knapp and K. Y. Chen (2008). "Trans- and cis-stilbene polyphenols induced rapid perinuclear mitochondrial clustering and p53-independent apoptosis in cancer cells but not normal cells." Eur J Pharmacol **587**(1-3): 25-34.

Greer, A. K., N. R. Madadi, S. M. Bratton, S. D. Eddy, Z. Mazerska, H. Hendrickson, P. A. Crooks and A. Radominska-Pandya (2014). "Novel Resveratrol-Based Substrates for Human Hepatic, Renal and Intestinal UDP-Glucuronosyltransferases." Chemical Research in Toxicology, **27**(4): 536-545.

Gundersen, G. G., M. H. Kalnoski and J. C. Bulinski (1984). "Distinct populations of microtubules: tyrosinated and nontyrosinated alpha tubulin are distributed differently in vivo." Cell **38**(3): 779-789.

Hadfield, J. A., S. Ducki, N. Hirst and A. T. McGown (2003). "Tubulin and microtubules as targets for anticancer drugs." Prog Cell Cycle Res **5**: 309-325.

Hasenbrink, G., A. Sievernich, L. Wildt, J. Ludwig and H. Lichtenberg-Frate (2006). "Estrogenic effects of natural and synthetic compounds including tibolone assessed in Saccharomyces cerevisiae expressing the human estrogen alpha and beta receptors." FASEB J **20**(9): 1552-1554.

Heredia, A., C. Davis and R. Redfield (2000). "Synergistic inhibition of HIV-1 in activated and resting peripheral blood mononuclear cells, monocyte-derived macrophages, and selected drug-resistant isolates with nucleoside analogues combined with a natural product, resveratrol." J Acquir Immune Defic Syndr **25**(3): 246-255.

Heron, M. (2012). "Deaths: leading causes for 2008." Natl Vital Stat Rep **60**(6): 1-94.

Howitz, K. T., K. J. Bitterman, H. Y. Cohen, D. W. Lamming, S. Lavu, J. G. Wood, R. E. Zipkin, P. Chung, A. Kisielewski, L. L. Zhang, B. Scherer and D. A. Sinclair (2003). "Small molecule activators of sirtuins extend Saccharomyces cerevisiae lifespan." Nature **425**(6954): 191-196.

Hsieh, H. P., J. P. Liou and N. Mahindroo (2005). "Pharmaceutical design of antimitotic agents based on combretastatins." Curr Pharm Des **11**(13): 1655-1677.

Huang, X. F., B. F. Ruan, X. T. Wang, C. Xu, H. M. Ge, H. L. Zhu and R. X. Tan (2007). "Synthesis and cytotoxic evaluation of a series of resveratrol derivatives modified in C2 position." Eur J Med Chem **42**(2): 263-267.

Hwang, J. T., D. W. Kwak, S. K. Lin, H. M. Kim, Y. M. Kim and O. J. Park (2007). "Resveratrol induces apoptosis in chemoresistant cancer cells via modulation of AMPK signaling pathway." Ann N Y Acad Sci **1095**: 441-448.

Jang, D. S., B. S. Kang, S. Y. Ryu, I. M. Chang, K. R. Min and Y. Kim (1999). "Inhibitory effects of resveratrol analogs on unopsonized zymosan-induced oxygen radical production." Biochem Pharmacol **57**(6): 705-712.

Jang, M., L. Cai, G. O. Udeani, K. V. Slowing, C. F. Thomas, C. W. Beecher, H. H. Fong, N. R. Farnsworth, A. D. Kinghorn, R. G. Mehta, R. C. Moon and J. M. Pezzuto (1997). "Cancer chemopreventive activity of resveratrol, a natural product derived from grapes." Science **275**(5297): 218-220.

Jockovich, M. E., F. Suarez, A. Alegret, Y. Pina, B. Hayden, C. Cebulla, W. Feuer and T. G. Murray (2007). "Mechanism of retinoblastoma tumor cell death after focal chemotherapy, radiation, and vascular targeting therapy in a mouse model." Invest Ophthalmol Vis Sci **48**(12): 5371-5376.

Johnson, I. S., J. G. Armstrong, M. Gorman and J. P. Burnett, Jr. (1963). "The Vinca Alkaloids: A New Class of Oncolytic Agents." Cancer Res **23**: 1390-1427.

Jordan, A., J. A. Hadfield, N. J. Lawrence and A. T. McGown (1998). "Tubulin as a target for anticancer drugs: agents which interact with the mitotic spindle." Med Res Rev **18**(4): 259-296.

Jordan, M. A. (2002). "Mechanism of action of antitumor drugs that interact with microtubules and tubulin." Curr Med Chem Anticancer Agents **2**(1): 1-17.

Jordan, M. A. and L. Wilson (2004). "Microtubules as a target for anticancer drugs." Nat Rev Cancer **4**(4): 253-265.

Kim, A. L., Y. Zhu, H. Zhu, L. Han, L. Kopelovich, D. R. Bickers and M. Athar (2006). "Resveratrol inhibits proliferation of human epidermoid carcinoma A431 cells by modulating MEK1 and AP-1 signalling pathways." Exp Dermatol **15**(7): 538-546.

Koduru, S., S. Sowmyalakshmi, R. Kumar, R. Gomathinayagam, J. Rohr and C. Damodaran (2009). "Identification of a potent herbal molecule for the treatment of breast cancer." BMC Cancer **9**: 41.
Kopp, P. (1998). "Resveratrol, a phytoestrogen found in red wine. A possible explanation for the conundrum of the 'French paradox'?" Eur J Endocrinol **138**(6): 619-620.

Krasiński, A., V. V. Fokin and K. B. Sharpless (2004). "Direct Synthesis of 1,5-Disubstituted-4-magnesio-1,2,3-triazoles, Revisited." Organic Letters **6**(8): 1237-1240.

Kurkela, M., J. A. Garcia-Horsman, L. Luukkanen, S. Morsky, J. Taskinen, M. Baumann, R. Kostiainen, J. Hirvonen and M. Finel (2003). "Expression and characterization of recombinant human UDP-glucuronosyltransferases (UGTs). UGT1A9 is more resistant to detergent inhibition than other UGTs and was purified as an active dimeric enzyme." J Biol Chem **278**(6): 3536-3544.

Kuuranne, T., M. Kurkela, M. Thevis, W. Schanzer, M. Finel and R. Kostiainen (2003). "Glucuronidation of anabolic androgenic steroids by recombinant human UDP-glucuronosyltransferases." Drug Metab Dispos **31**(9): 1117-1124.

Lagouge, M., C. Argmann, Z. Gerhart-Hines, H. Meziane, C. Lerin, F. Daussin, N. Messadeq, J. Milne, P. Lambert, P. Elliott, B. Geny, M. Laakso, P. Puigserver and J. Auwerx (2006). "Resveratrol improves mitochondrial function and protects against metabolic disease by activating SIRT1 and PGC-1alpha." Cell **127**(6): 1109-1122.

Lanzilli, G., M. P. Fuggetta, M. Tricarico, A. Cottarelli, A. Serafino, R. Falchetti, G. Ravagnan, M. Turriziani, R. Adamo, O. Franzese and E. Bonmassar (2006). "Resveratrol down-regulates the growth and telomerase activity of breast cancer cells in vitro." Int J Oncol **28**(3): 641-648.

Lee, J. E. and S. Safe (2001). "Involvement of a post-transcriptional mechanism in the inhibition of CYP1A1 expression by resveratrol in breast cancer cells." Biochem Pharmacol **62**(8): 1113-1124.

Li, H., W. K. Wu, Z. Zheng, C. T. Che, L. Yu, Z. J. Li, Y. C. Wu, K. W. Cheng, J. Yu, C. H. Cho and M. Wang (2009). "2,3',4,4',5'-Pentamethoxy-trans-stilbene, a resveratrol derivative, is a potent inducer of apoptosis in colon cancer cells via targeting microtubules." Biochem Pharmacol **78**(9): 1224-1232.

Liang, Y. C., S. H. Tsai, L. Chen, S. Y. Lin-Shiau and J. K. Lin (2003). "Resveratrol-induced G2 arrest through the inhibition of CDK7 and p34CDC2 kinases in colon carcinoma HT29 cells." Biochem Pharmacol **65**(7): 1053-1060.

Ma, G., S. I. Khan, J. Mustafa, L. A. Walker and I. A. Khan (2005). "Anticancer activity and possible mode of action of 4-O-podophyllotoxinyl 12-hydroxyl-octadec-Z-9-enoate." Lipids **40**(3): 303-308.

Madadi, N. R., S. Parkin and P. A. Crooks (2012). "(Z)-2-{2,4-Dimeth-oxy-6-[(E)-4-meth-oxy-styr-yl]benzyl-idene}quinuclidin-3-one." Acta Crystallogr Sect E Struct Rep Online **68**(Pt 3): o730.

Madadi, N. R., N. R. Penthala, L. K. Brents, B. M. Ford, P. L. Prather and P. A. Crooks (2013). "Evaluation of (< i> Z</i>)-2-((1-benzyl-1< i> H</i>-indol-3-yl) methylene)-quinuclidin-3-one analogues as novel, high affinity ligands for CB1 and CB2 cannabinoid receptors." Bioorganic & Medicinal Chemistry Letters **23**(7): 2019-2021.

Madadi, N. R., N. R. Penthala, V. Janganati and P. A. Crooks (2014). "Synthesis and anti-proliferative activity of aromatic substituted 5-((1-benzyl-1< i> H</i>-indol-3-yl) methylene)-1, 3-dimethylpyrimidine-2, 4, 6 (1< i> H</i>, 3< i> H</i>, 5< i> H</i>)-trione analogs against human tumor cell lines." Bioorganic & Medicinal Chemistry Letters **24**(2): 601-603.

Madadi, N. R., N. R. Penthala, L. Song, H. P. Hendrickson and P. A. Crooks (2014). "Preparation of 4,5 disubstituted-2H-1,2,3-triazoles from (Z)-2,3-diaryl substituted acrylonitriles." Tetrahedron Letters **45**(30): 4207-4211.

Madadi, N. R., T. R. Y. Reddy, N. R. Penthala, S. Parkin and P. A. Crooks (2010). "(Z)-2-Amino-5-[2, 4-dimethoxy-6-(4-methoxystyryl) benzylidene]-1, 3-thiazol-4 (5H)-one methanol solvate." Acta Crystallographica Section E: Structure Reports Online **66**(7): o1792-o1792.

Majireck, M. M. and S. M. Weinreb (2006). "A Study of the Scope and Regioselectivity of the Ruthenium-Catalyzed [3 + 2]-Cycloaddition of Azides with Internal Alkynes." Journal of Organic Chemistry **71**(22): 8680-8683.

Marier, J. F., P. Vachon, A. Gritsas, J. Zhang, J. P. Moreau and M. P. Ducharme (2002). "Metabolism and disposition of resveratrol in rats: extent of absorption, glucuronidation, and enterohepatic recirculation evidenced by a linked-rat model." J Pharmacol Exp Ther **302**(1): 369-373.

Mason, R. P., D. Zhao, L. Liu, M. L. Trawick and K. G. Pinney (2011). "A perspective on vascular disrupting agents that interact with tubulin: preclinical tumor imaging and biological assessment." Integr Biol (Camb) **3**(4): 375-387.

Mikstacka, R., T. Stefanski and J. Rozanski (2013). "Tubulin-interactive stilbene derivatives as anticancer agents." Cell Mol Biol Lett **18**(3): 368-397.

Mitchison, T. and M. Kirschner (1984). "Microtubule assembly nucleated by isolated centrosomes." Nature **312**(5991): 232-237.

Mouria, M., A. S. Gukovskaya, Y. Jung, P. Buechler, O. J. Hines, H. A. Reber and S. J. Pandol (2002). "Food-derived polyphenols inhibit pancreatic cancer growth through mitochondrial cytochrome C release and apoptosis." Int J Cancer **98**(5): 761-769.

Munson, A. E., L. S. Harris, M. A. Friedman, W. L. Dewey and R. A. Carchman (1975). "Antineoplastic activity of cannabinoids." J Natl Cancer Inst **55**(3): 597-602.

Nambu, H., R. Nambu, M. Melia and P. A. Campochiaro (2003). "Combretastatin A-4 phosphate suppresses development and induces regression of choroidal neovascularization." Invest Ophthalmol Vis Sci **44**(8): 3650-3655.

Nathwani, S. M., L. Hughes, L. M. Greene, M. Carr, N. M. O'Boyle, S. McDonnell, M. J. Meegan and D. M. Zisterer (2013). "Novel cis-restricted beta-lactam combretastatin A-4 analogues display anti-vascular and anti-metastatic properties in vitro." Oncol Rep **29**(2): 585-594.

Nguy, N. M., I. C. Chiu and H. Kohn (1987). "Synthesis and reactivity of 6- and 7-methoxyindano[1,2-b]aziridines." Journal of Organic Chemistry **52**(9): 1649-1655.

Noble, R. L., C. T. Beer and J. H. Cutts (1959). "Further biological activities of vincaleukoblastine—an alkaloid isolated from Vinca rosea (L.)." Biochemical Pharmacology **1**(4): 347-348.

Nogales, E., S. G. Wolf and K. H. Downing (1998). "Structure of the alpha beta tubulin dimer by electron crystallography." Nature **391**(6663): 199-203.

Nonn, L., D. Duong and D. M. Peehl (2007). "Chemopreventive anti-inflammatory activities of curcumin and other phytochemicals mediated by MAP kinase phosphatase-5 in prostate cells." Carcinogenesis **28**(6): 1188-1196.

Ohsumi, K., R. Nakagawa, Y. Fukuda, T. Hatanaka, Y. Morinaga, Y. Nihei, K. Ohishi, Y. Suga, Y. Akiyama and T. Tsuji (1998). "Novel combretastatin analogues effective against murine solid tumors: design and structure-activity relationships." J Med Chem **41**(16): 3022-3032.

Pace-Asciak, C. R., O. Rounova, S. E. Hahn, E. P. Diamandis and D. M. Goldberg (1996). "Wines and grape juices as modulators of platelet aggregation in healthy human subjects." Clinica Chimica Acta **246**(1–2): 163-182.

Pålhagen, S., R. Canger, O. Henriksen, J. A. van Parys, M.-E. Rivière and M. A. Karolchyk (2001). "Rufinamide: a double-blind, placebo-controlled proof of principle trial in patients with epilepsy." Epilepsy Research **43**(2): 115-124.

Paul, B., I. Masih, J. Deopujari and C. Charpentier (1999). "Occurrence of resveratrol and pterostilbene in age-old darakchasava, an ayurvedic medicine from India." Journal of Ethnopharmacology **68**(1–3): 71-76.

Paul, S., C. S. Mizuno, H. J. Lee, X. Zheng, S. Chajkowisk, J. M. Rimoldi, A. Conney, N. Suh and A. M. Rimando (2010). "In vitro and in vivo studies on stilbene analogs as potential treatment agents for colon cancer." Eur J Med Chem **45**(9): 3702-3708.

Penthala, N. R., V. Janganati, S. Bommagani and P. A. Crooks (2014). "Synthesis and evaluation of a series of quinolinyl trans-cyanostilbene analogs as anticancer agents." MedChemComm.

Penthala, N. R., V. N. Sonar, J. Horn, M. Leggas, J. S. Yadlapalli and P. A. Crooks (2013). "Synthesis and evaluation of a series of benzothiophene acrylonitrile analogs as anticancer agents." MedChemComm **4**(7): 1073-1078.

Pertwee, R. G. (2006). "Cannabinoid pharmacology: the first 66 years." Br J Pharmacol **147 Suppl 1**: S163-171.

Pettit, G. R., S. B. Singh, M. R. Boyd, E. Hamel, R. K. Pettit, J. M. Schmidt and F. Hogan (1995). "Antineoplastic Agents. 291. Isolation and Synthesis of Combretastatins A-4, A-5, and A-6." Journal of Medicinal Chemistry **38**(10): 1666-1672.

Pisanti, S., A. M. Malfitano, C. Grimaldi, A. Santoro, P. Gazzerro, C. Laezza and M. Bifulco (2009). "Use of cannabinoid receptor agonists in cancer therapy as palliative and curative agents." Best Pract Res Clin Endocrinol Metab **23**(1): 117-131.

Pozo-Guisado, E., A. Alvarez-Barrientos, S. Mulero-Navarro, B. Santiago-Josefat and P. M. Fernandez-Salguero (2002). "The antiproliferative activity of resveratrol results in apoptosis in MCF-7 but not in MDA-MB-231 human breast cancer cells: cell-specific alteration of the cell cycle." Biochem Pharmacol **64**(9): 1375-1386.

Pozo-Guisado, E., J. M. Merino, S. Mulero-Navarro, M. J. Lorenzo-Benayas, F. Centeno, A. Alvarez-Barrientos and P. M. Fernandez-Salguero (2005). "Resveratrol-induced apoptosis in MCF-7 human breast cancer cells involves a caspase-independent mechanism with downregulation of Bcl-2 and NF-kappaB." Int J Cancer **115**(1): 74-84.

Qamri, Z., A. Preet, M. W. Nasser, C. E. Bass, G. Leone, S. H. Barsky and R. K. Ganju (2009). "Synthetic cannabinoid receptor agonists inhibit tumor growth and metastasis of breast cancer." Mol Cancer Ther **8**(11): 3117-3129.

Quiclet-Sire, B. and S. Z. Zard (2005). "The Synthesis of 1,2,3-Triazoles from Nitroalkenes - Revisited." Synthesis **2005**(19): 3319-3326.

Quiney, C., D. Dauzonne, C. Kern, J. D. Fourneron, J. C. Izard, R. M. Mohammad, J. P. Kolb and C. Billard (2004). "Flavones and polyphenols inhibit the NO pathway during apoptosis of leukemia B-cells." Leuk Res **28**(8): 851-861.

Ravelli, R. B., B. Gigant, P. A. Curmi, I. Jourdain, S. Lachkar, A. Sobel and M. Knossow (2004). "Insight into tubulin regulation from a complex with colchicine and a stathmin-like domain." Nature **428**(6979): 198-202.

Ruan, B.-F., X. Lu, J.-F. Tang, Y. Wei, X.-L. Wang, Y.-B. Zhang, L.-S. Wang and H.-L. Zhu (2011). "Synthesis, biological evaluation, and molecular docking studies of resveratrol derivatives possessing chalcone moiety as potential antitubulin agents." Bioorganic & Medicinal Chemistry **19**(8): 2688-2695.

Rubinstein, L. V., R. H. Shoemaker, K. D. Paull, R. M. Simon, S. Tosini, P. Skehan, D. A. Scudiero, A. Monks and M. R. Boyd (1990). "Comparison of in vitro anticancer-drug-screening data generated with a tetrazolium assay versus a protein assay against a diverse panel of human tumor cell lines." J Natl Cancer Inst **82**(13): 1113-1118.

Sabolovic, N., A. C. Humbert, A. Radominska-Pandya and J. Magdalou (2006). "Resveratrol is efficiently glucuronidated by UDP-glucuronosyltransferases in the human gastrointestinal tract and in Caco-2 cells." Biopharm Drug Dispos **27**(4): 181-189.

Sanchez, C., M. L. de Ceballos, T. Gomez del Pulgar, D. Rueda, C. Corbacho, G. Velasco, I. Galve-Roperh, J. W. Huffman, S. Ramon y Cajal and M. Guzman (2001). "Inhibition of glioma growth in vivo by selective activation of the CB(2) cannabinoid receptor." Cancer Res **61**(15): 5784-5789.

Sarfaraz, S., V. M. Adhami, D. N. Syed, F. Afaq and H. Mukhtar (2008). "Cannabinoids for cancer treatment: progress and promise." Cancer Res **68**(2): 339-342.

Sengupta, S., H. Duan, W. Lu, J. L. Petersen and X. Shi (2008). "One Step Cascade Synthesis of 4,5-Disubstituted-1,2,3-(NH)-Triazoles." Organic Letters **10**(7): 1493-1496.

Seve, M., F. Chimienti, S. Devergnas, M. Aouffen, T. Douki, J. Chantegrel, J. Cadet and A. Favier (2005). "Resveratrol enhances UVA-induced DNA damage in HaCaT human keratinocytes." Med Chem **1**(6): 629-633.

Shih, A., F. B. Davis, H. Y. Lin and P. J. Davis (2002). "Resveratrol induces apoptosis in thyroid cancer cell lines via a MAPK- and p53-dependent mechanism." J Clin Endocrinol Metab **87**(3): 1223-1232.

Shirai, R., H. Takayama, A. Nishikawa, Y. Koiso and Y. Hashimoto (1998). "Asymmetric synthesis of antimitotic combretadioxolane with potent antitumor activity against multi-drug resistant cells." Bioorganic & Medicinal Chemistry **8**(15): 1997-2000.

Shoemaker, R. H. (2006). "The NCI60 human tumour cell line anticancer drug screen." Nat Rev Cancer **6**(10): 813-823.

Siemann, D. W., D. J. Chaplin and P. A. Walicke (2009). "A review and update of the current status of the vasculature-disabling agent combretastatin-A4 phosphate (CA4P)." Expert Opin Investig Drugs **18**(2): 189-197.

Singh, P., K. Rathinasamy, R. Mohan and D. Panda (2008). "Microtubule assembly dynamics: an attractive target for anticancer drugs." IUBMB Life **60**(6): 368-375.

Stervbo, U., O. Vang and C. Bonnesen (2006). "Time- and concentration-dependent effects of resveratrol in HL-60 and HepG2 cells." Cell Prolif **39**(6): 479-493.

Sun, B., J. Hoshino, K. Jermihov, L. Marler, J. M. Pezzuto, A. D. Mesecar and M. Cushman (2010). "Design, synthesis, and biological evaluation of resveratrol analogues as aromatase and quinone reductase 2 inhibitors for chemoprevention of cancer." Bioorganic & Medicinal Chemistry **18**(14): 5352-5366.

Tarleton, M., J. Gilbert, M. J. Robertson, A. McCluskey and J. A. Sakoff (2011). "Library synthesis and cytotoxicity of a family of 2-phenylacrylonitriles and discovery of an estrogen dependent breast cancer lead compound." MedChemComm **2**(1): 31-37.

Thomas, C. J., N. J. Rahier and S. M. Hecht (2004). "Camptothecin: current perspectives." Bioorganic & Medicinal Chemistry **12**(7): 1585-1604.

Thomson, P., M. A. Naylor, S. A. Everett, M. R. Stratford, G. Lewis, S. Hill, K. B. Patel, P. Wardman and P. D. Davis (2006). "Synthesis and biological properties of bioreductively targeted nitrothienyl prodrugs of combretastatin A-4." Mol Cancer Ther **5**(11): 2886-2894.

Thorpe, P. E. (2004). "Vascular targeting agents as cancer therapeutics." Clin Cancer Res **10**(2): 415-427.

Tozer, G. M., C. Kanthou, C. S. Parkins and S. A. Hill (2002). "The biology of the combretastatins as tumour vascular targeting agents." Int J Exp Pathol **83**(1): 21-38.

Trincheri, N. F., G. Nicotra, C. Follo, R. Castino and C. Isidoro (2007). "Resveratrol induces cell death in colorectal cancer cells by a novel pathway involving lysosomal cathepsin D." Carcinogenesis **28**(5): 922-931.

Tron, G. C., F. Pagliai, E. Del Grosso, A. A. Genazzani and G. Sorba (2005). "Synthesis and cytotoxic evaluation of combretafurazans." J Med Chem **48**(9): 3260-3268.

Tron, G. C., T. Pirali, G. Sorba, F. Pagliai, S. Busacca and A. A. Genazzani (2006). "Medicinal chemistry of combretastatin A4: present and future directions." J Med Chem **49**(11): 3033-3044.

Tsai, C.-W., S.-C. Yang, Y.-M. Liu and M.-J. Wu (2009). "Microwave-assisted cycloadditions of 2-alkynylbenzonitriles with sodium azide: selective synthesis of tetrazolo[5,1-a]pyridines and 4,5-disubstituted-2H-1,2,3-triazoles." Tetrahedron **65**(40): 8367-8372.

Waite, K. A., M. R. Sinden and C. Eng (2005). "Phytoestrogen exposure elevates PTEN levels." Hum Mol Genet **14**(11): 1457-1463.

Walle, T., F. Hsieh, M. H. DeLegge, J. E. Oatis, Jr. and U. K. Walle (2004). "High absorption but very low bioavailability of oral resveratrol in humans." Drug Metab Dispos **32**(12): 1377-1382.

Wang, T. T., N. W. Schoene, Y. S. Kim, C. S. Mizuno and A. M. Rimando (2010). "Differential effects of resveratrol and its naturally occurring methylether analogs on cell cycle and apoptosis in human androgen-responsive LNCaP cancer cells." Mol Nutr Food Res **54**(3): 335-344.

Wasik, A. M., B. Christensson and B. Sander (2011). "The role of cannabinoid receptors and the endocannabinoid system in mantle cell lymphoma and other non-Hodgkin lymphomas." Semin Cancer Biol **21**(5): 313-321.

Weiss, J. N. (1997). "The Hill equation revisited: uses and misuses." FASEB J **11**(11): 835-841.
Young, S. L. and D. J. Chaplin (2004). "Combretastatin A4 phosphate: background and current clinical status." Expert Opin Investig Drugs **13**(9): 1171-1182.

Yu, C., Y. G. Shin, J. W. Kosmeder, J. M. Pezzuto and R. B. van Breemen (2003). "Liquid chromatography/tandem mass spectrometric determination of inhibition of human cytochrome P450 isozymes by resveratrol and resveratrol-3-sulfate." Rapid Commun Mass Spectrom **17**(4): 307-313.

Zhou, J. and P. Giannakakou (2005). "Targeting microtubules for cancer chemotherapy." Curr Med Chem Anticancer Agents **5**(1): 65-71.

VITA

Nikhil Reddy Madadi

Education:

Bachelors in Pharmacy (2003-2007) Osmania University

Professional Positions:

Teaching Assistant, Eastern Kentucky University (2008-2009)

Research Assistant, University of Kentucky (2009-2011)

Research Assistant, University of Arkansas for Medical Sciences (2011-2014)

Professional Publications:

Madadi, Nikhil Reddy, Narsimha Reddy Penthala, Lisa K Brents, Benjamin M Ford, Paul L Prather and Peter A Crooks. "Evaluation of (< I> Z</I>)-2-((1-Benzyl-1< I> H</I>-Indol-3-Yl) Methylene)-Quinuclidin-3-One Analogues as Novel, High Affinity Ligands for Cb1 and Cb2 Cannabinoid Receptors." *Bioorganic & Medicinal Chemistry Letters* 23, no. 7 (2013): 2019-2021.

Madadi, Nikhil Reddy, Narsimha Reddy Penthala, Venumadhav Janganati and Peter A Crooks. "Synthesis and Anti-Proliferative Activity of Aromatic Substituted 5-((1-Benzyl-1< I> H</I>-Indol-3-Yl) Methylene)-1, 3-Dimethylpyrimidine-2, 4, 6 (1< I> H</I>, 3< I> H</I>, 5< I> H</I>)-Trione Analogs against Human Tumor Cell Lines." *Bioorganic & Medicinal Chemistry Letters* 24, no. 2 (2014): 601-603.

Madadi, Nikhil Reddy, Narsimha Reddy Penthala, Lin Song, Howard P. Hendrickson and Peter A. Crooks. "Preparation of 4,5 Disubstituted-2*H*-1,2,3-Triazoles from (*Z*)-2,3-Diaryl Substituted Acrylonitriles." *Tetrahedron Letters*, 55 (2014) 4207–4211.

Franks, Lirit N., Benjamin M. Ford, **Nikhil R. Madadi**, Narsimha R. Penthala, Peter A. Crooks and Paul L. Prather. "Characterization of the Intrinsic Activity for a Novel Class of Cannabinoid Receptor Ligands: Indole Quinuclidine Analogues." *European Journal of Pharmacology*, 737 (2014), 140–148.

Greer, Aleksandra K, **Nikhil R Madadi**, Stacie M Bratton, Sarah D Eddy, Zofia Mazerska, Howard Hendrickson, Peter A Crooks and Anna Radominska-Pandya. "Novel Resveratrol-Based Substrates for Human Hepatic, Renal and Intestinal Udp-Glucuronosyltransferases." *Chemical Research in Toxicology*, 2014, 27, 536−545.

Janganati, Venumadhav, Narsimha Reddy Penthala, **Nikhil Reddy Madadi**, Zheng Chen and Peter A. Crooks. "Anti-Cancer Activity of Carbamate Derivatives of Melampomagnolide B." *Bioorganic & Medicinal Chemistry Letters*, no. 0 (2014).

Janganati, Venumadhav, Narsimha Reddy Penthala, **Nikhil Reddy Madadi**, Sean Parkin and Peter A Crooks. "Monosuccinate Ester of Melampomagnolide B." *Acta Crystallographica Section E: Structure Reports Online* 70, no. 3 (2014): o372-o373.

Penthala, Narsimha Reddy, Thirupathi Reddy Yerramreddy, **Nikhil Reddy Madadi** and Peter A Crooks. "Synthesis and in Vitro Evaluation of< I> N</I>-Alkyl-3-Hydroxy-3-(2-Imino-3-Methyl-5-Oxoimidazolidin-4-Yl) Indolin-2-One Analogs as Potential Anticancer Agents." *Bioorganic & Medicinal Chemistry Letters* 20, no. 15 (2010): 4468-4471.

Reddy, P Narsimha, Y Thirupathi Reddy, **M Nikhil Reddy**, B Rajitha and Peter A Crooks. Cellulose Sulfuric Acid: An Efficient Biodegradable and Recyclable Solid Acid Catalyst for the One-Pot Synthesis of 3, 4-Dihydropyrimidine-2 (1 H)-Ones. *Synthetic Communications* 39, no. 7 (2009): 1257-1263.

Reddy, Y Thirupathi, P Narsimha Reddy, **M Nikhil Reddy**, B Rajitha and Peter A Crooks. "Convenient and Scalable Process for the Preparation of Bupropion Hydrochloride Via Efficient Bromination of M-Chloropropiophenone with N-Bromosuccinimide." *Synthetic Communications*® 40, no. 11 (2010): 1566-1573.

Reddy, Y Thirupathi, P Raghotham Reddy, **M Nikhil Reddy**, B Rajitha and Peter A Crooks. "Sulfamic Acid: An Efficient, Cost-Effective, and Reusable Solid Acid Catalyst for the Synthesis of 1, 8-Naphthyridines under Solvent-Free Heating and Microwave Irradiation." *Synthetic Communications*® 38, no. 18 (2008): 3201-3207.

Venu Madhav, J, Y Thirupathi Reddy, P Narsimha Reddy, **M Nikhil Reddy**, Suresh Kuarm, Peter A Crooks and B Rajitha. "Cellulose Sulfuric Acid: An Efficient Biodegradable and Recyclable Solid Acid Catalyst for the One-Pot Synthesis of Aryl-14h-Dibenzo [< I> Aj</I>] Xanthenes under Solvent-Free Conditions." *Journal of Molecular Catalysis A: Chemical* 304, no. 1 (2009): 85-87.

Narsimha R Penthala, Shobanbabu Bommagani, Venumadhav Janganati, Kenzie B. MacNicol, Chad E. Cragle, **Nikhil R. Madadi**, Linda L. Hardy, Angus M. MacNicol, and Peter A. Crooks. Synthesis of C-C bond analogs of parthenolide and melampomagnolide B as anticancer modulators that modify cell cycle progression. *European Journal of Medicinal Chemistry*. **Accepted** (***In press) (2014).***

Nikhil Reedy Madadi, Hongliang Zong, Amit Ketkar, Chen Zheng, Narsimha Reddy Penthala, Venumadhav Janganati, Shobanbabu Bommagani, Robert Eoff, Monica L. Guzman, Peter A. Crooks. Synthesis and evaluation of a series of combretastatin/resveratrol analogs as anti-cancer agents**.** MedChemComm. ***Ready for submission.***

Narsimha Reddy Penthala, **Nikhil Reddy Madadi**, Janganati, Venumadhav and Peter A Crooks. L-Proline catalyzed one-step synthesis of 4,5-diaryl-2*H*-1,2,3-triazoles from cyanostilbenes via [3+2] cycloaddition of azide. *Tetrahedron Letters*. **Accepted** (***In press) (2014).***

4,5 disubstituted-2*H*-1,2,3-triazoles as potent and stable combretastatin A4 analogues. ***In preparation***

3,4-(methylenedioxy)-substituted cyanostilbenes as selective and high affinity ligands for CB1 and CB2 cannabinoid receptors. ***In preparation***

PATENTS

- **M. Nikhil Reddy,** P. Narsimha Reddy, Peter A. Crooks, M. Leena and E. Robert. 4,5-Disubstituted-2*H*-1,2,3-triazoles as anticancer agents, US Provisional Patent Application No. 61/972,938, submitted on March 10th, (**2014)**.

- Peter A. Crooks, Y. Thirupathi Reddy, P. Narsimha Reddy, **M. Nikhil Reddy**, and B. Rajitha. Process Development for the Synthesis of Bupropion Hydrochloride and Hydroxybupropion *via* Efficient Bromination using *N*-Bromosuccinimide, US Provisional Patent Application No. 61/198,802, submitted on November 10th, (**2009)**.